The effect of cover cropping and P fertilization on soil P pools and forms in a no-till corn soybean rotation system

by

Elaheh Khosh Manzar

B.S., University of Tabriz, 2013
M.S., University of Tabriz, 2016

AN ABSTRACT OF A DISSERTATION

submitted in partial fulfillment of the requirements for the degree

DOCTOR OF PHILOSOPHY

Department of Agronomy
College of Agriculture

KANSAS STATE UNIVERSITY
Manhattan, Kansas

2026

Abstract

Sustainable phosphorus (P) management in no-till agroecosystems requires balancing crop nutrient requirements with the critical need to mitigate environmental impacts, particularly the loss of dissolved reactive P (DRP) in surface runoff. While cover crops (CC) are widely implemented to control soil erosion, recent field-scale monitoring indicates they can paradoxically increase DRP losses. To elucidate the biogeochemical mechanisms driving this phenomenon, this dissertation evaluated the interactive effects of long-term cover cropping and distinct P fertilization strategies on soil P pools, molecular P speciation, soil fertility indicators, and iron (Fe) chemistry.

A long-term field study was conducted at the Kansas Agricultural Watershed (KAW) field laboratory (Manhattan, KS, USA) in a continuous no-till corn–soybean rotation. The experiment utilized a randomized complete block design with a 2 × 3 factorial treatment structure. The two cover crop treatments consisted of no cover crop (NC) and a winter cover crop (CC, primarily cereal rye). The three P fertilization strategies included an unfertilized control (CN; 0 kg P ha^{-1} yr^{-1}), a build-and-drawdown/sufficiency strategy (BD/SF; initially fertilized at 27 kg P ha^{-1} yr^{-1}, unfertilized from 2020 to 2022 to draw down legacy P, and then transitioned to a targeted sufficiency rate of 10 kg P ha^{-1} yr^{-1}), and a continuous build-and-maintain strategy (BM; receiving 27 kg P ha^{-1} yr^{-1} from 2015 to 2019 and ~24 kg P ha^{-1} yr^{-1} thereafter). Soil samples across multiple depth increments (0–2.5, 2.5–5, and 5–15 cm) were analyzed using standard chemical extractions, Hedley sequential fractionation, selective Fe extractions, bulk Fe K-edge X-ray absorption near-edge structure (XANES) spectroscopy, and solution ^{31}P nuclear magnetic resonance (^{31}P-NMR) spectroscopy.

Agronomic and sequential fractionation results indicated that continuous P fertilization (BM) significantly increased total P, Mehlich-3 P, and highly labile inorganic pools (Resin-P_i and $NaHCO_3$-P_i), establishing a concentration gradient of BM > BD > CN. However, the BM strategy caused severe vertical stratification, with Mehlich-3 P concentrations exceeding 80 mg kg^{-1} strictly at the 0–2.5 cm surface interface, directly escalating the vulnerability to DRP runoff. In contrast, the BD strategy operated under a highly negative P budget but successfully sustained combined cash crop and cover crop P uptake equivalent to the BM strategy by drawing upon legacy inorganic P reserves accumulated during prior fertilization phases.

The integration of cover crops significantly enhanced foundational soil health, progressively increasing surface total carbon and total nitrogen over the seven-year period. While CC actively depleted highly mobile inorganic P pools (Resin-P_i, $NaHCO_3$-P_i, and Mehlich-3 P) in the fertilized plots, sequential fractionation and ^{31}P-NMR spectroscopy revealed that CC concurrently increased moderately stable and biologically mediated organic P (P_o) reservoirs. Specifically, NaOH-P_o and *myo*-inositol hexakisphosphate (*myo*-IHP) accumulated significantly under cover cropping, with *myo*-IHP comprising 12% to 15% of the total organic P pool. This demonstrates that cover crops actively scavenge and redistribute legacy P from vulnerable inorganic fractions into stable, plant-derived organic forms that can gradually mineralize to replenish crop demands.

To resolve the paradox of increased DRP runoff under cover cropping despite this organic stabilization, concurrent Fe speciation was evaluated. Selective extractions revealed that cover cropping significantly increased organically associated Fe (pyrophosphate-extractable) while proportionally decreasing amorphous, highly reactive Fe oxides (oxalate-extractable). Bulk Fe-XANES spectroscopy confirmed no shift toward reduced Fe(II) species, ruling out

widespread reductive dissolution. Instead, these trends indicate ligand-promoted dissolution driven by root exudates, which destabilizes Fe oxides through organic complexation. The ligand-driven transition of Fe effectively reduces the soil's inorganic sorption sites normally available to retain phosphate, leaving phosphate unbound and highly susceptible to runoff.

These integrated findings confirm that while cover crops enhance internal P cycling and soil health, their root-driven ligand-promoted dissolution of amorphous Fe oxides and formation of organo-Fe complexes reduce the abundance of reactive inorganic mineral surfaces available for phosphate adsorption. Therefore, continuing a high-input BM fertilization strategy in cover-cropped, no-till systems continuously loads fewer remaining mineral sorption sites and maintains elevated soluble phosphate at the acidified soil surface, maximizing DRP runoff risk. Implementing a strategic P drawdown and sufficiency approach is a mandatory adaptation when utilizing cover crops, providing a robust management framework that safely utilizes legacy P, leverages internal organic P cycling, and proactively mitigates water quality degradation without sacrificing agronomic productivity.

The effect of cover cropping and P fertilization on soil P pools and forms in a no-till corn soybean rotation system

by

Elaheh Khosh Manzar

B.S., University of Tabriz, 2013
M.S., University of Tabriz, 2016

A DISSERTATION

submitted in partial fulfillment of the requirements for the degree

DOCTOR OF PHILOSOPHY

Department of Agronomy
College of Agriculture

KANSAS STATE UNIVERSITY
Manhattan, Kansas

2026

Approved by:

Co-Major Professor
Nathan O. Nelson

Approved by:

Co-Major Professor
Ganga M. Hettiarachchi

Copyright

© Elaheh Khosh Manzar 2026.

Abstract

Sustainable phosphorus (P) management in no-till agroecosystems requires balancing crop nutrient requirements with the critical need to mitigate environmental impacts, particularly the loss of dissolved reactive P (DRP) in surface runoff. While cover crops (CC) are widely implemented to control soil erosion, recent field-scale monitoring indicates they can paradoxically increase DRP losses. To elucidate the biogeochemical mechanisms driving this phenomenon, this dissertation evaluated the interactive effects of long-term cover cropping and distinct P fertilization strategies on soil P pools, molecular P speciation, soil fertility indicators, and iron (Fe) chemistry.

A long-term field study was conducted at the Kansas Agricultural Watershed (KAW) field laboratory (Manhattan, KS, USA) in a continuous no-till corn–soybean rotation. The experiment utilized a randomized complete block design with a 2 × 3 factorial treatment structure. The two cover crop treatments consisted of no cover crop (NC) and a winter cover crop (CC, primarily cereal rye). The three P fertilization strategies included an unfertilized control (CN; 0 kg P ha^{-1} yr^{-1}), a build-and-drawdown/sufficiency strategy (BD/SF; initially fertilized at 27 kg P ha^{-1} yr^{-1}, unfertilized from 2020 to 2022 to draw down legacy P, and then transitioned to a targeted sufficiency rate of 10 kg P ha^{-1} yr^{-1}), and a continuous build-and-maintain strategy (BM; receiving 27 kg P ha^{-1} yr^{-1} from 2015 to 2019 and ~24 kg P ha^{-1} yr^{-1} thereafter). Soil samples across multiple depth increments (0–2.5, 2.5–5, and 5–15 cm) were analyzed using standard chemical extractions, Hedley sequential fractionation, selective Fe extractions, bulk Fe K-edge X-ray absorption near-edge structure (XANES) spectroscopy, and solution ^{31}P nuclear magnetic resonance (^{31}P-NMR) spectroscopy.

Agronomic and sequential fractionation results indicated that continuous P fertilization (BM) significantly increased total P, Mehlich-3 P, and highly labile inorganic pools (Resin-P_i and $NaHCO_3$-P_i), establishing a concentration gradient of BM > BD > CN. However, the BM strategy caused severe vertical stratification, with Mehlich-3 P concentrations exceeding 80 mg kg^{-1} strictly at the 0–2.5 cm surface interface, directly escalating the vulnerability to DRP runoff. In contrast, the BD strategy operated under a highly negative P budget but successfully sustained combined cash crop and cover crop P uptake equivalent to the BM strategy by drawing upon legacy inorganic P reserves accumulated during prior fertilization phases.

The integration of cover crops significantly enhanced foundational soil health, progressively increasing surface total carbon and total nitrogen over the seven-year period. While CC actively depleted highly mobile inorganic P pools (Resin-P_i, $NaHCO_3$-P_i, and Mehlich-3 P) in the fertilized plots, sequential fractionation and ^{31}P-NMR spectroscopy revealed that CC concurrently increased moderately stable and biologically mediated organic P (P_o) reservoirs. Specifically, NaOH-P_o and *myo*-inositol hexakisphosphate (*myo*-IHP) accumulated significantly under cover cropping, with *myo*-IHP comprising 12% to 15% of the total organic P pool. This demonstrates that cover crops actively scavenge and redistribute legacy P from vulnerable inorganic fractions into stable, plant-derived organic forms that can gradually mineralize to replenish crop demands.

To resolve the paradox of increased DRP runoff under cover cropping despite this organic stabilization, concurrent Fe speciation was evaluated. Selective extractions revealed that cover cropping significantly increased organically associated Fe (pyrophosphate-extractable) while proportionally decreasing amorphous, highly reactive Fe oxides (oxalate-extractable). Bulk Fe-XANES spectroscopy confirmed no shift toward reduced Fe(II) species, ruling out

widespread reductive dissolution. Instead, these trends indicate ligand-promoted dissolution driven by root exudates, which destabilizes Fe oxides through organic complexation. The ligand-driven transition of Fe effectively reduces the soil's inorganic sorption sites normally available to retain phosphate, leaving phosphate unbound and highly susceptible to runoff.

These integrated findings confirm that while cover crops enhance internal P cycling and soil health, their root-driven ligand-promoted dissolution of amorphous Fe oxides and formation of organo-Fe complexes reduce the abundance of reactive inorganic mineral surfaces available for phosphate adsorption. Therefore, continuing a high-input BM fertilization strategy in cover-cropped, no-till systems continuously loads fewer remaining mineral sorption sites and maintains elevated soluble phosphate at the acidified soil surface, maximizing DRP runoff risk. Implementing a strategic P drawdown and sufficiency approach is a mandatory adaptation when utilizing cover crops, providing a robust management framework that safely utilizes legacy P, leverages internal organic P cycling, and proactively mitigates water quality degradation without sacrificing agronomic productivity.

Table of Contents

Table of Contents ..... **x**
List of Figures ..... **xv**
List of Tables ..... **xviii**
Acknowledgements ..... **xx**
Dedication ..... **xxiv**
Preface ..... **xxv**
Acknowledgment of Artificial Intelligence (AI) Use ..... **xxvii**
Chapter 1 - General Introduction **1**
Research Objectives and Structure of the Dissertation 5
References 8
Chapter 2 - Literature Review **11**
Overview of Soil Phosphorus Cycle 11
Phosphorus and Environmental Concerns 14
Major P forms in Soils 15
Inorganic P compounds 15
Organic P compounds 17
Processes controlling the cycling of P compounds in the soil 18
Adsorption and Desorption 18
Dissolution and Precipitation 18
Mineralization and Immobilization 19
Factors impacting the cycling of P compounds 20
Soil Properties 20
Soil pH 20
Organic matter 21
Organic acids 22
Organic P Desorption and Enzymatic Hydrolysis 24
Soil Moisture, Aeration, and Redox Dynamics 24
Temperature Dynamics across Coupled Biogeochemical Processes 26
Microbial Activity 28

Soil Mineralogy 29
Management Practices 30
Cover Crops 30
Tillage 32
P Fertilization 32
Methods of P fertilization 34
Methods to identify and quantify P forms and pools in soils 34
Extractions 35
Agronomic Soil Test P 35
Oxalate Extractable P 36
Water and Dilute Salt Extractable P 36
Total Soil P Determination: High-Temperature Ignition versus Strong Acid Digestion 37
Sequential P fractionation 39
Different fractionation methods 39
Common sources of errors in fractionation schemes 40
Advanced methods 41
Phosphorus K-edge X-ray Absorption Near-Edge Structure (P-XANES) Spectroscopy 41
Limitations and challenges in P-XANES 42
P-XANES and its application in P fertilizer management 43
Introduction to ^{31}P-NMR 44
Principles of ^{31}P-NMR 45
Accurate ^{31}P-NMR Data Acquisition: Critical Factors 46
Advantages 46
Limitations and challenges 46
^{31}P-NMR and its application in P fertilizer management 47
References 49
Chapter 3 - Changes in soil P pools under long-term cover crop and phosphorus fertilization in a corn-soybean rotation system 65
Abstract 65
Introduction 66
Material and Methods 70

Experimental site and design 70
Agronomic management 71
Sampling and Analysis of Biomass for Phosphorus Uptake 71
Equations used to calculate P uptake and return 72
Soil Sample Collection and Processing 74
Hedley Sequential Fractionation Method 74
Statistical Analysis 76
Results 76
Phosphorus uptake and redeposition (return) 76
Phosphorus Pools Determined by Sequential Fractionation 78
Discussion 87
Conclusion 93
References 95
Chapter 4 - Effects of long-term cover crop and phosphorus fertilization on soil organic phosphorus forms and soil P pools under a corn-soybean rotation system 102
Abstract 102
Introduction 103
Material and Methods 107
Experimental site, design, and agronomic management 107
Soil sample collection 109
Hedley sequential fractionation method 109
Solution ^{31}P-NMR spectroscopy method 111
Statistical analysis 113
Results and Discussion 114
Phosphorus Pools Determined by Sequential Fractionation 114
Phosphorus Forms and Compound Classes Determined by ^{31}P-NMR 117
NaOH-EDTA Extraction Efficiency 117
Inorganic P Compounds (Orthophosphate, Pyrophosphate, Polyphosphate) 118
Organic P compounds (Monoesters, Diester degradation products, Phosphonates, *myo*-inositol hexakisphosphate) 124
Correlations between Soil Phosphorus Pools and Agronomic Indicators 129

Implications for soil fertility and potential P loss in runoff 131
Conclusion 133
References 135
Chapter 5 - The effect of P fertilization and cover cropping on soil fertility indicators in a no-till corn soybean rotation system 141
Abstract 141
Introduction 142
Material and Methods 145
Experimental site and design 145
Agronomic management 146
Plant sampling and P uptake analysis 148
Soil sampling 149
Soil Analysis 149
Statistical Analysis 150
Results 150
Mehlich-3 P 152
Total P 153
Total Carbon 155
Total Nitrogen 157
Soil pH Dynamics 159
Annual P budget dynamics 161
Discussion 163
Cover crops 163
Cover Cropping, P Fertilization, and Soil pH Interactions 167
Phosphorus fertilizer management and P budget dynamics 168
Conclusion 172
References 173
Chapter 6 - Effects of Cover Cropping and Phosphorus Fertilization on Soil Iron Chemistry: Evidence from Selective Extractions and Fe-XANES 180
Abstract 180
Introduction 181

Material and Methods 184
Experimental site and design 184
Soil Sample Collection and Processing 185
Soil pH Dynamics in the Surface Layer 186
Pyrophosphate Extraction 186
Ammonium Oxalate Extraction 187
Iron K-edge XANES Study 187
Data Collection 187
Data Analysis 188
Results 189
Pyrophosphate-Extractable Fe and Al 189
Oxalate-Extractable Fe, Al, and P 191
Iron K-edge XANES Spectroscopy 194
Discussion 200
Pyrophosphate- and ammonium oxalate-extractable Fe and Al 200
The Role of Soil pH in Iron Solubilization and Complexation 201
Iron K-edge XANES Spectroscopy 203
Conclusion 205
References 207
Chapter 7 - General Summary, Synthesis, and Conclusions 211
Research Overview and Rationale 211
Synthesis of Key Findings across Chapters 212
Mechanistic Synthesis: Resolving the Cover Crop–Phosphorus Paradox 215
Practical Implications for Sustainable Phosphorus Management 216
Future Research Directions 216
Appendix A - Supplementary ^{31}P-NMR Data 220
Reference 224

List of Figures

Figure 2-1. Integrated overview of the soil phosphorus cycle. 14
Figure 3-1. The main effect of cover cropping (a) and the main effect of P fertilization (b) on mean annual total plant P uptake (main crops plus cover crop, kg P ha^{-1} yr^{-1}) across the 8-year study period (2015 to 2022). 77
Figure 3-2. The main effect of cover cropping on mean annual total plant P return (a), and the main effect of P fertilization on mean annual total plant P return (b) and mean annual grain P removal (c) (kg P ha^{-1} yr^{-1}) across the 8-year study period (2015 to 2022). 78
Figure 3-3. The interaction of phosphorus (P) fertilization and cover cropping on Resin-P_i (a) and the interaction of P fertilization and year on Resin-P_i concentrations (b). 80
Figure 3-4.The interaction of cover cropping, year, and P fertilization on $NaHCO_3$-P_t concentration. 81
Figure 3-5. The main effect of cover cropping (a) and the interaction of P fertilization and year (b) on $NaHCO_3$-P_i concentration. 82
Figure 3-6.The interaction of P fertilization and year on $NaHCO_3$-P_o concentration. 83
Figure 3-7. The interaction of P fertilization and year on NaOH-P_t (a) and NaOH-P_i (b) concentrations. 84
Figure 3-8. The main effect of cover cropping on NaOH-P_o (a) and the interaction of P fertilization and year on NaOH-P_o (b). 85
Figure 3-9. Mean concentration of the residual phosphorus (Residual-P) fraction over the four-year study period (2019–2022). 86
Figure 4-1. An overview of the Kansas Agricultural Watershed (KAW) field laboratory with 18 plots, including cover crop (green plots) and no cover crop plots (brown plots) (left). Soil sampling points where three geo-referenced subplots were sampled within each plot (right). 107
Figure 4-2. Representative liquid-state one-dimensional ^{31}P-NMR spectra of NaOH-EDTA soil extracts for the six different agronomic treatments. ppm). 113
Figure 4-3. Percentage of total soil phosphorus (P) extracted in the topsoil (0–5 cm) under different long-term fertilization strategies. 118

Figure 4-4. The main effect of P fertilization on different forms of inorganic phosphorus (a. orthophosphate, b. pyrophosphate, and c. total polyphosphate). 122
Figure 4-5. The main effects of phosphorus (P) fertilization and cover cropping on selected organic P pools: (a) the corrected monoester-to-diester (cM:D) ratio, (b) *myo*-inositol hexakisphosphate (*myo*-IHP) response to cover cropping, (c) *myo*-IHP response to P fertilization, and (d) total phosphonates response to P fertilization. 125
Figure 5-1. The interaction of P fertilization, depth, and year on Mehlich-3 P (a, b, and c), and the main effect of CC on soil Mehlich-3 P (d). 153
Figure 5-2. The interaction of P fertilization and year on soil total P (a), and the interaction of depth and P fertilization on soil total P (b). 155
Figure 5-3. The interaction of cover crop and depth on soil total carbon (a), and the interaction of year and cover crop on soil total carbon (b) and the interaction of depth and P fertilization on soil total carbon (c). 156
Figure 5-4. The interaction of P fertilization and depth on soil total nitrogen (a), and the interaction of depth and cover crop on soil total nitrogen (b). 158
Figure 5-5. The three-way interaction of year, P fertilization, and cover cropping on soil total nitrogen concentration (g kg^{-1}) in the surface soil layer. Panel (a) represents the cover crop (CC) treatment, and panel (b) represents the no cover crop (NC) treatment. 159
Figure 5-6. The interaction of soil depth and cover cropping (a), and the interaction of soil depth and sampling year (b) on soil pH averaged across other treatments (2019–2025). 160
Figure 5-7. Annual phosphorus (P) balance components (kg P ha^{-1} yr^{-1}) from 2020 to 2024 under different fertilization strategies: (a) annual P fertilizer inputs (P_{in}), (b) annual crop P removal through grain harvest (P_{out}), and (c) the resulting annual net P budget ($P_{in} - P_{out}$). 162
Figure 6-1. The interaction of P fertilization and cover cropping on pyrophosphate-extractable Al (a) and pyrophosphate-extractable Fe (b). 191
Figure 6-2. The interaction of P fertilization and cover cropping on oxalate-extractable Fe (a) and the interaction of P fertilization and year on oxalate-extractable P (b). 193
Figure 6-3. Overlay of ammonium oxalate-extractable Fe (representing total reactive and poorly crystalline Fe) and sodium pyrophosphate-extractable Fe (representing organically associated Fe) across different phosphorus fertilization and cover crop treatments. The

overlaid bars illustrate the proportion of organically bound Fe (foreground) relative to the broader reactive Fe pool (background). 194
Figure 6-4. Normalized Fe K-edge X-ray absorption near-edge structure spectra of soil collected in 2015 and 2022. CN-CC, control-with cover crops; CN-NC, control-no cover crops; BD-CC, build-and-drawdown with cover crops; BD-NC, build-and-drawdown-no cover crops; BM-CC, build-and-maintain with cover crops; BM-NC, build-and-maintain no cover crops. 196
Figure 6-5. Normalized Fe K-edge X-ray absorption near-edge structure spectra of soil collected in 2022 and 2023. CN-CC, control-with cover crops; CN-NC, control-no cover crops; BD-CC, build-and-drawdown with cover crops; BD-NC, build-and-drawdown-no cover crops; BM-CC, build-and-maintain with cover crops; BM-NC, build-and-maintain no cover crops. 199

List of Tables

Table 3-1. Summary of the extractants and operational procedure used for the modified Hedley sequential P fractionation in this study (Tiessen and Moir, 1993)..... 75

Table 3-2. Analysis of variance (p-values) for the main and interacting effects of cover crop and phosphorus fertilization on mean annual total plant P uptake (main crops plus cover crop), total plant P return, and grain P removal across the 8-year study period (2015–2022)..... 77

Table 3-3. Analysis of variance (p-values) for the main and interacting effects of cover crop, phosphorus fertilization, and sampling year on sequentially extracted soil phosphorus pools. 79

Table 3-4. Main effects of cover cropping and P fertilization on HCl-P_i and Residual-P concentrations (mg kg^{-1})..... 85

Table 4-1. Summary of the extractants, procedures, and defined fractions for the Hedley sequential extraction. 110

Table 4-2. Effect of cover crop and phosphorus (P) fertilization treatment on different soil phosphorus fractions. 115

Table 4-3. Chemical shifts of peaks detected in ^{31}P NMR spectra of NaOH-EDTA samples, present in at least 9 of 18 samples..... 119

Table 4-4. Analysis of variance (ANOVA) results (P-values) for testing fixed effects of cover crop (Cover), phosphorus (P) fertilizer management (Fert), and their interactions on different compound classes and forms of inorganic and organic phosphorus. Significant effects ($P < 0.05$) are highlighted in bold. 123

Table 4-5. Effect of cover crop and phosphorus (P) fertilization treatment on broad soil organic P pools and inositol phosphates, determined by ^{31}P-NMR spectroscopy. 126

Table 4-6.Effect of cover crop and phosphorus (P) fertilization treatment on specific orthophosphate monoesters, diesters, and phosphonates, determined by ^{31}P-NMR spectroscopy..... 128

Table 4-7. Pearson correlation coefficients (r) between selected soil phosphorus pools, agronomic soil test P (STP), crop yield, and crop P uptake. 130

Table 5-1. Summary of P fertilizer and cover crop treatments for three time periods. 148

Table 5-2.Analysis of variance (p-values) for the effects of cover crop, phosphorus fertilizer, year, soil depth, and their interactions on soil pH, Mehlich-3 P, total P, total carbon, and total nitrogen. 151
Table 5-3. The interaction of soil depth and sampling year on soil pH across cover crop and P fertilization treatments (2019–2025)..... 161
Table 6-1. Baseline soil physicochemical properties (pH, total carbon, and Mehlich-3 extractable P) across experimental treatments in 2023. 186
Table 6-2. The relative contributions of the Fe reference spectra obtained from Fe-XANES linear combination fitting for all treatments in 2015. 197
Table 6-3. The relative contributions of the Fe reference spectra obtained from Fe-XANES linear combination fitting for all treatments in 2022. 200
Table 6-4. The relative contributions of the Fe reference spectra obtained from Fe-XANES linear combination fitting for all treatments in 2023. 200

Acknowledgements

First and foremost, I would like to express my deepest gratitude and sincere appreciation to my major professor and advisor, Dr. Nathan O. Nelson, for his continuous guidance, rigorous mentorship, constructive critiques, and unwavering support throughout my doctoral journey. His high scientific standards, sharp insights into nutrient dynamics, and encouragement to pursue precision in research have fundamentally shaped my development as an independent scientist.

I would also like to express my sincere gratitude to my co-major advisor, Dr. Ganga M. Hettiarachchi, for sharing her extensive knowledge and expertise in soil chemistry, which greatly enriched my research and broadened my understanding of the field. Beyond her academic guidance, I am deeply grateful for her kindness, encouragement, and unwavering support throughout my doctoral journey. Her warmth and willingness to support me made a meaningful difference in my experience and development as a researcher.

I am also deeply grateful to my committee member, Dr. Barbara Cade-Menun, for her invaluable expertise in soil organic phosphorus, particularly her extensive knowledge of ^{31}P NMR spectroscopy, which provided important insights and strengthened my understanding of phosphorus dynamics throughout my research.

I would also like to thank Dr. Om Prakash for serving on my doctoral committee. I appreciate his time and service throughout my doctoral program.

I would like to sincerely thank Dr. Darshani Kumaragamage for providing some data used in this dissertation. Her contribution and willingness to share these data are greatly appreciated and have been valuable to this research.

Special thanks are extended to the faculty and research staff of the Kansas Agricultural Watershed (KAW) field laboratory, Dr. Gerard J. Kluitenberg, Dr. Kraig L. Roozeboom, Dr. Peter J. Tomlinson, and Dr. Dean Presley, for their valuable contributions, support, and collaboration throughout my doctoral journey. I am grateful for the opportunity to be part of this research team and for the knowledge, perspectives, and experiences shared by everyone involved, which have enriched my research experience and contributed to my growth as a researcher.

I also acknowledge the Structural Biology Center at the University of Kansas for their technical support with liquid-state ^{31}P-NMR spectroscopy analysis, as well as the staff at the National Synchrotron Light Source II (NSLS-II), Brookhaven National Laboratory, for their operational assistance during Fe K-edge XANES data collection at beamline 7-ID-2. Appreciation is also expressed to the Kansas State University Soil Testing Laboratory for their analytical support.

This research was supported by funding from the Kansas Agricultural Experiment Station, the Kansas Corn Commission, the Kansas Soybean Commission, and relevant USDA-NIFA grants. Their dedication to advancing agricultural science and innovation provided the valuable resources, support, and opportunities that made this research possible and contributed to the successful completion of my doctoral work.

I would also like to express my sincere appreciation to the Water Quality Laboratory for welcoming me as a part-time laboratory assistant and providing me with the opportunity to expand my knowledge and skills beyond my doctoral research. I am especially grateful to Madhubhashini Galkaduwa and Kushan Kompalage for their support, guidance, and willingness

to share their knowledge, which have made my experience in the lab both rewarding and enjoyable.

I would like to extend my special thanks to Sarah Moylan for her dedication, tireless efforts, and positive spirit, which have contributed greatly to the smooth functioning of our laboratory.

I am also grateful to my fellow graduate students and postdoctoral researchers in the Department of Agronomy, Dr. Tamjid Us Sakib, Dr. Eduardo Gutierrez, Dr. Kasuni Gamage, Dr. Amber Pasket, Dr. Gustavo Roa, and Sumit Chowdhury, for their friendship, support, and encouragement throughout my doctoral journey. Their willingness to lend a helping hand and share their knowledge made this journey a collaborative, supportive, and enjoyable experience.

I would also like to express my deepest gratitude to my dear friend, Braden McCune-Streit, for being a constant source of support, encouragement, and strength throughout my doctoral journey. Your kindness, generosity, and willingness to be there whenever I needed help have meant more to me than I can fully express. Your friendship made the challenges of this journey easier to navigate and the memorable moments even more meaningful. I am truly grateful to have had you by my side throughout this important chapter of my life.

I would like to express my deepest gratitude to my dear friend, Susan Ataei Masjedloo, for her kindness, compassion, and unwavering support during one of the most challenging periods of my PhD journey. Your care, encouragement, and presence when I was dealing with health difficulties meant more to me than words can express. I am truly grateful to have had you by my side during such a difficult time.

Above all, I am profoundly grateful to my parents, especially my father, for their unwavering love, patience, encouragement, and sacrifices throughout my academic journey. Their constant support and belief in me gave me the strength and motivation to persevere through the challenges along the way. This dissertation would not have been possible without their love and support, and I will always be deeply grateful for everything they have done for me.

Dedication

This dissertation is dedicated to my parents, who taught me the value of perseverance, curiosity, and hard work, and whose sacrifices made this dream possible.

To my loved ones, thank you for standing by my side through the challenges and triumphs of this endeavor.

Preface

This dissertation is presented in a manuscript-based format in accordance with the Graduate School guidelines of Kansas State University. It comprises seven chapters designed to provide a cohesive and mechanistic understanding of the interactive impacts of cover cropping and phosphorus (P) fertilization management on soil P pools, molecular speciation, fertility indicators, and iron (Fe) biogeochemistry in a continuous no-till corn-soybean rotation.

Chapter 2 provides a comprehensive literature review, following the general introduction in Chapter 1, contextualizing soil P cycling, operational chemical fractionation methods, and advanced spectroscopic approaches including solution ^{31}P nuclear magnetic resonance (^{31}P-NMR) and synchrotron-based X-ray absorption near-edge structure (XANES) spectroscopy. Chapters 3 through 6 are organized as independent research manuscripts prepared for submission to peer-reviewed scientific journals:

- **Chapter 3** evaluates the redistribution of soil P pools using the Hedley sequential fractionation scheme across eight years of management.
- **Chapter 4** investigates the molecular speciation of organic and inorganic soil P forms using solution ^{31}P-NMR spectroscopy.
- **Chapter 5** examines the vertical stratification of soil fertility indicators (Mehlich-3 P, total carbon, and total nitrogen) and evaluates the annual P budget dynamics.
- **Chapter 6** elucidates the mechanisms regulating P mobility and dissolved reactive P runoff through selective Fe extractions and bulk Fe K-edge XANES spectroscopy.
- **Chapter 7** provides an overarching synthesis and general summary of key findings across all experimental chapters, discusses practical management implications, and identifies future research directions.

The candidate was the primary investigator responsible for experimental implementation, laboratory extractions, spectroscopic data processing, statistical modeling, and the drafting of all manuscripts under the supervisory guidance of Dr. Nathan O. Nelson and the supervisory committee.

Acknowledgment of Artificial Intelligence (AI) Use

ChatGPT (OpenAI) was used as an AI-assisted writing tool during the preparation of this dissertation. Its use was limited to improving the clarity and readability of written text, revising sentences without altering their original meaning or scientific content, checking grammar, assisting with the preparation of descriptive notes and footnotes for tables, and identifying potentially relevant scientific publications for the literature review based on specific research topics and keywords. All AI-generated suggestions and literature recommendations were independently reviewed and verified by the author. The author takes full responsibility for the accuracy, interpretation, and final content of this dissertation.

Chapter 1 - General Introduction

Phosphorus (P) is an essential macronutrient for crop growth and development, playing an indispensable role in sustaining global food production. At the same time, P is a major contributor to environmental degradation when transported from agricultural lands to receiving water bodies, where elevated concentrations stimulate harmful cyanobacterial blooms and impair water quality, posing severe ecological and toxicological risks to both ecosystems and public health (Sharpley et al., 2015). Consequently, understanding the chemical forms, cycling, distribution, and transformations of P in soils is fundamental for maintaining agricultural productivity while safeguarding vulnerable water resources.

Although agricultural soils often contain substantial total P concentrations, only a small fraction is immediately available in the soil solution for plant uptake (Stevenson & Cole, 1999). However, soil P availability is not static. Various biogeochemical processes continuously transform and partition P among different soil pools, potentially mobilizing previously unavailable or recalcitrant forms and increasing their susceptibility to transport through surface runoff and erosion. Excessive anthropogenic inputs of P to agricultural systems can therefore contribute to chronic P buildup and accelerated losses to surface waters, where elevated P concentrations promote algal blooms and accelerate freshwater eutrophication (Qin et al., 2019).

To address these challenges, considerable attention has been directed toward implementing best management practices (BMPs) that simultaneously improve soil conservation, protect water quality, and optimize fertilizer use efficiency. Among these practices, cover cropping has been widely adopted because of its ability to reduce soil erosion during fallow periods. Several field-scale studies have reported substantial reductions in soil erosion following the incorporation of cover crops into cropping systems. For example, Carver et al. (2022)

empirically measured an approximately 70% reduction in sediment-bound soil erosion at the watershed scale, while similar benefits were extensively documented in comprehensive syntheses and literature reviews conducted by Dabney et al. (2001) and Blanco-Canqui et al. (2015).

Despite their well-documented effects on erosion control and particulate P mitigation, the influence of cover crops on dissolved reactive phosphorus (DRP) loss remains highly variable and complex across published studies. While vegetative cover consistently curbs sediment-bound P transport by intercepting raindrops and stabilizing aggregate structure, edge-of-field water quality monitoring has demonstrated that cover cropping can paradoxically increase DRP concentrations and annual loads in surface runoff (Carver et al., 2022). This apparent discrepancy is not an artifact of erratic behavior, but rather the manifestation of distinct biological, physical, and hydrological mechanisms operating across disparate scales (Baker et al., 2017; Cober et al., 2019). First, laboratory evaluations using simulated rainfall on excised cover crop biomass have proven that freezing and desiccating conditions rupture plant cell membranes, causing rapid intracellular P leaching directly from terminated residues without interacting with the soil mineral matrix (Miller et al., 1994). Second, controlled runoff-box and small-plot rainfall simulations have demonstrated that surface-applied residues and manure release significant pulses of soluble molybdate-reactive P during early snowmelt or high-intensity storm events (Bechmann et al., 2005; Kleinman et al., 2005). Third, field trials in no-till terraced systems and cold-climate watersheds reveal that winter cover-crop tissue decomposition and subsequent P release interact strongly with species selection, termination timing, and seasonal freeze-thaw cycles (Cober et al., 2019; Kaur et al., 2024). Furthermore, the physical accumulation and vertical stratification of biomass P at the immediate 0–2.5 cm soil surface under continuous no-

till management substantially increases dissolved P desorption kinetics during runoff events, as documented in regional watershed assessments (Baker et al., 2017; Macrae et al., 2021).

These diverse experimental observations demonstrate that cover-crop impacts on P transport depend fundamentally on the balance between plant P uptake, residue decomposition rates, and field-scale hydrological pathways. For instance, Soltangheisi et al. (2018) observed that some cover crop species, including black oat, fodder radish, white lupine, and common vetch, increased fertilizer P solubility more than ryegrass due to differing root exudation capacities. Similarly, Kleinman et al. (2005) found that cover crops reduced total P and dissolved molybdate-reactive phosphorus (DMRP) losses when established prior to manure application. However, manure additions increased DMRP concentrations in runoff and largely overshadowed the beneficial effects of cover crops.

The complex responses of P to cover cropping highlight the importance of understanding the biogeochemical mechanisms that regulate P availability and mobility in soils. The behavior of P compounds is strongly influenced by their chemical associations with soil constituents, particularly iron (Fe) and aluminum (Al) minerals and organic matter (OM). Changes in Fe speciation can alter the retention and release processes of P compounds, thereby affecting P speciation and bioavailability. Likewise, OM does not exert a simple or erratic effect on soil P; rather, it governs P compound dynamics through dual and competing biogeochemical pathways operating simultaneously (Chen et al., 2018; Gerke, 2010). On one hand, low-molecular-weight organic acids (LMWOAs) such as citrate, malate, and oxalate directly compete with phosphate and other P compounds for sorption sites on variable-charge mineral surfaces and promote the ligand-induced dissolution of poorly crystalline Fe and Al oxides, thereby decreasing phosphate sorption and releasing it into the soil solution (Guppy et al., 2005; Hu et al., 2001; Mikutta et al.,

2006). On the other hand, high-molecular-weight humic substances can enhance phosphate retention by providing alternative organo-mineral binding pathways through the formation of stable Fe- and Al-mediated ternary complexes (phosphate–metal–OM bridges), while simultaneously modifying or inhibiting the crystalline precipitation of secondary P minerals (Chen et al., 2018; Du et al., 2013; Hiradate & Uchida, 2004; Sundman et al., 2016). These competing organo-mineral interactions underscore the need to better understand how management-induced changes in soil chemistry affect P speciation and, ultimately, P loss from agricultural systems.

In addition to cover cropping, fertilizer management represents another important BMP for improving nutrient-use efficiency and minimizing environmental losses. The rate, source, timing, and method of fertilizer application can all influence P availability and transport. Among fertilizer recommendation strategies, the build-and-maintain (BM) and sufficiency (SF) approaches are widely used by soil testing laboratories. The build-and-maintain approach aims to increase soil test phosphorus levels to a critical threshold and subsequently maintain those levels through fertilizer applications based on crop P removal (Macnack et al., 2017). In contrast, the sufficiency approach recommends fertilizer rates designed to achieve approximately 90–95% of maximum crop yield while avoiding excessive P application (Leikam et al., 2003). Consequently, P application rates and cumulative soil P loadings under the build-and-maintain approach are generally greater than those under the sufficiency approach.

Phosphorus fertilizer source can also influence soil P availability and distribution among different soil pools because fertilizer materials differ in their solubility and behavior in soil. However, the effectiveness of a given fertilizer source is often influenced by soil properties and management practices. Soltangheisi et al. (2018) reported that single superphosphate (SSP)

maintained greater P availability than rock phosphate (RP) over six years of cultivation when cover crops were included in the system. In contrast, Pavinato et al. (2017) observed greater plant-available P following RP application than SSP application. These authors further reported that the interaction between cover crops and P source was not significant, suggesting that soil-related factors may have been more important drivers of P availability.

Beyond fertilizer source, P fertilization itself can substantially alter P distribution among soil pools and affect overall P bioavailability. Biassoni et al. (2023) demonstrated that inorganic P pools were particularly sensitive to fertilization practices. Inorganic fertilizer applications increased P concentrations in both labile ($NaHCO_3$-Pi) and moderately labile (NaOH-Pi and HCl-Pi) fractions compared with unfertilized treatments. Such findings indicate that management practices can modify not only the quantity of P present in soils but also its chemical forms and potential availability.

Although numerous studies have evaluated the effects of cover crops, fertilizer sources, and P fertilization on soil P availability and fractionation, integrated assessments of these factors remain limited. In particular, comparisons of the build-and-maintain and sufficiency fertilizer strategies in systems that include cover crops have not been widely investigated. A better understanding of how these common P management approaches influence soil P pools, P speciation, and bioavailability under cover-cropped systems is needed to improve nutrient management while minimizing environmental P losses.

Research Objectives and Structure of the Dissertation

While extensive research has evaluated conservation practices, fertilizer placement methods, and soil P forms independently, comprehensive investigations examining how long-

term cover cropping interacts with contrasting P fertilization philosophies (build-and-maintain versus sufficiency and intentional drawdown) to modify soil P biogeochemistry remain scarce.

Accordingly, the overarching objective of this dissertation is to evaluate the interactive effects of long-term cover cropping and distinct P fertilization strategies on soil P pools, molecular speciation, vertical fertility stratification, and iron (Fe) biogeochemical reactivity in a continuous no-till corn–soybean cropping system. By integrating wet chemical fractionation schemes with advanced spectroscopic techniques, this research aims to provide a mechanistic understanding of soil P retention and transport dynamics that can be broadly applied to conservation agroecosystems. To accomplish this overarching goal, specific objectives correspond to the following sequential chapters:

1. To quantify the redistribution of soil P among operationally defined labile, moderately stable, and highly recalcitrant inorganic and organic pools across multi-year management using sequential chemical fractionation (Chapter 3).
2. To identify, characterize, and quantify the molecular speciation of soil organic and inorganic P forms—specifically resolving orthophosphate monoester stereoisomers and labile diesters—using high-resolution solution ^{31}P-NMR spectroscopy (Chapter 4).
3. To evaluate the vertical stratification of agronomic fertility indicators (Mehlich-3 P, total carbon, and total nitrogen) and establish comprehensive field-scale P mass balances under continuous no-till management (Chapter 5).
4. To determine the biogeochemical mechanisms regulating P mobilization by characterizing soil Fe solid-phase speciation, mineral crystallinity, and coordination environments using selective chemical extractions and bulk Fe K-edge XANES spectroscopy (Chapter 6).

5. To synthesize the collective experimental findings, resolve the mechanistic paradox of P mobilization under cover cropping, and outline practical management implications alongside future research directions (Chapter 7).

Collectively, addressing these objectives and synthesizing their outcomes will elucidate how conservation practices alter organo-mineral associations and internal nutrient cycling, offering crucial foundational insights for designing agronomic management frameworks that sustain high crop productivity while mitigating agricultural dissolved P export to sensitive aquatic ecosystems.

References

Baker, D. B., Johnson, L. T., Confesor, R. B., & Crumrine, J. P. (2017). Vertical stratification of soil phosphorus as a concern for dissolved phosphorus runoff in the Lake Erie Basin. Journal of Environmental Quality, 46(6), 1287–1295. https://doi.org/10.2134/jeq2016.09.0337

Bechmann, M. E., Kleinman, P. J. A., Sharpley, A. N., & Saporito, L. S. (2005). Freeze-thaw effects on phosphorus loss in runoff from manured and catch-cropped soils. Journal of Environmental Quality, 34(6), 2301–2309. https://doi.org/10.2134/jeq2004.0415

Biassoni, M. M., Vivas, H., Gutiérrez-Boem, F. H., & Salvagiotti, F. (2023). Changes in soil phosphorus (P) fractions and P bioavailability after 10 years of continuous P fertilization. Soil and Tillage Research, 232, 105777. https://doi.org/10.1016/j.still.2023.105777

Blanco-Canqui, H., Shaver, T. M., Lindquist, J. L., Shapiro, C. A., Elmore, R. W., Francis, C. A., & Hergert, G. W. (2015). Cover crops and ecosystem services: Insights from studies in temperate soils. Agronomy Journal, 107(6), 2449–2474. https://doi.org/10.2134/agronj15.0086

Carver, R. E., Nelson, N. O., Roozeboom, K. L., Kluitenberg, G. J., Tomlinson, P. J., Kang, Q., & Abel, D. S. (2022). Cover crop and phosphorus fertilizer management impacts on surface water quality from a no-till corn-soybean rotation. Journal of Environmental Management, 301, 113818. https://doi.org/10.1016/j.jenvman.2021.113818

Chen, K.-Y., Hsu, L.-C., Chan, Y.-T., Cho, Y.-L., Tsao, F.-Y., Tzou, Y.-M., Hsieh, Y.-C., & Liu, Y.-T. (2018). Phosphate removal in relation to structural development of humic acid-iron coprecipitates. Scientific Reports, 8, 10363. https://doi.org/10.1038/s41598-018-28568-7

Cober, J. R., Macrae, M. L., & Van Eerd, L. L. (2019). Winter phosphorus release from cover crops and linkages with runoff chemistry. Journal of Environmental Quality, 48(4), 907–914. https://doi.org/10.2134/jeq2018.08.0307

Dabney, S. M., Delgado, J. A., & Reeves, D. W. (2001). Using winter cover crops to improve soil and water quality. Communications in Soil Science and Plant Analysis, 32(7–8), 1221–1250. https://doi.org/10.1081/CSS-100104110

Du, Z. Y., Wang, Q. H., Liu, F. C., Ma, H. L., Ma, B. Y., & Malhi, S. S. (2013). Movement of phosphorus in a calcareous soil as affected by humic acid. Pedosphere, 23(2), 229–235. https://doi.org/10.1016/S1002-0160(13)60011-9

Gerke, J. (2010). Humic (organic matter)-Al(Fe)-phosphate complexes: An underestimated phosphate form in soils and source of plant-available phosphate. Soil Science, 175(9), 417–425. https://doi.org/10.1097/SS.0b013e3181f1b4dd

Guppy, C. N., Menzies, N. W., Moody, P. W., & Blamey, F. P. C. (2005). Competitive sorption reactions between phosphorus and organic matter in soil: A review. Australian Journal of Soil Research, 43(2), 189–202. https://doi.org/10.1071/SR04049

Hiradate, S., & Uchida, N. (2004). Effects of soil organic matter on pH-dependent phosphate sorption by soils. Soil Science and Plant Nutrition, 50(5), 665–675. https://doi.org/10.1080/00380768.2004.10408523

Hu, H. Q., He, J. Z., Li, X. Y., & Liu, F. (2001). Effect of several organic acids on phosphate adsorption by variable charge soils of central China. Environment International, 26(5–6), 353–358. https://doi.org/10.1016/S0160-4120(01)00012-5

Kaur, H., Nelson, K. A., Singh, G., Kaur, G., & Davis, M. P. (2024). Spring applied phosphorus loss with cover crops in no-till terraced field. Journal of Environmental Management, 355, 120431. https://doi.org/10.1016/j.jenvman.2024.120431

Kleinman, P. J. A., Salon, P., Sharpley, A. N., & Saporito, L. S. (2005). Effect of cover crops established at time of corn planting on phosphorus runoff from soils before and after dairy manure application. Journal of Soil and Water Conservation, 60(6), 311–322.

Leikam, D. F., Lamond, R. E., & Mengel, D. B. (2003). Providing flexibility in phosphorus and potassium fertilizer recommendations. Better Crops with Plant Food, 87(3), 6–10.

Macnack, N. E., Chim, B. K., Amedy, B., & Arnall, D. B. (2017). Fertilization based on sufficiency, build-up and maintenance concept (Fact Sheet PSS-2266). Oklahoma Cooperative Extension Service. https://extension.okstate.edu/fact-sheets/fertilization-based-on-sufficiency-build-up-and-maintenance-concept.html

Macrae, M. L., Jarvie, H. P., Brouwer, R., Gunn, G., Reid, K., Joosse, P., King, K. W., Kleinman, P. J. A., Smith, D. R., Williams, M. R., & Zwonitzer, M. (2021). One size does not fit all: Toward regional conservation practice guidance to reduce phosphorus

loss risk in the Lake Erie watershed. Journal of Environmental Quality, 50(3), 529–546. https://doi.org/10.1002/jeq2.20218

Mikutta, C., Lang, F., & Kaupenjohann, M. (2006). Citrate impairs the micropore diffusion of phosphate into pure and C-coated goethite. Geochimica et Cosmochimica Acta, 70(3), 595–607. https://doi.org/10.1016/j.gca.2005.10.032

Miller, M. H., Beauchamp, E. G., & Lauzon, J. D. (1994). Leaching of nitrogen and phosphorus from the biomass of three cover crop species. Journal of Environmental Quality, 23(2), 267–272. https://doi.org/10.2134/jeq1994.00472425002300020007x

Pavinato, P. S., Rodrigues, M., Soltangheisi, A., Sartor, L. R., & Withers, P. J. A. (2017). Effects of cover crops and phosphorus sources on maize yield, phosphorus uptake, and phosphorus use efficiency. Agronomy Journal, 109(3), 1039–1047. https://doi.org/10.2134/agronj2016.06.0323

Qin, B., Paerl, H. W., Brookes, J. D., Liu, J., Jeppesen, E., Zhu, G., Zhang, L., Xu, H., Shi, K., & Deng, J. (2019). Why Lake Taihu continues to be plagued with cyanobacterial blooms through 10 years (2007–2017) efforts. Science Bulletin, 64(6), 354–356. https://doi.org/10.1016/j.scib.2019.02.008

Sharpley, A. N., Bergström, L., Aronsson, H., Bechmann, M., Bolster, C. H., Börling, K., Djodjic, F., Jarvie, H. P., Schoumans, O. F., Stamm, C., Tonderski, K. S., Ulén, B., Uusitalo, R., & Withers, P. J. A. (2015). Future agriculture with minimized phosphorus losses to waters: Research needs and direction. Ambio, 44(Suppl. 2), S163–S179. https://doi.org/10.1007/s13280-014-0612-x

Soltangheisi, A., Rodrigues, M., Coelho, M. J. A., Gasperini, A. M., Sartor, L. R., & Pavinato, P. S. (2018). Changes in soil phosphorus lability promoted by phosphate sources and cover crops. Soil and Tillage Research, 179, 20–28. https://doi.org/10.1016/j.still.2018.01.006

Stevenson, F. J., & Cole, M. A. (1999). Cycles of soils: Carbon, nitrogen, phosphorus, sulfur, micronutrients (2nd ed.). John Wiley & Sons.

Sundman, A., Karlsson, T., Sjöberg, S., & Persson, P. (2016). Impact of iron–organic matter complexes on aqueous phosphate concentrations. Chemical Geology, 426, 109–117. https://doi.org/10.1016/j.chemgeo.2016.02.008

Chapter 2 - Literature Review

Overview of Soil Phosphorus Cycle

Before delineating the three major paired processes controlling reactions of P compounds in the soil at the molecular scale, it is essential to contextualize the pathways through which P enters and exits the soil profile. The primary agronomic output from agricultural soils is crop harvest removal, which permanently exports accumulated P in grain and vegetative biomass from the field. Additional environmental export pathways include surface runoff (transporting both dissolved and sediment-bound particulate P compounds), subsurface lateral flow, tile drainage, and vertical leaching down the soil profile. In agricultural soils, external P inputs replenish these losses through the application of commercial mineral P fertilizers, crop residues, municipal biosolids, and livestock manures. The immediate addition of water-soluble fertilizer P directly supplements the dissolved phosphate concentration in the soil solution, whereas organic amendments (manure and biosolids) deliver a heterogeneous mixture of immediately soluble phosphate and recalcitrant inorganic and organic P compounds that require subsequent biological transformation.

Generally, there are three major paired processes controlling the reactions of P compounds in the soil at the molecular scale: mineralization/immobilization, dissolution/precipitation, and sorption/desorption. All these fundamental processes are chemically and biologically reversible; depending on dynamic environmental conditions, microbial activity, and soil physicochemical properties, they continuously operate in forward and reverse directions to maintain equilibria with the soil solution (Figure 2-1).

Biological Mineralization and Immobilization: Through enzymatic mineralization, organic P compounds are hydrolyzed and converted to phosphate ($H_2PO_4^-$ and HPO_4^{2-}) in the soil solution; conversely, biological immobilization is the conversion of phosphate into cellular organic P structures via two major biological pathways (Condron et al., 2005). First, soil microorganisms assimilate dissolved phosphate from the soil solution and labile solid phases, either converting it into cellular organic P compounds or storing it as intracellular phosphate and complex inorganic P compounds (pyrophosphate and polyphosphates); these P forms are subsequently stabilized or returned to the soil organic matter (OM) pool as microbial cells undergo turnover, senescence, and lysis (Condron et al., 2005; Richardson & Simpson, 2011). Second, growing plants absorb dissolved phosphate from the soil solution via root transporters and either convert it into organic P compounds to synthesize plant tissues or store it as inorganic phosphate and pyro-/polyphosphates. During the subsequent decomposition of senesced root biomass, unharvested stubble, and fallen plant leaves, this stored P is returned to the soil as phosphate, complex inorganic P compounds (pyro- and polyphosphates), and organic P compounds. While the released phosphate enters the soil solution directly, the organic P compounds must be enzymatically mineralized and the complex inorganic P compounds must be hydrolyzed to release bioavailable phosphate.

Mineral Dissolution and Precipitation: Dissolution refers to the thermodynamic process by which primary P minerals (e.g., hydroxyapatite or fluorapatite inherited from parent materials) and secondary P minerals (e.g., strengite, variscite, octacalcium phosphate) dissolve, releasing phosphate into the soil solution. These minerals dissolve to resupply dissolved $H_2PO_4^-$ and HPO_4^{2-} as solution P is depleted by plant uptake or leaching. Precipitation, in contrast, is a three-dimensional nucleation and phase-transformation process, occurring when the

thermodynamic activity products of dissolved phosphate and associated metal cations (Fe^{3+}, Al^{3+}, or Ca^{2+}) exceed the solubility product (K_{sp}) of secondary mineral phases, thereby precipitating solid-phase secondary P minerals out of the soil solution and reducing aqueous P concentrations (Sims & Pierzynski, 2005). Similarly, dissolved organic P compounds—most notably *myo*-inositol hexakisphosphate (*myo*-IHP or phytate)—can react with polyvalent metal cations (Fe^{3+}, Al^{3+}, and Ca^{2+}) to precipitate out of solution as insoluble metal-phytate salts (Celi & Barberis, 2005).

Interfacial Adsorption and Desorption: Adsorption refers to the two-dimensional surface accumulation of dissolved phosphate ions and some organic P compounds onto the reactive surfaces of soil particles, including edge surfaces of phyllosilicate clay minerals, iron and aluminum oxyhydroxides, calcium carbonates, and OM. Depending on the underlying mechanism, adsorption proceeds either as reversible physical sorption via outer-sphere electrostatic interactions and hydration bridges (non-specific adsorption) or as chemical sorption via direct ligand-exchange reactions with surface hydroxyl groups, forming stable monodentate and bidentate inner-sphere surface complexes (specific chemisorption) (Sims & Pierzynski, 2005). Desorption is the direct reverse reaction, releasing adsorbed P compounds from mineral and organic surfaces back into the soil solution, a process that frequently exhibits significant hysteresis due to solid-state diffusion and micropore entrapment (Sims & Pierzynski, 2005).

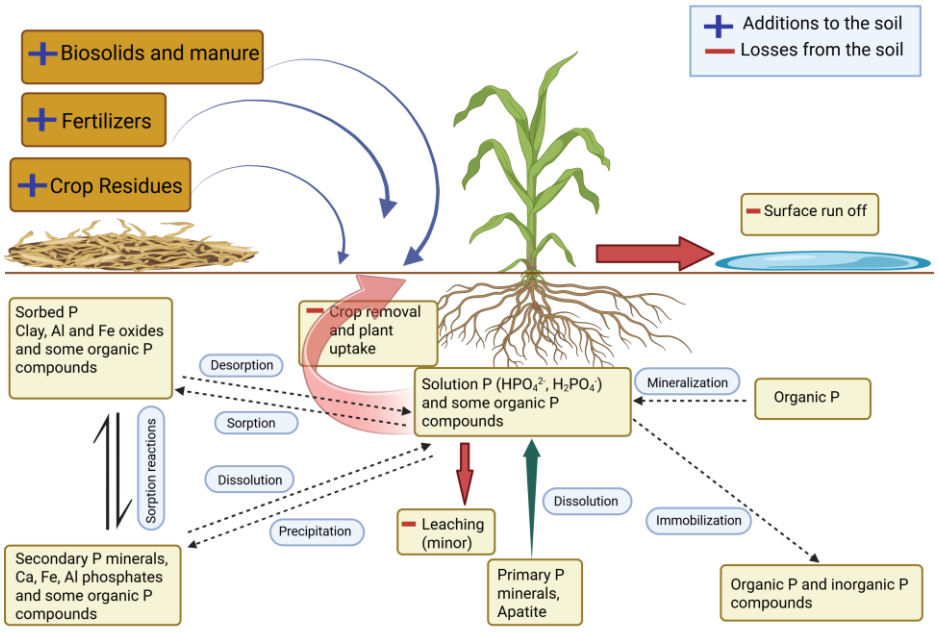


Figure 2-1. Integrated overview of the soil phosphorus cycle illustrating primary input pathways (mineral fertilizers directly feeding the soil solution P pool; organic amendments and plant residues feeding the unified soil organic P pool), central solution-solid equilibria governed by paired transformation mechanisms (mineralization/immobilization, dissolution/precipitation, adsorption/desorption), and export pathways (crop removal and environmental runoff losses).

Phosphorus and Environmental Concerns

While P is an indispensable plant nutrient, excessive P transport from agricultural landscapes into aquatic ecosystems accelerates freshwater eutrophication (Dodds et al., 2009; Sharpley et al., 2003). Eutrophication is fundamentally an ecological degradation process characterized by excessive nutrient enrichment and subsequent biological oxygen (O_2) depletion; however, it is critical to recognize that eutrophication itself does not directly cause severe neurological or hepatotoxic illnesses in exposed human and animal populations. Rather, these adverse health impacts are explicitly driven by potent cyanotoxins (e.g., microcystins, cylindrospermopsin, and anatoxins) produced by proliferating harmful cyanobacterial blooms

(HABs; blue-green algae) that thrive under elevated P loadings (Hudnell, 2010). Degradation of drinking water supplies, closure of recreational surface waters, and ecological hypoxia represent widespread economic and environmental crises linked directly to agricultural P losses.

Agricultural runoff carries P in two distinct physical forms: particulate P (sediment-bound P compounds associated with eroded soil mineral particles and OM) and dissolved reactive P (DRP, consisting primarily of phosphate). Although conservation management practices such as no-till and cover cropping are highly effective at mitigating soil erosion and particulate P export, their impacts on DRP export are often neutral or detrimental (Carver et al., 2022). Dissolved reactive P is 100% bioavailable to downstream algae and can immediately stimulate cyanobacterial growth upon entering receiving water bodies. Therefore, resolving whether agricultural best management practices effectively mitigate total P versus DRP export remains one of the most pressing challenges in contemporary soil and water conservation research.

Major P forms in Soils

Inorganic P compounds

Soil inorganic P (P_i) compounds include dissolved phosphate ions ($H_2PO_4^-$ and HPO_4^{2-} within the pH range of agricultural soils) and polyphosphates (chains of phosphate tetrahedra linked by phosphoanhydride bonds, including pyrophosphates with two phosphate groups). These compounds do not contain carbon (C) groups (Condron et al., 2005).

Inorganic P in the soil solution participates in dynamic equilibria with the solid phase; it can precipitate out as secondary P minerals or can be adsorbed to mineral surfaces, depending on the concentration of P compounds in solution, concentrations of other soluble metal cations in

solution, and the surface charge characteristics and reactive site density of the adsorptive surfaces. Soil pH plays a significant role in determining the speciation of both phosphate in solution and variable-charge mineral surfaces. At pH 7.2, $H_2PO_4^- \approx HPO_4^{2-}$. Below this pH, $H_2PO_4^- > HPO_4^{2-}$, whereas $HPO_4^{2-} > H_2PO_4^-$ above pH 7.2. This speciation strongly dictates the availability of these ions for plant uptake: $H_2PO_4^-$ tends to be more readily absorbed by plant root transporters as it carries a single negative charge, whereas HPO_4^{2-} carries a double negative charge.

Soil minerals, especially hydroxylated surfaces of Fe and Al oxides and oxyhydroxides, possess pH-dependent charge properties, developing positively charged sites under acidic conditions via surface protonation (e.g., $Fe–OH + H^+ \rightarrow Fe–OH_2^+$); therefore, the more negatively charged the ion, the stronger the electrostatic attraction to these sites. To maintain clear geochemical distinctions between dissolved aqueous species and solid-phase minerals, their reactions must be categorized accurately. In acidic soils, dissolved phosphate in the soil solution reacts with soluble aqueous species of Al and Fe (such as Al^{3+}, Fe^{3+}, and their monomeric hydroxy species like $Al(OH)^{2+}$ and $Fe(OH)^{2+}$) to precipitate out as discrete solid-phase Al-phosphate (e.g., variscite) and Fe-phosphate (e.g., strengite) minerals when ion activity products exceed thermodynamic solubility thresholds. Simultaneously, dissolved phosphate can undergo ligand exchange and chemisorb directly onto the reactive surface hydroxyl groups of pre-existing solid-phase Al and Fe oxide minerals (such as gibbsite, goethite, and ferrihydrite).

Conversely, in alkaline and neutral soils, solid-phase calcium carbonate ($CaCO_3$) minerals alongside soluble calcium (Ca^{2+}) and magnesium (Mg^{2+}) cations dictate phosphate partitioning. Dissolved phosphate initially chemisorbs onto the active surface exchange sites of solid $CaCO_3$ minerals; with increasing P activity and the high

availability of soluble Ca^{2+} in the soil solution, it precipitates out as secondary Ca-phosphate mineral phases (transitioning from dicalcium phosphate dihydrate to octacalcium phosphate and eventually stable hydroxyapatite). In soils characterized by elevated soluble Mg^{2+} concentrations, the precipitation of Mg-phosphate phases (such as bobierrite) or the incorporation of Mg^{2+} into Ca-phosphate crystal lattices further modulates secondary mineral solubility and P retention (Havlin et al., 1999).

Organic P compounds

Soil total P concentrations vary between 100 and 3000 mg kg^{-1}. Between 30-60% of soil total P is made of organic P (Condron et al., 2005), although high OM soils can contain up to 90% organic P (Harrison, 1987). Organic P is defined as P bonded in some way with C (Condron et al., 2005).

Various biochemical processes are involved in converting phosphate to organic P compounds through phosphorylation (adding P to C moieties via a covalent bond), and this process is governed by soil microorganisms and plants (Condron et al., 2005). Organic P compound classes include orthophosphate monoesters (one ester linkage of phosphate to C moieties; e.g., sugar phosphates, mononucleotides, and inositol hexakisphosphate (IHP) stereoisomers), orthophosphate diesters (phosphate linked to two C moieties, including deoxyribonucleic acid (DNA), RNA, phospholipids, and lipoteichoic acids), and phosphonates with a direct C–P bond, which include natural compounds such as phosphonoalanine or agricultural chemicals such as the herbicide glyphosate (Condron et al., 2005; Cade-Menun, 2015; Cade-Menun, 2017).

Processes controlling the cycling of P compounds in the soil

Adsorption and Desorption

Phosphate and organic P compounds, such as DNA and inositol phosphates, can adsorb onto reactive soil surfaces (edges of phyllosilicates, carbonates, and metal oxyhydroxides) through specific and non-specific adsorption. If the adsorption occurs via purely physical electrostatic interactions (Van der Waals forces and outer-sphere complexation with retained hydration waters), it is referred to as non-specific adsorption; however, if it occurs through inner-sphere complexation involving direct ligand exchange reactions with surface hydroxyls, it is classified as specific adsorption or chemisorption (Sims & Pierzynski, 2005). Desorption, on the other hand, is the detachment of these adsorbed compounds back into the soil solution, representing the direct reverse of adsorption.

Different factors such as soil pH, phosphate concentration gradient, OM, clay content, soluble metal cations (Al and Fe), and $CaCO_3$ mineral content impact the adsorption/desorption of P (Loganathan et al., 1987). For example, competition for adsorption sites with P compounds and preventing iron oxides from crystallization, ultimately impacting phosphate availability, are direct and indirect effects of OM on phosphate adsorption/desorption, respectively (Loganathan et al., 1987; Zhang et al., 2022).

Dissolution and Precipitation

In general, dissolution is the process determining the solubility of P minerals and precipitated P compounds, and the release of phosphate and other precipitated P compounds into the soil solution (Pierzynski et al., 2005); however, it is important not to overlook the factors influencing this process. Soil pH (the most important factor), availability of other ions such as

soluble metal cations (Fe and Al species), Ca^{2+}, Mg^{2+}, and the concentration of dissolved P compounds determine the solubility and dissolution of P minerals (Rajan et al., 1996). In neutral to alkaline soils, Ca-phosphate minerals such as dicalcium phosphate or octacalcium phosphate, hydroxyapatite, and less soluble fluorapatite are the main forms of precipitated phosphates (Lindsay, 1979). In acidic soils, however, Al phosphates (berlinite, variscite, sterretite, taranakite) and Fe phosphate minerals (strengite, vivianite, tinticite) are the major forms of P minerals (Norrish & Rosser, 1983; Sims & Pierzynski, 2005). In addition to soil pH, the soil weathering stage is also another determining factor in the occurrence of soil P minerals. In moderately weathered soils, apatite minerals, and in highly weathered soils, secondary Fe and Al minerals are the dominant forms of P minerals in the soil (Pierzynski et al., 2005). These minerals replenish solution P compounds through the dissolution process as soluble P compounds are depleted through crop removal, runoff, or leaching. On the other hand, P compounds in solution can also precipitate out as secondary P minerals depending on the availability of the other counter-ions and phosphate itself (added P into the soil as fertilizers or crop residues can enter this precipitation pathway). Furthermore, organic P compounds such as *myo*-IHP (phytate) can also undergo precipitation reactions with soluble Fe^{3+}, Al^{3+}, and Ca^{2+} cations to form poorly soluble metal-phytate precipitates, which strongly governs organic P accumulation and recalcitrance across pH gradients (Yan et al., 2020).

Mineralization and Immobilization

Phosphatase enzymes, which originate from both microbial and plant exudates, are involved in mineralization by releasing phosphate from organic P compounds. This process requires the enzymatic hydrolysis of ester bonds in phosphate compounds (Nannipieri et al., 2011). In addition to hydrolyzing organic phosphoester bonds, extracellular phosphatases and

pyrophosphatases also catalyze the enzymatic hydrolysis of phosphoanhydride bonds in complex inorganic P compounds, such as pyrophosphate and polyphosphates, converting them into bioavailable orthophosphate (Condron et al., 2005; Nannipieri et al., 2011). Immobilization, on the other hand, refers to the biological uptake of dissolved phosphate and its storage or transformation into cellular organic and complex inorganic P compounds through biochemical reactions (Condron et al., 2005). Several factors impact the mineralization/immobilization of P in the soil, including temperature, soil pH, moisture, aeration, soil parent material, C:P ratio, and nitrogen availability (Nannipieri et al., 2011).

Factors impacting the cycling of P compounds

Soil Properties

Several soil properties influence phosphate transformations, among which are soil pH, OM, Al and Fe (hydr)oxides, Mn oxides, and $CaCO_3$, which represent primary master variables affecting its availability as stated by Al-Rohily et al. (2013); however, the influence of other factors such as soil moisture and aeration, temperature, redox condition, microbial activity, and soil mineralogy must also be comprehensively evaluated to understand P partitioning across environmental gradients.

Soil pH

The soil pH range for maximum soil P availability is usually a pH range of 6.5–6.8 (Havlin et al., 1999). Below and above this range, the acidity and alkalinity of soil respectively reduce phosphate availability, each for different reasons. Under acidic conditions, soil phosphate precipitates as Fe/Al-phosphate secondary minerals or adsorbs strongly to the surfaces of Fe/Al oxides and clay minerals. Under alkaline and neutral conditions, however, precipitation of

secondary Ca-phosphate minerals and/or Mg-phosphate (in high-Mg soils), and P compounds adsorbed to the surface of clay minerals and $CaCO_3$ are dominant (Havlin et al., 1999).

Although Fe/Al oxides play a significant role in adsorbing phosphate ions in acidic soils, this does not necessarily translate into not playing a role in calcareous and neutral soils. These oxides continue to contribute to the adsorption of solution phosphate in calcareous soils even though they are present in small quantities (Havlin et al., 1999); however, their ability to retain phosphate increases under acidic conditions as their surface charge is pH dependent and protonation of these surfaces enhances their ability to adsorb and retain phosphate ions (Arai & Sparks, 2007). Although these oxides play a significant role in acidic conditions, their role in phosphate retention and availability becomes complicated when the weathering stage of the soil comes into play. This is mainly due to the higher content of oxides in highly weathered soils and at the same time increased crystallinity (a factor that reduces chemical reactivity) of these oxides (Shi et al., 2011).

Organic matter

Soil OM, a crucial component of soil systems, plays a substantial role in the P cycle. It interacts with metal ions and phosphate ions, forming phosphate–metal–OM complexes. These complexes represent a significant P pool in soil and a more bioavailable source of phosphate compared to other pools of phosphate (bonded to inorganic surfaces or precipitated forms; Gerke, 2010).

The contribution of OM to soil phosphate availability occurs through direct or indirect mechanisms. Organic compounds compete with phosphate ions for adsorption sites on soil mineral surfaces, increasing the concentration of soluble phosphate (Zhang et al., 2022). Stimulating microbial reduction of Fe(III), thereby releasing phosphate from Fe-PO_4 minerals, is

an indirect role of OM to increase the concentration of soluble P, as humic and non-humic fractions provide organic substrates for soil microbes, enhancing their growth and activity (Chacon et al., 2006). In fact, OM provides C and electrons (OM is an electron donor) for microbial communities. Microbial reduction of Fe(III) (Fe(III); electron acceptor) under O_2^- depleted conditions releases Fe from Fe-PO_4 minerals, thereby enhancing soil soluble phosphate concentration (Lindsay, 1991).

In a study conducted by Schreeg et al. (2013), OM increased the bioavailable phosphate concentration while decreasing the immobilized phosphate fraction. Detailed information and mechanisms were not fully resolved in that work due to methodological constraints. However, Sundman et al. (2016) referred to the complexation of Fe(III) with OM, which further decreases the availability of this cation to react with phosphate and precipitate out as Fe-phosphate. As a result, enhanced soluble phosphate concentrations were observed in solution. This effect serves as another indirect biogeochemical pathway of OM in enhancing P concentration in the solution.

Organic acids

Organic acids are made up of C, H, and O. Based on their size, they are categorized into two major groups: high molecular weight organic acids (HMWOAs; ranging in size from a few hundred to millions of Daltons (Da)) and low molecular weight organic acids (LMWOAs; ranging in size from 46 to a few hundred Da) (Adeleke et al., 2017). These compounds (LMWOAs and HMWOAs) differ in structure (one to three carboxylic acid groups and more than three carboxylic groups for LMWOAs and HMWOAs, respectively). Examples of LMWOAs are malic, succinic, acetic, malonic, citric, oxalic, and maleic. Humic and fulvic acids, on the other hand, are examples of HMWOAs (Adeleke et al., 2017).

Various mechanisms are involved in enhancing the availability of soil P compounds through the contribution of LMWOAs. Competing for adsorption sites with phosphate ions, decreasing pH and enhancing the solubility of recalcitrant P compounds, and chelating metal cations to reduce their activity for precipitation with P ions, are major mechanisms driven by organic acids ultimately impacting phosphorus availability (Arcand & Schneider, 2006; Calvaruso et al., 2006; Thammaiah et al., 2023).

Competing for adsorption sites, inhibiting P compounds from sorption, as well as desorbing P compounds from these sites is stimulated in the presence of organic acids (Sims & Pierzynski, 2005); however, desorption of a substantial amount of phosphate ions from adsorption sites is highly dependent on organic acid concentration (citrate above 100 μM can desorb phosphate, while for oxalate, malate, and tartrate the required concentration is more than 1 mM) (Earl et al., 1979; Jones & Darrah, 1994). Whether a given organic acid is more efficient than another depends on its functional group in addition to its concentration. For example, dicarboxylic acids and tricarboxylic acids are more efficient than monocarboxylic acids in ligand exchange and metal chelation. Additionally, organic acids' effectiveness depends on how long they remain in the soil solution because they undergo rapid microbial assimilation and degradation in soils (Adeleke et al., 2017). According to Thammaiah et al. (2023), external application of LMWOAs may not enhance P solubilization, P fertilizer use efficiency, and plant growth mainly due to the rapid microbial degradation of organic acids.

Jalali and Jalali (2022) reported that the addition of poultry manure and sewage sludge, rich in LMWOAs, solubilized phosphate through desorption mechanisms from inorganic surfaces such as calcium carbonate and Fe/Al oxides when added at low concentrations, while at higher concentrations, dissolution of Ca phosphate and release of phosphate ions occurred.

Organic P Desorption and Enzymatic Hydrolysis

Organic P compounds, which constitute a substantial portion of total soil P (typically 30% to 65%), represent a critical reservoir of biological P that requires multi-step mobilization before entering the plant-available pool. Because many organic P compounds, particularly inositol hexakisphosphates (such as phytate) and nucleic acids, possess high negative charge densities, they are strongly chemisorbed onto the edges of clay minerals and the surfaces of amorphous Fe and Al oxyhydroxides. Consequently, these sorbed organic P molecules are sterically protected and must undergo chemical desorption into the soil solution before extracellular phosphatase and phytase enzymes can access and hydrolyze their phosphoester bonds. Giles et al. (2018) experimentally demonstrated that the synergistic co-exudation of carboxylate ligands (citrate) and phytase by plant roots substantially enhanced organic P acquisition in P-deficient soils: citrate displaced sorbed phytate via ligand exchange, rendering the desorbed organic substrate directly accessible to enzymatic cleavage.

Soil Moisture, Aeration, and Redox Dynamics

Soil moisture plays a significant role in phosphate movement, mineralization, and immobilization (Lewis & McGechan, 2002; Shapiro et al., 1960). Mineralization of organic P compounds can proceed across a broad spectrum of moisture regimes (Dalal, 1977); however, the frequency and severity of drying and rewetting (D/W) cycles fundamentally govern the direction and magnitude of biological P transformations (Bünemann et al., 2013; Dinh et al., 2017). Rapid rewetting of dry soil imposes severe osmotic shock on the soil microbial community, inducing cell lysis and releasing labile intracellular inorganic and organic P into the soil solution (Dinh et al., 2017). Concurrently, rapid hydration triggers the slaking and physical disruption of macroaggregates, exposing previously occluded OM and organically bound P to

extracellular enzymes and microbial attack, which accounts for the substantial surge in P mineralization rates observed following rainfall events (Bünemann et al., 2013; Dalal, 1977). In contrast, during extended dry periods, matric potential decreases, pore water connectivity is severed, and solute diffusion rates decline precipitously; this physical isolation constrains extracellular enzyme diffusion and restricts microbial substrate access, causing microbial biomass immobilization and physical sorption to predominate over net mineralization (Devi & Yadava, 2006).

The response of P cycling to moisture shifts is further dictated by soil aeration and O_2 availability. Under waterlogged or poorly drained conditions, excess soil water displaces air from soil pore spaces, rapidly depleting dissolved O and halting aerobic microbial respiration. This O_2 limitation substantially suppresses biological P immobilization by obligate aerobic microorganisms, as demonstrated by the marked decrease in microbial biomass P under prolonged saturation in Mollisols (Wright et al., 2001). Concurrently, facultative and obligate anaerobic microorganisms switch to alternative terminal electron acceptors in a thermodynamically predictable sequence, driving the reductive dissolution of crystalline and amorphous Fe(III) (hydr)oxides (e.g., ferrihydrite and goethite) to soluble Fe^{2+} (Chacon et al., 2006; Lindsay, 1991):

$$\text{Fe(III)–PO}_4\text{ (solid)} + e^- \rightarrow Fe^{2+}\text{ (aqueous)} + PO_4^{3-}\text{ (aqueous)}$$

This reductive dissolution releases large pulses of co-precipitated and surface-sorbed phosphate into the soil solution, drastically increasing soil solution P availability under submerged conditions (such as flooded rice paddy culture) compared to upland soils with adequate internal drainage (Havlin et al., 1999).

However, in upland, well-drained no-till soils managed with conservation practices such as winter cover cropping, the mechanisms regulating Fe and phosphate mobilization operate under entirely different biogeochemical constraints. While prolonged saturation and macroscale anaerobiosis are rare in these well-aerated systems, cover crops substantially enhance the concentrations of LMWOAs, root exudates, and decomposing biomass residues in the near-surface soil layers. In these aerated environments, Fe and associated phosphate mobilization is predominantly governed by ligand-promoted dissolution rather than anaerobic reductive dissolution. Root-derived organic ligands (e.g., citrate, oxalate, and malate) and microbial siderophores complex structural Fe^{3+} at oxyhydroxide surfaces, weakening Fe–O bonds and accelerating the detachment of soluble Fe(III)–organic complexes without requiring a change in the Fe oxidation state (Reichard et al., 2007). Although high-resolution microspectroscopy shows that microscale anaerobic microsites can transiently support localized Fe reduction within dense rhizosphere aggregates (van Veelen et al., 2020), bulk spectroscopic evaluations (bulk Fe K-edge XANES) confirm that the overall Fe pool remains dominantly Fe(III). Thus, as will be demonstrated in Chapter 6, cover-crop-induced shifts toward organically associated Fe and subsequent increases in DRP mobility in no-till agroecosystems are driven primarily by ligand-mediated chelation and surface complexation rather than bulk-scale reductive Fe dissolution.

Temperature Dynamics across Coupled Biogeochemical Processes

Temperature exerts a profound, multifaceted influence on the soil P cycle, regulating both biologically mediated transformations and abiotic chemical equilibria. Rather than merely modifying enzyme kinetics in isolation, temperature shifts simultaneously govern sorption kinetics, mineral dissolution thresholds, and microbial metabolic demands across soil profiles.

Biologically, microbial mineralization of organic P and extracellular phosphatase activity respond dynamically to temperature gradients; however, this response is strongly mediated by substrate availability and ecosystem-specific constraints. While Nadelhoffer et al. (1991) observed that net P mineralization rates decreased with rising temperatures in certain high-latitude soils while increasing in others, Shaw and Cleveland (2020) demonstrated that rising temperatures consistently enhanced microbial and root phosphatase enzyme activities and elevated extractable P concentrations across tropical and temperate biomes, yet showed no direct linear relationship with net mineralized P. This decoupled response reflects the concurrent acceleration of microbial P immobilization, wherein microbial communities rapidly assimilate newly hydrolyzed phosphate to sustain elevated metabolic maintenance requirements under warmer soil conditions (Bergkemper et al., 2016).

Abiotically, temperature fundamentally governs the thermodynamic equilibrium and kinetics of both precipitation/dissolution and adsorption/desorption processes. Mineral solubility products (Ksp) of secondary crystalline Fe, Al, and Ca phosphates are intrinsically temperature-dependent; elevated soil temperatures increase the solubility and dissolution kinetics of meta-stable secondary minerals (such as dicalcium phosphate dihydrate), thereby accelerating the resupply of phosphate to the soil solution (Lindsay, 1979). Concurrently, temperature regulates interfacial sorption reactions. Because phosphate chemisorption via inner-sphere ligand exchange is typically an endothermic process characterized by an activation energy barrier, rising temperatures accelerate ion diffusion across hydrodynamic boundary layers and enhance solid-state intraparticle diffusion into aggregate micropores, increasing the overall P sorption capacity and fixation rate in mineral soils (Arai & Sparks, 2007; Barrow et al., 2021). Conversely, desorption kinetics and the temperature sensitivity of organic-matter-mediated

desorption exhibit pronounced hysteresis, meaning that seasonal temperature fluctuations induce coupled shifts in both biological hydrolysis and abiotic surface equilibria.

Microbial Activity

Microorganisms act on both sides of the P cycle, not only mineralizing organic forms and solubilizing precipitated phosphate and organic P forms but also taking up and immobilizing phosphate (Bergkemper et al., 2016). Some genes such as *pit* and *pstABCS* are involved in P transportation and some others such as *phoB*, *phoR*, and *phoU* are involved in P regulations and can result in enhanced microbial phosphate immobilization, thereby assimilating bioavailable P and reducing soil plant-available phosphate (Richardson & Simpson, 2011). Conditions such as P deficiency in soils can stimulate microbial P solubilization and mineralization, enhancing crop P uptake (Bergkemper et al., 2016; Liang et al., 2020). Some enzymes involved in the solubilization of less available mineral phosphates, Ca-phosphates, and rock phosphates can be encoded through the *gcd* gene, indicating microbial phosphate solubilization capacity (Wu et al., 2022).

Extracellular enzymes released by microbes and roots can catalyze the hydrolysis of organic P compounds. Tarafdar and Jungk (1987) found that there was a significant correlation between depletion of organic P and phosphatase activity in the rhizosphere soil of wheat and clover. Microorganisms secrete both acid and alkaline phosphatases, mineralizing organic P and thus enhancing plant P uptake. Plant roots, on the other hand, only release acid phosphatase (Spohn & Kuzyakov, 2013). Plant roots can either directly or indirectly affect the P cycle. pH regulation and phosphatase enzyme release are direct effects of plants on P mineralization. The indirect effect, however, refers to stimulated microbial growth and activity due to the C sources

provided by plant roots, leading to enhanced microbial phosphate mineralization and immobilization in the rhizosphere.

Soil Mineralogy

Soil mineralogy plays a significant role in the P biogeochemical cycle and availability of phosphate. Clay minerals as active components of the soil systems with high surface area and a significant cation exchange capacity (CEC) substantially contribute to nutrient availability through adsorption and desorption (Sparks et al., 2022). Generally, soils containing greater amounts of clay minerals tend to have less available phosphate due to their higher reactive surface area and greater adsorption of P compounds compared to soils with small quantities of clay minerals (Havlin et al., 1999). In a study conducted by Hadgu et al. (2014), five different types of soils (Fluvisols, Cambisols, Vertisols, Arenosols, and Nitosols) with different properties including clay content were examined to understand the relationship between clay content and phosphate adsorption capacity. They reported that soils with higher clay content (Vertisols with 46% and Nitosols with 42% clay content) resulted in greater phosphate adsorption compared to soils with lower clay content (Fluvisols with 10%, Cambisols with 14%, and Arenosols with 20% clay content).

Additionally, clay types, as well as their interfacial properties resulting from surface reactivity and acid-base chemistry (amphoteric properties of clay minerals), have a significant impact on phosphate availability and its adsorption to clay mineral surfaces or desorption from them (Adams & McCabe, 2006). In other words, the extent to which clay plays a significant role in adsorbing nutrients depends largely on the structure of its layers. There are two major types of structural layers, including 1:1 (one tetrahedral sheet, Si–O, and one octahedral sheet, Al–O) and 2:1 (one octahedral sheet, Al–O octahedrons, sandwiched by two tetrahedral sheets) (Tournassat

et al., 2015). Kaolinite and montmorillonite are examples of layered silicates with 1:1 and 2:1 layer structures, respectively. Kaolinite clays possess greater amounts of associated hydrated iron and aluminum oxides, leading to a significant amount of P fixation. The hydroxyl groups associated with Al and Fe present in the structure and edge faces of kaolinite can exchange with P. Furthermore, pH-dependent charges on its edges can enter adsorption reactions with P (Havlin et al., 1999; Tournassat et al., 2015). In addition to the quantity of Fe/Al oxides, the degree of crystallization of these oxides highly impacts P availability. Soils with more amorphous Fe/Al oxides (reactive Fe/Al oxides) will result in lower available P because of their greater surface area and high density of reactive hydroxyl coordination sites (Havlin et al., 1999).

Management Practices

Cover Crops

Cover crops do not directly contribute to a large net external addition of P into the soil; instead, they impact nutrient cycling and availability, including P for subsequent crops, through various biological and physical mechanisms (Varela et al., 2017). Increased soil biological activity and enhanced phosphate uptake even in soils with higher sorption capacity for P compounds, thereby improving P use efficiency, are only some benefits of cover crops on P cycling (Kuo et al., 2005).

In response to low soil solution concentrations of bioavailable P, plant roots and rhizosphere microorganisms upregulate the synthesis and exudation of extracellular phosphatase and phytase enzymes, which subsequently hydrolyze ester bonds to cleave phosphate from organic P compounds (Pang et al., 2024). However, some organic P compounds need to be desorbed from mineral surfaces before enzymatic mineralization can occur (Giles et al., 2018).

Inclusion of cover crops has increased microbial activity and phosphatase enzyme production, especially when plant-available P is deficient (Hallama et al., 2019).

Depending on the cover crop species and edaphic properties of the studied soils, the effect of cover crops on soil P pools and availability varies. For example, in a study conducted by Pavinato et al. (2008), radish was the most efficient crop for increasing soil P availability in comparison to other tested cover crops. This cover crop, with greater root excretion of malic acid and higher P content in its tissue, was able to increase P availability in the soil.

Cover crop residue containing both organic and inorganic P compounds impacts soil P pools after being decomposed and releasing P into the soil (Noack et al., 2012). Some studies reported an increase in organic P pools when implementing cover crops (Maltais-Landry et al., 2015); however, other studies did not detect a significant change in soil organic P (Kuo et al., 2005). This could be due to differences in soil type, cover crop species, climatic conditions, management practices, and the duration of the study.

Furthermore, cover crops can influence the transformation of specific soil inorganic P fractions. Gamage et al. (2025) reported that Fe-associated phosphate in soil and sediments for cover crop treatments decreased, suggesting that Fe-associated phosphate was more vulnerable to transformation due to the presence of the cover crop. They further reported that exchangeable phosphate increased in both sediment and soil samples for cover crop treatments. Additionally, the mechanisms implemented by cover crops to enhance nutrient availability vary between cover crops. For example, gramineous cover crops mostly scavenge nutrients from deeper layers of the soil through their dense and fibrous root systems (Clark, 2008). Legume cover crops, on the other hand, can release organic exudates that desorb and/or solubilize P compounds, ultimately enhancing P availability (Nuruzzaman et al., 2005).

Tillage

Although the no-till system benefits the soil in various aspects, it is still associated with several significant challenges, making it not applicable in all places. Reduced soil erosion is one of the great advantages of no-till systems. In these systems, the concentration of soil organic C particularly at the surface of the soil profile increases, which leads to greater soil structural stability, ultimately reducing soil erosion in addition to fostering greater nutrient storage, in particular at the surface (Aguilera et al., 2013; Conceição et al., 2013). However, vertical stratification of immobile nutrients, especially phosphate and potassium, causes various challenges for crops regarding nutrient uptake, root distribution, growth, and development (Ma et al., 2007).

Additionally, the buildup of P on the soil surface in these systems because of stratification leads to increased dissolved P loss through runoff (Sharpley & Smith, 1994), even though several studies have reported reduced particulate P loss under conservation tillage due to enhanced aggregate stability (Daryanto et al., 2017). A greater amount of organic residues deposited on the soil surface in no-till systems results in higher concentrations of total P and organic C accumulated on the soil surface. Higher concentrations of organic anions derived from decomposing residues and root exudates on the soil surface compete directly with P compounds for adsorption sites (Fink et al., 2016), leading to increased phosphate desorption from the surface soil into moving surface runoff.

P Fertilization

Fertilization with products derived from non-renewable phosphate rock sources is a common way to cope with P deficiency in agricultural systems (Cordell et al., 2009); however, only 10% to 20% of applied fertilizer is typically taken up by crops during the growing season of

application, and the remaining unrecovered fraction (approximately 80%) accumulates in the soil profile as diverse inorganic and organic P compounds that can subsequently become available through biogeochemical transformations and utilized by subsequent crops (Black, 2013). In other words, when cumulative external P inputs (from commercial fertilizers, manures, or biosolids) consistently exceed total crop P harvest removal, a positive net P balance (surplus P) is established, driving the progressive accumulation of residual or "legacy P" within the soil matrix; however, its subsequent availability to future crops will significantly depend on other soil physicochemical factors such as soil pH, mineralogy, texture, and biological activity (Rowe et al., 2016).

Seemingly, P fertilization does not impact all pools of P equally as it has been reported that some pools of P are more sensitive to fertilization in terms of change in the concentration. Biassoni et al. (2023) reported that inorganic fractions of both labile ($NaHCO_3$-Pi) and moderately labile (NaOH-Pi and HCl 1 M-Pi) have been increased in P fertilized treatments compared to controls after 10 years of continuous P fertilization and this increase was greater for labile pools compared to other pools. Additionally, moderately labile P has the highest concentration in fertilized treatments compared to non-fertilized treatments. They further stated that these fractions could be responsible for legacy-P after 10 years of continuous P fertilization.

Additionally, P fertilization may not equally impact P pools in all depths of the soil. Teles et al. (2017) reported that near-surface soils showed greater accumulation of labile and nonlabile P pools when treated with P fertilizer, but only the recalcitrant organic P pool was affected in deeper layers of clayey soils of Brazil rich in Fe/Al oxides.

Phosphate fertilizers from different sources could also have a significant impact on the distribution of soil P pools. In a study conducted by Soltangheisi et al. (2018), single

superphosphate (SSP) resulted in a higher proportion of labile P pools compared to rock phosphate (RP) mainly due to the greater solubility of SSP compared to RP, which only presents 1/3 soluble phosphate.

Methods of P fertilization

The method of P fertilizer application is one of the most crucial and determining factors regarding the efficiency of P fertilizers. Some of the methods such as band application could result in higher efficiency and crop yield as they reduce the contact area of phosphate with the soil and chemical compounds in soil such as Al and Fe oxides and Ca (Grant et al., 2001); however, it should be mentioned that this is not always the case and depending on other factors such as STP, band application may not always result in higher yield (Edwards, 2017).

There are different methods of band application including surface band, deep band, sideband, mid-row band, single band and double band (Shahena et al., 2021); yet, fall broadcast applications of P fertilizers is preferred by farmers because of its effectiveness in terms of economics, labor and timing. Additionally, fall broadcasting is simpler and quicker (Carver et al., 2022), and it also does not interfere with other field operations (Mallarino et al., 2009); however, subsurface placement of fertilizer has been reported to reduce both total and dissolved P loss in different management systems by 30 and 75% respectively compared to broadcasting (Baker & Laflen, 1982; Mostaghimi et al., 1988; Zeimen et al., 2006; Yuan et al., 2018; Wiens et al., 2019).

Methods to identify and quantify P forms and pools in soils

This section reviews the commonly used techniques for identifying and quantifying different P forms and pools in soils.

Extractions

Soil P is often quantified or estimated using chemical extraction methods. These extractions target different P pools based on their solubility in the soil matrix.

Agronomic Soil Test P

There are four primary soil test P extractants standardized and widely utilized across the United States and Canada: Bray and Kurtz P-1, Mehlich-1, Mehlich-3, and Olsen P. The primary objective of agronomic soil testing is to provide a relative chemical index of soil P supply calibrated against field crop response probabilities, establishing critical threshold values to predict crop yield response to added P fertilizer and guide economically and environmentally sound fertilizer recommendations.

- The Bray and Kurtz P-1 method (Bray & Kurtz, 1945; Frank et al., 1998) is widely used in acidic to neutral soils of the Midwestern and North Central United States. The extractant incorporates ammonium fluoride (NH_4F) in a dilute hydrochloric acid (HCl) matrix (pH 2.6). Fluoride forms stable complexes with aluminum (Al-F), thereby decreasing Al^{3+} activity in solution and facilitating the release of phosphate from secondary Al-phosphate minerals. Concurrently, the dilute acid dissolves basic Ca- and Fe-phosphates, while fluoride ions suppress the rapid resorption of solubilized phosphate onto exposed mineral surfaces.
- The Mehlich-1 extractant (0.05 M HCl + 0.0125 M H_2SO_4), commonly termed the double-acid method, serves as a multi-element extractant (P, K, Ca, Mg, Cu, Fe, Mn, Zn) for highly weathered, coarse-textured, acidic soils (pH < 6.5) of the Southeastern and Mid-Atlantic regions. In calcareous or neutral soils, the limited buffering capacity of this dilute acid extractant is neutralized by soil carbonates, rendering it ineffective.

- The Mehlich-3 extractant (Mehlich, 1984) is an advanced, multi-element extractant formulated with acetic acid (CH_3COOH), ammonium nitrate (NH_4NO_3), ammonium fluoride (NH_4F), nitric acid (HNO_3), and ethylenediaminetetraacetic acid (EDTA) buffered at pH 2.5. It is applicable across a broad spectrum of soil types ranging from strongly acidic to calcareous. Mehlich-3 exhibits superior extraction efficacy over Mehlich-1 because its enhanced buffering capacity resists rapid neutralization by free carbonates, while EDTA chelates micronutrients and suppresses secondary precipitation.
- The Olsen P method (0.5 M $NaHCO_3$ buffered at pH 8.5) was specifically engineered for neutral, calcareous, and alkaline soils (Olsen et al., 1954). The bicarbonate anion decreases soluble Ca^{2+} activity in the soil solution by precipitating calcium as calcium carbonate ($CaCO_3$), which in turn enhances the solubility and dissolution of secondary calcium phosphate minerals according to the common-ion effect.

Oxalate Extractable P

Acid ammonium oxalate extraction (pH 3.0, conducted in the dark) provides a selective quantitative estimate of P associated with amorphous, poorly crystalline Fe and Al oxyhydroxides (e.g., ferrihydrite). Because poorly crystalline minerals possess immense reactive surface areas, oxalate-extractable P (P_{ox}) alongside oxalate-extractable Fe and Al (Fe_{ox} and Al_{ox}) is routinely used to calculate the Soil Degree of Phosphorus Saturation (DPS = $[P_{ox} / (Fe_{ox} + Al_{ox})] \times 100$), which serves as an environmental indicator of potential P desorption into surface runoff and leachate.

Water and Dilute Salt Extractable P

Agronomic chemical extractants are either markedly more acidic or more alkaline than the ambient soil solution, which can induce dissolution of non-labile solid-phase minerals that

are not immediately accessible to plant roots or runoff waters. Extracting soil with deionized water or dilute unbuffered salts (e.g., 0.01 M $CaCl_2$) circumvents this limitation by closely mirroring the ionic strength and ambient pH of the native soil solution (Pote et al., 1996). Water-extractable P represents the most readily desorbable, immediately mobile fraction, and dissolved reactive P concentrations in surface runoff and subsurface tile drain waters correlate strongly with water-extractable soil P across diverse cropping systems (Pote et al., 1996; Sharpley, 1995).

Total Soil P Determination: High-Temperature Ignition versus Strong Acid Digestion

Quantifying total soil P is fundamental for establishing field-scale nutrient mass balances, evaluating long-term legacy P accumulation, and determining the overall recovery efficiency of sequential chemical fractionation schemes. Two principal analytical methodologies are widely employed to quantify total soil P: the high-temperature ignition method and wet chemical strong-acid digestion methods (Olsen & Sommers, 1982).

The high-temperature ignition method (Saunders & Williams, 1955; Walker & Adams, 1958) is a classical, widely utilized approach for estimating total organic P (P_o) by difference across large sample sets, rather than true total soil P. In this procedure, soil aliquots are incinerated in a muffle furnace at 550°C for 1 to 2 hours to thermally oxidize organic carbon and convert all organic P moieties into inorganic phosphate. The ignited sample is subsequently extracted with dilute sulfuric acid (0.5 M or 1.0 M H_2SO_4), alongside an identical unignited sample extracted with the same acid matrix. Total organic P is calculated as the mathematical difference between the ignited and unignited extracts (Olsen & Sommers, 1982). Although the ignition method is operationally straightforward, rapid, and eliminates hazardous wet acid handling, it is subject to analytical artifacts: high-temperature heating can enhance the acid

solubility of certain crystalline inorganic Fe and Al minerals, occasionally leading to the overestimation of total organic P in mineral soils high in sesquioxides (Condron et al., 1990; Turner et al., 2006). Crucially, because thermal oxidation completely destroys organic molecular structures, ignition cannot be utilized if individual organic P species (e.g., inositol phosphates, phospholipids) are to be characterized.

For total P concentrations, wet chemical acid digestion methods utilize concentrated strong acid mixtures under elevated temperatures to achieve complete oxidative dissolution of both organic and inorganic soil P matrices. While alkaline fusion (using sodium carbonate or lithium metaborate) followed by acid dissolution represents the definitive reference standard for true total soil P recovery across all mineral matrices, wet chemical digestion with concentrated perchloric acid ($HClO_4$) following preliminary nitric acid (HNO_3) treatment has historically served as a benchmark digestion procedure (Olsen & Sommers, 1982; Sommers & Nelson, 1972). Perchloric acid acts as a powerful dehydrating and oxidizing agent at boiling temperatures, completely destroying recalcitrant OM and dissolving primary and secondary mineral lattices (with the exception of resistant silicate minerals, which require hydrofluoric acid, HF). However, perchloric acid digestion has been banned in many locations due to associated hazards.

In modern environmental and agronomic testing laboratories, rapid multi-acid block digestion—specifically utilizing concentrated sulfuric acid (H_2SO_4) combined with salicylic acid, hydrogen peroxide (H_2O_2), and a selenium or copper catalyst—is extensively utilized for the simultaneous determination of total nitrogen and total P in soil and plant tissue digests (Thomas et al., 1967). Comparative methodological evaluations consistently demonstrate that while both perchloric acid digestion and sulfuric-salicylic-peroxide digestion yield comparable and precise

recoveries of total soil P across agricultural soils, wet acid digestion methods provide superior reproducibility over the high-temperature ignition method, particularly in soils characterized by low organic carbon contents or high sesquioxide mineralogies (Kuo, 1996; Olsen & Sommers, 1982). Following digestion, the solubilized phosphate concentration in the clear digestate is quantified spectrophotometrically via the ascorbic acid-molybdate blue colorimetric procedure (Murphy & Riley, 1962) or determined directly via Inductively Coupled Plasma Optical Emission Spectrometry (ICP-OES).

Sequential P fractionation

For more than five decades, sequential fractionation schemes have served as an important tool to study P dynamics in soils and sediments (Condron & Newman, 2011). These methods utilize a series of selective acid and base reagents to sequentially extract P from loosely bound P to occluded P, which is a common feature of all fractionation methods (Pierzynski et al., 2005).

Different fractionation methods

Chang and Jackson (1957) developed a fractionation scheme for the first time. Hedley et al. (1982) and its modified version by Tiessen and Moir (1993) were the most common methods used until today (Cross & Schlesinger, 1995; Negassa & Leinweber, 2009; Tamburini et al., 2014). Methods introduced by Chang and Jackson (1957) and Zhang and Kovar (2009) assumed that Al-P could be separated from Fe-P using NH_4F extractant; however, Hedley et al. (1982) and its modified version (Tiessen & Moir, 1993) did not attempt to separate these forms of P using NH_4F as they stated that using NH_4F is unreliable due to ligand-exchange artifacts and the precipitation of insoluble fluorite (CaF_2) in calcareous systems (Bromfield, 1967; Williams & Walker, 1969). Accordingly, using NaOH solution in these methods provides an operational

estimate for the sum of (Al+Fe)-P (Condron & Newman, 2011; Hedley et al., 1982; Hieltjes & Lijklema, 1980).

Common sources of errors in fractionation schemes

The extracts from sequential extractions are analyzed colorimetrically (Murphy & Riley, 1962) for total P after digestion and molybdate-reactive-P (MRP) concentrations before digestion. The MRP and the molybdate-unreactive P (MUP; the subtraction of MRP from total P) are considered as inorganic-P and organic-P, respectively (Chen et al., 2021); however, errors may arise as not all forms of inorganic-P, including pyrophosphate and polyphosphate, can react directly with molybdate during the analysis of extracts (Condron & Newman, 2011), meaning that MUP values can include both organic-P and inorganic-P forms, potentially leading to an underestimation of inorganic P and an overestimation of organic P. However, an underestimation of organic P can also occur due to the acid hydrolysis of labile organic P during the inorganic P analysis after adding a color-forming acid–molybdate reagent (Condron & Newman, 2011).

Before adding the acid–molybdate reagent, it has been recommended to reduce the pH of the alkaline (NaOH and $NaHCO_3$) soil extracts to 1.5 to precipitate out humic acids, which are further removed through centrifugation, as unprecipitated organic macromolecules induce severe spectral interference with MRP analysis (Tiessen & Moir, 2008); however, this approach can also cause systematic errors in inorganic-P measurement, as acidifying the extract to pH 1.5 induces the co-precipitation of inorganic P onto aggregating humic macromolecules (Turner et al., 2006), ultimately distorting organic P estimation. Complexation and/or occlusion of inorganic P and incomplete extraction (Condron & Newman, 2011) are additional confounding factors, making the fractionation scheme hard to rely on as the only method of studying P dynamics.

Fundamentally, sequential fractionation schemes are operationally-defined procedures rather than definitive chemical or mineralogical characterizations. The core limitation of these operational definitions is their complete lack of species-specific resolution: chemical reagents extract P pools based strictly on empirical solubility thresholds in arbitrary acid or alkaline solutions rather than selective affinity for discrete chemical compounds or mineral phases (Barrow et al., 2021; Gu & Margenot, 2021). For example, the 0.1 M NaOH extraction is broadly defined as "Fe- and Al-associated P," yet it indiscriminately dissolves poorly crystalline Fe oxides, crystalline Fe oxyhydroxides, amorphous Al minerals, and a heterogeneous mixture of chemically diverse organic P compounds without distinguishing among them. Furthermore, sequential extractions cannot prevent readsorption artifacts, wherein P solubilized from one mineral phase readsorbs onto exposed surfaces of another mineral during extraction shaking, falsely shifting P into subsequent recalcitrant pools (Condron & Newman, 2011). Because these fractions represent continuum pools defined solely by the method of extraction rather than unique thermodynamic compounds (McLaughlin et al., 2011), relying solely on this method can lead to substantial discrepancies in interpreting soil P availability and its different forms (Liu et al., 2020). The combination of advanced analytical methods such as phosphorus K-edge X-ray absorption near-edge structure (P-XANES) and ^{31}P-NMR spectroscopy with wet chemical extraction methods has been proposed to interpret P speciation comprehensively (Helfenstein et al., 2018; Koch et al., 2018; Liu et al., 2013).

Advanced methods

Phosphorus K-edge X-ray Absorption Near-Edge Structure (P-XANES) Spectroscopy

P-XANES spectroscopy is a nondestructive chemical speciation technique used to study the solid-phase chemical forms and coordination environments of P in soils and environmental

matrices (Brown & Sturchio, 2002). This method is a powerful technique for soil investigations because it directly probes P speciation in intact or minimally prepared solid samples without requiring chemical extraction.

Fundamentally, X-ray absorption spectroscopy provides direct insights into the electronic state and local coordination environment of the target element. When an incident X-ray beam is directed at a sample and the photon energy equals or exceeds the binding energy of a core electron (such as the 1s shell electron at the P K-edge, approximately 2145 eV), that core electron is ejected into unbound or unoccupied continuum states; this threshold energy corresponds to the absorption edge of the element (Kizewski et al., 2011). Because core electron binding energies are unique to each atomic number, the absorption edge position and near-edge spectral features directly reflect the identity, formal oxidation state, and local geometry of the absorbing atom. For instance, in elements with multiple accessible oxidation states such as Fe (Fe^{2+} versus Fe^{3+}), the absorption edge shifts toward higher energies with increasing positive valence because the lower electron density around the nucleus increases the effective nuclear charge experienced by remaining core electrons.

Limitations and challenges in P-XANES

Although this method provides species-specific information about inorganic-P forms with unique spectral features, it fails to discriminate more than four to five chemical species in most soils because of the inherent similarity and broad nature of P K-edge resonance features, as well as limitations in spectral sensitivity (Kizewski et al., 2011; Prietzel et al., 2013). In addition, the linear combination fitting (LCF) model standards used in this technique may not be a true representation of actual, poorly crystalline, and heterogeneous soil species (Khare et al., 2004; Khare et al., 2005).

Some of the challenges in studying P speciation using advanced methods such as P-XANES arise from the nature of the soil matrix itself rather than analytical flaws in the technique. The highly heterogeneous chemical bonding environments of P in soils and its relatively low concentrations create uncertainty when deconvoluting multi-component spectra into distinct mineral phases; however, attempts have been made to overcome these limitations using spatially resolved spectroscopies, e.g., micro X-ray fluorescence (μ-XRF; providing elemental distribution maps of P in diverse matrices) and microscopically focused XANES (μ-XANES; studying P coordination at specific micron-scale regions of interest). Costs, beamline availability, and competitive access to national synchrotron light source facilities represent additional practical constraints that must be accounted for.

P-XANES and its application in P fertilizer management

Analysis by P-XANES has revealed detailed information about P speciation as impacted by P fertilizer management practices. For example, the application of NPK fertilizer along with sheep manure has shown a significant increase in available Mg content (Liu et al., 2020), leading to an increase in the formation of dimagnesium phosphate trihydrate ($MgHPO_4$) and a substantial decrease in the formation of insoluble Ca-phosphates, which resulted in greater P availability.

In a study by Liu et al. (2018), the use of P-XANES to study soils in pastures, croplands, and roadside ditches adjacent to their fields, along with lab experiments, revealed a close association between soil properties obtained from lab experiments and information obtained from advanced methods. They reported a higher proportion of tricalcium phosphate (TCP) based on XANES results in soils with neutral pH (~7.1) and greater ammonium acetate-extractable (NH_4OAc-extractable) Ca.

Liu et al. (2017) in another study utilized advanced methods (P-XANES and ^{31}P-NMR) to investigate the effect of P fertilization on soil legacy P transformation. According to them, long-term P fertilization (27 years) resulted in hydroxyapatite (HAP) depletion and an increase in $FePO_4$-like species in these soils, possibly due to the release of labile phosphate from HAP and subsequent strong chemisorption onto Fe (hydr)oxides due to the exceptionally high affinity of phosphate for these oxide surfaces. Information about soil legacy P and its contribution to crop P uptake could explain why lower soil test P does not always align with a reduction in crop yield, as traditional soil test P methods neglect the contribution of slowly releasing legacy P reserves to crop nutrition (Blake et al., 2003; Liu et al., 2015; Selles et al., 2011; Shen et al., 2011).

This technique is effective and successful for studying inorganic P (Pi) species (Ca-associated phosphates such as hydroxyapatite and octacalcium phosphate; Fe-associated phosphates such as strengite; and Al-associated phosphates such as variscite) (Kizewski et al., 2011; Liu et al., 2015; Prietzel et al., 2013); however, it has severe limitations in resolving individual organic P species because the energy differences among diverse ester bonds (monoesters, diesters, phosphonates) are too small to produce distinct, resolvable K-edge post-edge features. Therefore, strategically combining P-XANES with solution ^{31}P-NMR spectroscopy enables a complete, complementary characterization of both inorganic and organic soil P speciation across agroecosystems.

Introduction to ^{31}P-NMR

Phosphorus-31 nuclear magnetic resonance spectroscopy (^{31}P-NMR) is a powerful and definitive analytical technique to identify and quantify specific P compounds at the molecular level. These include inorganic P compounds (orthophosphate, polyphosphates, and pyrophosphate) and organic P compounds that can be grouped into the compound classes

orthophosphate monoesters, orthophosphate diesters, and phosphonates based on the chemical environment of various P nuclei (Cade-Menun, 2015; Cade-Menun, 2017). The term orthophosphate is specifically used here because the high pH of P-NMR analysis fully deprotonates phosphates.

Principles of ^{31}P-NMR

NMR spectroscopy is the study of molecules by recording the interaction of radiofrequency electromagnetic radiation with the nuclei of the molecules placed in a strong magnetic field. Radiofrequency radiation causes nuclei in the sample to transition between different energy states when exposed to it. A spectrometer measures the nuclei's energy as they move between states and generates a spectrum based on the energy absorbed or emitted.

According to NMR principles, many nuclei possess spin and an associated magnetic moment. When an external magnetic field (B_0) is applied, the magnetic moments of spin-active nuclei align either parallel (lower energy state) or antiparallel (higher energy state) to the magnetic field. Energy is transferred from the base energy state to the higher energy level when radiofrequency pulses match the Larmor precession frequency of the targeted nuclei. By detecting the electromagnetic signals emitted as the nuclei relax back to the ground state (free induction decay), the NMR spectrum can be processed via Fourier transformation. Because the local electronic cloud shields the nucleus, different chemical environments induce specific resonant chemical shifts, allowing NMR to distinguish among discrete molecular species. The isotopic specificity of NMR allows it to detect only one active isotope at a time (such as ^{1}H, ^{13}C, and ^{31}P).

Accurate ^{31}P-NMR Data Acquisition: Critical Factors

Cade-Menun and Liu (2014), in a comprehensive review, provided a thorough discussion of the critical factors that must be considered to obtain accurate ^{31}P-NMR data. These critical factors include the type of extractant, pre- and post-extraction treatments, extraction duration, the physical state of soil samples, the soil-to-extractant ratio, and the procedures used to concentrate extracts prior to spectroscopic analysis.

Advantages

Due to its high gyromagnetic ratio and complete natural abundance, ^{31}P is readily detectable using NMR spectroscopy, making it particularly useful for analyzing organic P in soils (Wilson, 1987; Condron et al., 1997). One major benefit is that it allows for the simultaneous identification of all P species in a sample without requiring elaborate purification or separation steps. In addition, solution ^{31}P-NMR analysis requires a relatively small mass of bulk soil (typically 3 to 5 g), which is chemically extracted with NaOH–EDTA and freeze-dried prior to spectral acquisition (Cade-Menun & Liu, 2014).

Limitations and challenges

A critical analytical threshold for reliable spectral signal detection is an extracted solution P concentration of approximately 1.0×10^3 mg kg^{-1} (1 mg g^{-1}), whereas natural total and extractable P concentrations in many soils fall below this threshold. Furthermore, elevated concentrations of paramagnetic cations (particularly Fe^{3+} and Mn^{2+}) accelerate transverse relaxation, causing severe spectral line broadening and drastically decreasing the signal-to-noise ratio. To mitigate this, chemical extractants incorporate EDTA to chelate paramagnetic metals, and alkaline soil extracts must be concentrated via freeze-drying prior to analysis, introducing additional sample preparation steps.

During spectral acquisition, the sample probe temperature must be regulated below 20°C to 25°C to reduce the enzymatic or alkaline hydrolysis of labile diesters (e.g., RNA and phospholipids) into monoester degradation products. For quantitative reproducibility, relaxation recycle delays (T_1) must be sufficiently long to permit complete magnetization recovery between pulses; underestimating relaxation delays can lead to the severe underestimation of specific compounds (e.g., pyrophosphate and phosphonates) (McDowell et al., 2006). Another major challenge is the extensive spectral overlap of chemical shifts in the orthophosphate monoester region (approximately 3.5 to 6.0 ppm), requiring specialized baseline correction, deconvolution algorithms, and standardized chemical shift libraries to distinguish specific stereoisomers (such as *myo*-, *scyllo*-, D-*chiro*-, and *neo*-inositol hexakisphosphate) (Cade-Menun, 2015).

^{31}P-NMR and its application in P fertilizer management

After partially replacing inorganic P fertilizer with manure, Liu et al. (2020) assessed P speciation via solution ^{31}P-NMR spectroscopy in agricultural soils, observing greater overall P availability compared with soils receiving chemical fertilizer alone. They also reported that manure applications significantly increased soil organic P and elevated the orthophosphate diester-to-monoester ratio, reflecting greater biological lability. In another study conducted by Abdi et al. (2019), long-term P fertilization altered P distribution in grassland soils: total orthophosphate diesters and *scyllo*-inositol hexakisphosphate decreased with continuous fertilization, while soluble inorganic orthophosphate and total extractable P increased.

Rodrigues et al. (2023) evaluated how land-use transitions from native Cerrado into conventional and no-till cropping systems impacted soil P pools. They observed that across all cultivated soils, recalcitrant orthophosphate monoesters constituted the predominant organic P fraction, whereas labile diester P was preserved primarily in undisturbed native vegetation soils.

Furthermore, transitioning from native vegetation to continuous no-till or conventional cultivation resulted in the progressive depletion of phytate reserves.

References

Abdi, D., Cade-Menun, B. J., Ziadi, N., Shi, Y., Bélanger, G., Lajeunesse, J., & Lafond, J. (2019). A ^{31}P-NMR spectroscopic study of phosphorus forms in two phosphorus-fertilized grassland soils in eastern Canada. Canadian Journal of Soil Science, 99(2), 161–172. https://doi.org/10.1139/cjss-2018-0125

Adams, J. M., & McCabe, R. W. (2006). Clay minerals as catalysts. In F. Bergaya, B. K. G. Theng, & G. Lagaly (Eds.), Developments in Clay Science (Vol. 1, pp. 541–581). Elsevier. https://doi.org/10.1016/S1572-4352(05)01017-2

Adeleke, R., Nwangburuka, C., & Oboirien, B. (2017). Origins, roles and fate of organic acids in soils: A review. South African Journal of Botany, 108, 393–406. https://doi.org/10.1016/j.sajb.2016.09.002

Aguilera, E., Lassaletta, L., Gattinger, A., & Gimeno, B. S. (2013). Managing soil carbon for climate change mitigation and adaptation in Mediterranean cropping systems: A meta-analysis. Agriculture, Ecosystems & Environment, 168, 25–36. https://doi.org/10.1016/j.agee.2013.02.003

Al-Rohily, K. M., Ghoneim, A. M., Modaihsh, A. S., & Mahjoub, M. O. (2013). Phosphorus availability in calcareous soil amend with chemical phosphorus fertilizer, cattle manure compost and sludge manure. International Journal of Soil Science, 8(1), 17–24. https://doi.org/10.3923/ijss.2013.17.24

Arai, Y., & Sparks, D. L. (2007). Phosphate reaction dynamics in soils and soil components: A multiscale approach. Advances in Agronomy, 94, 135–179. https://doi.org/10.1016/S0065-2113(06)94003-6

Arcand, M. M., & Schneider, K. D. (2006). Plant- and microbial-based mechanisms to improve the agronomic effectiveness of phosphate rock: A review. Anais da Academia Brasileira de Ciências, 78(4), 791–807. https://doi.org/10.1590/S0001-37652006000400013

Baker, J. L., & Laflen, J. M. (1982). Effects of corn residue and fertilizer management on soluble nutrient runoff losses. Transactions of the ASAE, 25(2), 344–348. https://doi.org/10.13031/2013.33533

Barrow, N. J., Sen, A., Roy, N., & Debnath, A. (2021). The soil phosphate fractionation fallacy. Plant and Soil, 459(1–2), 1–11. https://doi.org/10.1007/s11104-020-04476-6

Bergkemper, F., Schöler, A., Engel, M., Lang, F., Krüger, J., Schloter, M., & Schulz, S. (2016). Phosphorus depletion in forest soils shapes bacterial communities towards phosphorus recycling systems. Environmental Microbiology, 18(6), 1988–2000. https://doi.org/10.1111/1462-2920.13188

Biassoni, M. M., Vivas, H., Gutiérrez-Boem, F. H., & Salvagiotti, F. (2023). Changes in soil phosphorus (P) fractions and P bioavailability after 10 years of continuous P fertilization. Soil and Tillage Research, 232, 105777. https://doi.org/10.1016/j.still.2023.105777

Black, C. A. (2013). Soil fertility evaluation and control. CRC Press.

Blake, L., Johnston, A. E., Poulton, P. R., & Goulding, K. W. T. (2003). Changes in soil phosphorus fractions following positive and negative phosphorus balances for long periods. Plant and Soil, 254(2), 245–261. https://doi.org/10.1023/A:1025544817872

Bray, R. H., & Kurtz, L. T. (1945). Determination of total, organic, and available forms of phosphorus in soils. Soil Science, 59(1), 39–46. https://doi.org/10.1097/00010694-194501000-00006

Bromfield, S. M. (1967). An examination of the use of ammonium fluoride as a selective extractant for aluminium-bound phosphate in partially phosphated systems. Australian Journal of Soil Research, 5(2), 225–234. https://doi.org/10.1071/SR9670225

Brown, G. E., Jr., & Sturchio, N. C. (2002). An overview of synchrotron radiation applications to low temperature geochemistry and environmental science. Reviews in Mineralogy and Geochemistry, 49(1), 1–115. https://doi.org/10.2138/rmg.2002.49.01

Bünemann, E. K., Keller, B., Hoop, D., Jud, K., Boivin, P., & Frossard, E. (2013). Increased availability of phosphorus after drying and rewetting of a grassland soil: Processes and plant use. Plant and Soil, 370(1–2), 511–526. https://doi.org/10.1007/s11104-013-1651-y

Cade-Menun, B. J. (2015). Improved peak identification in ^{31}P-NMR spectra of environmental samples with a standardized method and peak library. Geoderma, 257–258, 102–114. https://doi.org/10.1016/j.geoderma.2014.12.016

Cade-Menun, B. J. (2017). Characterizing phosphorus forms in cropland soils with solution ^{31}P-NMR: Past studies and future research needs. Chemical and Biological Technologies in Agriculture, 4, 19. https://doi.org/10.1186/s40538-017-0098-4

Cade-Menun, B. J., & Liu, C. W. (2014). Solution phosphorus-31 nuclear magnetic resonance spectroscopy of soils from 2005 to 2013: A review of sample preparation and experimental parameters. Soil Science Society of America Journal, 78(1), 19–37. https://doi.org/10.2136/sssaj2013.05.0187dgs

Calvaruso, C., Turpault, M. P., & Frey-Klett, P. (2006). Root-associated bacteria contribute to mineral weathering and to mineral nutrition in trees: A budgeting analysis. Applied and Environmental Microbiology, 72(2), 1258–1266. https://doi.org/10.1128/AEM.72.2.1258-1266.2006

Carver, R. E., Nelson, N. O., Roozeboom, K. L., Kluitenberg, G. J., Tomlinson, P. J., Kang, Q., & Abel, D. S. (2022). Cover crop and phosphorus fertilizer management impacts on surface water quality from a no-till corn-soybean rotation. Journal of Environmental Management, 301, 113818. https://doi.org/10.1016/j.jenvman.2021.113818

Celi, L., & Barberis, E. (2005). Abiotic stabilization of organic phosphorus in the environment. In B. L. Turner, A. E. Richardson, & E. J. Mullaney (Eds.), Inositol phosphates: Linking agriculture and the environment (pp. 111–133). CABI Publishing. https://doi.org/10.1079/9780851998220.0111

Chacon, N., Silver, W. L., Dubinsky, E. A., & Cusack, D. F. (2006). Iron reduction and soil phosphorus solubilization in humid tropical forest soils: The roles of labile carbon pools and an electron shuttle compound. Biogeochemistry, 78(1), 67–84. https://doi.org/10.1007/s10533-005-2343-3

Chang, S. C., & Jackson, M. L. (1957). Fractionation of soil phosphorus. Soil Science, 84(2), 133–144. https://doi.org/10.1097/00010694-195708000-00005

Chen, S., Cade-Menun, B. J., Bainard, L. D., Luce, M. S., Hu, Y., & Chen, Q. (2021). The influence of long-term N and P fertilization on soil P forms and cycling in a wheat/fallow cropping system. Geoderma, 404, 115274. https://doi.org/10.1016/j.geoderma.2021.115274

Clark, A. (Ed.). (2008). Managing cover crops profitably (3rd ed.). Sustainable Agriculture Network.

Conceição, P. C., Dieckow, J., & Bayer, C. (2013). Combined role of no-tillage and cropping systems in soil carbon stocks and stabilization. Soil and Tillage Research, 129, 40–47. https://doi.org/10.1016/j.still.2013.01.003

Condron, L. M., & Newman, S. (2011). Revisiting the fundamentals of phosphorus fractionation of sediments and soils. Journal of Soils and Sediments, 11(5), 830–840. https://doi.org/10.1007/s11368-011-0364-2

Condron, L. M., Frossard, E., Tiessen, H., Newman, R. H., & Stewart, J. W. B. (1990). Chemical nature of organic phosphorus in cultivated and uncultivated soils under different environmental conditions. Journal of Soil Science, 41(1), 41–50. https://doi.org/10.1111/j.1365-2389.1990.tb00045.x

Condron, L. M., Newman, R. H., & Frossard, E. (1997). Nuclear magnetic resonance spectroscopy of soil phosphorus. In M. A. Nanny, R. A. Minear, & J. A. Leenheer (Eds.), Nuclear Magnetic Resonance Spectroscopy in Environmental Chemistry (pp. 187–208). Oxford University Press.

Condron, L. M., Turner, B. L., & Cade-Menun, B. J. (2005). Chemistry and dynamics of soil organic phosphorus. In J. T. Sims & A. N. Sharpley (Eds.), Phosphorus: Agriculture and the environment (pp. 87–121). American Society of Agronomy, Crop Science Society of America, & Soil Science Society of America. https://doi.org/10.2134/agronmonogr46.c4

Cordell, D., Drangert, J. O., & White, S. (2009). The story of phosphorus: Global food security and food for thought. Global Environmental Change, 19(2), 292–305. https://doi.org/10.1016/j.gloenvcha.2008.10.009

Cross, A. F., & Schlesinger, W. H. (1995). A literature review and evaluation of the Hedley fractionation: Applications to the biogeochemical cycle of soil phosphorus in natural ecosystems. Geoderma, 64(3–4), 197–214. https://doi.org/10.1016/0016-7061(94)00023-6

Dalal, R. C. (1977). Soil organic phosphorus. Advances in Agronomy, 29, 83–117. https://doi.org/10.1016/S0065-2113(08)60236-2

Daryanto, S., Wang, L., & Jacinthe, P. A. (2017). Meta-analysis of phosphorus loss from no-till soils. Journal of Environmental Quality, 46(5), 1028–1037. https://doi.org/10.2134/jeq2016.12.0462

Devi, N. B., & Yadava, P. S. (2006). Seasonal dynamics in soil microbial biomass C, N, and P in a mixed-oak forest ecosystem of Manipur, North-east India. Applied Soil Ecology, 31(3), 220–227. https://doi.org/10.1016/j.apsoil.2005.05.005

Dinh, M.-V., Guhr, A., Spohn, M., & Matzner, E. (2017). Release of phosphorus from soil bacterial and fungal biomass following drying/rewetting. Soil Biology and Biochemistry, 110, 1–7. https://doi.org/10.1016/j.soilbio.2017.02.014

Dodds, W. K., Bouska, W. W., Eitzmann, J. L., Pilger, T. J., Pitts, K. L., Riley, A. J., Schloesser, J. T., & Thornbrugh, D. J. (2009). Eutrophication of U.S. freshwaters: Analysis of potential economic damages. Environmental Science & Technology, 43(1), 12–19. https://doi.org/10.1021/es801217q

Earl, K. D., Syers, J. K., & McLaughlin, J. R. (1979). Origin of the effects of citrate, tartrate, and acetate on phosphate sorption by soils and synthetic gels. Soil Science Society of America Journal, 43(4), 674–678. https://doi.org/10.2136/sssaj1979.03615995004300040008x

Edwards, C. L. (2017). Evaluation of long-term phosphorus fertilizer placement, rate, and source, and research in the US Midwest [Master's thesis, Kansas State University]. https://hdl.handle.net/2097/35425

Fink, J. R., Inda, A. V., Bavaresco, J., Barrón, V., Torrent, J., & Bayer, C. (2016). Phosphorus adsorption and desorption in undisturbed samples from subtropical soils under conventional tillage or no-tillage. Journal of Plant Nutrition and Soil Science, 179(2), 198–205. https://doi.org/10.1002/jpln.201500017

Frank, K., Beegle, D., & Denning, J. (1998). Phosphorus. In J. R. Brown (Ed.), Recommended chemical soil test procedures for the North Central Region (North Central Regional Research Publication No. 221, pp. 21–26). Missouri Agricultural Experiment Station.

Gamage, K. H. H., Hettiarachchi, G. M., Nelson, N. O., Roozeboom, K. L., Kluitenberg, G. J., Tomlinson, P. J., & Presley, D. R. (2025). Phosphorus and cover crop management practices affect phosphorus speciation in soils and eroded sediments. Journal of Environmental Quality, 54(2), 382–396. https://doi.org/10.1002/jeq2.20677

Gerke, J. (2010). Humic (organic matter)-Al(Fe)-phosphate complexes: An underestimated phosphate form in soils and source of plant-available phosphate. Soil Science, 175(9), 417–425. https://doi.org/10.1097/SS.0b013e3181f1b4dd

Giles, C. D., Richardson, A. E., Cade-Menun, B. J., Mezeli, M. M., Brown, L. K., Menezes-Blackburn, D., Darch, T., Blackwell, M. S., Shand, C. A., Stutter, M. I., Wendler, R., Cooper, P., Lumsdon, D. G., Wearing, C., Zhang, H., Haygarth, P. M., & George, T. S. (2018). Phosphorus acquisition by citrate- and phytase-exuding Nicotiana tabacum plant

mixtures depends on soil phosphorus availability and root intermingling. Physiologia Plantarum, 163(3), 356–371. https://doi.org/10.1111/ppl.12686

Grant, C. A., Flaten, D. N., Tomasiewicz, D. J., & Sheppard, S. C. (2001). The importance of early season phosphorus nutrition. Canadian Journal of Plant Science, 81(2), 211–224. https://doi.org/10.4141/P00-093

Gu, C., & Margenot, A. J. (2021). Navigating limitations and opportunities of soil phosphorus fractionation. Plant and Soil, 459(1–2), 13–17. https://doi.org/10.1007/s11104-020-04552-x

Hadgu, F., Gebrekidan, H., Kibret, K., & Yitaferu, B. (2014). Study of phosphorus adsorption and its relationship with soil properties, analyzed with Langmuir and Freundlich models. Agriculture, Forestry and Fisheries, 3(1), 40–51. https://doi.org/10.11648/j.aff.20140301.15

Hallama, M., Pekrun, C., Lambers, H., & Kandeler, E. (2019). Hidden miners–the roles of cover crops and soil microorganisms in phosphorus cycling through agroecosystems. Plant and Soil, 434(1–2), 7–45. https://doi.org/10.1007/s11104-018-3810-7

Harrison, A. F. (1987). Soil organic phosphorus: A review of world literature. CAB International.

Havlin, J. L., Beaton, J. D., Tisdale, S. L., & Nelson, W. L. (1999). Soil fertility and fertilizers: An introduction to nutrient management (6th ed.). Prentice Hall.

Hedley, M. J., Stewart, J. W. B., & Chauhan, B. S. (1982). Changes in inorganic and organic soil phosphorus fractions induced by cultivation practices and by laboratory incubations. Soil Science Society of America Journal, 46(5), 970–976. https://doi.org/10.2136/sssaj1982.03615995004600050017x

Helfenstein, J., Tamburini, F., von Sperber, C., Massey, M. S., Pistocchi, C., Chadwick, O. A., Vitousek, P. M., Kretzschmar, R., & Frossard, E. (2018). Combining spectroscopic and isotopic techniques gives a dynamic view of phosphorus cycling in soil. Nature Communications, 9, 3226. https://doi.org/10.1038/s41467-018-05731-2

Hieltjes, A. H. M., & Lijklema, L. (1980). Fractionation of inorganic phosphates in calcareous sediments. Journal of Environmental Quality, 9(3), 405–407. https://doi.org/10.2134/jeq1980.00472425000900030015x

Hudnell, H. K. (2010). The state of U.S. freshwater harmful algal blooms assessments, policy and legislation. Toxicon, 55(5), 1024–1034. https://doi.org/10.1016/j.toxicon.2009.07.021

Jalali, M., & Jalali, M. (2022). Effect of low-molecular-weight organic acids on the release of phosphorus from amended calcareous soils: Experimental and modeling. Journal of Soil Science and Plant Nutrition, 22(4), 4179–4193. https://doi.org/10.1007/s42729-022-00996-3

Jones, D. L., & Darrah, P. R. (1994). Role of root derived organic acids in the mobilization of nutrients from the rhizosphere. Plant and Soil, 166(2), 247–257. https://doi.org/10.1007/BF00008338

Khare, N., Hesterberg, D., Beauchemin, S., & Wang, S. L. (2004). XANES determination of adsorbed phosphate distribution between ferrihydrite and boehmite in mixtures. Soil Science Society of America Journal, 68(2), 460–469. https://doi.org/10.2136/sssaj2004.4600

Kizewski, F., Liu, Y. T., Morris, A., & Hesterberg, D. (2011). Spectroscopic approaches for phosphorus speciation in soils and other environmental systems. Journal of Environmental Quality, 40(3), 751–766. https://doi.org/10.2134/jeq2010.0169

Koch, M., Kruse, J., Eichler-Löbermann, B., Zimmer, D., Willbold, S., Leinweber, P., & Siebers, N. (2018). Phosphorus stocks and speciation in soil profiles of a long-term fertilizer experiment: Evidence from sequential fractionation, P K-edge XANES, and ^{31}P NMR spectroscopy. Geoderma, 316, 115–126. https://doi.org/10.1016/j.geoderma.2017.12.003

Kuo, S. (1996). Phosphorus. In D. L. Sparks, A. L. Page, P. A. Helmke, R. H. Loeppert, P. N. Soltanpour, M. A. Tabatabai, C. T. Johnston, & M. E. Sumner (Eds.), Methods of soil analysis: Part 3—Chemical methods (pp. 869–919). Soil Science Society of America & American Society of Agronomy. https://doi.org/10.2136/sssabookser5.3.c32

Kuo, S., Huang, B., & Bembenek, R. (2005). Effects of long-term phosphorus fertilization and winter cover cropping on soil phosphorus transformations in less weathered soil. Biology and Fertility of Soils, 41(2), 116–123. https://doi.org/10.1007/s00374-004-0807-6

Lewis, D. R., & McGechan, M. B. (2002). SW—Soil and water: A review of field-scale phosphorus dynamics models. Biosystems Engineering, 82(4), 359–380. https://doi.org/10.1006/bioe.2002.0102

Liang, J.-L., Liu, J., Jia, P., Yang, T.-T., Zeng, Q.-W., Zhang, S.-C., Liao, B., Shu, W.-S., & Li, J.-T. (2020). Novel phosphate-solubilizing bacteria enhance soil phosphorus cycling

following ecological restoration of land degraded by mining. The ISME Journal, 14(6), 1600–1613. https://doi.org/10.1038/s41396-020-0628-0

Lindsay, W. L. (1979). Chemical equilibria in soils. John Wiley & Sons.

Lindsay, W. L. (1991). Iron oxide solubilization by organic matter and its effect on iron availability. In Y. Chen & Y. Hadar (Eds.), Iron nutrition and interactions in plants (pp. 29–36). Springer. https://doi.org/10.1007/978-94-011-3294-7_5

Liu, J., Cade-Menun, B. J., Yang, J., Hu, Y., Liu, C. W., Tremblay, J., LaForge, K., Schellenberg, M., Hamel, C., & Bainard, L. D. (2018). Long-term land use affects phosphorus speciation and the composition of phosphorus cycling genes in agricultural soils. Frontiers in Microbiology, 9, 1643. https://doi.org/10.3389/fmicb.2018.01643

Liu, J., Han, C., Zhao, Y., Yang, J., Cade-Menun, B. J., Hu, Y., Li, J., Liu, H., Sui, P., Chen, Y., & Ma, Y. (2020). The chemical nature of soil phosphorus in response to long-term fertilization practices: Implications for sustainable phosphorus management. Journal of Cleaner Production, 272, 123093. https://doi.org/10.1016/j.jclepro.2020.123093

Liu, J., Hu, Y., Yang, J., Abdi, D., & Cade-Menun, B. J. (2015). Investigation of soil legacy phosphorus transformation in long-term agricultural fields using sequential fractionation, P K-edge XANES and solution ^{31}P-NMR spectroscopy. Environmental Science & Technology, 49(1), 168–176. https://doi.org/10.1021/es504420n

Liu, J., Yang, J., Cade-Menun, B. J., Hu, Y., Li, J., Peng, C., & Ma, Y. (2017). Molecular speciation and transformation of soil legacy phosphorus with and without long-term phosphorus fertilization: Insights from bulk and microprobe spectroscopy. Scientific Reports, 7, 15354. https://doi.org/10.1038/s41598-017-14741-7

Liu, J., Yang, J., Cade-Menun, B. J., Liang, X., Hu, Y., Liu, C. W., Zhao, Y., Li, L., & Shi, J. (2013). Complementary phosphorus speciation in agricultural soils by sequential fractionation, solution ^{31}P nuclear magnetic resonance, and phosphorus K-edge X-ray absorption near-edge structure spectroscopy. Journal of Environmental Quality, 42(6), 1763–1770. https://doi.org/10.2134/jeq2013.04.0127

Loganathan, P., Isirimah, N. O., & Nwachuku, D. A. (1987). Phosphorus sorption by Ultisols and Inceptisols of the Niger delta in southern Nigeria. Soil Science, 144(5), 330–338. https://doi.org/10.1097/00010694-198711000-00004

Ma, Q., Rengel, Z., & Bowden, B. (2007). Heterogeneous distribution of phosphorus and potassium in soil influences wheat growth and nutrient uptake. Plant and Soil, 291(1–2), 301–309. https://doi.org/10.1007/s11104-007-9194-6

Mallarino, A. P., Barcos, S. R., Prater, J. R., & Wittry, D. J. (2009). Timing of broadcast phosphorus fertilization for no-till corn and soybean. Soil Science Society of America Journal, 73(6), 2143–2150. https://doi.org/10.2136/sssaj2008.0383

Maltais-Landry, G., Scow, K., Brennan, E., & Vitousek, P. (2015). Long-term effects of compost and cover crops on soil phosphorus in two California agroecosystems. Soil Science Society of America Journal, 79(2), 688–697. https://doi.org/10.2136/sssaj2014.08.0335

McDowell, R. W., Stewart, I., & Cade-Menun, B. J. (2006). An examination of spin-lattice relaxation times for analysis of soil and manure extracts by liquid state phosphorus-31 nuclear magnetic resonance spectroscopy. Journal of Environmental Quality, 35(1), 293–302. https://doi.org/10.2134/jeq2005.0298

McLaughlin, M. J., McBeath, T. M., Smernik, R., Stacey, S. P., Ajiboye, B., & Guppy, C. (2011). The chemical nature of P accumulation in agricultural soils—implications for fertiliser management and design: An Australian perspective. Plant and Soil, 349(1–2), 69–87. https://doi.org/10.1007/s11104-011-0907-3

Mehlich, A. (1984). Mehlich 3 soil test extractant: A modification of Mehlich 2 extractant. Communications in Soil Science and Plant Analysis, 15(12), 1409–1416. https://doi.org/10.1080/00103628409367568

Mikutta, C., Lang, F., & Kaupenjohann, M. (2006). Citrate impairs the micropore diffusion of phosphate into pure and C-coated goethite. Geochimica et Cosmochimica Acta, 70(3), 595–607. https://doi.org/10.1016/j.gca.2005.10.032

Mostaghimi, S., Flagg, J. M., Dillaha, T. A., & Shanholtz, V. O. (1988). Phosphorus loss from cropland as affected by tillage system and fertilizer application method. Water Resources Bulletin, 24(4), 735–742. https://doi.org/10.1111/j.1752-1688.1988.tb00924.x

Murphy, J., & Riley, J. P. (1962). A modified single solution method for the determination of phosphate in natural waters. *Analytica Chimica Acta*, 27, 31–36. https://doi.org/10.1016/S0003-2670(00)88444-5

Nadelhoffer, K. J., Giblin, A. E., Shaver, G. R., & Laundre, J. A. (1991). Effects of temperature and substrate quality on element mineralization in six Arctic soils. Ecology, 72(1), 242–253. https://doi.org/10.2307/1938919

Nannipieri, P., Giagnoni, L., Landi, L., & Renella, G. (2011). Role of phosphatase enzymes in soil. In E. K. Bünemann, A. Oberson, & E. Frossard (Eds.), Phosphorus in action: Biological processes in soil phosphorus cycling (pp. 215–243). Springer. https://doi.org/10.1007/978-3-642-15271-9_9

Negassa, W., & Leinweber, P. (2009). How does the Hedley sequential phosphorus fractionation reflect impacts of land use and management on soil phosphorus: A review. Journal of Plant Nutrition and Soil Science, 172(3), 305–325. https://doi.org/10.1002/jpln.200800223

Noack, S. R., McLaughlin, M. J., Smernik, R. J., McBeath, T. M., & Armstrong, R. D. (2012). Crop residue phosphorus: Speciation and potential bio-availability. Plant and Soil, 359(1–2), 375–385. https://doi.org/10.1007/s11104-012-1212-4

Norrish, K., & Rosser, H. (1983). Mineral phosphate. In Soils: An Australian viewpoint (pp. 335–361). CSIRO / Academic Press.

Nuruzzaman, M., Lambers, H., Bolland, M. D. A., & Veneklaas, E. J. (2005). Phosphorus benefits of different legume crops to subsequent wheat grown in different soils of Western Australia. Plant and Soil, 271(1–2), 175–187. https://doi.org/10.1007/s11104-004-2296-2

Olsen, S. R., & Sommers, L. E. (1982). Phosphorus. In A. L. Page, R. H. Miller, & D. R. Keeney (Eds.), Methods of soil analysis: Part 2—Chemical and microbiological properties (2nd ed., pp. 403–430). American Society of Agronomy & Soil Science Society of America. https://doi.org/10.2134/agronmonogr9.2.2ed.c24

Olsen, S. R., Cole, C. V., Watanabe, F. S., & Dean, L. A. (1954). Estimation of available phosphorus in soils by extraction with sodium bicarbonate (USDA Circular No. 939). U.S. Department of Agriculture.

Pang, F., Li, Q., Solanki, M. K., Wang, Z., Xing, Y. X., & Dong, D. F. (2024). Soil phosphorus transformation and plant uptake driven by phosphate-solubilizing microorganisms. Frontiers in Microbiology, 15, 1383813. https://doi.org/10.3389/fmicb.2024.1383813

Pavinato, P. S., Merlin, A., & Rosolem, C. A. (2008). Organic compounds from plant extracts and their effect on soil phosphorus availability. Pesquisa Agropecuária Brasileira, 43(10), 1379–1388. https://doi.org/10.1590/S0100-204X2008001000015

Pierzynski, G. M., McDowell, R. W., & Sims, J. T. (2005). Chemistry, cycling, and potential movement of inorganic phosphorus in soils. In J. T. Sims & A. N. Sharpley (Eds.), Phosphorus: Agriculture and the environment (pp. 53–86). American Society of Agronomy, Crop Science Society of America, & Soil Science Society of America. https://doi.org/10.2134/agronmonogr46.c3

Pote, D. H., Daniel, T. C., Sharpley, A. N., Moore, P. A., Jr., Edwards, D. R., & Nichols, D. J. (1996). Relating extractable soil phosphorus to phosphorus losses in runoff. Soil Science Society of America Journal, 60(3), 855–859. https://doi.org/10.2136/sssaj1996.03615995006000030025x

Prietzel, J., Dümig, A., Wu, Y., Zhou, J., & Klysubun, W. (2013). Synchrotron-based P K-edge XANES spectroscopy reveals rapid changes of phosphorus speciation in the topsoil of two glacier foreland chronosequences. Geochimica et Cosmochimica Acta, 108, 154–171. https://doi.org/10.1016/j.gca.2013.01.009

Rajan, S. S. S., Watkinson, J. H., & Sinclair, A. G. (1996). Phosphate rocks for direct application to soils. Advances in Agronomy, 57, 77–159. https://doi.org/10.1016/S0065-2113(08)60923-6

Reichard, P. U., Kretzschmar, R., & Kraemer, S. M. (2007). Dissolution mechanisms of goethite in the presence of siderophores and organic acids. Geochimica et Cosmochimica Acta, 71(23), 5635–5650. https://doi.org/10.1016/j.gca.2006.12.022

Richardson, A. E., & Simpson, R. J. (2011). Soil microorganisms mediating phosphorus availability: Update on microbial phosphorus. Plant Physiology, 156(3), 989–996. https://doi.org/10.1104/pp.111.175448

Rodrigues, M., Soltangheisi, A., Abdala, D. B., Ebuele, V. O., Thoss, V., Withers, P. J. A., & Pavinato, P. S. (2023). Long-term land use and tillage influence on phosphorus species in Brazilian Oxisols: A multi-technique assessment by chemical P fractionation, ^{31}P NMR and P K-edge XANES spectroscopies. Soil and Tillage Research, 229, 105683. https://doi.org/10.1016/j.still.2023.105683

Rowe, H., Withers, P. J. A., Baas, P., Chan, N. I., Doody, D., Holiman, J., Jacobs, B., Li, H., MacDonald, G. K., McDowell, R., Sharpley, A. N., Shen, J., Taheri, W., Wallenstein, M., & Weintraub, M. N. (2016). Integrating legacy soil phosphorus into sustainable nutrient

management strategies for future food, bioenergy and water security. Nutrient Cycling in Agroecosystems, 104(3), 393–412. https://doi.org/10.1007/s10705-015-9726-1

Saunders, W. M. H., & Williams, E. G. (1955). Observations on the determination of total organic phosphorus in soils. Journal of Soil Science, 6(2), 254–267. https://doi.org/10.1111/j.1365-2389.1955.tb00849.x

Schreeg, L. A., Mack, M. C., & Turner, B. L. (2013). Nutrient-specific solubility patterns of leaf litter across 41 lowland tropical plant species. Ecology, 94(1), 94–105. https://doi.org/10.1890/11-1958.1

Selles, F., Campbell, C. A., Zentner, R. P., Curtin, D., James, D. C., & Basnyat, P. (2011). Phosphorus use efficiency and long-term trends in soil available phosphorus in wheat production systems with and without nitrogen fertilizer. Canadian Journal of Soil Science, 91(1), 39–52. https://doi.org/10.4141/cjss10051

Shahena, S., Rajan, M., Chandran, V., & Mathew, L. (2021). Conventional methods of fertilizer release. In F. B. Lewu, T. Volova, S. Thomas, & R. K. Rakhimol (Eds.), Controlled release fertilizers for sustainable agriculture (pp. 1–24). Academic Press. https://doi.org/10.1016/B978-0-12-819555-0.00001-6

Shapiro, R. E., Armiger, W. H., & Fried, M. (1960). The effect of soil water movement vs. phosphate diffusion on growth and phosphorus content of corn and soybeans. Soil Science Society of America Journal, 24(3), 161–164. https://doi.org/10.2136/sssaj1960.03615995002400030008x

Sharpley, A. N. (1995). Dependence of runoff phosphorus on extractable soil phosphorus. Journal of Environmental Quality, 24(5), 920–926. https://doi.org/10.2134/jeq1995.00472425002400050020x

Sharpley, A. N., & Smith, S. J. (1994). Wheat tillage and water quality in the Southern Plains. Soil and Tillage Research, 30(1), 33–48. https://doi.org/10.1016/0167-1987(94)90069-8

Sharpley, A. N., Daniel, T., Sims, T., Lemunyon, J., Stevens, R., & Parry, R. (2003). Agricultural phosphorus and eutrophication (2nd ed., ARS-149). U.S. Department of Agriculture, Agricultural Research Service.

Shaw, A. N., & Cleveland, C. C. (2020). The effects of temperature on soil phosphorus availability and phosphatase enzyme activities: A cross-ecosystem study from the tropics to

the Arctic. Biogeochemistry, 151(2–3), 113–125. https://doi.org/10.1007/s10533-020-00703-3

Shen, J., Yuan, L., Zhang, J., Li, H., Bai, Z., Chen, X., Zhang, W., & Zhang, F. (2011). Phosphorus dynamics: From soil to plant. Plant Physiology, 156(3), 997–1005. https://doi.org/10.1104/pp.111.175232

Shi, Z., Krom, M. D., Bonneville, S., Baker, A. R., Bristow, C., Drake, N., Mann, G., Carslaw, K., McQuaid, J. B., Jickells, T., & Benning, L. G. (2011). Influence of chemical weathering and aging of iron oxides on the potential iron solubility of Saharan dust during simulated atmospheric processing. Global Biogeochemical Cycles, 25(2), GB2010. https://doi.org/10.1029/2010GB003837

Sims, J. T., & Pierzynski, G. M. (2005). Chemistry of phosphorus in soils. In M. A. Tabatabai & D. L. Sparks (Eds.), Chemical processes in soils (SSSA Book Series No. 8, pp. 151–192). Soil Science Society of America. https://doi.org/10.2136/sssabookser8.c2

Soltangheisi, A., Rodrigues, M., Coelho, M. J. A., Gasperini, A. M., Sartor, L. R., & Pavinato, P. S. (2018). Changes in soil phosphorus lability promoted by phosphate sources and cover crops. Soil and Tillage Research, 179, 20–28. https://doi.org/10.1016/j.still.2018.01.006

Sommers, L. E., & Nelson, D. W. (1972). Determination of total phosphorus in soils: A rapid perchloric acid digestion procedure. Soil Science Society of America Journal, 36(6), 902–904. https://doi.org/10.2136/sssaj1972.03615995003600060020x

Sparks, D. L., Singh, B., & Siebecker, M. G. (2022). Environmental soil chemistry (3rd ed.). Elsevier.

Spohn, M., & Kuzyakov, Y. (2013). Distribution of microbial- and root-derived phosphatase activities in the rhizosphere depending on P availability and C allocation – Coupling soil zymography with ^{14}C imaging. Soil Biology and Biochemistry, 67, 106–113. https://doi.org/10.1016/j.soilbio.2013.08.011

Sundman, A., Karlsson, T., Sjöberg, S., & Persson, P. (2016). Impact of iron–organic matter complexes on aqueous phosphate concentrations. Chemical Geology, 426, 109–117. https://doi.org/10.1016/j.chemgeo.2016.02.008

Tamburini, F., Pfahler, V., von Sperber, C., Frossard, E., & Bernasconi, S. M. (2014). Oxygen isotopes for unraveling phosphorus transformations in the soil–plant system: A review. Soil

Science Society of America Journal, 78(1), 38–46. https://doi.org/10.2136/sssaj2013.05.0186dgs

Tarafdar, J. C., & Jungk, A. (1987). Phosphatase activity in the rhizosphere and its relation to the depletion of soil organic phosphorus. Biology and Fertility of Soils, 3(4), 199–204. https://doi.org/10.1007/BF00640630

Teles, A. P. B., Rodrigues, M., Bejarano Herrera, W. F., Soltangheisi, A., Sartor, L. R., Withers, P. J. A., & Pavinato, P. S. (2017). Do cover crops change the lability of phosphorus in a clayey subtropical soil under different phosphate fertilizers? Soil Use and Management, 33(1), 34–44. https://doi.org/10.1111/sum.12327

Thammaiah, M., Pandey, R. N., Purakayastha, T. J., Chobhe, K. A., Vashisth, A., Chandra, S., Singh, G., Das, T. K., & Trivedi, A. (2023). Impact of low molecular weight organic acids on soil Olsen phosphorus and its phyto-availability to soybean (Glycine max). Journal of Plant Nutrition, 46(5), 765–781. https://doi.org/10.1080/01904167.2022.2155543

Thomas, R. L., Sheard, R. W., & Moyer, J. R. (1967). Comparison of conventional and automated procedures for nitrogen, phosphorus, and potassium analysis of plant material using a single digestion. Agronomy Journal, 59(3), 240–243. https://doi.org/10.2134/agronj1967.00021962005900030010x

Tiessen, H., & Moir, J. O. (1993). Characterization of available P by sequential extraction. In M. R. Carter (Ed.), Soil sampling and methods of analysis (pp. 75–86). CRC Press.

Tiessen, H., & Moir, J. O. (2008). Characterization of available P by sequential extraction. In M. R. Carter & E. G. Gregorich (Eds.), Soil sampling and methods of analysis (2nd ed., pp. 293–306). CRC Press.

Tournassat, C., Steefel, C. I., Bourg, I. C., & Bergaya, F. (Eds.). (2015). Natural and engineered clay barriers (Developments in Clay Science, Vol. 6). Elsevier.

Turner, B. L., Newman, S., & Reddy, K. R. (2006). Overestimation of organic phosphorus in wetland soils by alkaline extraction and molybdate colorimetry. Environmental Science & Technology, 40(10), 3349–3354. https://doi.org/10.1021/es052506y

van Veelen, A., Koebernick, N., Scotson, C. S., McKay-Fletcher, D., Huthwelker, T., Borca, C. N., Mosselmans, J. F. W., & Roose, T. (2020). Root-induced soil deformation influences Fe, S and P: Rhizosphere chemistry investigated using synchrotron XRF and XANES. New Phytologist, 225(4), 1476–1490. https://doi.org/10.1111/nph.16242

Varela, M. F., Barraco, M., Gili, A., Taboada, M. A., & Rubio, G. (2017). Biomass decomposition and phosphorus release from residues of cover crops under no-tillage. Agronomy Journal, 109(1), 317–326. https://doi.org/10.2134/agronj2016.03.0168

Walker, T. W., & Adams, A. F. R. (1958). Studies on soil organic matter: 1. Influence of phosphorus content of parent materials on accumulations of carbon, nitrogen, sulfur, and organic phosphorus in grassland soils. Soil Science, 85(6), 307–318. https://doi.org/10.1097/00010694-195806000-00004

Wiens, J. T., Cade-Menun, B. J., Weiseth, B., & Schoenau, J. J. (2019). Potential phosphorus export in snowmelt as influenced by fertilizer placement method in the Canadian prairies. Journal of Environmental Quality, 48(3), 586–593. https://doi.org/10.2134/jeq2018.10.0368

Williams, J. D. H., & Walker, T. W. (1969). Fractionation of phosphate in a maturity sequence of New Zealand basaltic soil profiles: 2. Soil Science, 107(3), 213–219. https://doi.org/10.1097/00010694-196903000-00007

Wilson, M. A. (1987). NMR techniques and applications in geochemistry and soil chemistry. Pergamon Press.

Wright, R. B., Lockaby, B. G., & Walbridge, M. R. (2001). Phosphorus availability in an artificially flooded southeastern floodplain forest soil. Soil Science Society of America Journal, 65(4), 1293–1302. https://doi.org/10.2136/sssaj2001.6541293x

Wu, X., Cui, Z., Peng, J., Zhang, F., & Liesack, W. (2022). Genome-resolved metagenomics identifies the particular genetic traits of phosphate-solubilizing bacteria in agricultural soil. ISME Communications, 2, 17. https://doi.org/10.1038/s43705-022-00099-2

Yan, J., Yang, Y., Liang, X., Hou, J., Liu, H., Li, W., & Sparks, D. L. (2020). Molecular mechanisms of phytate precipitation with calcium, iron, and aluminum. Environmental Science & Technology, 54(17), 10608–10617. https://doi.org/10.1021/acs.est.0c02465

Yuan, M., Fernández, F. G., Pittelkow, C. M., Greer, K. D., & Schaefer, D. (2018). Tillage and fertilizer management effects on phosphorus runoff from minimal slope fields. Journal of Environmental Quality, 47(3), 462–470. https://doi.org/10.2134/jeq2017.08.0314

Zeimen, M. B., Janssen, K. A., Sweeney, D. W., Pierzynski, G. M., Mankin, K. R., Devlin, D. L., Regehr, D. L., Barnes, P. L., & McVay, K. A. (2006). Combining management

practices to reduce sediment, nutrients, and herbicides in runoff. Journal of Soil and Water Conservation, 61(5), 258–267.

Zhang, H., & Kovar, J. L. (2009). Fractionation of soil phosphorus. In J. L. Kovar & G. M. Pierzynski (Eds.), Methods of phosphorus analysis for soils, sediments, residuals, and waters (2nd ed., Southern Cooperative Series Bulletin No. 408, pp. 50–60). Virginia Tech University.

Zhang, S., Wang, L., Chen, S., Fan, B., Huang, S., & Chen, Q. (2022). Enhanced phosphorus mobility in a calcareous soil with organic amendments additions: Insights from a long term study with equal phosphorus input. Journal of Environmental Management, 306, 114451. https://doi.org/10.1016/j.jenvman.2022.114451

Chapter 3 - Changes in soil P pools under long-term cover crop and phosphorus fertilization in a corn-soybean rotation system

Abstract

Sustainable phosphorus (P) management requires an improved understanding of how conservation practices and fertilizer strategies interact to influence soil P dynamics and legacy P utilization. This study evaluated the interacting effects of cover cropping (CC) and long-term P fertilization strategies on soil P pools and crop P uptake in a no-till corn-soybean rotation. A field experiment included two cover crop treatments (with and without) and three P fertilization strategies: a control (CN, no P), build-and-drawdown (BD), and build-and-maintain (BM). Soil samples (0–5 cm) collected annually from 2019 to 2022 were analyzed using the Hedley sequential fractionation method. Results indicated that mean annual plant P uptake and redeposition were significantly greater under CC and fertilized treatments (BD and BM). Soil fractionation revealed that P fertilization primarily drove the accumulation of labile inorganic pools (Resin-P_i and $NaHCO_3$-P_i), following the order BM > BD > CN. In fertilized plots (BM and BD), the inclusion of cover crops significantly reduced the concentrations of readily soluble inorganic pools (Resin-P_i and $NaHCO_3$-P_i) while concurrently enriching the moderately stable organic P pool (NaOH-P_o) relative to no-cover treatments. This indicates that cover crops temporarily partition highly soluble fertilizer and legacy P into biomass and subsequently cycle it into moderately stable organic forms. Highly stable P fractions (HCl-P_i and Residual-P) were not significantly affected by the treatments, though Residual-P exhibited annual temporal fluctuations. These findings suggest that cover crops do not merely deplete legacy P but actively

redistribute it. By assimilating soluble, runoff-vulnerable phosphate into winter biomass and ultimately transferring it into soil organic pools, cover crops alter near-surface P pools. Although this biological cycling increases total agronomic P uptake and enhances organic P reserves, earlier runoff data from this site demonstrate that cover crops simultaneously elevate dissolved reactive P losses, highlighting an unavoidable environmental trade-off. Integrating cover cropping with a drawdown fertilization strategy thus offers a mechanistic approach to managing and biologically cycling legacy P in agroecosystems.

Introduction

Sustainable phosphorus (P) management in agroecosystems depends on an improved understanding of how management practices influence the chemical composition of P compounds in soil. Because P compounds occur in multiple inorganic and organic fractions with differing reactivity, changes in their chemical composition directly affect plant availability and the risk of P loss to surface waters (Condron et al., 2005). Management practices designed to enhance soil conservation, such as cover cropping, can alter soil physical, chemical, and biological processes that regulate the transformation of P compounds; however, their effects on soil P pools defined by sequential P fractionation are not well resolved. In parallel, the source, rate, and method of P fertilizer application play key roles in determining the retention and mobility of P compounds in soil, yet these factors are rarely evaluated in combination with cover cropping. A clearer understanding of how cover cropping interacts with P fertilization strategies to influence soil P pools/fractions is therefore needed to inform integrated nutrient management approaches that balance agronomic productivity with environmental protection.

Cover crops are widely recognized as a conservation practice in agricultural systems for their ability to improve soil health, reduce erosion, minimize sediment-associated nutrient runoff,

and enhance long-term soil fertility (Carver et al., 2022; Maltais-Landry & Frossard, 2015; Sharpley & Smith, 1994). In addition, cover crops are known for decreasing sediment-bound P losses; however, edge-of-field monitoring and rainfall simulation studies have reported that cover crops can paradoxically increase dissolved reactive P (DRP) concentrations and cumulative loads in runoff (Carver et al., 2022; Cober et al., 2019; Daryanto et al., 2017), which can lead to eutrophication. These trade-offs associated with cover cropping highlight important gaps in current conservation practices. Addressing these gaps requires integrating conservation practices with phosphorus fertilization approaches.

A build-and-maintain approach to fertilization aims to raise soil test P (STP) concentrations to an established critical threshold at which no yield response to P fertilization is expected, and then maintain P concentrations by applying P fertilizers at rates equal to the P removed in harvested crops (Brooker et al., 2017; Patel et al., 2024). As a result of this strategy, a nutrient reserve is created to mitigate yield-limiting P shortages. Continual P applications equal to crop removal can maintain high STP concentrations, resulting in P being reserved in soil as "legacy P". When STP concentrations are maintained substantially above the agronomic critical threshold, there is greater risk of P being lost to surface waters in runoff (McDowell et al., 2001; Wortmann et al., 2009). To minimize potential P loss, it is essential to manage STP concentrations as close to the agronomic critical threshold as practical (Bergström et al., 2015; Kleinman et al., 2015; Withers et al., 2014). By intentionally withholding P inputs, STP concentrations can be gradually drawn down to the critical threshold, allowing crops to utilize legacy P accumulated from years of build-and-maintain fertilization. Drawdown P management offers a viable alternative for reducing P inputs by minimizing fertilizer applications and

allowing crops to utilize existing soil P reserves until STP approaches the agronomic critical level.

Integrating cover crops into drawdown strategies may further enhance this process by promoting biological access to soil P pools not readily available to other crops. For example, the ability of some cover crop species, such as lupin (Lupinus *spp.*) and ruzigrass (*Urochloa ruziziensis*), to acquire P from less-available soil fractions suggests a potential role in mobilizing legacy P pools, as has been reported in previous studies (Almeida & Rosolem, 2016; Braum & Helmke, 1995; Wang et al., 2008). While cash crops in a drawdown system successfully utilize labile legacy P, the inclusion of a winter cover crop extends the duration of active root exploration, biological P scavenging, and rhizosphere acidification, thereby increasing the total annual assimilation of residual soil P.

Assessing changes in soil P fractionation across contrasting fertilization rates and cover crop treatments will help elucidate the mechanisms underlying observed changes in DRP loss. Sequential P extraction provides a valuable, albeit operational, framework for characterizing these changes. While this approach has inherent limitations such as a lack of strict chemical specificity and the potential for unintended extraction or reprecipitation of non-target P species, it remains a fundamental tool for partitioning soil P into pools based on relative solubility. Acknowledging these limitations, sequential fractionation still enables a robust, comparative evaluation of how cover cropping and P fertilization strategies mobilize or stabilize legacy P dynamics in agricultural soils.

Wang et al. (2021) reported that the long-term use of cover crops enhanced P bioavailability. Specifically, cover crop treatments significantly increased concentrations of total P, microbial P, organic P, and certain inorganic P fractions. Although the phosphate in these

fractions is considered not immediately plant-available, these fractions represent potentially bioavailable phosphate that could be mobilized through biological processes, such as root exudates and microbial interactions, under cover cropping systems (Vance et al., 2003; Wang et al., 2018; Zhou et al., 2017). Eichler-Löbermann et al. (2008) also reported that some cover crops could enhance the availability of phosphate during their growth period, potentially through the mobilization of soil phosphate. Rhizosphere acidification through proton release is one of the mechanisms by which cover crop roots facilitate nutrient uptake and, under low-P conditions, mobilize otherwise unavailable soil phosphate for plant absorption (Zhang et al., 2021).

In a study conducted by Raniro et al. (2025), growth of a single cover crop reduced soil pools of inorganic P (P_i) and organic P (P_o) extracted by $NaHCO_3$ ($NaHCO_3$-P_i and $NaHCO_3$-P_o), indicating a greater reliance on, and likely uptake from this pool; however, a cover crop mixture showed a greater depletion of P in pools extracted by NaOH and HCl (NaOH-P_i, NaOH-P_o, and HCl-P_i), likely due to complementary P acquisition strategies that enabled access to less available soil P pools. In another study conducted by Ye et al. (2020), cover cropping increased organic P stocks in the topsoil, which were dominated by NaOH-extractable organic P.

The objectives of this study were to evaluate the effects of cover cropping and P fertilization on soil P pools using the Hedley fractionation scheme. We hypothesized that cover crops take up phosphate from moderately soluble soil P fractions and recycle it into more soluble soil P fractions, thereby altering the distribution of soil P fractions as determined by Hedley fractionation. We further hypothesized that the effects of cover crops on soil P pools would vary with P fertilization rate due to differences in quantities of readily plant-available phosphate. Specifically, we hypothesized that the build-and-maintain (BM) strategy would disproportionately accumulate P in highly labile inorganic pools, whereas the build-and-

drawdown (BD) strategy would force the system to utilize these labile reserves, thereby reducing the highly soluble P pools and increasing the reliance on moderately stable P fractions.

Material and Methods

Experimental site and design

This research was carried out at the Kansas Agricultural Watershed field laboratory near Manhattan, Kansas from September 2019 through September 2022. The site was managed under a continuous no-till system with a corn–soybean rotation. Soils at the location are mapped as eroded Smolan silty clay loam (fine, smectitic, mesic Pachic Argiustoll) on slopes ranging from 3 to 7%. Before plot establishment for this experiment, the field was operated under a conventionally tilled winter wheat (*Triticum aestivum*)–soybean rotation, with the most recent tillage occurring in fall 2014. The region receives an average of 889 mm of precipitation annually based on 30-year records and experiences a continental climate characterized as hot and humid, with a mean annual temperature of 12.9 °C. This experiment, established in 2015, employed a randomized complete block design with a 2 × 3 factorial treatment structure. Two cover crop management treatments were included: plots with a cover crop (CC) and plots without a cover crop (NC). There were three levels of P fertilizer application rate: a control with no added P (CN), Build and draw down (BD), and Build and maintain (BM). Each treatment combination was replicated three times (n=3 per treatment; n = 18 total for plots), with replications blocked by landscape position.

Agronomic management

From fall 2014 through the 2019 crop year, the CC treatment consisted of either winter wheat or winter triticale (×Triticosecale Wittm.), grown alone or in combination with rapeseed (*Brassica napus* L.). From fall 2019 planting through fall 2022, the CC was cereal rye (Secale cereale), which was terminated with herbicide at or prior to planting the main crop. From fall 2014 through the 2019 cropping year, P fertilizer was applied annually to the BM and BD treatments at 27 kg P ha^{-1} yr^{-1} following Kansas State University's build-and-maintain recommendations (Leikam et al., 2003). Phosphorus was applied to the BM treatment as ammonium polyphosphate placed 5 cm below and 5 cm to the side of the seed at planting, and P was applied to the BD treatment as diammonium phosphate broadcast on the soil surface in the fall prior to planting.

From the fall 2019 planting through the fall 2022 crop year, the BM treatment received ammonium polyphosphate placed 5 cm below and 5 cm to the side of the seed at planting. The exact application rates to maintain soil test P over this period were 29, 22, and 21 kg P ha^{-1} in the 2020, 2021, and 2022 cropping years, respectively, averaging 24 kg P ha^{-1} yr^{-1}. From 2019 through fall 2022, the BD treatment did not receive any P fertilizer. The CN treatment did not receive any P fertilizer from the start of the experiment (fall 2014) through fall 2022. Additional details on agronomic management can be found in Nelson et al. (2023) and Bourns et al. (2026).

Sampling and Analysis of Biomass for Phosphorus Uptake

Biomass samples of the cover crop and main crops, including soybean and corn, were collected from three georeferenced subsample locations within each main plot. Samples of cover crop biomass were taken as close to the termination of the crop as possible, occurring nine days prior to termination in 2020, and within one day of termination in 2021 and 2022. To avoid loss

of plant biomass due to leaf drop, whole-plant soybean biomass samples were collected at the end of growth stage R6 or beginning of R7. For corn, ears were harvested at physiological maturity from an area measuring two rows by 9.1 m to quantify grain yield and cob biomass. After ear removal, ten intact plants were randomly chosen from the harvested area to assess stalk and leaf biomass. Plant tissue and grain samples were oven-dried, ground, and analyzed for P using a sulfuric-peroxide digestion method (Thomas et al., 1967) followed by analysis with an inductively coupled plasma optical emission spectrometer (ICP-OES; 720-ES, Varian, Santa Clara, CA). Additional details on biomass data collection are provided in Bourns et al. (2024).

To calculate the P uptake by different parts of the corn (cob, stover, and grain), the P concentration in each part was multiplied by the biomass (kg ha^{-1}) for that part. The P uptake for each part of the plant was summed to determine total P uptake by the corn plant for each plot in a given year. Finally, to evaluate the long-term biological P mobilization and removal over the course of the study, the annual data for each treatment were summed over the entire 8-year period (from 2015 to 2022) and divided by eight to determine the mean annual P uptake, residue P return, and grain P removal (kg P ha^{-1} yr^{-1}).

Equations used to calculate P uptake and return

To accurately quantify the annual and 8-year mean annual flow of P through the cropping system across the study period (t, where t = 2015 to 2022; n = 8 years), the following equations were utilized:

1. **Annual P Uptake by Corn (Ucorn,t):**

$$Ucorn, t = (Bcob, t \times \%Pcob, t) + (Bstover, t \times \%Pstover, t) + (Bcorn\ grain, t \times \%Pcorn\ grain, t)$$

2. **Annual P Uptake by Soybean (Usoybean,t):**

$$Usoybean, t = Bsoybean\ whole\ plant, t \times \%Psoybean\ whole\ plant$$

3. Annual P Uptake by Cover Crop (Ucover crop,t):

$U_{cover\ crop,\ t} = B_{cover\ crop\ whole\ plant,\ t} \times \%P_{cover\ crop\ whole\ plant}$

4. Mean Annual Total Plant P Uptake (UTotal):

$$U_{Total} = [\sum_{t=2015}^{2022} U_{corn,\ t} + \sum_{t=2015}^{2022} U_{soybean,\ t} + \sum_{t=2015}^{2022} U_{cover\ crop,\ t}] / 8$$

5. Annual P Return by Corn (Rcorn,t):

$R_{corn,\ t} = U_{corn,\ t} - U_{corn\ grain,\ t}$

6. Annual P Return by Soybean (Rsoybean,t):

$R_{soybean,\ t} = U_{soybean\ whole\ plant,\ t} - U_{soybean\ grain,\ t}$

7. Annual P Return by Cover Crop (Rcover crop,t):

$R_{cover\ crop,\ t} = U_{cover\ crop,\ t}$

8. Mean Annual Total Plant P Return (RTotal):

$$R_{Total} = [\sum_{t=2015}^{2022} R_{corn,\ t} + \sum_{t=2015}^{2022} R_{soybean,\ t} + \sum_{t=2015}^{2022} R_{cover\ crop,\ t}] / 8$$

9. Mean Annual Grain P Removal (RemovalTotal):

$$Removal_{Total} = [\sum_{t=2015}^{2022} U_{corn\ grain,\ t} + \sum_{t=2015}^{2022} U_{soybean\ grain,\ t}] / 8$$

Where U and R represent the annual P uptake and residue P return (kg P ha^{-1} in year t, and kg P ha^{-1} yr^{-1} for the 8-year mean annual fluxes UTotal, RTotal, and RemovalTotal), B and %P denote the dry biomass yield (kg ha^{-1}) and tissue P concentration (expressed as a decimal fraction) of the specified plant components in year t, and $U_{corn\ grain,t}$ ($B_{corn\ grain,t} \times \%P_{corn\ grain,t}$) and $U_{soybean\ grain,t}$ ($B_{soybean\ grain,t} \times \%P_{soybean\ grain,t}$) indicate the P permanently exported from the field via grain harvest in year t. For soybean, because whole-plant biomass was sampled at growth stage R5 prior to leaf drop to capture total P uptake ($U_{soybean,t}$), annual

soybean P return (Rsoybean,t) was calculated by subtracting harvested soybean grain P removal (Usoybean grain,t) from whole-plant soybean P uptake.

Soil Sample Collection and Processing

From 2019 to 2022, composite soil samples (21 cores per composite) were collected from three depth intervals (0–2.5, 2.5–5, and 5–15 cm) after harvest each fall at three geo-referenced subplot locations within each plot. Samples were air-dried, ground, and sieved to <2 mm. Composite soil samples representing 0 to 5-cm were made by combining 10 g of soil from the 0–2.5 cm depth and 10 g from the 2.5–5 cm depth for each sampling point. The resulting subsamples from the three points were then thoroughly mixed to form a single 0 to 5-cm composite sample for each plot.

Hedley Sequential Fractionation Method

Air-dried soil (0.5 g) was weighed into 50-mL centrifuge tubes and subjected sequentially to a series of extraction procedures following the method of Tiessen and Moir (1993). After each extraction step, samples were centrifuged at 10,000 rpm for 15 min, and the supernatants were carefully filtered through Whatman 0.45-µm syringe filters. The filtered supernatants were stored at 4 °C until analysis. A summary of the extraction procedure can be found in Table 3-1.

Concentrations of P in extracts from the first step (resin-extractable P) were analyzed with the molybdate-blue colorimetric method (Murphy & Riley, 1962) using a Beckman Coulter DU-800 spectrophotometer (Brea, CA). Samples from the second and third extraction steps were analyzed for inorganic P (P_i) using the molybdate-blue colorimetric method via a spectrophotometer, and for total extractable P (P_t) using an ICP-OES. The colorimetric P or

molybdate reactive P (MRP) is assumed to be inorganic P (P_i), while ICP-OES measures total P (P_t) in each extract. The difference between P_t and MRP is called molybdate-unreactive P (MUP), which is assumed to be organic P (P_o). Samples from the HCl extraction step were analyzed only by ICP-OES, as it was assumed that $P_t = P_i$ in this fraction. Residual P was calculated by subtracting the sum of all extracted P pools from the soil total P concentration, which had been determined previously by perchloric acid digestion and ICP-OES analysis (Olsen & Sommers, 1982; Sommers & Nelson, 1972).

Table 3-1. Summary of the extractants and operational procedure used for the modified Hedley sequential P fractionation in this study (Tiessen and Moir, 1993).

Step	Extractant	Method Detail	Defined Fraction	Analytical Method
Step 1	Water and Resin	Weighed 0.5 g of soil into a 50 ml tube, added 2 resin strips and 30 ml deionized water, and shaken overnight (16 h). Removed resins, washed with water, placed in clean tubes with 30 ml of 0.5 M NaCl, and shaken overnight (16 h).	Resin-P_i	Determined P_i colorimetrically
Step 2	$NaHCO_3$ (0.5 M)	Centrifuged the soil suspension from Step 1, filtered through 0.45 µm, added 30 ml of $NaHCO_3$, and shaken overnight (16 h).	$NaHCO_3$-P_i, $NaHCO_3$-P_o	Determined TP (ICP-OES) and P_i (colorimetrically); P_o calculated as TP - P_i
Step 3	NaOH (1.0 M)	Centrifuged the suspension from Step 2, filtered through 0.45 µm, added 30 ml of NaOH, and shaken overnight (16 h).	NaOH-P_i, NaOH-P_o	Determined TP (ICP-OES) and P_i (colorimetrically); P_o calculated as TP - P_i
Step 4	HCl (1.0 M)	Centrifuged the suspension from Step 3, filtered through 0.45 µm, added 30 ml of HCl, and shaken overnight (16 h).	HCl-TP	Determined TP (ICP-OES)
Step 5	Residual P	Calculated fraction.	Residual-TP	Subtracted the sum of all extracted fractions from the total soil P

Statistical Analysis

Analysis of variance was used to determine if treatments affected P concentrations in sequential extraction. Fixed effects of the model include replication, P fertilizer management practice, cover crop, soil sampling year, and all high-order interactions among fertilizer practice, cover crop, and soil sampling year. The protected LSD test with $\alpha = 0.05$ was used for mean separation within the year. Statistical analysis was performed using Statistical Analysis Software (SAS version 9.4; Cary, NC) proc glimmix with the option DDFM = KR. Transformed least squares means and standard errors (log(n + 0.5) or centered log-ratio transformed) for all ^{31}P-NMR soil phosphorus compounds and compound classes are provided for reference in the supplementary material (Appendix A, Table A1).

Results

Phosphorus uptake and redeposition (return)

Total annual P uptake (the sum of P assimilated by both the main crops and the cover crops, expressed as kg ha^{-1} yr^{-1}) was greater under CC than under NC (Figure 3-1a). Additionally, P fertilization significantly influenced P uptake; the CN treatment had lower total annual P uptake than both fertilized treatments (BD and BM), whereas BD and BM did not differ significantly from each other (Figure 3-1b).

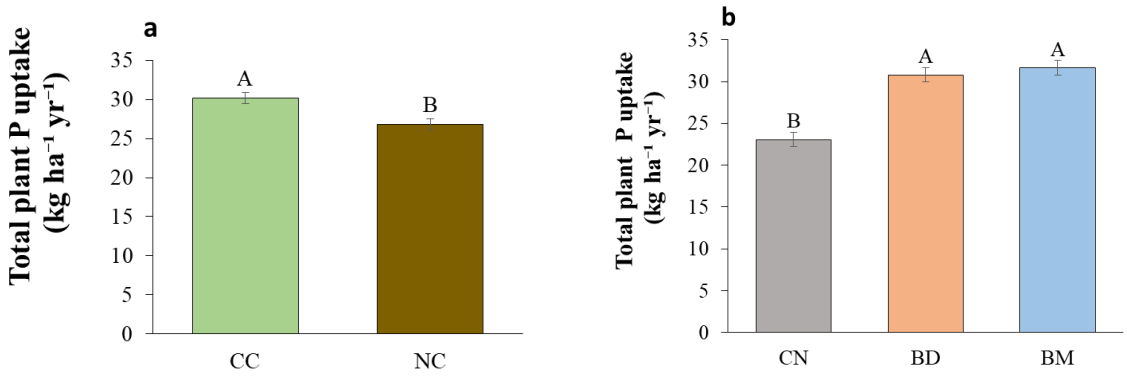


Figure 3-1. The main effect of cover cropping (a) and the main effect of P fertilization (b) on mean annual total plant P uptake (main crops plus cover crop, kg P ha^{-1} yr^{-1}) across the 8-year study period (2015 to 2022). Means within a panel containing the same letter are not significantly different at α = 0.05. Error bars represent the standard error of the mean. Abbreviations: control (CN), build and drawdown (BD), build and maintain (BM), no cover crop (NC), and with cover crop (CC).

To quantitatively evaluate the main and interacting effects of treatments on these crop parameters, an analysis of variance was conducted (Table 3-2).

Table 3-2. Analysis of variance (p-values) for the main and interacting effects of cover crop and phosphorus fertilization on mean annual total plant P uptake (main crops plus cover crop), total plant P return, and grain P removal across the 8-year study period (2015–2022).

Source of Variation	df	Total Plant P Uptake	Total Plant P Return	Grain P Removal
Block	2	0.280	0.536	0.098
Cover Crop (CC)	1	**0.007**	**< 0.001**	0.146
Fertilizer (Fert)	2	**< 0.001**	**0.001**	**< 0.001**
CC × Fert	2	0.884	0.247	0.580

Mean annual total plant P return (kg P ha^{-1} yr^{-1} returned to the soil via unharvested main crop and cover crop residues across the 8-year period) was significantly greater under

CC than under NC (Figure 3-2a). Additionally, P fertilization significantly influenced mean annual P return; the CN treatment had lower P return than both fertilized treatments (BD and BM), while BD and BM did not differ significantly from each other (Figure 3-2b). Mean annual grain P removal via harvested corn and soybean grain (kg P ha^{-1} yr^{-1} across the 8-year period) was significantly lower in the CN treatment compared to BD and BM, with no significant difference between BD and BM (Figure 3-2c) or between CC and NC (p = 0.146; Table 3-2).

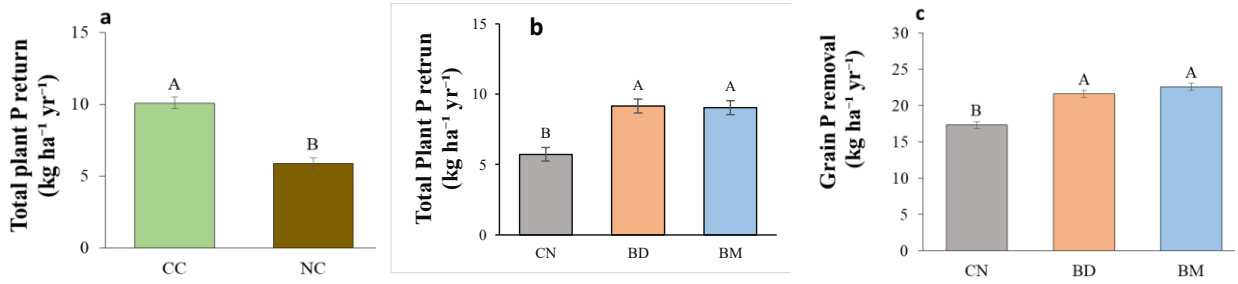


Figure 3-2. The main effect of cover cropping on mean annual total plant P return (a), and the main effect of P fertilization on mean annual total plant P return (b) and mean annual grain P removal (c) (kg P ha^{-1} yr^{-1}) across the 8-year study period (2015 to 2022). Means within a panel containing the same letter are not significantly different at α = 0.05. Error bars represent the standard error of the mean. Abbreviations: control (CN), build and drawdown (BD), build and maintain (BM), no cover crop (NC), and cover crop (CC).

Phosphorus Pools Determined by Sequential Fractionation

The significant interaction between P fertilization and cover cropping for Resin-P_i indicates that the influence of cover crops on soil labile P concentration depended on fertilization level. Cover cropping significantly reduced Resin-P_i in the BD and BM treatments, whereas no difference was observed between CC and NC plots in the CN treatment (**Error! Reference source not found.**a).

Table 3-3. Analysis of variance (p-values) for the main and interacting effects of cover crop, phosphorus fertilization, and sampling year on sequentially extracted soil phosphorus pools.

Source of Variation	Resin-P_i	$NaHCO_3$-P_t	$NaHCO_3$-P_i	$NaHCO_3$-P_o	NaOH-P_t	NaOH-P_i	NaOH-P_o	HCl-P_i	Residual-P
Cover	**0.003**	0.131	**0.020**	0.296	0.338	0.285	**0.035**	0.872	0.064
Fert	**< 0.001**	**< 0.001**	**< 0.001**	**0.002**	**< 0.001**	**< 0.001**	0.117	0.507	0.611
Cover × Fert	**0.013**	0.479	0.075	0.379	0.688	0.828	0.290	0.109	0.837
Year	**< 0.001**	**< 0.001**	**< 0.001**	0.132	**< 0.001**	**< 0.001**	**< 0.001**	0.184	**0.001**
Cover × Year	0.055	0.207	0.598	0.700	0.708	0.619	0.945	0.145	0.496
Fert × Year	**< 0.001**	**< 0.001**	**< 0.001**	**0.006**	**0.003**	**< 0.001**	**< 0.001**	0.162	0.486
Cover × Fert × Year	0.084	**0.030**	0.316	0.323	0.291	0.354	0.120	0.199	0.536

Note: Statistically significant effects ($p < 0.05$) are highlighted in bold.

The interaction of year and P fertilization was also significant for Resin-P_i concentrations. The Resin-P_i fraction differed markedly among P fertilization strategies and exhibited distinct temporal trends (**Error! Reference source not found.**b). Across all years, Resin-P_i was greatest in the BM treatment, intermediate in the BD treatment, and lowest in CN. Resin-P_i declined from 2019 to 2020 across all fertilized treatments; however, Resin-P_i in BM recovered after 2020 and increased through 2022, whereas BD remained at intermediate levels thereafter. Resin-P_i in the control treatment remained consistently low and showed no significant change after 2020. These patterns indicate that fertilization strategy influenced both the magnitude and temporal dynamics of Resin-P_i.

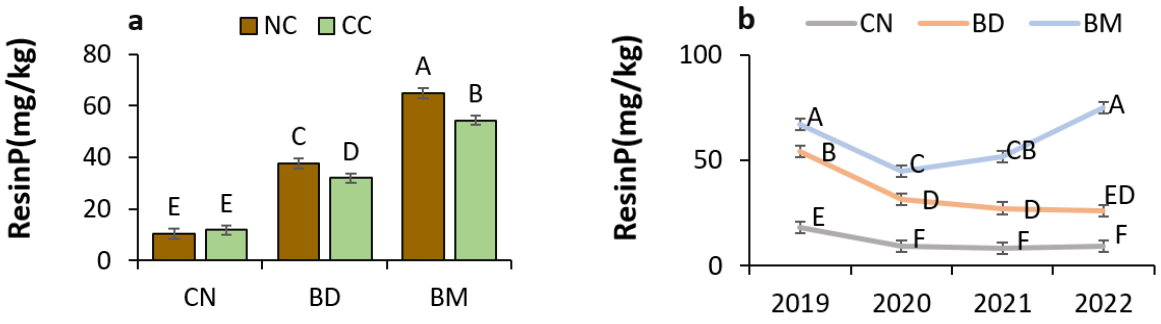


Figure 3-3. The interaction of phosphorus (P) fertilization and cover cropping on Resin-P_i (a) and the interaction of P fertilization and year on Resin-P_i concentrations (b). Means within a treatment containing the same letter are not significantly different at $\alpha = 0.05$. Abbreviations: control (CN), build and drawdown (BD), build and maintain (BM), no cover crop (NC), and with cover crop (CC).

A significant three-way interaction among P fertilization, cover cropping, and year was observed for $NaHCO_3$-P_t concentration. Comparing the effect of CC within each fertilization treatment and year reveals that the presence of cover crops did not significantly alter $NaHCO_3$-P_t concentrations compared to NC in any treatment from 2019 to 2021. The only significant CC effect emerged in 2022 under the BM treatment, where the inclusion of CC significantly reduced $NaHCO_3$-P_t compared to the NC-BM plot. Furthermore, while the BM treatment generally exhibited the highest $NaHCO_3$-P_t concentrations in later years, BM and BD were not statistically different from each other under NC in 2019 and 2020, nor were they different under CC in 2020 (**Error! Reference source not found.**4).

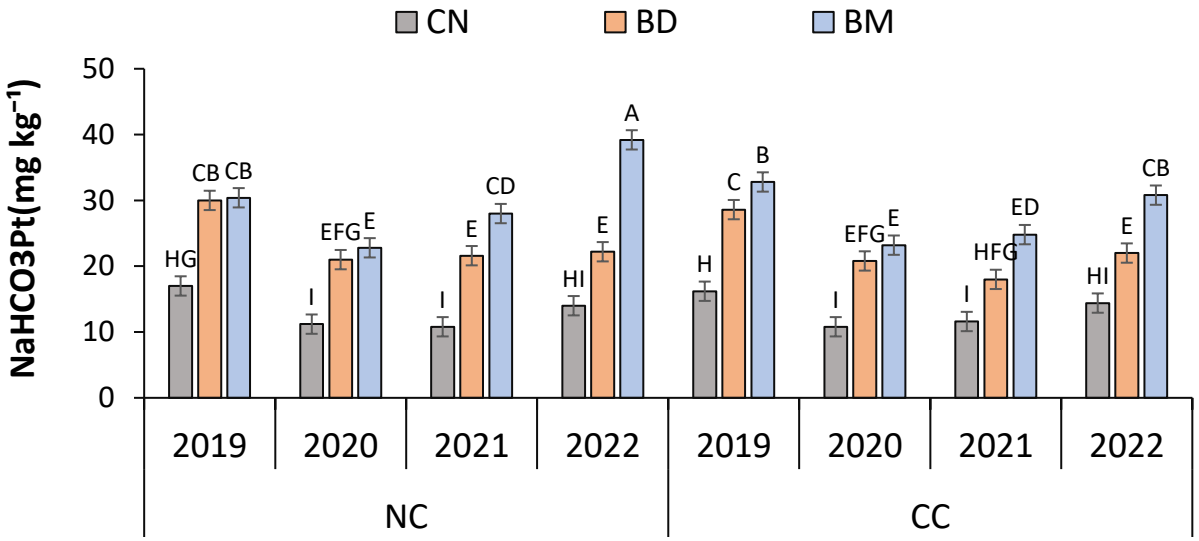


Figure 3-4.The interaction of cover cropping, year, and P fertilization on $NaHCO_3$-P_t concentration. Means within a treatment containing the same letter are not significantly different at $\alpha = 0.05$. Abbreviations: control (CN), build and drawdown (BD), build and maintain (BM), no cover crop (NC), and with cover crop (CC).

The main effect of cover cropping was significant for $NaHCO_3$-P_i concentrations, with the NC treatment higher than the CC treatment (**Error! Reference source not found.**a). The interaction of year and P fertilization was also significant for $NaHCO_3$-P_i concentrations ; **Error! Reference source not found.**b). In CN and BD, the $NaHCO_3$-P_i concentration decreased from 2019 to 2020 and then remained constant. For the BM treatment, the $NaHCO_3$-P_i concentration decreased from 2019 to 2020 but then increased in each of the remaining years.

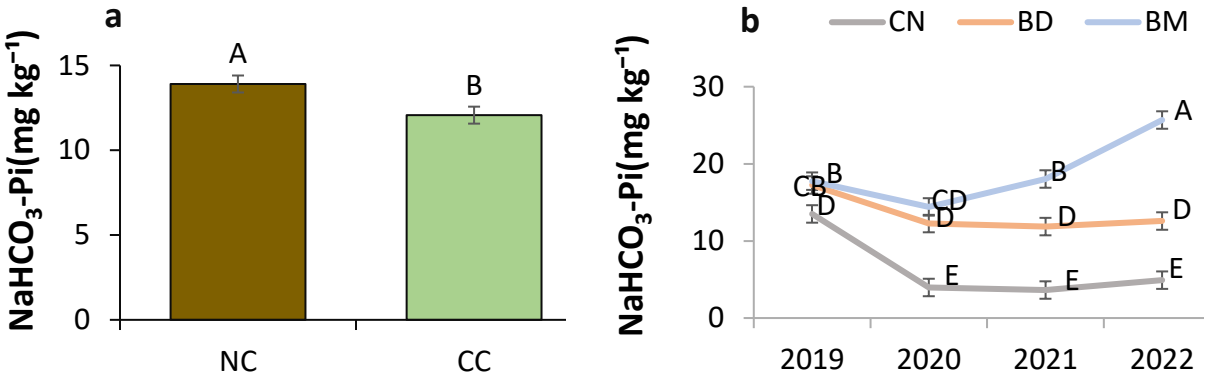


Figure 3-5. The main effect of cover cropping (a) and the interaction of P fertilization and year (b) on $NaHCO_3$-P_i concentration. Means within a treatment containing the same letter are not significantly different at $\alpha = 0.05$. Abbreviations: control (CN), build and drawdown (BD), build and maintain (BM), no cover crop (NC), and with cover crop (CC).

The interaction of year and P fertilization was significant for $NaHCO_3$-P_o concentrations (Table 3-3). In 2019, the $NaHCO_3$-P_o concentration for the CN treatment was significantly less than that of the BD and BM treatments; however, there were no significant P fertilization treatment effects in the subsequent years from 2020 through 2022 (Figure 3-6).

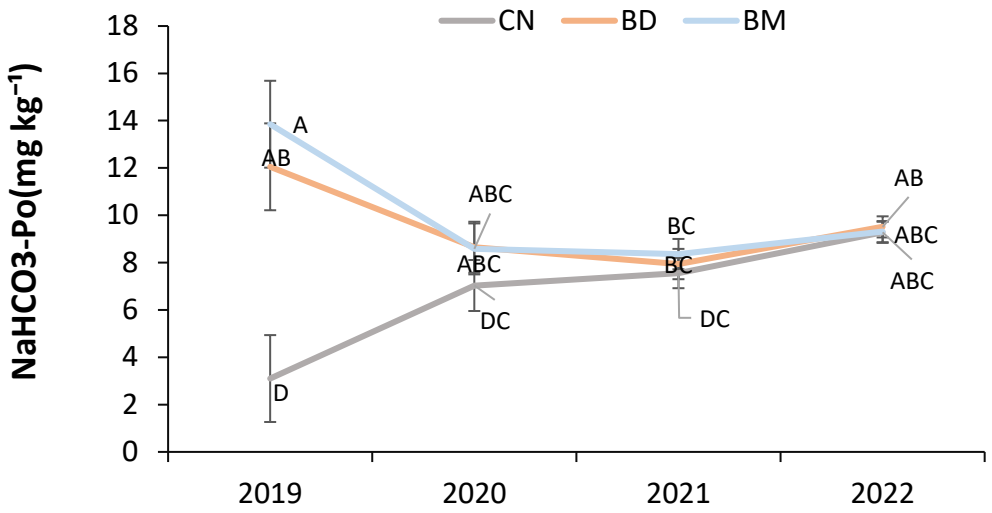


Figure 3-6.The interaction of P fertilization and year on $NaHCO_3$-P_o concentration. Means within a treatment containing the same letter are not significantly different at $\alpha = 0.05$. Abbreviations: control (CN), build and drawdown (BD), and build and maintain (BM).

The interaction of P fertilization and year was significant for NaOH-P_t and NaOH-P_i concentrations. In CN, NaOH-P_t concentration remained constant from 2019 to 2022 and was always significantly lower than the BD and BM treatments (**Error! Reference source not found.**7a). The NaOH-P_t concentrations were not significantly different between the BD and BM treatments from 2019 to 2021; however, in 2022, the concentration increased for the BM treatment. The NaOH-P_i concentration was significantly lower in CN than BD and BM treatments in 2019, 2020, and 2022, but was not significantly different from BD in 2021 (**Error! Reference source not found.**7b). In all treatments, the NaOH-P_i concentration decreased significantly from 2019 to 2020. In 2022, the concentration increased for the BM treatment only.

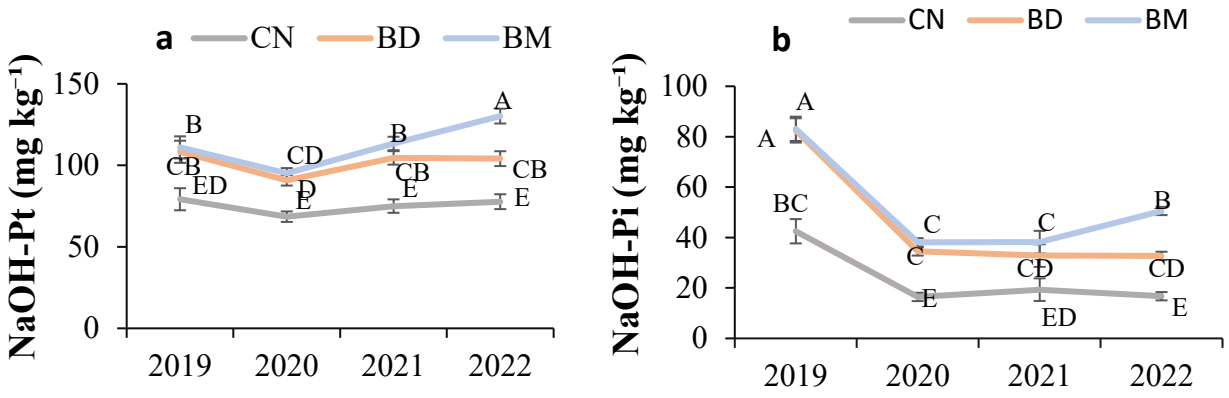


Figure 3-7. The interaction of P fertilization and year on NaOH-P_t (a) and NaOH-P_i (b) concentrations. Means within a treatment containing the same letter are not significantly different at $\alpha = 0.05$. Abbreviations: control (CN), build and drawdown (BD), and build and maintain (BM).

The main effect of cover cropping on NaOH-P_o concentration was significant with greater NaOH-P_o concentrations under CC compared to NC (**Error! Reference source not found.**8a). Also, the interaction of P fertilization and year was significant for NaOH-P_o . In all P fertilizer treatments, the NaOH-P_o concentration increased from 2019 to 2022. The BD and BM treatments were not significantly different from each other in any year, and both were significantly greater than the CN treatment in 2021 and 2022 (**Error! Reference source not found.**8b).

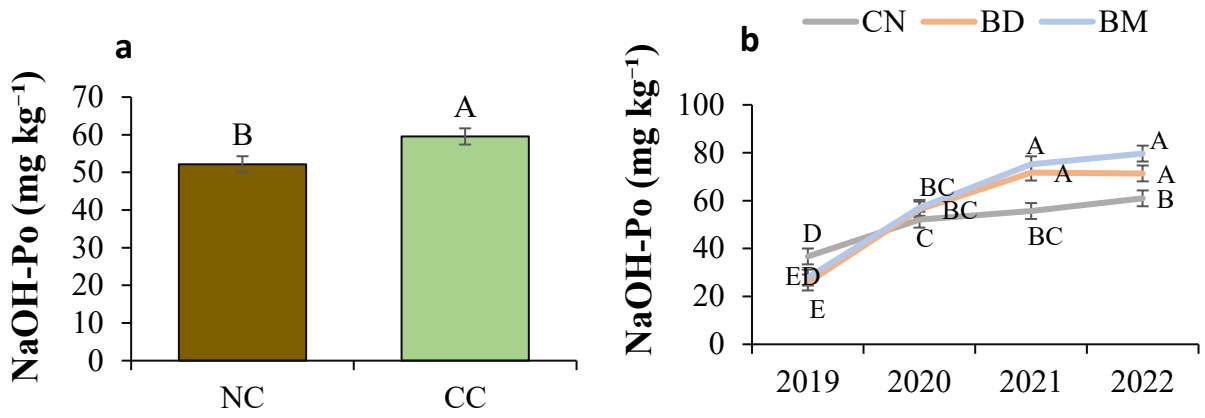


Figure 3-8. The main effect of cover cropping on NaOH-P_o (a) and the interaction of P fertilization and year on NaOH-P_o (b). Means within a treatment containing the same letter are not significantly different at $\alpha = 0.05$. Abbreviations: control (CN), build and drawdown (BD), build and maintain (BM), no cover crop (NC), and with cover crop (CC).

Neither cover cropping, P fertilization, nor year significantly affected HCl-P_i concentrations (Table 3-3). The main effects of the treatments on the highly stable pools (HCl-P_i and Residual-P) are summarized in Table 3-4.

Table 3-4. Main effects of cover cropping and P fertilization on HCl-P_i and Residual-P concentrations (mg kg^{-1}).

Treatment	Level	HCl-P_i	Residual-P
Cover Crop	NC	76.8 ± 5.3 a	173.3 ± 4.3 a
	CC	78.1 ± 5.3 a	161.2 ± 4.3 a
Fertilizer	CN	71.2 ± 6.4 a	166.1 ± 5.3 a
	BD	79.7 ± 6.4 a	171.5 ± 5.3 a
	BM	81.4 ± 6.4 a	164.3 ± 5.3 a

Note: Values are presented as Mean ± Standard Error. Means followed by the same letter within a column and treatment group are not significantly different at α = 0.05.

However, the concentration of the residual P fraction varied significantly across the four years of the study (2019–2022) (Figure 3-9). The highest accumulation of residual P was observed in 2020 (194.6 ± 8.8 mg P kg^{-1}), which was significantly greater than all other years ($p < 0.05$). Following this peak, the residual P pool exhibited a significant and progressive decline, dropping to 169.8 ± 5.7 mg P kg^{-1} in 2021 and reaching its lowest concentration of 149.8 ± 3.6 mg P kg^{-1} in 2022. The baseline concentration in 2019 (154.8 ± 6.8 mg P kg^{-1}) acted as an intermediate, showing no significant statistical difference from either 2021 or 2022. This temporal dynamic suggests a significant fluctuation in the highly recalcitrant P pool, likely driven by annual variations in weather, crop uptake demands, or shifts in long-term P fixation mechanisms. Furthermore, it is highly possible that this temporal fluctuation was additionally influenced by inherent sampling variations from one year to the next; although sampling protocols were strictly standardized, the random year effect and minor spatial variabilities cannot be entirely ruled out.

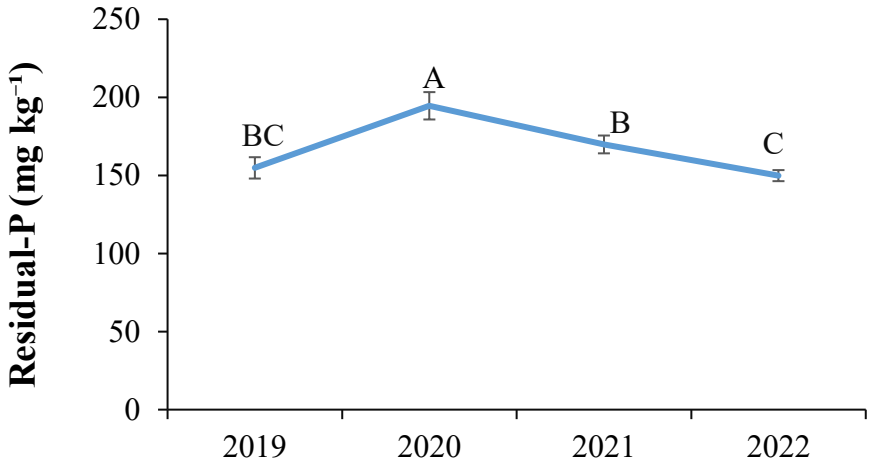


Figure 3-9. Mean concentration of the residual phosphorus (Residual-P) fraction over the four-year study period (2019–2022). Error bars represent the standard error of the mean.

Discussion

In the Hedley sequential fractionation scheme, soil P is operationally separated into pools that differ in their relative solubility, ranging from readily soluble to highly stable forms. Resin-P_i and $NaHCO_3$-P_i, which are considered to be more labile P, consist of P_i adsorbed on the surfaces of more crystalline P compounds, sesquioxides, or carbonates (Mattingly, 1975). The organic fraction extracted by sodium bicarbonate ($NaHCO_3$-P_o) is thought to be easily mineralizable and contributes to plant-available phosphate (Bowman & Cole, 1978). Furthermore, the NaOH-P_i fraction has lower solubility (Marks, 1977) and is thought to be associated with amorphous and some crystalline Al and Fe phosphates. Additionally, the NaOH-P_o fraction represents a more stable form of P_o involved in the long-term transformations of P in soils (Batsula & Krivonosova, 1973). The HCl-P_i fraction is typically associated with relatively insoluble phosphates, including Ca-phosphates and is considered relatively stable. Although these operationally defined fractions are often interpreted in terms of specific chemical associations and relative availability, more recent studies using advanced analytical techniques suggest that it is not possible to assign strict chemical specificity to individual P fractions derived from sequential extraction procedures (Barrow et al., 2021; Gu & Margenot, 2021).

In contrast to our hypothesis that cover crops would mobilize phosphate from less soluble soil P fractions and recycle it into more labile pools, our results showed that Residual-P was not influenced by either cover cropping or P fertilization. Similar findings have been reported in tropical oxisols under soybean/cotton rotation by Rodrigues et al. (2016, 2021) and in highly weathered soils under long-term no-till cropping systems (Tiecher et al., 2012a, 2012b).

Notably, we observed no depletion of Residual-P in either the CN or BD treatments, despite the absence of P fertilizer application. This lack of depletion was consistent even in the

control treatment with cover crops (CN-CC). Rather than tapping into highly recalcitrant pools, crops and microorganisms under P scarcity likely upregulated phosphatase enzyme exudation to extract P from more accessible moderately labile organic pools (Richardson & Simpson, 2011). This differs from the results of Gatiboni et al. (2007), who documented a profound depletion of the Residual-P fraction after twelve consecutive crops without fertilization, suggesting that residual P can become available only when more labile fractions are severely depleted (McLaren et al., 2014; Wang et al., 2008). In our study, moderately labile pools such as NaOH-P_t remained sufficiently large to buffer plant uptake in the control treatments. Therefore, the soil did not reach the extreme deficiency threshold required to trigger the mobilization of the highly recalcitrant Residual-P pool, unlike the severe starvation conditions induced in the highly weathered soils studied by Gatiboni et al. (2007).

Consistent with our finding that fertilization did not alter the highly stable P fraction, Gatiboni et al. (2007) also reported that P fertilizer additions failed to enrich the Residual-P pool. This is further supported by the findings of Pätzold et al. (2013), where long-term P fertilization (applied at rates significantly exceeding crop removal over a 14-year period) resulted in only minor changes in Residual-P compared to massive accumulations in the more reactive fractions, indicating limited transfer of added P into highly recalcitrant pools. However, this contrasts with Teles et al. (2017), who, in a field study on highly weathered tropical soils under repeated rock phosphate and soluble P fertilizer application, found that Residual-P increased in the 0–5 cm soil layer. Similarly, HCl-P_i was unaffected by our treatments, aligning with Rodrigues et al. (2021), who observed no changes in HCl-P_i under their management practices, including cover crops.

Our data also suggests that P fertilization is the dominant driver of Resin-P_i, with a clear gradient of BM > BD > CN, regardless of CC. Ammonium polyphosphate has been applied as a

fertilizer that can hydrolyze to plant-available phosphate shortly after application. A portion of the added phosphate remains in the soil solution or loosely adsorbed to exchange sites, resulting in higher Resin-P_i in fertilized treatments. Teles et al. (2017) also reported that P fertilizers (applied annually at 35 kg P ha^{-1}, vastly exceeding crop removal on clayey subtropical Oxisols) significantly increased all the labile P fractions, including Resin-P_i, $NaHCO_3$-P_i, and $NaHCO_3$-P_o in the top 0–5 cm layer. In another study, Silva et al. (2025) reported that intensive application of lime and gypsum to correct soil acidity combined with P fertilization and legume cultivation in tropical soils increased labile P pools.

In another study conducted by Wu et al. (2022), which was a long-term field fertilization experiment in China (different rates of P fertilizer application for 25 years in calcareous soils), Hedley sequential fractionation showed that long-term application of P fertilizers increased the proportion of labile P (Resin-P_i, $NaHCO_3$-P_i, and $NaHCO_3$-P_o) and moderately labile P fractions (such as NaOH-P_i, NaOH-P_o) while decreasing the proportion of non-labile P (HCl-P_i and Residual-P) relative to the unfertilized control plots, indicating a shift toward more soluble and potentially more plant-available forms with P addition. These findings are consistent with a study on P pool composition in soils and sediments of transitional ecotones under agricultural influence, which also reported that agricultural inputs shift P pools toward more labile (Resin-P_i and $NaHCO_3$-P_i) fractions (Neidhardt et al., 2019). Similar results have also been reported by Pätzold et al. (2013), where long-term P fertilization resulted in increased P concentrations in labile (Resin-P_i and $NaHCO_3$-P_i) and moderately labile (NaOH-P_i and NaOH-P_o) fractions.

Our study also indicated that Resin-P_i was lower in cover crop treatments in comparison to no cover crop treatments, and this was similar to the findings of Rodrigues et al. (2021) who found that in one study site, cover crop did deplete Resin-P_i; however, in another study site,

cover crop increased Resin-P_i and $NaHCO_3$-P_i. In addition, Teles et al. (2017) also reported that cover crops, including ryegrass, depleted Resin-P_i compared to fallow treatments. They further stated that this depletion might be explained by the plant uptake of the added fertilizer P by the cover crops. This mechanism is strongly corroborated by our data: both total cover crop P uptake and the subsequent depletion of Resin-P_i were significantly greater in the fertilized treatments (BM and BD) compared to the unfertilized control. This suggests that vigorous uptake by the cover crop actively depleted the labile soil P pool wherever the P supply was sufficient.

Plant P uptake was also higher in BD and BM than in CN treatments, consistent with greater P availability in those treatments due to active or historical fertilization. Together, these results indicate that P fertilization established a larger available P pool, which enabled greater cover crop P uptake and subsequent drawdown of resin-extractable P. In contrast, limited P availability in the control constrained both plant uptake and changes in resin-extractable P. Furthermore, the lack of significant changes in the more stable P fractions during the BD phase indicates that the relatively short duration of the drawdown period (three years) was simply not long enough to significantly remobilize the highly recalcitrant residual P pool.

In contrast, studies of green manure decomposition have reported that the release of P from rapidly decomposing biomass and microbial activity can increase labile P fractions, such as H_2O-P_i and $NaHCO_3$-P_i, through mineralization of organic P and solubilization of inorganic P (Khan et al., 2025). This rise in labile P was accompanied by a decline in non-labile P pools, especially more stable fractions such as concentrated HCl-P_o relative to initial pre-amendment soil tests, indicating a transformation of P from less available to more available forms. This contrast highlights that the fate of soil P under plant residue inputs depends on initial soil P availability, microbial activity, and residue type. While Khan et al. (2025) added highly labile,

low C:P ratio leguminous green manure to severely P-deficient soils, our study utilized a high C:P ratio cereal rye cover crop in historically fertilized soils; consequently, our results show that under these specific field conditions, strong plant uptake drives a net shift from highly labile phosphate pools to less labile MUP (organic P) fractions.

The lower Resin-P_i concentration observed under CC coincided with greater NaOH-extractable organic P (NaOH-P_o) concentration, indicating a redistribution of fertilizer-derived P from immediately available pools (Resin-P_i) into less labile MUP (organic) forms (NaOH-P_o). This pattern suggests enhanced biological assimilation (immobilization) of fertilizer-derived P followed by stabilization in organic soil P pools, rather than accumulation in resin-extractable forms. However, an alternative explanation is that the decline in Resin-P_i primarily reflects preferential plant and microbial uptake of labile phosphate, resulting in a relative enrichment of the more stable NaOH-P_o fraction. Thus, the observed shift may arise from a combination of active transformation of phosphate into organic forms and the selective depletion of labile phosphate pools.

Similar increases in NaOH-P_o under cover cropping have been reported by Rodrigues et al. (2021) in tropical soils from Brazil, where *Brachiaria* promoted the accumulation of this fraction. In other words, CC appears to shift P from immediately available pools to more stable organic forms (Linquist et al., 1997; Teles et al., 2017; Tiecher et al., 2012a, 2012b). While this organic pool requires subsequent enzymatic mineralization before it can be utilized by cash crops—thus temporarily reducing the immediately bioavailable pool—it acts as a protected, slow-release reservoir that buffers against immediate dissolved P runoff losses associated with elevated Resin-P_i, ultimately maintaining long-term P cycling within the agroecosystem (Helfenstein et al., 2020). Similar results have also been reported by Leite et al. (2024) in a long-

term field study conducted under a no-tillage system on a highly weathered tropical soil, where they observed that a single cover crop promoted the conversion of Resin-P_i and $NaHCO_3$-P_i to NaOH-P_i in the 0–0.1 m soil layer, suggesting a comparable shift from readily available to more strongly bound P pools, although in their case the increase occurred in the inorganic NaOH fraction rather than the organic fraction. However, given the strong differences in soil mineralogy and weathering status between those highly weathered tropical soils and the soils in the present study, direct comparisons should be made with caution.

In the BM treatment, Resin-P_i, $NaHCO_3$-P_i, and NaOH-P_i decreased from 2019 to 2020. This decline corresponded with a sharp reduction in the actual P fertilizer applied in 2020 to match updated soil test requirements, dropping from the historical rate of 27 kg P ha^{-1} and averaging 24 kg P ha^{-1} over the 2020–2022 period. Between 2021 and 2022, however, these P pools (Resin-P_i, $NaHCO_3$-P_i, and NaOH-P_i) increased again. This buildup is directly corroborated by our crop P removal data, which demonstrated significantly lower P harvest removal in 2022 compared to previous years due to reduced grain yields, resulting in less P being exported from the field and a consequent accumulation in the labile pools.

In the BD treatment, Resin-P_i, $NaHCO_3$-P_i, and NaOH-P_i also declined from 2019 to 2020, again coinciding with a reduction in the P fertilizer application rate. During the subsequent drawdown period, when no P fertilizer was applied, these pools remained relatively stable. Interestingly, there was no significant decrease in the residual P pool or the HCl-P_i pool. This raises an important question: if these more stable P pools did not significantly decline, from which source did the crop obtain the P required to sustain its growth? One possible explanation is that the crops may have accessed P from deeper soil layers, because the present analysis was conducted only on surface soil samples (0–5 cm). Another possible explanation is that surface-

retained crop residues likely contributed to P availability during the drawdown period through decomposition and leaching of soluble phosphate. However, it is also highly possible that the sequential P fractionation method lacks the analytical sensitivity required to capture these subtle changes. Because the extraction process can unintentionally extract non-target species and cause the reprecipitation of the extracted P, minor shifts in stable pools may be obscured. Therefore, relying solely on operational extractions may mask true mechanistic shifts. Future assessments would benefit from integrating more direct spectroscopic techniques, such as solution ^{31}P nuclear magnetic resonance (NMR) to successfully differentiate specific organic P compounds, and X-ray absorption near-edge structure (XANES) spectroscopy to successfully differentiate inorganic forms, such as Fe-bound P from Ca-bound P.

Although NaOH-P_o increased under cover cropping, the specific chemical forms comprising this pool cannot be resolved using the fractionation approach employed in this study. The NaOH-P_o fraction represents an operationally defined pool that may include a range of P_o compounds with differing stability and bioavailability. Advanced spectroscopic techniques, such as solution ^{31}P-NMR spectroscopy, are therefore required to directly characterize P_o speciation. Furthermore, because ^{31}P-NMR is not necessarily capable of speciating all P pools and is limited in separating inorganic P pools, Fe K-edge and P K-edge XANES spectroscopy should also be employed to accurately characterize inorganic P speciation.

Conclusion

Overall, these results suggest that cover crops redistributed legacy P among soil pools rather than simply depleting it. While the treatments did not significantly alter the overall mean of the residual P pool, the significant temporal depletion of residual P observed after 2020 highlights that this recalcitrant pool is not entirely static and can be influenced by annual

biological or climatic fluctuations, which ultimately impacts the P fractionation outcome. The decrease in Resin-P_i and $NaHCO_3$-P_i indicates that the most labile, plant-available fractions of previously accumulated P were reduced, likely due to plant uptake and biological immobilization. At the same time, the increase in NaOH-P_o under cover cropping suggests that part of this P was incorporated into P_o forms associated with microbial biomass or OM, which are extracted in the NaOH-P_o fraction. Therefore, instead of indicating a net loss of legacy P, our data imply that cover crops shift legacy P from readily available inorganic pools toward more biologically mediated organic pools, potentially enhancing long-term availability of P in soil while temporarily reducing the size of the immediately available P pool.

References

Almeida, D. S., & Rosolem, C. A. (2016). Ruzigrass grown in rotation with soybean increases soil labile phosphorus. Agronomy Journal, 108(6), 2444–2452. https://doi.org/10.2134/agronj2015.0478

Barrow, N. J., Sen, A., Roy, N., & Debnath, A. (2021). The soil phosphate fractionation fallacy. Plant and Soil, 459(1–2), 1–11. https://doi.org/10.1007/s11104-020-04476-6

Batsula, A. A., & Krivonosova, G. M. (1973). Phosphorus in the humic and fulvic acids of some Ukrainian soils. Soviet Soil Science, 5, 347–350.

Bergström, L., Kirchmann, H., Djodjic, F., Kyllmar, K., Ulén, B., Liu, J., Andersson, H., Aronsson, H., Börjesson, G., Kynkäänniemi, P., Svanbäck, A., & Villa, A. (2015). Turnover and losses of phosphorus in Swedish agricultural soils: Long-term changes, leaching trends, and mitigation measures. Journal of Environmental Quality, 44(2), 512–523. https://doi.org/10.2134/jeq2014.04.0165

Bourns, M. A., Nelson, N. O., Carver, R. E., Roozeboom, K. L., Kluitenberg, G. J., Tomlinson, P. J., Kang, Q., & Hettiarachchi, G. M. (2024). Cover crops impact phosphorus cycling and environmental efficiency in a corn–soybean system. Agronomy Journal, 116(1), 109–120. https://doi.org/10.1002/agj2.21498

Bourns, M., Yeager, E., Nelson, N., Kluitenberg, G., Roozeboom, K., Hettiarachchi, G., Tomlinson, P., & Presley, D. (2026). Phosphorus drawdown improves net return and water quality in a no-till corn–soybean system. Journal of Soil and Water Conservation, 81(3), 222–235. https://doi.org/10.1080/00224561.2026.2651052

Bowman, R. A., & Cole, C. V. (1978). Transformations of organic phosphorus substrates in soils as evaluated by $NaHCO_3$ extraction. Soil Science, 125(1), 49–54. https://doi.org/10.1097/00010694-197801000-00008

Braum, S. M., & Helmke, P. A. (1995). White lupin utilizes soil phosphorus that is unavailable to soybean. Plant and Soil, 176(1), 95–100. https://doi.org/10.1007/BF00017679

Brooker, A. P., Lindsey, L. E., Culman, S. W., Subburayalu, S. K., & Thomison, P. R. (2017). Low soil phosphorus and potassium limit soybean grain yield in Ohio. Crop, Forage & Turfgrass Management, 3(1), 1–5. https://doi.org/10.2134/cftm2016.12.0081

Carver, R. E., Nelson, N. O., Roozeboom, K. L., Kluitenberg, G. J., Tomlinson, P. J., Kang, Q., & Abel, D. S. (2022). Cover crop and phosphorus fertilizer management impacts on surface water quality from a no-till corn–soybean rotation. Journal of Environmental Management, 301, 113818. https://doi.org/10.1016/j.jenvman.2021.113818

Cober, J. R., Macrae, M. L., & Van Eerd, L. L. (2019). Winter phosphorus release from cover crops and linkages with runoff chemistry. Journal of Environmental Quality, 48(4), 907–914. https://doi.org/10.2134/jeq2018.08.0307

Condron, L. M., Turner, B. L., & Cade-Menun, B. J. (2005). Chemistry and dynamics of soil organic phosphorus. In J. T. Sims & A. N. Sharpley (Eds.), Phosphorus: Agriculture and the environment (pp. 87–121). American Society of Agronomy, Crop Science Society of America, & Soil Science Society of America. https://doi.org/10.2134/agronmonogr46.c4

Daryanto, S., Wang, L., & Jacinthe, P. A. (2017). Meta-analysis of phosphorus loss from no-till soils. Journal of Environmental Quality, 46(5), 1028–1037. https://doi.org/10.2134/jeq2016.12.0462

Eichler-Löbermann, B., Köhne, S., Kowalski, B., & Schnug, E. (2008). Effect of catch cropping on phosphorus bioavailability in comparison to organic and inorganic fertilization. Journal of Plant Nutrition, 31(4), 659–676. https://doi.org/10.1080/01904160801926517

Gatiboni, L. C., Kaminski, J., Rheinheimer, D. S., & Flores, J. P. C. (2007). Biodisponibilidade de formas de fósforo acumuladas em solo sob sistema plantio direto. Revista Brasileira de Ciência do Solo, 31(4), 691–699. https://doi.org/10.1590/S0100-06832007000400010

Gu, C., & Margenot, A. J. (2021). Navigating limitations and opportunities of soil phosphorus fractionation. Plant and Soil, 459(1–2), 13–17. https://doi.org/10.1007/s11104-020-04552-x

Helfenstein, J., Pistocchi, C., Oberson, A., Tamburini, F., Goll, D. S., & Frossard, E. (2020). Estimates of mean residence times of phosphorus in commonly considered inorganic soil phosphorus pools. Biogeosciences, 17(2), 441–454. https://doi.org/10.5194/bg-17-441-2020

Khan, A. A., Chen, Y., Asghar, R. M. A., Azeem, I., Shah, T., Cao, W., Zhang, D., & Gao, Y. (2025). P-solubilising bacteria and P-cycling genes drive soil P transformation during green manure decomposition. Agriculture, Ecosystems & Environment, 394, 109875. https://doi.org/10.1016/j.agee.2025.109875

Kleinman, P. J. A., Smith, D. R., Bolster, C. H., & Easton, Z. M. (2015). Phosphorus fate, management, and modeling in artificially drained systems. Journal of Environmental Quality, 44(2), 460–466. https://doi.org/10.2134/jeq2015.02.0090

Leikam, D. F., Lamond, R. E., & Mengel, D. B. (2003). Providing flexibility in phosphorus and potassium fertilizer recommendations. Better Crops with Plant Food, 87(3), 6–10.

Leite, H. M., Calonego, J. C., de Moraes, M. F., Mota, L. H., da Silva, G. F., & do Nascimento, C. A. (2024). How a long-term cover crop cultivation impacts soil phosphorus availability in a no-tillage system? Plants, 13(15), 2057. https://doi.org/10.3390/plants13152057

Linquist, B. A., Singleton, P. W., & Cassman, K. G. (1997). Inorganic and organic phosphorus dynamics during a build-up and decline of available phosphorus in an Ultisol. Soil Science, 162(4), 254–264. https://doi.org/10.1097/00010694-199704000-00004

Maltais-Landry, G., & Frossard, E. (2015). Similar phosphorus transfer from cover crop residues and water-soluble mineral fertilizer to soils and a subsequent crop. Plant and Soil, 393(1–2), 193–205. https://doi.org/10.1007/s11104-015-2477-6

Marks, G. (1977). Beitrag zur präzisierten Charakterisierung von pflanzenverfügbarem Phosphat in Ackerböden. Archiv für Acker- und Pflanzenbau und Bodenkunde, 21, 447–456.

Mattingly, G. E. G. (1975). Labile phosphate in soils. Soil Science, 119(5), 369–375. https://doi.org/10.1097/00010694-197505000-00008

McDowell, R. W., Sharpley, A. N., Condron, L. M., Haygarth, P. M., & Brookes, P. C. (2001). Processes controlling soil phosphorus release to runoff and implications for agricultural management. Nutrient Cycling in Agroecosystems, 59(3), 269–284. https://doi.org/10.1023/A:1014419206761

McLaren, T. I., Guppy, C. N., Tighe, M. K., Moody, P., & Bell, M. (2014). Dilute acid extraction is a useful indicator of the supply of slowly available phosphorus in Vertisols. Soil Science Society of America Journal, 78(1), 139–146. https://doi.org/10.2136/sssaj2013.05.0188

Murphy, J., & Riley, J. P. (1962). A modified single solution method for the determination of phosphate in natural waters. Analytica Chimica Acta, 27, 31–36. https://doi.org/10.1016/S0003-2670(00)88444-5

Neidhardt, H., Achten, F., Kern, S., Schwientek, M., & Oelmann, Y. (2019). Phosphorus pool composition in soils and sediments of transitional ecotones under the influence of agriculture. Journal of Environmental Quality, 48(5), 1325–1335. https://doi.org/10.2134/jeq2019.01.0012

Nelson, N. O., Roozeboom, K. L., Yeager, E. A., Williams, J. R., Zerger, S. E., Kluitenberg, G. J., Tomlinson, P. J., Abel, D. S., & Carver, R. E. (2023). Agronomic and economic implications of cover crop and phosphorus fertilizer management practices for water quality improvement. Journal of Environmental Quality, 52(1), 113–125. https://doi.org/10.1002/jeq2.20427

Olsen, S. R., & Sommers, L. E. (1982). Phosphorus. In A. L. Page, R. H. Miller, & D. R. Keeney (Eds.), Methods of soil analysis: Part 2—Chemical and microbiological properties (2nd ed., pp. 403–430). American Society of Agronomy & Soil Science Society of America. https://doi.org/10.2134/agronmonogr9.2.2ed.c24

Patel, S., Shapiro, C. A., & Iqbal, J. (2024). Long-term comparison of targeted soil test values and crop removal as a phosphorus fertilization strategy in corn. Agronomy Journal, 116(6), 3240–3255. https://doi.org/10.1002/agj2.21677

Pätzold, S., Hejcman, M., Barej, J., & Schellberg, J. (2013). Soil phosphorus fractions after seven decades of fertilizer application in the Rengen Grassland Experiment. Journal of Plant Nutrition and Soil Science, 176(6), 910–920. https://doi.org/10.1002/jpln.201300152

Raniro, H. R., Staudinger, C., Hage-Ahmed, K., Müller-Stöver, D. S., & Santner, J. (2025). Tailored cover crop mixtures enhance soil phosphorus cycling but not wheat yield in a short-term column experiment. Plant and Soil, 514(2), 1783–1809. https://doi.org/10.1007/s11104-025-07488-2

Richardson, A. E., & Simpson, R. J. (2011). Soil microorganisms mediating phosphorus availability: Update on microbial phosphorus. Plant Physiology, 156(3), 989–996. https://doi.org/10.1104/pp.111.175448

Rodrigues, M., Pavinato, P. S., Withers, P. J. A., Teles, A. P. B., & Bejarano Herrera, W. F. (2016). Legacy phosphorus and no tillage agriculture in tropical oxisols of the Brazilian savanna. Science of the Total Environment, 542, 1050–1061. https://doi.org/10.1016/j.scitotenv.2015.08.118

Rodrigues, M., Withers, P. J. A., Soltangheisi, A., Vargas, V., Holzschuh, M., & Pavinato, P. S. (2021). Tillage systems and cover crops affecting soil phosphorus bioavailability in Brazilian Cerrado Oxisols. Soil and Tillage Research, 205, 104770. https://doi.org/10.1016/j.still.2020.104770

Sharpley, A. N., & Smith, S. J. (1994). Wheat tillage and water quality in the Southern Plains. Soil and Tillage Research, 30(1), 33–48. https://doi.org/10.1016/0167-1987(94)90069-8

Silva, R. S. da, Alovisi, A. M. T., Kurihara, C. H., Rocha Neto, D. P., Lima, N. D., Medeiros, E. S. de, Staut, L. A., & Silva, C. J. da. (2025). Soil phosphorus fractions in response to cropping system, liming, and phosphate fertilization in an expanding sugarcane plantation area. Acta Scientiarum. Agronomy, 47(1), e71726. https://doi.org/10.4025/actasciagron.v47i1.71726

Sommers, L. E., & Nelson, D. W. (1972). Determination of total phosphorus in soils: A rapid perchloric acid digestion procedure. Soil Science Society of America Journal, 36(6), 902–904. https://doi.org/10.2136/sssaj1972.03615995003600060020x

Teles, A. P. B., Rodrigues, M., Bejarano Herrera, W. F., Soltangheisi, A., Sartor, L. R., Withers, P. J. A., & Pavinato, P. S. (2017). Do cover crops change the lability of phosphorus in a clayey subtropical soil under different phosphate fertilizers? Soil Use and Management, 33(1), 34–44. https://doi.org/10.1111/sum.12327

Thomas, R. L., Sheard, R. W., & Moyer, J. R. (1967). Comparison of conventional and automated procedures for nitrogen, phosphorus, and potassium analysis of plant material using a single digestion. Agronomy Journal, 59(3), 240–243. https://doi.org/10.2134/agronj1967.00021962005900030010x

Tiecher, T., Rheinheimer dos Santos, D., & Calegari, A. (2012a). Soil organic phosphorus forms under different soil management systems and winter crops, in a long-term experiment. Soil and Tillage Research, 124, 57–67. https://doi.org/10.1016/j.still.2012.05.001

Tiecher, T., Rheinheimer dos Santos, D., Kaminski, J., & Calegari, A. (2012b). Forms of inorganic phosphorus in soil under different long-term soil tillage systems and winter crops. Revista Brasileira de Ciência do Solo, 36(1), 271–282. https://doi.org/10.1590/S0100-06832012000100028

Tiessen, H., & Moir, J. O. (1993). Characterization of available P by sequential extraction. In M. R. Carter (Ed.), Soil sampling and methods of analysis (pp. 75–86). CRC Press.

Vance, C. P., Uhde-Stone, C., & Allan, D. L. (2003). Phosphorus acquisition and use: Critical adaptations by plants for securing a nonrenewable resource. New Phytologist, 157(3), 423–447. https://doi.org/10.1046/j.1469-8137.2003.00695.x

Wang, X., Tang, C., Guppy, C. N., & Sale, P. W. G. (2008). Phosphorus acquisition characteristics of cotton (Gossypium hirsutum L.), wheat (Triticum aestivum L.), and white lupin (Lupinus albus L.) under P-deficient conditions. Plant and Soil, 312(1–2), 117–128. https://doi.org/10.1007/s11104-008-9589-1

Wang, Y. J., Huang, Q. Q., Gao, H., Zhang, R. Q., Yang, L., Guo, Y. R., Li, H. K., Awasthi, M. K., & Li, G. C. (2021). Long-term cover crops improved soil phosphorus availability in a rain-fed apple orchard. Chemosphere, 275, 130093. https://doi.org/10.1016/j.chemosphere.2021.130093

Wang, Y., Shen, Z., & Zhang, Z. (2018). Phosphorus speciation and nutrient stoichiometry in the soil–plant system during primary ecological restoration of copper mine tailings. Pedosphere, 28(3), 530–541. https://doi.org/10.1016/S1002-0160(18)60031-1

Withers, P. J. A., Sylvester-Bradley, R., Jones, D. L., Healey, J. R., & Talboys, P. J. (2014). Feed the crop not the soil: Rethinking phosphorus management in the food chain. Environmental Science & Technology, 48(12), 6523–6530. https://doi.org/10.1021/es501670j

Wortmann, C. S., Dobermann, A. R., Ferguson, R. B., Hergert, G. W., Shapiro, C. A., Tarkalson, D. D., & Walters, D. T. (2009). High-yielding corn response to applied phosphorus, potassium, and sulfur in Nebraska. Agronomy Journal, 101(3), 546–555. https://doi.org/10.2134/agronj2008.0103x

Wu, Q., Huang, Z., Zhu, P., Wang, B., Zhang, S., & Ao, J. (2022). Long-term change in phosphorus behavior and the degree of P saturation in typical cropland after different fertilization practices. Soil Science and Plant Nutrition, 68(1), 202–214. https://doi.org/10.1080/00380768.2021.2014745

Ye, R., Parajuli, B., Ducey, T. F., Novak, J. M., Bauer, P. J., & Szogi, A. A. (2020). Cover cropping increased phosphorus stocks in surface sandy Ultisols under long-term conservation and conventional tillage. Agronomy Journal, 112(4), 3163–3173. https://doi.org/10.1002/agj2.20227

Zhang, S., Yang, X., Hsu, L.-C., Liu, Y.-T., Wang, S.-L., White, J. R., Shaheen, S. M., Chen, Q., & Rinklebe, J. (2021). Soil acidification enhances the mobilization of phosphorus under anoxic conditions in an agricultural soil: Investigating the potential for loss of phosphorus to water and the associated environmental risk. Science of the Total Environment, 793, 148531. https://doi.org/10.1016/j.scitotenv.2021.148531

Zhou, Y., Zhu, H., Fu, S., & Yao, Q. (2017). Variation in soil microbial community structure associated with different legume species is greater than that associated with different grass species. Frontiers in Microbiology, 8, 1007. https://doi.org/10.3389/fmicb.2017.01007

Chapter 4 - Effects of long-term cover crop and phosphorus fertilization on soil organic phosphorus forms and soil P pools under a corn-soybean rotation system

Abstract

Understanding the impact of long-term agronomic management on soil phosphorus (P) speciation is critical for balancing crop requirements with environmental quality. This study evaluated the effects of cover cropping and three P fertilization strategies — a control with no added P (CN), a sufficiency approach (SF), and a build-and-maintain approach (BM) — on soil P pools in a continuous no-till corn-soybean rotation in the Central Great Plains, USA. Soil samples were analyzed using Hedley sequential fractionation and solution ^{31}P nuclear magnetic resonance (^{31}P-NMR) spectroscopy. Sequential fractionation revealed that the BM strategy significantly increased inorganic P (P_i) fractions, particularly the labile (Resin-P_i) and moderately labile (NaOH-P_i) pools, while cover cropping had no significant main effect on these broadly-defined extraction pools. Advanced speciation using ^{31}P-NMR spectroscopy found the BM approach significantly elevated orthophosphate, pyrophosphate, and polyphosphate concentrations, reflecting direct fertilizer inputs and potential microbial storage. The integration of cover crops significantly increased *myo*-inositol hexakisphosphate (*myo*-IHP), indicating an accumulation of plant-derived or microbially synthesized organic P (P_o). Furthermore, unknown monoester peaks exhibited significant interactions between cover cropping and fertilization, suggesting shifts in uncharacterized P_o forms based on P fertilizer management. Our findings demonstrate that while the BM strategy builds agronomic soil test P, it disproportionately accumulates P in highly mobile inorganic fractions, which are intrinsically more vulnerable to

environmental loss. In contrast, managing systems with cover crops promotes the accumulation of biologically mediated P_o reservoirs (e.g., *myo*-IHP and NaOH-P_o). By physically transferring fertilizer and native soil P into winter biomass and subsequent soil organic pools, cover crops actively shift soil P speciation away from immediately soluble inorganic forms. Ultimately, transitioning from a BM to an SF fertilization strategy, coupled with cover cropping, presents a more sustainable approach to optimize internal P cycling and mitigate the accumulation of highly mobile inorganic P pools in agricultural systems.

Introduction

Phosphorus (P) is an essential element for all organisms. In soils, P compounds are grouped into inorganic P (P_i) compounds, including phosphate ($H_2PO_4^-$ or HPO_4^{2-}) and polyphosphates (chains of phosphate, including pyrophosphates with two phosphate groups), and organic P (P_o) compounds that contain carbon (C) groups. Organic P compound classes include orthophosphate monoesters with one P–O–C bond per phosphate (e.g., sugar phosphates, and inositol hexakisphosphate (IHP) stereoisomers which contain six phosphate groups each with a single P–O–C bond), orthophosphate diesters with two P–O–C bonds per phosphate (e.g., DNA, phospholipids), and phosphonates with a direct C–P bond (Cade-Menun, 2017; Condron et al., 2005). Organic P compounds can comprise 30–65% of total soil P, and up to 90% in soils with high OM (Harrison, 1987), making P_o a significant reservoir of potentially plant-available phosphate.

A key component of improved P management is understanding how different management practices affect the chemical forms of P and the processes that control their cycling, as the chemical speciation of P dictates its availability for crop uptake and loss to the environment (Condron et al., 2005). The main processes controlling the cycling of soil P

compounds are adsorption/desorption, dissolution/precipitation, and mineralization/immobilization (Arai & Sparks, 2007; Pierzynski et al., 2005). Adsorption/desorption and dissolution/precipitation primarily govern the solubility and availability of P_i compounds by controlling their interactions with soil minerals, such as iron (Fe) and aluminum (Al) oxides. Importantly, P_o compounds can also be adsorbed to soil minerals, which significantly affects their mineralization rates and subsequent mobility. Mineralization and immobilization are biologically driven processes that regulate the transformation between P_o and P_i, directly impacting the replenishment of the soil solution P pool (Arai & Sparks, 2007; Pierzynski et al., 2005). Advanced spectroscopic techniques, such as ^{31}P-NMR, are required to accurately identify and quantify these specific P compounds, as traditional sequential extraction techniques (e.g., Hedley fractionation) only determine the relative solubility of broad soil P pools.

Fertilizer applications to agricultural soils are often needed to maintain soil phosphate levels that support optimal crop yields (Cade-Menun, 2022). However, excessive use of P fertilizers can lead to the discharge of P into water bodies via surface runoff, subsurface flow, and vertical leaching, causing eutrophication and harmful algal blooms (Dodds et al., 2009; Hudnell, 2010; Sharpley et al., 2015; Verheyen et al., 2015). Consequently, fertilization strategies strongly dictate soil P pools. Two common P fertilization strategies, build-maintain (BM) and sufficiency (SF), differ fundamentally in their objectives. The BM approach builds the soil test P (STP) values to a critical level and maintains it with applications based on crop removal (Macnack et al., 2017; Schefe et al., 2015). The SF approach, however, applies fertilizer only when STP concentrations are below the critical level to alleviate deficiency for the current crop, without aiming to build soil P levels (Leikam et al., 2003). Although the short-term impacts

of these strategies are established, the cumulative effects of these approaches on soil P forms, particularly when transitioning to an SF strategy or during complete fertilizer cessation, remain a critical area of investigation (Cade-Menun et al., 2017; Liu et al., 2015).

The integration of cover crops is an increasingly adopted strategy to protect soil and improve internal nutrient cycling. Cover crops can influence soil P dynamics in contrasting but biologically significant ways. On one hand, they may decrease soil P_o accumulation by expanding root systems and releasing organic acids or enzymes (e.g., phosphatases) to mineralize sparingly soluble P_o forms, transferring P into labile P_i pools to meet crop demands (Guppy et al., 2005; Hallama et al., 2019). On the other hand, cover crops can simultaneously increase P_o pools due to enhanced P uptake by the cover crop and the subsequent return of high organic carbon inputs, stimulating microbial biomass and the synthesis of stable P_o compounds (Tiecher et al., 2012a, 2012b). Despite these established mechanisms, the specific influence of cover cropping on P speciation remains insufficiently documented. Recent studies have begun to highlight that cover crops and companion crops can significantly modulate soil organic P forms and overall P speciation (Barbosa et al., 2026; Gamage et al., 2025; Tiecher et al., 2012a, 2012b), reinforcing the need for additional speciation studies in diverse cropping systems and soils. Furthermore, extending this high-resolution speciation research to the slightly acidic, smectitic soils of the Central Great Plains under continuous no-till management provides critical novel insights, as there has been little research to date on P speciation in soils of this region.

The dynamics of P_o mineralization become particularly vital in systems with reduced P inputs. In soils with low phosphate availability, the mineralization of P_o compounds can serve as a primary source of phosphate (Condron et al., 2005), often explaining the lack of crop response to P fertilizers where STP predicts a deficiency (Dodd & Sharpley, 2015). Furthermore, P

availability directly alters the P composition within the plants themselves. Plants grown at high P fertilizer rates typically accumulate greater concentrations of phosphate, whereas plants grown at low P fertilization rates tend to partition a significantly greater proportion of their total P into organic P_o forms. This shift ultimately dictates the specific forms of P returned to the soil post-harvest through crop residues (Noack et al., 2014).

Understanding the complex interactions between fertilization strategies and conservation practices like cover cropping is essential for improving P use efficiency and minimizing environmental loss. The core justification of this study lies in exploring this specific interaction, as the combined effects of cover crops and targeted P fertilizer management on P_o speciation are still not well characterized.

Accordingly, the objective of this study was to evaluate the interactive effects of cover cropping and three distinct P fertilization approaches (CN, SF, and BM) on soil P_o forms and soil P pools. We hypothesized that cover cropping, interacting with P fertilization strategies, would fundamentally alter the distribution of soil P_i and P_o forms. Specifically, we hypothesized that long-term cover cropping would actively drive P_o cycling, either by decreasing stable P_o compounds through enhanced mineralization to support crop requirements, or conversely, by increasing P_o accumulation via continuous residue inputs and microbial synthesis. Furthermore, we hypothesized that the BM strategy would primarily inflate highly mobile P_i fractions, whereas the unfertilized and SF strategies would result in a significantly greater proportion of soil P existing in P_o forms, thereby yielding distinctly different overall P speciation profiles.

Material and Methods

Experimental site, design, and agronomic management

This study was conducted at the Kansas Agricultural Watershed (KAW) field laboratory near Manhattan, KS, and included 18 watersheds ranging in size from 0.46 to 0.65 ha (Figure 4-1).

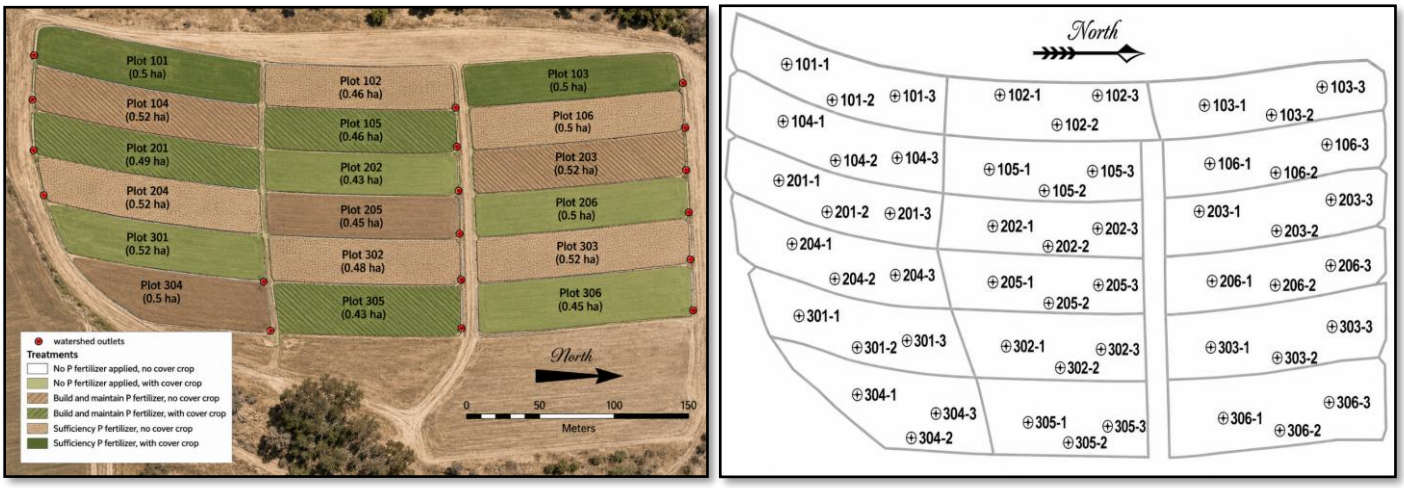


Figure 4-1. An overview of the Kansas Agricultural Watershed (KAW) field laboratory with 18 plots, including cover crop (green plots) and no cover crop plots (brown plots) (left). Soil sampling points where three geo-referenced subplots were sampled within each plot (right).

The soils are mapped as eroded Smolan silty clay loam (fine, smectitic, mesic Pachic Argiustolls) with 3 to 7% slopes. Prior to the establishment of the current study, the field was managed under conventional tillage in a winter wheat (*Triticum aestivum L.*)–soybean [*Glycine max (L.) Merr.*] rotation, with the last tillage event occurring in fall 2014. Since then, the site has been managed under a continuous no-till corn (*Zea mays L.*) soybean rotation.

General agronomic management applied equally across all plots included standard regional practices for seeding rates, weed control, and nitrogen fertilization (Bourns et al., 2026;

Nelson et al., 2023). From fall 2014 through the 2019 crop year, the CC treatment consisted of either winter wheat or winter triticale (×*Triticosecale Wittm. Ex A. Camus*), grown alone or mixed with rapeseed (*Brassica napus L.*). From fall 2019 planting through fall 2022, the CC species was changed exclusively to cereal rye (*Secale cereale*).

The study was arranged as a 2 × 3 factorial randomized complete block design with three replications (blocked by landscape position), resulting in 18 experimental plots. The two factors were cover crop management (cover crop [CC] and no cover crop [NC]) and phosphorus fertilization strategy. The specific P fertilization treatments evolved through three distinct phases:

Phase 1 (2015–2019): Treatments included a control with no P application (CN), a fall surface-broadcast (FB) application of diammonium phosphate, and a spring injected (SI) application of ammonium polyphosphate, applied 5 cm to the side and 5 cm below the seed. Both FB and SI received 27 kg P ha^{-1} yr^{-1} following Kansas State University's build-and-maintain (BM) recommendations (Leikam et al., 2003).

Phase 2 (2020–2022): The plots previously receiving SI fertilizer were transitioned into a continuous BM treatment, receiving an average of 24 kg P ha^{-1} yr^{-1} as ammonium polyphosphate applied at planting (placed 5 cm below and 5 cm to the side of the seed). The plots previously receiving FB fertilizer entered a drawdown phase where no P fertilizer was applied. The CN plots continued to receive no P.

Phase 3 (2023): The BM and CN treatments continued as described for Phase 2. The drawdown plots were transitioned into a sufficiency (SF) treatment. In 2023, based on soil analysis and expected crop response under the SF framework, these plots received 10 kg P ha^{-1}

as ammonium polyphosphate applied at planting 5 cm below and 5 cm to the side of the seed. Therefore, the SF treatment only received fertilizer in 2023 during the post-2019 period.

Soil sample collection

Each fall, composite soil samples consisting of 21 cores were collected at each of three geo-referenced subplot locations within a plot (Figure 4-1b). Soil cores were divided into three depth intervals: 0 to 2.5 cm, 2.5 to 5 cm, and 5 to 15 cm. For this study, composite soil samples were prepared using dried, ground (<2 mm), and sieved soils collected in the fall of 2023, following the corn harvest. To create these composites, 10 g of soil from each of the two upper depth intervals (0 to 2.5 cm and 2.5 to 5 cm) at each of the three sampling points within a plot were combined and thoroughly mixed. This resulted in 18 composite 60-g soil samples representing the 0 to 5-cm depth for the 18 experimental plots.

Hedley sequential fractionation method

Sequential extraction was performed using 0.5 g of soil following the method of Tiessen and Moir (1993), as detailed in Table 4-1. After each extraction step, samples were centrifuged at 10,000 rpm for 15 minutes, and the supernatants were filtered through 0.45-µm syringe filters and stored at 4 °C. Following the standard protocol of Tiessen and Moir (1993), no biocides were added during the sequential extraction steps, and filtered extracts were immediately stored at 4 °C prior to analysis to minimize microbial transformations.

For the analytical determination of P forms, total P (TP) in the extracts from the second and third steps ($NaHCO_3$ and NaOH) was measured using an inductively coupled plasma optical emission spectrometer (ICP-OES; 720-ES, Varian, Santa Clara, CA). Molybdate-reactive P (MRP), representing inorganic P (P_i), was analyzed using the molybdate-blue colorimetric

method (Murphy & Riley, 1962) with a Beckman Coulter DU-800 spectrophotometer (Brea, CA). Molybdate-unreactive P (MUP), representing organic P (P_o), was calculated as the difference between TP and MRP (P_o = TP - MRP).

For the first step (Resin), P_i was measured colorimetrically and assumed to equal TP. For the fourth step (HCl), only TP was analyzed via ICP-OES. Residual P was calculated by subtracting the sum of all extracted TP fractions from the total soil P, which was determined separately by perchloric acid digestion and ICP-OES analysis (Olsen & Sommers, 1982; Sommers & Nelson, 1972).

Table 4-1. Summary of the extractants, procedures, and defined fractions for the Hedley sequential extraction.

Step	Extractant	Method Detail	Defined Fraction	Analytical Method
Step 1	Water and Resin	Weighed 0.5 g of soil into a 50 ml tube, added 2 resin strips and 30 ml deionized water, and shaken overnight (16 h). Removed resins, washed with water, placed in clean tubes with 30 ml of 0.5 M NaCl, and shaken overnight (16 h).	Resin-P_i	Determined P_i colorimetrically
Step 2	$NaHCO_3$ (0.5 M)	Centrifuged the soil suspension from Step 1, filtered through 0.45 µm, added 30 ml of $NaHCO_3$, and shaken overnight (16 h).	$NaHCO_3$-P_i, $NaHCO_3$-P_o	Determined TP (ICP-OES) and P_i (colorimetrically); P_o calculated as TP - P_i
Step 3	NaOH (1.0 M)	Centrifuged the suspension from Step 2, filtered through 0.45 µm, added 30 ml of NaOH, and shaken overnight (16 h).	NaOH-P_i, NaOH-P_o	Determined TP (ICP-OES) and P_i (colorimetrically); P_o calculated as TP - P_i
Step 4	HCl (1.0 M)	Centrifuged the suspension from Step 3, filtered through 0.45 µm, added 30 ml of HCl, and shaken overnight (16 h).	HCl-TP	Determined TP (ICP-OES)
Step 5	Residual P	Calculated fraction.	Residual-TP	Subtracted the sum of all extracted fractions from the total soil P

Solution ^{31}P-NMR spectroscopy method

Composite soil samples were extracted for ^{31}P-NMR following Cade-Menun et al. (2017). Briefly, 3 g of soil was shaken with 30 mL of NaOH–EDTA solution (0.5 mol L^{-1} NaOH plus 0.1 mol L^{-1} Na_2EDTA) for 4 h in the dark. Samples were centrifuged at 10,000 rpm for 10 min, and the extracts were frozen at −80 °C and subsequently freeze-dried for 2 days. Prior to the NMR analysis, the lyophilized extracts were re-dissolved by adding 850 µL each of H_2O, D_2O, and NaOH–EDTA solution, and 450 µL of 10 M NaOH. Samples were sonicated for 3 min and allowed to stand for 20 min before centrifuging at 10,000 rpm for 15 min. An aliquot of the supernatant was analyzed by ICP-OES for TP, Fe, Al, and Mn concentrations. The ratio of TP to Fe + Mn concentrations was used to estimate relaxation times (T_1) for P nuclei in each sample (Cade-Menun & Liu, 2014; McDowell et al., 2006).

The remaining supernatant was transferred to a 10-mm NMR tube, frozen at -20 °C, and transported in a chilled state to the Structural Biology Center (University of Kansas), where the samples were maintained at -20 °C until immediate analysis to prevent degradation of labile organic esters.

Liquid-state one-dimensional ^{31}P-NMR spectra were acquired using a Bruker Avance 500-MHz spectrometer (202.5 MHz for P) with a 45° pulse, a spectral width of 14,124 Hz (35 to −35 ppm), an acquisition time of 3.2 sec, a temperature of 20 °C, and no proton decoupling. Experimental delay times were calculated as $4 \times T_1$, using the estimated T_1 values, ranging from 4.2 to 13.3 sec (av. 7.9 sec). Samples were analyzed for 4 h each, collecting 912–2,200 scans. Spiking experiments were conducted to confirm peak identifications based on Cade-Menun (2015), using ten standards including pyrophosphate, tripolyphosphate, *myo*-IHP,

phosphocholine, β-glycerophosphate, adenosine 5'-monophosphate, D-glucose 6-phosphate, glucose 1-phosphate, *α*-glycerol 6-phosphate, and DNA.

Spectra were processed using the NMR Utility Transform Software (NUTS) from Acorn NMR, with 7 and 2 Hz line broadening for full spectra and zoomed-in regions, respectively (Figure 4-2). Peak picking and integration were performed manually, with the orthophosphate peak set to 6.00 ppm. Compound identification was based on the literature and confirmed with spiking experiments. Peak areas were converted to mg P kg^{-1} soil on a dry basis using the TP concentration determined by ICP-OES. Individual phosphorus compounds were subsequently summed into functional categories for statistical analysis, including: total inorganic P, total organic P, total monoesters, and total diesters. The percentage of total P extracted by the NaOH-EDTA extraction method was calculated as the NaOH-EDTA extracted-P relative to the total soil P determined by acid digestion.

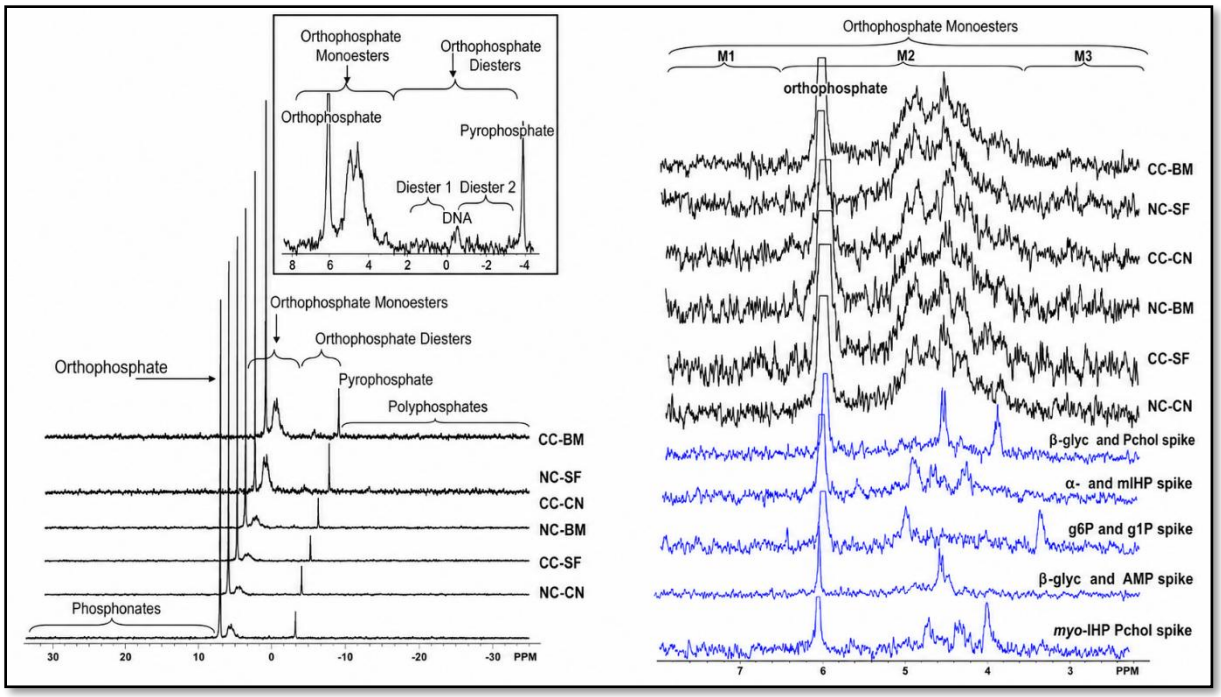


Figure 4-2. Representative liquid-state one-dimensional ^{31}P-NMR spectra of NaOH-EDTA soil extracts for the six different agronomic treatments. The spectra illustrate the specific chemical shift regions where different phosphorus species and compound classes are identified: orthophosphate (~6.0 ppm), orthophosphate monoesters (~3.0 to 7.5 ppm), orthophosphate diesters (~ -1.0 to 2.5 ppm), pyrophosphate (~ -4.0 ppm), polyphosphates (< -4.0 ppm), and phosphonates (> 10.0 ppm). Spectra from spiking experiments with known internal standards were utilized to confirm specific peak identities across these regions.

Statistical analysis

For the P fractionation data, the assumption of normality was evaluated by visual inspection of residual plots and distribution histograms. The fractionation data were found to be approximately normally distributed; therefore, no transformation was required before analysis. Prior to transformation, the assumption of normality for the ^{31}P-NMR data was assessed using residual plots. The ^{31}P-NMR data were transformed for statistical analysis using log (n + 0.5) for broad categories (e.g., total inorganic P, total organic P, total monoesters, and total diesters) or

centered log ratios for specific P compounds based on established compositional statistical analysis recommendations (Abdi et al., 2015). Treatment effects were determined by factorial ANOVA using SAS PROC GLIMMIX version 9.4 (SAS Institute, 2020) with replicate, cover crop, P fertilizer, and the cover crop by P fertilizer interaction as fixed effects and denominator degrees of freedom determined by the Kenward and Roger method. The protected LSD test with $\alpha = 0.05$ was used for mean separation. For ^{31}P-NMR data, to generate graphs, data were back-transformed, and means reported in figures are from back-transformed data. Untransformed least squares means and standard errors for all ^{31}P-NMR soil phosphorus compounds are provided for reference in the supplementary material (Appendix A, Table A1).

Results and Discussion

Phosphorus Pools Determined by Sequential Fractionation

The main effect of P fertilization significantly influenced the concentrations of Resin-P_i, $NaHCO_3$-P_i, $NaHCO_3$-P_o, NaOH-P_i, and NaOH-P_o (Table 4-2). Conversely, the effects of cover cropping and the interaction between cover crop and fertilization were not significant for any P fraction. Specifically, the BM treatment resulted in the highest P concentrations in both the Resin-P_i and NaOH-P_i pools, establishing a clear gradient based on P inputs (CN < SF < BM). The SF strategy maintained the labile $NaHCO_3$-P_i and moderately labile NaOH-P_o pools at levels statistically comparable to the BM treatment. However, both the SF and CN treatments exhibited a significant depletion of the labile organic pool ($NaHCO_3$-P_o) compared to BM. Furthermore, the highly recalcitrant pools (HCl-TP and Residual-TP) remained statistically unaffected by any agronomic treatment.

Table 4-2. Effect of cover crop and phosphorus (P) fertilization treatment on different soil phosphorus fractions.

Effect	Resin-P_i	$NaHCO_3$-P_i	$NaHCO_3$-P_o	NaOH-P_i	NaOH-P_o	HCl-TP	Residual-TP
	mg kg^{-1}	mg kg^{-1}	mg kg^{-1}	mg kg^{-1}	mg kg^{-1}	mg kg^{-1}	mg kg^{-1}
Cover Crop (n=9)							
NC	34.3 a	9.74 a	8.6 a	34.7 a	67.5 a	81.7 a	197.5 a
CC	32.5 a	9.44 a	10.00 a	32.6 a	72.3 a	80.7 a	216.1 a
Standard Error	*(3.0)*	*(1.57)*	*(1.50)*	*(2.3)*	*(2.51)*	*(4.73)*	*(21. 3)*
P-value	*0.672*	*0.891*	*0.839*	*0.534*	*0.210*	*0.892*	*0.550*
Fertilizer (n=6)							
CN	7.1 c	3.5 b	7.5 b	18.0 c	60.9 b	74.1 a	187.2 a
SF	31.1 b	13.1 a	5.5 b	34.3 b	75.2 a	82.5 a	205.8 a
BM	62.0 a	12.2 a	13.6 a	48.6 a	73.5 a	87.0 a	227.4 a
Standard Error	*(3.7)*	*(1.9)*	*(1. 8)*	*(2. 9)*	*(3. 1)*	*(5.8)*	*(26.1)*
P-value	*<0.001*	*0.010*	*0.027*	*<0.001*	*0.016*	*0.321*	*0.569*
Cover Crop × Fertilizer (n=3)							
P-value	*0.931*	*0.646*	*0.628*	*0.693*	*0.436*	*0.138*	*0.230*

Note: Values are least squares means. Means within a column for each main effect followed by the same letter are not significantly different at $\alpha = 0.05$.
Treatments: NC: No Cover Crop; CC: Cover Crop; CN: Control (No P fertilizer); SF: Sufficiency P fertilizer; BM: Build and Maintain P fertilizer.

Sequential extraction fractions reflect the decreasing relative solubility of soil P rather than specific chemical compounds (Hedley et al., 1982). The progressive, stepwise increase in the inorganic pools (Resin-P_i and NaOH-P_i) with increasing P inputs indicates that applied P fertilizer primarily accumulated in these labile and moderately labile pools. While Resin-P_i represents the most freely exchangeable and immediately bioavailable P fraction in the soil solution, $NaHCO_3$-P_o represents an organic pool that is thought to be easily mineralizable and may act as a vital buffer for plant-available P across all treatments (Hedley et al., 1982). The significant depletion of $NaHCO_3$-P_o in the SF treatment compared to BM suggests an increased biological reliance on this labile organic pool to sustain crop uptake when fertilizer P inputs are restricted. Furthermore, both SF and BM treatments exhibited significantly higher NaOH-P_o concentrations compared to CN. This suggests that the higher crop productivity and corresponding residue returns associated with active fertilization (both SF and BM) were sufficient to build and maintain this more stable, moderately labile pool, regardless of the strict differences in fertilizer P application rates between the SF and BM approaches.

A substantial proportion of the total P remained in the residual fraction across all treatments, representing highly recalcitrant P forms, which likely include highly stable inorganic P minerals and possibly recalcitrant organic P compounds associated with mineral-protected or occluded OM. Importantly, our sequential fractionation data demonstrated that fertilization strategies effectively altered specific MUP pools (elevating NaOH-P_o in SF/BM and depleting $NaHCO_3$-P_o in SF/CN). Additionally, while cover cropping did not significantly alter the broadly defined Hedley fractions in this specific sampling year, our previous long-term evaluations (Chapter 3) strongly indicate that cover crops actively may influence cycling of P_o compounds. Because the sequential fractionation scheme lacks the analytical sensitivity required to differentiate individual

chemical compounds within these operational pools, advanced analytical techniques such as ^{31}P-NMR spectroscopy are strictly necessary. NMR allows us to independently identify the specific P_o compounds responding to these fertilization shifts and to uncover targeted cover crop effects that are otherwise masked by broad chemical extractions.

Phosphorus Forms and Compound Classes Determined by ^{31}P-NMR

NaOH-EDTA Extraction Efficiency

The percentage of total soil P extracted by the NaOH-EDTA method was significantly affected by the long-term fertilization strategy ($P = 0.005$), whereas cover cropping and their interaction had no significant effect. The NaOH-EDTA extraction used for ^{31}P-NMR extracted a greater percentage of total P from soils in the BM and SF treatments than in the CN treatment (Figure 4-3).

The significantly lower extraction efficiency observed in the unfertilized control (CN) compared to the fertilized treatments (SF and BM) can be attributed to the nature of the NaOH-EDTA extractant and the chemical composition of the unextracted P. The NaOH-EDTA solution primarily recovers labile to moderately labile P pools. In the fertilized treatments (SF and BM), higher crop productivity and subsequent residue returns contribute to the accumulation of "new" or relatively accessible OM. In contrast, in the prolonged absence of P fertilization (CN), a greater proportion of the total soil P is tightly bound in highly recalcitrant forms. Prior research has indicated that this unextracted portion predominantly consists of stable inorganic minerals (e.g., apatite; Chen et al., 2021) but could also include a small portion of recalcitrant organic P that is physically inaccessible to the NaOH-EDTA extraction (Cade-Menun & Liu, 2014; Turner et al., 2005). Because the NaOH-EDTA extraction efficiency varied significantly among the fertilization treatments, analyzing raw extract concentrations could misrepresent the true soil P

dynamics. Therefore, to ensure an accurate and mathematically robust evaluation of the specific P pools, statistical analysis of the NMR data was conducted utilizing centered log ratios (CLR). The CLR transformation appropriately assesses the relative compositional shifts (the ratio of various P fractions) independently of the total extracted mass (Abdi et al., 2015).

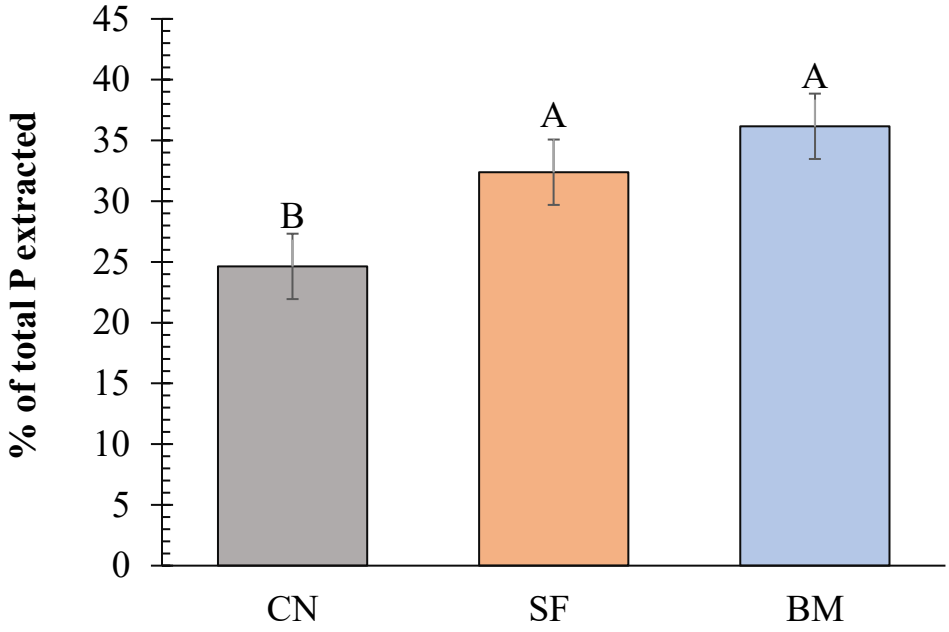


Figure 4-3. Percentage of total soil phosphorus (P) extracted in the topsoil (0–5 cm) under different long-term fertilization strategies. Values represent the least squares means of the percentage of total soil P extracted by the NaOH-EDTA method. Error bars indicate standard errors. Bars marked with different letters are significantly different at $\alpha = 0.05$. Treatments: CN: Control (No P fertilizer); SF: Sufficiency P fertilizer; BM: Build and Maintain P fertilizer.

Inorganic P Compounds (Orthophosphate, Pyrophosphate, Polyphosphate)

Peaks for orthophosphate, pyrophosphate, and polyphosphate were identified in all samples based on their specific chemical shifts (Table 4-3). There was a significant effect of P

fertilizer treatment on orthophosphate concentration, with the highest concentration observed in the BM treatment and the lowest in the CN treatment (Figure 4-4a; Table 4-3).

Consistent with findings from multiple studies, orthophosphate concentrations were lower in plots receiving no P fertilizer compared with P-fertilized treatments (Ahlgren et al., 2013; Annaheim et al., 2015; Liu et al., 2015). The greater orthophosphate concentration in the BM treatment likely reflects the direct contribution of higher P fertilizer inputs (Cade-Menun et al., 2017). Although crop residue can be a source of returned P, total P return from aboveground biomass did not differ significantly between the BM and SF treatments (Bourns et al., 2024), indicating that the elevated orthophosphate is more likely associated with direct fertilizer application.

Table 4-3. Chemical shifts of peaks detected in ^{31}P NMR spectra of NaOH-EDTA samples, present in at least 9 of 18 samples.

P Form or Compound Class	Chemical Shift (ppm)
	Inorganic P
Orthophosphate	6.00 ± 0.00
Pyrophosphate	-4.06 ± 0.02
Polyphosphates	-3.81 ± 0.02, -4.43 ± 0.19, -5.97 ± 0.12, -7.51 ± 0.27, -9.28 ± 0.33, -12.59 ± 0.30, -13.42 ± 0.30, -14.52 ± 0.31, -24.46 ± 0.28, -25.41 ± 0.30, -29.38 ± 0.26
	Organic P
Phosphonates	33.44 ± 0.40, 31.37 ± 0.43, 26.20 ± 0.16, 21.51 ± 0.28, 19.56 ± 0.27, 18.52 ± 0.25, 17.39 ± 0.30, 15.37 ± 0.29, 14.53 ± 0.21, 12.36 ± 0.37, 10.61 ± 0.36
	Orthophosphate Monoesters
myo-IHP	5.56 ± 0.03, 4.58 ± 0.03, 4.22 ± 0.03, 4.09 ± 0.02
scyllo-IHP	3.75 ± 0.03

neo-IHP 4e/2a	6.35 ± 0.02, 4.42 ± 0.03
neo-IHP 4a/2e	4.86 ± 0.03, 4.63 ± 0.03
D-*chiro*-IHP 4e/2a	6.63 ± 0.03, 5.35 ± 0.03, 4.04 ± 0.02
D-*chiro*-IHP 4a/2e	6.15 ± 0.01, 4.77 ± 0.03, 4.36 ± 0.03
scyllo-IP5	4.38 ± 0.02, 3.80 ± 0.04, 3.66 ± 0.03
Glucose 6-phosphate	4.99 ± 0.04
α-glycerophosphate	4.85 ± 0.02
ß-glycerophosphate	4.52 ± 0.02
Mononucleotides	4.49 ± 0.01, 4.46 ± 0.01, 4.43 ± 0.03, 4.33 ± 0.02, 4.30 ± 0.01, 4.28 ± 0.01
Choline phosphate	3.87 ± 0.05
Unknown 5.0 ppm	5.05 ± 0.03
Unknown 4.2 ppm	4.17 ± 0.02
Monoester 1	7.56 ± 0.03, 7.32 ± 0.05, 7.15 ± 0.05, 6.95 ± 0.05, 6.81 ± 0.06, 6.45 ± 0.03, 6.24 ± 0.03
Monoester 2	5.88 ± 0.01, 5.82 ± 0.01, 5.74 ± 0.03, 5.46 ± 0.04, 5.21 ± 0.04, 4.76 ± 0.03, 4.66 ± 0.02
Monoester 3	3.57 ± 0.02, 3.43 ± 0.02, 3.27 ± 0.04, 3.13 ± 0.05, 2.98 ± 0.04, 2.85 ± 0.06, 2.65 ± 0.06
Orthophosphate Diesters	
Diester 1	2.42 ± 0.07, 1.82 ± 0.06, 1.62 ± 0.05, 1.44 ± 0.04, 1.29 ± 0.04, 0.97 ± 0.05, 0.55 ± 0.04, 0.00 ± 0.04, -0.54 ± 0.07
DNA	-0.71 ± 0.03, -0.89 ± 0.04
Diester 2	-1.10 ± 0.06, -1.29 ± 0.07, -1.81 ± 0.07, -2.52 ± 0.08, -2.92 ± 0.08, -3.24 ± 0.07

Phosphorus fertilization also significantly affected pyrophosphate and total polyphosphate concentrations, with the highest concentrations observed in the BM treatment and the lowest in the CN (Figure 4-4b, c; Table 4-4). This increase in the fertilized treatments is primarily attributed to the P fertilizer source, ammonium polyphosphate, which directly supplies

phosphate, pyrophosphate, and polyphosphate to the soil (Hansen–Bruhn et al., 2025). Second, the higher P fertilizer application rate may have stimulated P uptake by soil microbial biomass. Previous studies at this site reported that microbial biomass P concentrations in the BM and SF treatments were 146% and 111% higher than in the CN treatment, respectively (Pasket, 2023). Because microorganisms can synthesize and store phosphorus as polyphosphates within their cells (Čapek et al., 2024), this increased microbial biomass may also have contributed to the greater polyphosphate and pyrophosphate concentrations observed in the fertilized plots.

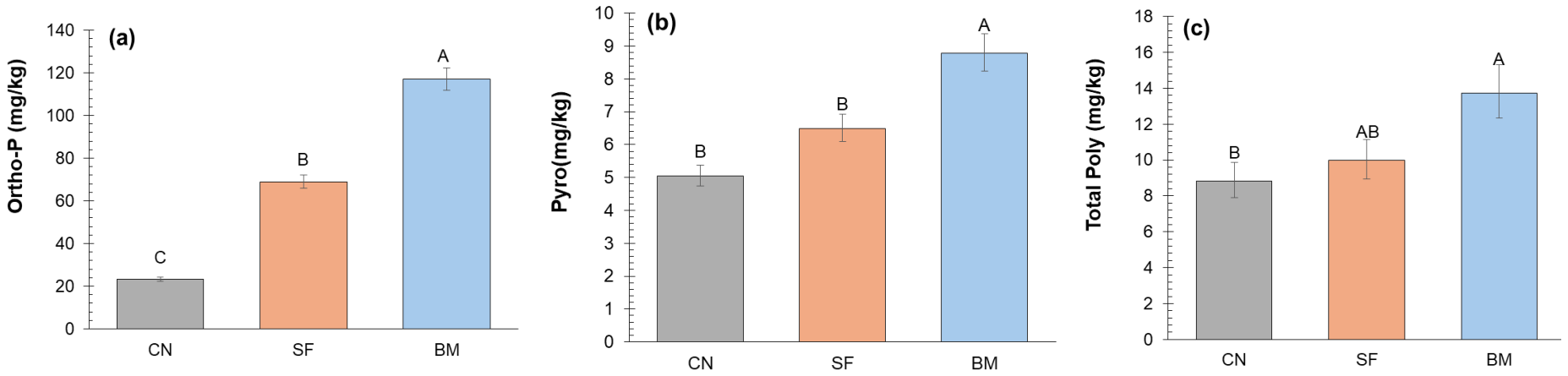


Figure 4-4. The main effect of P fertilization on different forms of inorganic phosphorus (a. orthophosphate, b. pyrophosphate, and c. total polyphosphate). Abbreviations used include control (CN), Sufficiency (SF), and build and maintain (BM) of phosphorus fertilizer application. Means within a treatment containing the same letter are not significantly different at α=0.05.

Table 4-4. Analysis of variance (ANOVA) results (P-values) for testing fixed effects of cover crop (Cover), phosphorus (P) fertilizer management (Fert), and their interactions on different compound classes and forms of inorganic and organic phosphorus. Significant effects (P < 0.05) are highlighted in bold.

Effect	P_i	P_o	TotPoly	TotIHP	Cmono	Cdiest	cM:D
Cover	0.894	0.268	0.933	0.229	0.556	0.404	0.932
Fert	**<0.001**	0.257	0.043	0.082	0.117	0.110	0.006
Fert * Cover	0.652	0.630	0.795	0.767	0.673	0.831	0.973
	OrthoP	**Pyro**	**Poly**	**Phn**	***myo*IHP**	**ScyIHP**	**sIP5**
Cover	0.148	0.969	0.317	0.723	0.015	0.374	0.598
Fert	<0.001	0.042	0.317	0.001	0.006	0.198	0.760
Fert * Cover	0.076	0.230	0.822	0.189	0.099	0.859	0.278
	ChiroIHP	**α-glyc**	**β-glyc**	**Nucl**	**Pchol**	**g6P**	**5 ppm**
Cover	0.314	0.205	0.277	0.516	0.219	0.785	0.408
Fert	0.365	0.128	0.076	0.127	0.389	0.052	0.611
Fert * Cover	0.396	0.627	0.531	0.582	0.111	0.326	0.386
	Mono1	**Mono2**	**Mono3**	**DNA**	**OthDi1**	**OthDi 2**	
Cover	0.947	**0.043**	**0.002**	0.216	0.774	0.566	
Fert	**0.017**	**<0.001**	**0.002**	0.092	0.562	0.053	
Fert * Cover	**0.029**	0.369	**0.013**	0.659	0.623	0.709	

Note: P_i: Inorganic Phosphorus; P_o: Organic Phosphorus; TotPoly: Total Polyphosphates; TotIHP: Total Inositol Hexakisphosphates; Cmono: Corrected Orthophosphate Monoesters; Cdiest: Corrected Orthophosphate Diesters; cM:D: Corrected Monoester-to-Diester ratio; OrthoP: Orthophosphate; Pyro: Pyrophosphate; Poly: Polyphosphate; Phn: Phosphonates; *myo*IHP: *myo*-Inositol Hexakisphosphate; ScyIHP: *scyllo*-Inositol Hexakisphosphate; sIP5: *scyllo*-Inositol Pentakisphosphate; neoIHP: *neo*-Inositol Hexakisphosphate; ChiroIHP: D-*chiro*-Inositol Hexakisphosphate; α-glyc: α-glycerophosphate; β-glyc: β-glycerophosphate; Nucl: Mononucleotides; Pchol: Choline phosphate; g6P: Glucose 6-phosphate; 5 ppm: Unknown peak at 5.0 ppm; 4.2 ppm: Unknown peak at 4.2 ppm; Mono1, Mono2, Mono3: Unknown Monoesters 1, 2, and 3; DNA: Deoxyribonucleic acid; OthDi1, OthDi 2: Other Diesters 1 and 2.

Organic P compounds (Monoesters, Diester degradation products, Phosphonates, *myo*-inositol hexakisphosphate)

The ^{31}P-NMR spectra contained several peaks within the orthophosphate monoester and diester regions (Table 4-3). Because some diesters can degrade into monoesters during the high-pH extraction and subsequent analysis, a degradation correction was applied. Corrected orthophosphate monoester (Cmono) and diester (Cdiest) concentrations were calculated by proportionally adjusting the raw monoester and diester pool sizes based on the degradation of specific diester compounds, primarily DNA and phospholipids, as described by Cade-Menun (2015). The Cmono and Cdiest pools were not significantly affected by the treatments (Table 4-4). However, the main effect of P fertilization significantly influenced the cM:D ratio (Figure 4-5a).

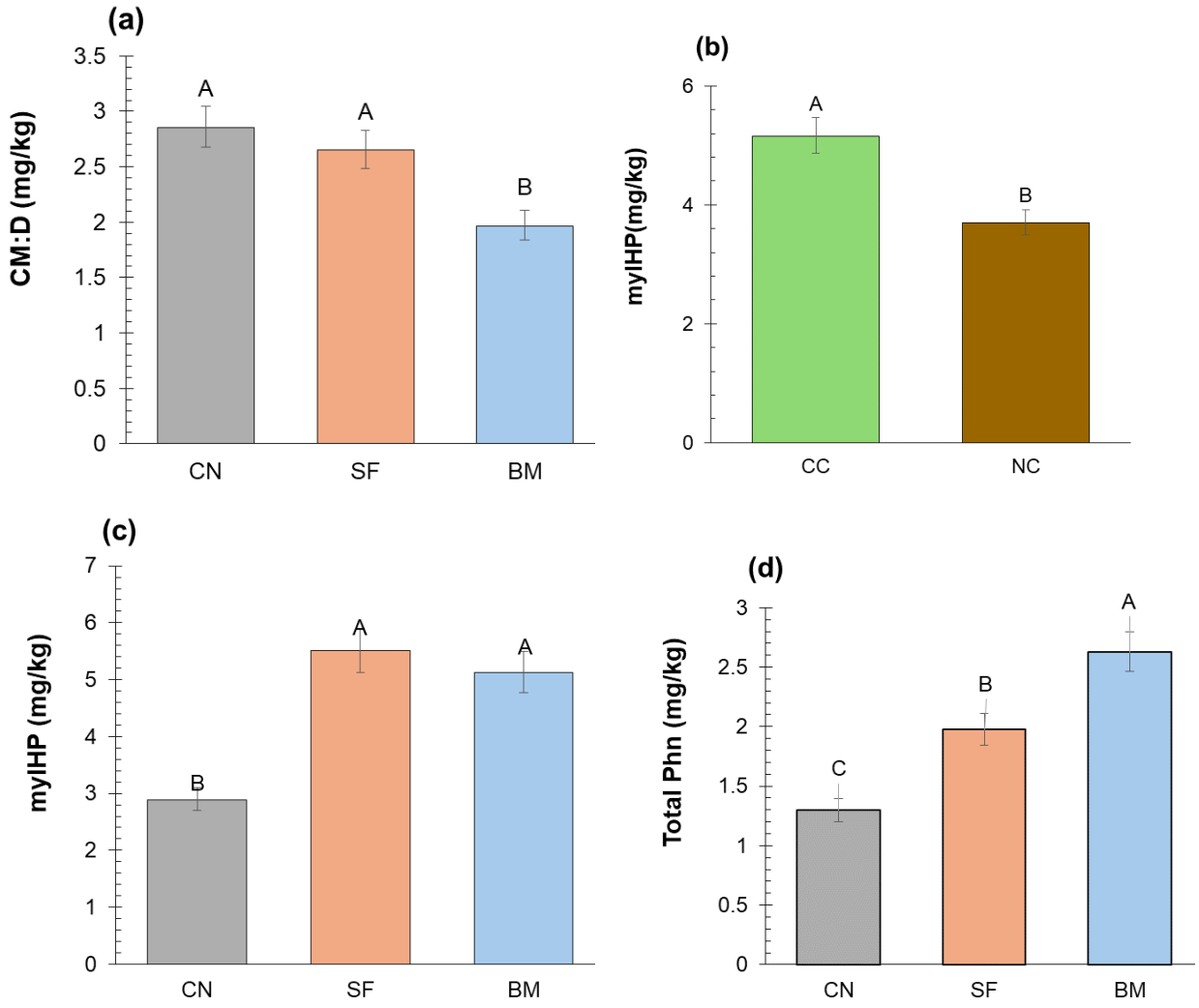


Figure 4-5. The main effects of phosphorus (P) fertilization and cover cropping on selected organic P pools: (a) the corrected monoester-to-diester (cM:D) ratio, (b) *myo*-inositol hexakisphosphate (*myo*-IHP) response to cover cropping, (c) *myo*-IHP response to P fertilization, and (d) total phosphonates response to P fertilization. Abbreviations: control (CN), sufficiency (SF), build and maintain (BM), no cover crop (NC), and cover crop (CC). Means within a treatment containing the same letter are not significantly different at α = 0.05.

Among the identified orthophosphate monoesters, *myo*-IHP (phytate) was the most abundant, representing approximately 12 to 15% of the total organic P pool. The main effect of cover crop significantly influenced *myo*-IHP concentrations, with higher concentrations observed in the cover crop (CC) treatments (8.77 mg P kg^{-1}) compared to the no cover crop (NC) treatments (7.68 mg P kg^{-1}) (Figure 4-5b; Table 4-5).

Table 4-5. Effect of cover crop and phosphorus (P) fertilization treatment on broad soil organic P pools and inositol phosphates, determined by ^{31}P-NMR spectroscopy.

Main Effect	Treatment	P_o (mg/kg)	Cmono (mg/kg)	Cdiest (mg/kg)	TotIHP (mg/kg)	ScyIHP (mg/kg)	sIP5 (mg/kg)	neoIHP (mg/kg)	ChiroIHP (mg/kg)
Cover	NC	55.3 a	35.0 a	14.3 a	7.68 a	1.22 a	1.17 a	1.90 a	1.99 a
Crop	CC	59.6 a	37.0 a	15.0 a	8.77 a	1.20 a	1.18 a	2.09 a	2.60 a
Fertilizer	CN	53.8 a	36.6 ab	12.9 b	6.82 b	1.18 a	0.92 a	1.59 a	1.95 a
	SF	61.6 a	39.0 a	14.8 ab	9.22 a	1.21 a	1.33 a	2.09 a	2.71 a
	BM	57.1 a	32.5 b	16.6 a	8.77 ab	1.21 a	1.30 a	2.33 a	2.18 a

Note: All values are expressed in mg kg^{-1} and rounded to three significant figures. Means within a column for each main effect followed by the same letter are not significantly different at $\alpha = 0.05$. Treatments: NC: No Cover Crop; CC: Cover Crop; CN: Control (No P fertilizer); SF: Sufficiency P fertilizer; BM: Build and Maintain P fertilizer. Phosphorus Compound Classes: P_o: Total Organic Phosphorus; Cmono: Corrected Orthophosphate Monoesters; Cdiest: Corrected Orthophosphate Diesters; TotIHP: Total Inositol Hexakisphosphate; ScyIHP: *scyllo*-Inositol Hexakisphosphate; sIP5: *scyllo*-Inositol Pentakisphosphate; neoIHP: *neo*-Inositol Hexakisphosphate; ChiroIHP: D-*chiro*-Inositol Hexakisphosphate.

The *myo*-IHP stereoisomers *scyllo*-IHP, *neo*-IHP, and D-*chiro*-IHP were also detected, though their concentrations were generally lower and were not significantly affected by the main treatments. Phytate (*myo*-IHP) is synthesized strictly by plants and accumulates in seeds and

roots. The origins of the other IHP stereoisomers are unknown; they may originate from plants or be synthesized via epimerization by soil microorganisms (Turner, 2007). The increase in *myo*-IHP in the CC treatment indicates an accumulation of plant-derived organic P, likely originating from the decomposition of cover crop biomass.

In addition to the known monoesters, several unknown monoester peaks were detected (Monoester 1, 2, and 3; Table 4-3). The main effects of fertilization and cover cropping were significant for Monoester 2 (Table 4-4; Table 4-5). Furthermore, the interaction of cover crop and fertilization was significant for Monoester 1, Monoester 3, and the unknown peak at 4.2 ppm (Table 4-4). Detailed interaction means and standard errors for these uncharacterized peaks are provided in the supplementary material (Appendix A, Table A2). The specific identity of these monoesters remains unknown, but their differential response to the treatment interactions suggests that the combination of cover crop residue inputs and specific fertilizer regimes selectively favors the accumulation or microbial synthesis of distinct, uncharacterized organic P forms. Overall, there was not a clear, uniform pattern of cover crop or P fertilizer management effects across these specific unknown P compounds, highlighting the complex and compound-specific nature of organic P cycling in these soils.

Table 4-6.Effect of cover crop and phosphorus (P) fertilization treatment on specific orthophosphate monoesters, diesters, and phosphonates, determined by ^{31}P-NMR spectroscopy.

Main Effect	Treatment	Phn	a-glyc	b-glyc	g6P	Mono 2	Nucl	Pchol	5 ppm	DNA	OthDi1	OthDi 2
		mg kg^{-1}	mg kg^{-1}	mg kg^{-1}	mg kg^{-1}	mg kg^{-1}	mg kg^{-1}	mg kg^{-1}	mg kg^{-1}	mg kg^{-1}	mg kg^{-1}	mg kg^{-1}
Cover Crop	NC	1.84 a	1.34 a	2.73 a	0.83 a	19.12 a	5.96 a	0.71 a	1.58 a	1.46 a	2.32 a	0.69 a
	CC	1.98 a	1.65 a	3.26 a	0.88 a	18.70 b	6.21 a	0.90 a	1.95 a	1.17 a	2.67 a	0.66 a
Fertilizer	CN	1.30 c	1.10 b	2.20 b	0.84 a	21.80 a	5.71 a	0.69 a	1.56 a	1.30 a	1.94 a	0.72 a
	SF	1.99 b	1.74 a	3.51 a	1.01 a	19.91 b	6.16 a	0.90 a	1.89 a	0.90 a	2.46 a	0.43 b
	BM	2.65 a	1.68 ab	3.36 ab	0.72 b	15.25 c	6.27 a	0.80 a	1.81 a	1.87 a	3.17 a	0.97 a

Note: All values are expressed in mg kg^{-1}. Means within a column for each main effect followed by the same letter are not significantly different at $\alpha = 0.05$. Phosphorus Forms: Phn: Phosphonates; a-glyc: a-glycerophosphate; b-glyc: b-glycerophosphate; g6P: Glucose 6-phosphate; Mono 2: Unknown Monoester 2; Nucl: Mononucleotides; Pchol: Choline phosphate; 5 ppm: Unknown peak at 5.0 ppm; DNA: Deoxyribonucleic acid; OthDi1: Other Diesters 1; OthDi 2: Other Diesters 2.

Phosphonates, characterized by a highly stable C-P bond, were also detected in the spectra (Table 4-3; Table 4-6; Figure 4-5d). There was a significant main effect of P fertilization on total phosphonates, with the highest concentrations in the BM treatment and the lowest in the CN. Phosphonates in agricultural soils may originate from agricultural chemicals such as herbicides and their breakdown products (e.g., glyphosate), or may originate from microbial synthesis (e.g., ciliates and fungi) rather than direct plant inputs (Cade-Menun, 2015; Condron et al., 2005). The origins of the elevated phosphonate concentrations in the fertilized plots cannot be directly determined from our current data, but could reflect enhanced microbial activity and biomass driven by the higher availability of inorganic P and root exudates. Furthermore, the

higher crop yields in fertilized treatments result in significantly greater carbon (C) inputs from crop residues, which additionally stimulates microbial activity and the biological synthesis of these compounds, leading to their subsequent stabilization in the soil. However, further research is needed to fully understand the origin of the phosphonates detected in these soils.

Previous studies comparing fertilized and unfertilized systems have reported varying responses in organic P pools. For instance, Liu et al. (2015) observed a reduction in total P_o with continued P fertilization in a wheat-fallow system. In contrast, our results demonstrate an overall increase in major organic P forms (such as NaOH-P_o and specific monoesters) in the fertilized (SF and BM) treatments. This difference likely arises from variations in crop rotation, soil types, and regional climate dynamics. The continuous corn-soybean rotation, coupled with cover cropping in our system, likely returns significantly more biomass and organic residues to the soil compared to the wheat-fallow rotation studied by Chen et al. (2021), thereby fostering a greater accumulation and active cycling of organic P pools alongside the inorganic fertilizer inputs.

Correlations between Soil Phosphorus Pools and Agronomic Indicators

Pearson correlation analysis was conducted to further evaluate the relationships among selected soil P pools, agronomic soil test P (Mehlich-3 P), crop yield, and crop P uptake (Table 4-7). Agronomic data utilized for this correlation analysis, including Mehlich-3 P concentrations, corn grain yields, and total crop P uptake, were collected and published in parallel evaluations of these experimental plots (Bourns et al., 2026; Nelson et al., 2023).

Table 4-7. Pearson correlation coefficients (r) between selected soil phosphorus pools, agronomic soil test P (STP), crop yield, and crop P uptake.

Phosphorus Pool	Mehlich 3-P (STP)	Crop Yield	Crop P Uptake
	Sequential Fractionation		
Resin-P_i	0.995***	0.686**	0.839***
$NaHCO_3$-P_i	0.738***	0.468*	0.598**
NaOH-P_i	0.951***	0.705**	0.834***
NaOH-P_o	0.501*	-	0.599**
	P-NMR Spectroscopy		
Orthophosphate	0.936***	0.714***	0.895***
Total Polyphosphate	0.724***	-	0.513*
myo-IHP	-	-	-
Total Phosphonates	0.918***	0.655**	0.839***

Note: Only significant correlations are shown. * $P < 0.05$, ** $P < 0.01$, *** $P < 0.001$. STP is represented by Mehlich-3 P.

The results revealed strong positive correlations between labile inorganic P fractions (such as Resin-P_i, orthophosphate, and $NaHCO_3$-P_i) and all agronomic indicators. The NaOH-P_i fraction also demonstrated a strong positive relationship across these metrics. These strong associations align with the speciation data; specifically, the strong correlation between the operationally-defined labile inorganic pool (Resin-P_i) and the analytically confirmed orthophosphate pool validates that these highly extractable fractions are indeed dominated by readily solublephosphate. As suggested by previous research, these inorganic pools represent

sources for plant available P and subsequent crop uptake. Furthermore, their direct correlation with STP is consistent with the hypothesis that there is a potential risk of environmental P loss through runoff when these pools are inflated, particularly under high-input management such as the build-and-maintain (BM) fertilization strategy (McDowell et al., 2001; Pote et al., 1996; Sharpley, 1995). However, because this study is based on a designed experiment, the observed correlations between specific P pools and agronomic parameters may partly reflect parallel responses to the applied fertilizer treatments rather than purely direct mechanistic dependencies. Nonetheless, these strong parallel trends critically underscore how specific fertilizer management strategies simultaneously govern both agronomic performance and the accumulation of environmentally sensitive P pools.

Implications for soil fertility and potential P loss in runoff

The integrated results from the sequential fractionation and ^{31}P-NMR spectroscopy offer important mechanistic insights for managing soil fertility and mitigating environmental risks. Agronomic background data from this site (Bourns et al., 2024) indicate that both the SF and BM strategies successfully maintained crop yields compared to the unfertilized control. However, our speciation data reveal that the fertilization strategies drive fundamentally different P accumulation patterns. The BM approach resulted in the highest concentrations of orthophosphate and moderately labile P (e.g., NaOH-P_i). While this ensures sufficient P availability, the continuous buildup of these inorganic pools could increase the saturation of Fe/Al oxide sorption sites (Condron et al., 2005; Tiessen & Moir, 1993).

As these sites become saturated, a greater proportion of P becomes susceptible to desorption, which has been widely associated with elevated risks of dissolved reactive P (DRP) loss in surface runoff during heavy rainfall events in other studies (McDowell et al., 2001; Sharpley, 1995). In fact, edge-of-field water quality monitoring at this specific study site directly corroborates this mechanism; Sakib et al. (2026) reported that the BM strategy significantly increased P loss in runoff compared to drawdown and sufficiency approaches.

Conversely, the accumulation of P_o pools and compounds, particularly *myo*-IHP and NaOH-P_o under cover-cropped treatments, represents an important reservoir of potentially plant-available P. Cover cropping successfully increased the P_o pool without inflating the highly mobile P_i pools. In soils where P fertilization is managed under the sufficiency (SF) strategy, the biologically driven mineralization of these organic pools can sustain plant requirements while minimizing the accumulation of excessive inorganic P. This mechanistic logic is strongly supported by recent agronomic evaluations at this site (Bourns et al., 2026), which demonstrated that the SF strategy produced corn and soybean yields equivalent to the BM strategy. Because the SF system maintained high crop yields despite having significantly lower concentrations of highly mobile inorganic P (Resin-P_i and orthophosphate), the crops likely fulfilled a portion of their physiological P requirements through the active, biologically driven mineralization of these enriched organic pools (e.g., *myo*-IHP and NaOH-P_o).

Therefore, shifting from a BM approach to an SF approach, coupled with cover cropping, appears to be a more sustainable management strategy. It balances the need for maintaining soil fertility through internal organic P cycling while proactively mitigating the potential environmental risks associated with agricultural P runoff.

Conclusion

This study demonstrated that long-term P fertilization strategies and cover cropping significantly, yet distinctly, alter soil P pools and speciation. Our findings fully support the hypothesis that the build-and-maintain (BM) fertilization strategy predominantly inflates P_i pools. The BM strategy significantly increased highly mobile and moderately labile P_i species and fractions, particularly Resin-P_i, NaOH-P_i, orthophosphate, and polyphosphates. While this ensures high agronomic soil test P, it concurrently elevates the potential risk of P loss by continuously loading soil sorption sites.

Conversely, our hypothesis regarding the impact of cover crops on P_o cycling was also supported: cover cropping actively promoted the accumulation of P_o compounds and increases in P_o pools, specifically *myo*-IHP and NaOH-P_o, likely driven by continuous plant residue inputs and subsequent microbial synthesis.

By integrating our high-resolution speciation results with parallel agronomic and water quality data from this site, a clear, evidence-based mechanistic pathway emerges. Because the sufficiency (SF) strategy sustained crop yields equivalent to the BM strategy despite maintaining significantly lower labile P_i concentrations (Bourns et al., 2026), we conclude that the enriched P_o pools act as a critical, biologically mediated reservoir. These P_o fractions can mineralize to sustain crop P requirements without requiring the excessive inflation of highly mobile phosphate concentrations that drive runoff losses.

Ultimately, transitioning from a BM to a sufficiency (SF) strategy, combined with cover cropping, offers a more sustainable approach; the SF strategy minimizes phosphate loading while the cover crops maintain an active, internal P_o cycle to support crop yields and mitigate

environmental risks. To further clarify these dynamics, future research should focus on the direct characterization of P forms in crop and cover crop residues using advanced techniques like ^{31}P-NMR spectroscopy to fully elucidate their role in replenishing specific soil P pools.

References

Abdi, D., Cade-Menun, B. J., Ziadi, N., & Parent, L.-É. (2015). Compositional statistical analysis of soil ^{31}P-NMR forms. *Geoderma*, 257–258, 40–47. https://doi.org/10.1016/j.geoderma.2014.11.030

Ahlgren, J., Djodjic, F., Börjesson, G., & Mattsson, L. (2013). Identification and quantification of organic phosphorus forms in soils from fertility experiments. Soil Use and Management, 29(1), 24–35. https://doi.org/10.1111/sum.12014

Annaheim, K. E., Doolette, A. L., Smernik, R. J., Mayer, J., Oberson, A., Frossard, E., & Bünemann, E. K. (2015). Long-term addition of organic fertilizers has little effect on soil organic phosphorus as characterized by ^{31}P-NMR spectroscopy and enzyme additions. Geoderma, 257–258, 67–77. https://doi.org/10.1016/j.geoderma.2015.01.014

Arai, Y., & Sparks, D. L. (2007). Phosphate reaction dynamics in soils and soil components: A multiscale approach. Advances in Agronomy, 94, 135–179. https://doi.org/10.1016/S0065-2113(06)94003-6

Barbosa, L. D., da Luz, J. H., dos Santos, R. A., de Souza, J. W., de Oliveira, H. P., Silva, D. M., Soltangheisi, A., Pavinato, P. S., & dos Santos, V. R. (2026). Cover crops modulate soil phosphorus dynamics under P fertilizer sources in dryland maize production on tropical soil. Geoderma Regional, 36, e01065. https://doi.org/10.1016/j.geodrs.2026.e01065

Bourns, M. A., Nelson, N. O., Carver, R. E., Roozeboom, K. L., Kluitenberg, G. J., Tomlinson, P. J., Kang, Q., & Hettiarachchi, G. M. (2024). Cover crops impact phosphorus cycling and environmental efficiency in a corn–soybean system. Agronomy Journal, 116(1), 109–120. https://doi.org/10.1002/agj2.21498

Bourns, M., Yeager, E., Nelson, N., Kluitenberg, G., Roozeboom, K., Hettiarachchi, G., Tomlinson, P., & Presley, D. (2026). Phosphorus drawdown improves net return and water quality in a no-till corn–soybean system. Journal of Soil and Water Conservation, 81(3), 222–235. https://doi.org/10.1080/00224561.2026.2651052

Cade-Menun, B. J. (2015). Improved peak identification in ^{31}P-NMR spectra of environmental samples with a standardized method and peak library. Geoderma, 257–258, 102–114. https://doi.org/10.1016/j.geoderma.2014.12.016

Cade-Menun, B. J. (2017). Characterizing phosphorus forms in cropland soils with solution ^{31}P-NMR: Past studies and future research needs. Chemical and Biological Technologies in Agriculture, 4(1), 19. https://doi.org/10.1186/s40538-017-0098-4

Cade-Menun, B. J. (2022). Changes in soil phosphorus pools in long-term wheat-based rotations in Saskatchewan, Canada, with and without phosphorus fertilization. Spanish Journal of Soil Science, 12, 10737. https://doi.org/10.3389/sjss.2022.10737

Cade-Menun, B. J., & Liu, C. W. (2014). Solution phosphorus-31 nuclear magnetic resonance spectroscopy of soils from 2005 to 2013: A review of sample preparation and experimental parameters. Soil Science Society of America Journal, 78(1), 19–37. https://doi.org/10.2136/sssaj2013.05.0187dgs

Cade-Menun, B. J., Doody, D. G., Liu, C. W., & Watson, C. J. (2017). Long-term changes in grassland soil phosphorus with fertilizer application and withdrawal. Journal of Environmental Quality, 46(3), 537–545. https://doi.org/10.2134/jeq2016.09.0373

Čapek, P., Tupá, A., & Choma, M. (2024). Exploring polyphosphates in soil: Presence, extractability, and contribution to microbial biomass phosphorus. Biology and Fertility of Soils, 60(5), 667–680. https://doi.org/10.1007/s00374-024-01829-6

Chen, S., Cade-Menun, B. J., Bainard, L. D., Luce, M. S., Hu, Y., & Chen, Q. (2021). The influence of long-term N and P fertilization on soil P forms and cycling in a wheat/fallow cropping system. Geoderma, 404, 115274. https://doi.org/10.1016/j.geoderma.2021.115274

Condron, L. M., Turner, B. L., & Cade-Menun, B. J. (2005). Chemistry and dynamics of soil organic phosphorus. In J. T. Sims & A. N. Sharpley (Eds.), Phosphorus: Agriculture and the environment (pp. 87–121). American Society of Agronomy, Crop Science Society of America, & Soil Science Society of America. https://doi.org/10.2134/agronmonogr46.c4

Dodd, R. J., & Sharpley, A. N. (2015). Recognizing the role of soil organic phosphorus in soil fertility and water quality. Resources, Conservation and Recycling, 105, 282–293. https://doi.org/10.1016/j.resconrec.2015.10.001

Dodds, W. K., Bouska, W. W., Eitzmann, J. L., Pilger, T. J., Pitts, K. L., Riley, A. J., Schloesser, J. T., & Thornbrugh, D. J. (2009). Eutrophication of U.S. freshwaters: Analysis of potential economic damages. Environmental Science & Technology, 43(1), 12–19. https://doi.org/10.1021/es801217q

Gamage, K. H. H., Hettiarachchi, G. M., Nelson, N. O., Roozeboom, K. L., Kluitenberg, G. J., Tomlinson, P. J., & Presley, D. R. (2025). Phosphorus and cover crop management practices affect phosphorus speciation in soils and eroded sediments. Journal of Environmental Quality, 54(2), 382–396. https://doi.org/10.1002/jeq2.20677

Guppy, C. N., Menzies, N. W., Moody, P. W., & Blamey, F. P. C. (2005). Competitive sorption reactions between phosphorus and organic matter in soil: A review. Australian Journal of Soil Research, 43(2), 189–202. https://doi.org/10.1071/SR04049

Hallama, M., Pekrun, C., Lambers, H., & Kandeler, E. (2019). Hidden miners–the roles of cover crops and soil microorganisms in phosphorus cycling through agroecosystems. Plant and Soil, 434(1–2), 7–45. https://doi.org/10.1007/s11104-018-3810-7

Hansen-Bruhn, I., Craig, J. L., Hinge, M., & Hull, T. R. (2025). Ammonium polyphosphates: Correlating structure to application. European Polymer Journal, 223, 113644. https://doi.org/10.1016/j.eurpolymj.2024.113644

Harrison, A. F. (1987). Soil organic phosphorus: A review of world literature. CAB International.

Hedley, M. J., Stewart, J. W. B., & Chauhan, B. S. (1982). Changes in inorganic and organic soil phosphorus fractions induced by cultivation practices and by laboratory incubations. Soil Science Society of America Journal, 46(5), 970–976. https://doi.org/10.2136/sssaj1982.03615995004600050017x

Hudnell, H. K. (2010). The state of U.S. freshwater harmful algal blooms assessments, policy and legislation. Toxicon, 55(5), 1024–1034. https://doi.org/10.1016/j.toxicon.2009.07.021

Leikam, D. F., Lamond, R. E., & Mengel, D. B. (2003). Providing flexibility in phosphorus and potassium fertilizer recommendations. Better Crops with Plant Food, 87(3), 6–10.

Liu, J., Hu, Y., Yang, J., Abdi, D., & Cade-Menun, B. J. (2015). Investigation of soil legacy phosphorus transformation in long-term agricultural fields using sequential fractionation, P K-edge XANES and solution ^{31}P-NMR spectroscopy. Environmental Science & Technology, 49(1), 168–176. https://doi.org/10.1021/es504420n

Macnack, N. E., Chim, B. K., Amedy, B., & Arnall, D. B. (2017). Fertilization based on sufficiency, build-up and maintenance concept (Fact Sheet PSS-2266). Oklahoma State University Extension. https://extension.okstate.edu/fact-sheets/fertilization-based-on-sufficiency-build-up-and-maintenance-concept.html

McDowell, R. W., Sharpley, A. N., Condron, L. M., Haygarth, P. M., & Brookes, P. C. (2001). Processes controlling soil phosphorus release to runoff and implications for agricultural management. Nutrient Cycling in Agroecosystems, 59(3), 269–284. https://doi.org/10.1023/A:1014419206761

McDowell, R. W., Stewart, I., & Cade-Menun, B. J. (2006). An examination of spin-lattice relaxation times for analysis of soil and manure extracts by liquid state phosphorus-31 nuclear magnetic resonance spectroscopy. Journal of Environmental Quality, 35(1), 293–302. https://doi.org/10.2134/jeq2005.0298

Murphy, J., & Riley, J. P. (1962). A modified single solution method for the determination of phosphate in natural waters. Analytica Chimica Acta, 27, 31–36. https://doi.org/10.1016/S0003-2670(00)88444-5

Nelson, N. O., Roozeboom, K. L., Yeager, E. A., Williams, J. R., Zerger, S. E., Kluitenberg, G. J., Tomlinson, P. J., Abel, D. S., & Carver, R. E. (2023). Agronomic and economic implications of cover crop and phosphorus fertilizer management practices for water quality improvement. Journal of Environmental Quality, 52(1), 113–125. https://doi.org/10.1002/jeq2.20427

Noack, S. R., McLaughlin, M. J., Smernik, R. J., McBeath, T. M., & Armstrong, R. D. (2014). Phosphorus speciation in mature wheat and canola plants as affected by phosphorus supply. Plant and Soil, 378(1–2), 125–137. https://doi.org/10.1007/s11104-013-2015-3

Olsen, S. R., & Sommers, L. E. (1982). Phosphorus. In A. L. Page, R. H. Miller, & D. R. Keeney (Eds.), Methods of soil analysis: Part 2—Chemical and microbiological properties (2nd

ed., pp. 403–430). American Society of Agronomy & Soil Science Society of America. https://doi.org/10.2134/agronmonogr9.2.2ed.c24

Pasket, A. (2023). Seasonal dynamics and impact of P fertilizer treatments and cover crops on soil health indicators in a no-till corn-soybean system [Ph.D., Kansas State University]. https://hdl.handle.net/2097/43115

Pierzynski, G. M., McDowell, R. W., & Sims, J. T. (2005). Chemistry, cycling, and potential movement of inorganic phosphorus in soils. In J. T. Sims & A. N. Sharpley (Eds.), Phosphorus: Agriculture and the environment (pp. 53–86). American Society of Agronomy, Crop Science Society of America, & Soil Science Society of America. https://doi.org/10.2134/agronmonogr46.c3

Pote, D. H., Daniel, T. C., Sharpley, A. N., Moore, P. A., Jr., Edwards, D. R., & Nichols, D. J. (1996). Relating extractable soil phosphorus to phosphorus losses in runoff. Soil Science Society of America Journal, 60(3), 855–859. https://doi.org/10.2136/sssaj1996.03615995006000030025x

Sakib, T. U., Hettiarachchi, G. M., Kluitenberg, G. J., Roozeboom, K. L., Tomlinson, P. J., Presley, D. R., & Nelson, N. O. (2026). Drawdown phosphorus management in cover cropping systems: A strategy for mitigating phosphorus loss in agroecosystems. Journal of Environmental Quality. (In review).

SAS Institute. (2020). SAS/STAT 15.2 user's guide (Version 9.4). SAS Institute Inc.

Schefe, C. R., Barlow, K. M., Robinson, N. J., Crawford, D. M., McLaren, T. I., Smernik, R. J., Croatto, G., Walsh, R. D., & Kitching, M. (2015). 100 years of superphosphate addition to pasture in an acid soil—current nutrient status and future management. Soil Research, 53(6), 662–676. https://doi.org/10.1071/SR14241

Sharpley, A. N. (1995). Dependence of runoff phosphorus on extractable soil phosphorus. Journal of Environmental Quality, 24(5), 920–926. https://doi.org/10.2134/jeq1995.00472425002400050020x

Sharpley, A. N., Bergström, L., Aronsson, H., Bechmann, M., Bolster, C. H., Börling, K., Djodjic, F., Jarvie, H. P., Schoumans, O. F., Stamm, C., Tonderski, K. S., Ulén, B., Uusitalo, R., & Withers, P. J. A. (2015). Future agriculture with minimized phosphorus

losses to waters: Research needs and direction. Ambio, 44(Suppl. 2), S163–S179. https://doi.org/10.1007/s13280-014-0612-x

Sommers, L. E., & Nelson, D. W. (1972). Determination of total phosphorus in soils: A rapid perchloric acid digestion procedure. Soil Science Society of America Journal, 36(6), 902–904. https://doi.org/10.2136/sssaj1972.03615995003600060020x

Tiecher, T., Rheinheimer dos Santos, D., & Calegari, A. (2012a). Soil organic phosphorus forms under different soil management systems and winter crops, in a long-term experiment. Soil and Tillage Research, 124, 57–67. https://doi.org/10.1016/j.still.2012.05.001

Tiecher, T., Rheinheimer dos Santos, D., Kaminski, J., & Calegari, A. (2012b). Forms of inorganic phosphorus in soil under different long-term soil tillage systems and winter crops. Revista Brasileira de Ciência do Solo, 36(1), 271–282. https://doi.org/10.1590/S0100-06832012000100028

Tiessen, H., & Moir, J. O. (1993). Characterization of available P by sequential extraction. In M. R. Carter (Ed.), Soil sampling and methods of analysis (pp. 75–86). CRC Press.

Tiessen, H., Stewart, J. W. B., & Cole, C. V. (1984). Pathways of phosphorus transformations in soils of differing pedogenesis. *Soil Science Society of America Journal*, 48(4), 853–858. https://doi.org/10.2136/sssaj1984.03615995004800040031x

Turner, B. L. (2007). Inositol phosphates in soil: Amounts and forms of the Earth's most abundant organic phosphorus compound. In B. L. Turner, A. E. Richardson, & E. J. Mullaney (Eds.), Inositol phosphates: Linking agriculture and the environment (pp. 186–206). CAB International. https://doi.org/10.1079/9781845931520.0186

Turner, B. L., Cade-Menun, B. J., Condron, L. M., & Richardson, A. E. (2005). Extraction of soil organic phosphorus. Talanta, 66(2), 294–306. https://doi.org/10.1016/j.talanta.2004.11.012

Verheyen, D., Van Gaelen, N., Ronchi, B., Batelaan, O., Struyf, E., Govers, G., Merckx, R., & Diels, J. (2015). Dissolved phosphorus transport from soil to surface water in catchments with different land use. Ambio, 44(Suppl. 2), S228–S240. https://doi.org/10.1007/s13280-014-0617-5

Chapter 5 - The effect of P fertilization and cover cropping on soil fertility indicators in a no-till corn soybean rotation system

Abstract

Sustainable phosphorus (P) management in no-till agricultural systems requires balancing crop nutrient requirements with the need to mitigate environmental impacts, including loss of dissolved reactive P. This study evaluated the interactive effects of cover cropping (CC) and distinct P fertilization strategies on the vertical distribution of soil fertility indicators and P budgets in a no-till corn-soybean rotation. The field experiment (2019–2025) included two cover crop treatments (with and without) and three P fertilization strategies: a control (CN, no P), build-and-drawdown (BD), and build-and-maintain (BM). Soil samples were collected annually at 0–2.5, 2.5–5, and 5–15 cm depths and analyzed for soil pH, Mehlich-3 P, total P (TP), total carbon (TC), and total nitrogen (TN). Results showed that P fertilization significantly increased TP and Mehlich-3 P, but this accumulation was highly stratified, occurring primarily in the uppermost soil layer (0–2.5 cm). Evaluation of the P budget (P_{in} - P_{out}) revealed that while the BM strategy generally maintained the highest concentrations of agronomic soil test P (Mehlich-3 P), it exacerbated surface P accumulation over time. Conversely, the BD strategy resulted in a progressive decline in surface Mehlich-3 P concentrations during the drawdown phase, demonstrating that crops successfully utilized legacy P reserves to sustain yields under a highly negative P budget without immediate yield penalties. Furthermore, cover cropping significantly increased surface TC and TN over time while decreasing surface Mehlich-3 P, regardless of P

fertilization rate. These findings demonstrate that integrating a strategic P drawdown approach with cover cropping provides a robust management framework that utilizes legacy P, enhances soil OM, and reduces environmental risks associated with excessive surface P accumulation without compromising agronomic productivity.

Introduction

Soil phosphorus (P) management remains a central challenge in agricultural systems due to its dual role in sustaining crop productivity and contributing to environmental degradation when lost from soils. Effective management of soil P depends on how agricultural practices influence its availability and cycling within the soil. In agricultural systems, these dynamics are shaped primarily through fertilization strategies and cropping system choices. Conservation practices, such as cover cropping, can alter soil physical, chemical, and biological processes that regulate nutrient cycling (Blanco-Canqui & Ruis, 2020; Haruna et al., 2020; McClelland et al., 2021; Poeplau & Don, 2015; Schipanski et al., 2014; Xu et al., 2024). In particular, cover crops are widely used due to their capacity to improve soil health, limit erosion, reduce sediment-associated nutrient transport, and support long-term soil fertility (Carver et al., 2022; Maltais-Landry & Frossard, 2015; Sharpley & Smith, 1994).

Beyond reducing erosion, cover crops play an important role in shaping soil fertility and nutrient dynamics. They contribute to improved soil carbon (C) and nitrogen (N) storage by increasing soil OM, enhancing microbial diversity, and promoting nutrient cycling (Hao et al., 2023; McClelland et al., 2021; Xu et al., 2024). Furthermore, cover crops can take up nutrients, including P as phosphate, from deeper soil layers and redistribute them to the surface through

biomass production and residue decomposition (Hallama et al., 2019; Soltangheisi et al., 2020). However, the extent to which cover cropping influences key soil fertility indicators—such as total P, Mehlich-3 P, total C, and total N—appears to be highly context-dependent and variable across studies (Barbosa et al., 2026; Kaur et al., 2024; Welch et al., 2016; White & Weil, 2011). These varying effects are heavily influenced by the specific cover crop species (e.g., legumes vs. grasses), the C:N and C:P ratios of the residue, the timing of termination relative to cash crop planting, initial soil nutrient status, and regional climatic conditions that dictate the rate of biomass decomposition and mineralization (Kaur et al., 2024; Maltais-Landry & Frossard, 2015).

In parallel, the source, rate, and method of P fertilizer application play critical roles in determining soil P accumulation and the potential for P losses (Bindraban et al., 2020; Sharpley, 2003). While cover cropping influences internal soil nutrient cycling, P fertilization directly regulates external inputs. Recent literature has extensively evaluated distinct P management paradigms, such as build-and-maintain versus drawdown strategies, to manage legacy P and optimize crop yields (Bourns et al., 2026). However, these specific P fertilization strategies are rarely evaluated in combination with cover cropping in stratified, no-till temperate systems (Barbosa et al., 2026; Soltangheisi et al., 2018).

In continuous no-till systems, the lack of mechanical mixing inherently leads to severe nutrient stratification, where broadcast fertilizers and decomposing crop residues progressively concentrate P, C, and N exclusively in the uppermost soil layer (typically 0–2.5 or 0–5 cm) (Robbins & Voss, 1991; Sharpley, 2003). Because surface runoff directly interacts with this highly concentrated, narrow surface layer, nutrient stratification exponentially increases the risk of dissolved reactive P loss during rainfall events (McDowell et al., 2001; Sharpley et al., 2015).

Understanding the interactive effects of these combined practices on the vertical distribution (e.g., 0–2.5, 2.5–5, and 5–15 cm depths) of soil fertility indicators is necessary to develop integrated P management systems that simultaneously maintain soil fertility and protect downstream water quality.

There are three main P fertilization approaches relevant to this study: build-and-maintain, drawdown, and sufficiency strategies. With the build-and-maintain approach, we build the soil test P (STP) above the critical level and then maintain those levels by adding P fertilizer based on crop removal (Macnack et al., 2017; Patel et al., 2024). Although this approach helps to prevent yield limitations due to P deficiency, high soil STP due to continued P fertilizer application increases the likelihood of phosphorus loss to surface waters via runoff (McDowell et al., 2001; Wortmann et al., 2009). The drawdown strategy, on the other hand, reduces the P inputs to allow STP to decline. This approach enables crops to utilize accumulated legacy P while minimizing further fertilizer applications. Once STP is drawn down near the critical agronomic threshold, a sufficiency strategy can be implemented. The sufficiency approach applies only the minimum amount of P fertilizer required to meet the immediate nutritional needs of the current crop, avoiding further depletion or unnecessary accumulation.

Differences in P application rates among build-and-maintain, drawdown, and sufficiency strategies are expected to influence soil P accumulation and availability over time. According to Syers et al. (2008), newly applied fertilizer P is rapidly distributed between readily available and less readily available soil P pools through adsorption and absorption processes; when P fertilizer inputs exceed crop P removal over time, surplus P accumulates in the soil and is progressively distributed among different soil P pools with varying degrees of reversibility through sorption

and fixation processes. Repeated fertilizer applications can therefore increase both soil test P concentrations and total soil P concentrations over time due to the buildup of residual P in the soil. It has also been reported by Hooda et al. (2001) that a higher rate of P fertilization increases soil total P and soil test P concentrations.

Therefore, the objective of this study was to evaluate the effect of P fertilization strategies (build-maintain and build-drawdown) and cover cropping on soil pH, Mehlich-3 P, total P (TP), total N (TN), and total C (TC) across multiple soil depths (0 to 2.5, 2.5 to 5, and 5 to 15 cm). We hypothesized that higher P application rates under the build-maintain strategy would increase both total P and soil test P concentrations, compared to build-drawdown and control treatments. Additionally, we hypothesized that the inclusion of cover crops would increase TP, TN, and TC in surface soils due to greater OM inputs and also greater P extraction from lower soil depths and cycling back to the soil surface.

Material and Methods

Experimental site and design

This study was conducted at the Kansas Agricultural Watershed (KAW) field laboratory near Manhattan, Kansas, from September 2019 to September 2025. Soils at the location are mapped as eroded Smolan silty clay loam (fine, smectitic, mesic Pachic Argiustoll) on slopes ranging from 3 to 7%. The study site has 18 watersheds ranging in size from 0.46 to 0.65 ha plots. The experiment was arranged as a 2 × 3 factorial randomized complete block design with three replications (blocked by landscape position). The two main factors were cover crop management (with and without cover crop) and three levels of P fertilization strategy, which

evolved through specific phases over time as detailed below. Further details on the overall experimental site can be found in Chapter 3.

Agronomic management

Prior to September 2019, there was another phase of this study at this site; further details on agronomic practices related to this time are provided in Nelson et al. (2023) and Bourns et al. (2024). In brief, the cropping system was a continuous no-till corn-soybean rotation. From 2015 to 2019, the cover crop species varied by season according to the preceding crop, consisting of either winter wheat or winter triticale (×*Triticosecale Wittm.*), grown alone or in combination with rapeseed (*Brassica napus L.*). More information on cover crop planting and harvest timing is available in Bourns et al. (2024).

The three P fertilization strategies, which serve as the primary treatments in this evaluation, progressed through three distinct management phases (Table 5-1):

- Phase 1 (2015–2019, Build Phase): There were three levels of P fertilization: fall broadcast (FB), spring injected (SI), and a control (CN) with no P applied. Both FB and SI treatments received 27 kg P ha^{-1} yr^{-1} in accordance with Kansas State University's build-and-maintain recommendations (Leikam et al., 2003). Diammonium phosphate was applied as a fall broadcast to the FB treatments, while liquid ammonium polyphosphate was injected in the spring for the SI treatments. These applications were carried out annually.
- Phase 2 (2020–2022, Maintain/Drawdown Phase): The cover crop was changed exclusively to cereal rye (*Secale cereale*), and the cropping system remained a no-till

corn-soybean rotation. For the P fertilization, the treatment previously managed as SI transitioned into a continuous Build-and-Maintain (BM) treatment, receiving an average of 24 kg P ha^{-1}. In contrast, no P fertilizer was applied to the treatment previously managed as FB, which formally entered the Build-and-Drawdown (BD) phase. For the BM treatment, ammonium polyphosphate served as the P source and was applied at planting each year, positioned 5 cm below and 5 cm to the side of the seed. The CN treatment continued to receive zero P.

- Phase 3 (2023–2025, Maintain/Sufficiency Phase): The cover crop remained cereal rye under the same rotation. Regarding P fertilization, the BM treatment received an average of 23 kg P ha^{-1} yr^{-1} as subsurface-injected ammonium polyphosphate. In contrast, the treatment that had been drawn down (BD) during the 2020–2022 phase was transitioned into a Sufficiency (SF) management strategy, receiving an average of 10 kg P ha^{-1} yr^{-1} as subsurface-injected ammonium polyphosphate. The detailed progression of P fertilization rates, fertilizer sources, application methods, and cover crop species across all three experimental phases is summarized in Table 5-1.

Table 5-1. Summary of P fertilizer and cover crop treatments for three time periods.

Treatment	2015-2019 (Build Phase)	2020-2022 (Maintain/Drawdown Phase)	2023-2025 (Maintain/Sufficiency Phase)
Control (CN)	Control, 0 kg P ha^{-1} yr^{-1}	Control, 0 kg P ha^{-1} yr^{-1}	Control, 0 kg P ha^{-1} yr^{-1}
Build-Maintain (BM)	Subsurface-injected ammonium polyphosphate (APP), 27 kg P ha^{-1} yr^{-1}	Subsurface-injected APP, 24 kg P ha^{-1} yr^{-1}	Subsurface-injected APP, 23 kg P ha^{-1} yr^{-1}
Build-Drawdown (BD/SF)	Fall surface-broadcast diammonium phosphate (DAP), 27 kg P ha^{-1} yr^{-1}	Drawdown (BD), no P applied, 0 kg P ha^{-1} yr^{-1}	Sufficiency (SF), subsurface-injected APP, 10 kg P ha^{-1} yr^{-1}
Cover crop	Wheat/Triticale/Rapeseed	Cereal rye	Cereal rye

Plant sampling and P uptake analysis

Plant biomass samples (corn and soybean) and cover crop biomass were collected annually to determine plant P uptake. Aboveground plant tissues and grain were harvested at physiological maturity, oven-dried, and ground. Phosphorus concentrations in the plant tissues and grain were determined following sulfuric peroxide digestion using an inductively coupled plasma (ICP) spectrometer. Total plant P uptake was calculated by multiplying the P concentration by the respective dry biomass yield (Thomas et al., 1967).

Soil sampling

Between 2019 and 2025, a total of 21 soil cores (0–15 cm) were collected per plot after fall harvest across three geo-referenced subplot locations within each plot. Immediately upon collection, the soil cores were separated into three discrete depth intervals (0–2.5, 2.5–5, and 5–15 cm) and combined by depth to form one composite sample per depth interval for each plot. The composite samples were air-dried, ground, and passed through a < 2 mm sieve prior to chemical analysis.

Soil Analysis

Soil pH was measured in a 1:1 (w/v) soil-to-deionized water slurry using a glass electrode pH meter (Watson & Brown, 1998). Mehlich-3 P was extracted following the procedures described by Mehlich (1984) using a 1:10 soil-to-solution extraction ratio and shaking for 5 minutes at 200 rpm. Phosphorus concentrations in the extracts were analyzed colorimetrically using the molybdate blue method with a Lachat QuickChem 8000 Series Automated Ion Analyzer and QuickChem Method 12-115-01-1-A. Soil TP concentration was measured after perchloric acid digestion (Olsen & Sommers, 1982; Sommers & Nelson, 1972) and analyzed with an inductively coupled plasma (ICP) spectrometer. Total C and total N were determined by combustion using a LECO TruSpec CN Analyzer (TruSpec Method “Carbon and Nitrogen in Soil and Sediment”). All soil samples were weighed prior to extraction. Chemical analyses were conducted at the Kansas State University Soil Testing Lab.

Statistical Analysis

Data collected from 2019–2025 were analyzed using a comprehensive linear mixed model that evaluated all soil depths and years together. Data were normally distributed and therefore did not require transformation. Fixed effects of the model included replication, fertilizer management practice, cover crop, year, soil depth, and all higher-order interactions among fertilizer management practice, cover crop, year, and depth. The random effects of the model included interactions incorporating replication, year, and depth to appropriately account for the repeated measures structure of the experimental design. Linear contrast statements were utilized within the model to specifically evaluate and partition the linear trends of soil parameters over time across the multiple sampling years. Statistical analysis was executed via Statistical Analysis Software (SAS version 9.4; Cary, NC) PROC GLIMMIX with the option DDFM=satterth.

Results

The analysis of variance (ANOVA) revealed interactive effects of the experimental factors, including cover cropping, P fertilization strategies, sampling years, and soil depths on all evaluated soil fertility indicators (Table 5-2). Soil depth was a dominant main effect across all parameters, indicating strong vertical stratification.

Table 5-2.Analysis of variance (p-values) for the effects of cover crop, phosphorus fertilizer, year, soil depth, and their interactions on soil pH, Mehlich-3 P, total P, total carbon, and total nitrogen.

Fixed Effect	Soil pH (p)	Mehlich-3 P (p)	Total P (p)	Total Carbon (p)	Total Nitrogen (p)
Cover Crop (CC)	0.2835	**0.0270**	0.9475	**0.0334**	**0.0043**
Fertilizer (Fert)	0.0505	**<.0001**	**<.0001**	0.7646	0.5837
CC × Fert	0.5334	0.4039	0.2081	0.7409	0.9362
Year	**<.0001**	**<.0001**	**<.0001**	**<.0001**	**<.0001**
CC × Year	0.6063	0.2978	0.0505	0.0547	**0.0075**
Fert × Year	0.3575	**<.0001**	**0.0002**	0.5498	0.4130
CC × Fert × Year	0.9044	0.1003	0.1369	0.3578	**0.0459**
Depth	**<.0001**	**<.0001**	**<.0001**	**<.0001**	**<.0001**
Depth × CC	**<.0001**	0.0668	0.0739	**<.0001**	**<.0001**
Depth × Fert	0.0676	**<.0001**	**<.0001**	**0.0169**	**0.0087**
Depth × CC × Fert	0.7604	0.3509	0.5458	0.1369	0.0680
Depth × Year	**<.0001**	**<.0001**	**0.0456**	**<.0001**	**<.0001**
Depth × CC × Year	0.9733	0.7508	0.9622	0.1590	0.2794
Depth × Fert × Year	0.6846	**<.0001**	0.1409	0.6416	0.9077
Depth × CC × Fert × Year	0.9958	0.8509	0.9999	0.9439	0.9882

Note: CC, cover crop; Fert, phosphorus fertilization strategy. p denotes the probability value. Statistically significant effects ($p < 0.05$ at the $\alpha = 0.05$ level) are highlighted in bold.

Mehlich-3 P

For Mehlich-3 P, a highly significant three-way interaction of depth × P fertilization × year was detected, indicating that Mehlich-3 P fluctuated differently across the soil layers depending on the sampling year (Table 5-2). From 2019 to 2025, in the 0 to 2.5-cm depth, linear contrast analysis indicated that Mehlich-3 P stayed almost stable in BM ($p = 0.252$), but decreased significantly for BD during this time period ($p < 0.001$), and stayed almost stable for the CN treatment ($p = 0.318$) (Figure 5-1a).

In the 2.5 to 5-cm depth, Mehlich-3 P increased significantly from 2019 to 2025 for the BM treatment ($p < 0.001$), but stayed almost stable for BD and CN treatment with the *p*-values of 0.776 and 0.829, respectively (Figure 5-1b). At the 5 to 15-cm depth, Mehlich-3 P showed a significant increasing trend under the BM treatment from 2019 to 2025 ($p = 0.0005$). For BD and CN at this depth and during this time period, Mehlich-3 P stayed stable ($p = 0.753$ for BD and $p = 0.884$ for CN) (Figure 5-1c). Also, the main effect of cover crop on soil Mehlich-3 P was significant, with greater Mehlich-3 P for the NC compared to the CC treatment (Figure 5-1d).

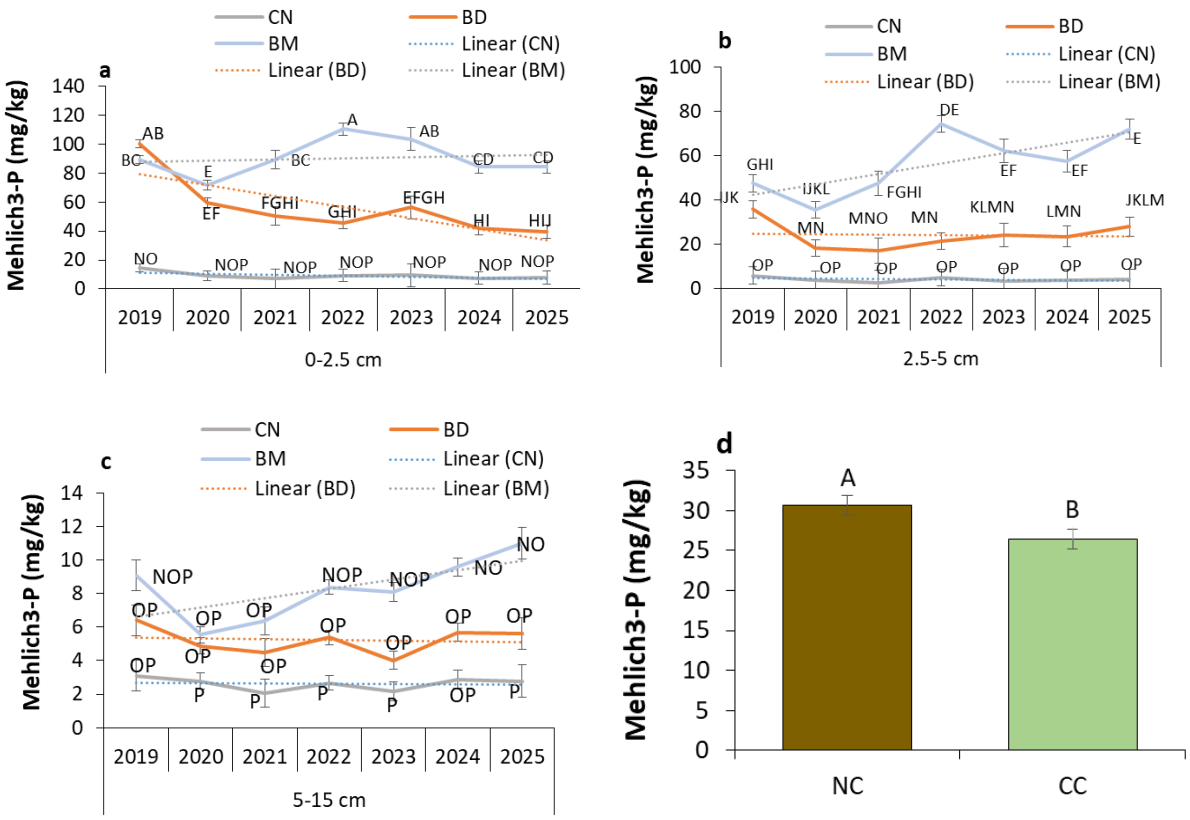


Figure 5-1. The interaction of P fertilization, depth, and year on Mehlich-3 P (a, b, and c), and the main effect of CC on soil Mehlich-3 P (d). Means within a treatment containing the same letter are not significantly different at α=0.05. Also, means within figures 1a, 1b, and 1c that have the same letter are not different. Abbreviations: control (CN), build and drawdown (BD), build and maintain (BM), no cover crop (NC), and with cover crop (CC).

Total P

Total P dynamics were primarily shaped by significant two-way interactions of P fertilization × year and depth × P fertilization (Table 5-2). Additionally, a marginally significant two-way interaction between cover crop and year was observed for soil total P (p = 0.0505).

Overall, BM maintained the highest P levels across the years, peaking around 2023 before slightly declining while remaining consistently above the other treatments (Figure 5-2a). Linear contrast analysis indicated a significant increase in TP over time at a rate of 3 mg kg^{-1} yr^{-1} (p = 0.025) for the BM treatment. Total P concentration for the BD treatment fluctuated but remained intermediate, generally greater than CN but less than BM. Linear contrast analysis for the BD treatment indicated a significant decrease in TP over time at a rate of -4.5 mg kg^{-1} yr^{-1} (p = 0.001). The control (CN) remained relatively stable and consistently lower than the fertilized treatments (BD and BM).

Also, there was a two-way interaction of P fertilization and depth on soil total P (Figure 5-2b). Total soil P decreased with depth across all treatments, with the highest concentrations in the 0 to 2.5-cm layer and lower values in deeper layers. At each depth, BM had the greatest TP, followed by BD, while CN remained the lowest. These treatment differences were most pronounced near the surface and diminished with depth.

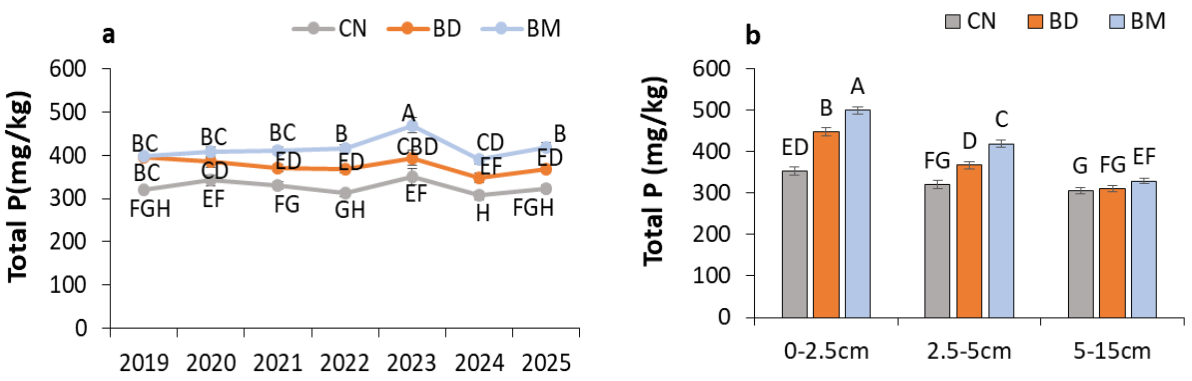


Figure 5-2. The interaction of P fertilization and year on soil total P (a), and the interaction of depth and P fertilization on soil total P (b). Means within a treatment containing the same letter are not significantly different at α=0.05. Abbreviations: control (CN), build and drawdown (BD), build and maintain (BM).

Total Carbon

Regarding soil OM dynamics, total C (TC) was strongly influenced by a significant depth × cover crop interaction (Table 5-2; Figure 5-3a). Because these slightly acidic surface soils (pH < 7.0) contain no detectable inorganic carbonates, TC predominantly represents soil organic C. Total C declined with soil depth in both CC and NC treatments, with the greatest concentrations at the 0 to 2.5-cm depth and the lowest at 5 to 15 cm. The CC treatment maintained significantly greater TC than NC at the 0 to 2.5-cm surface layer, whereas there were no significant differences between treatments in the deeper layers (Figure 5-3a).

Furthermore, the interaction between sampling year and cover crop on soil TC approached significance (p = 0.0547; Table 5-2). While not strictly significant at α = 0.05, a noticeable trend occurred where TC increased over time in the CC treatment (particularly peaking in 2024 and 2025) but remained relatively flat in the NC treatment (Figure 5-3b). Based

on linear contrast analysis, TC in the CC treatment increased at a rate of 0.33 g kg^{-1} yr^{-1}, while the NC treatment increased at a rate of 0.14 g kg^{-1} yr^{-1}. An additional contrast specifically comparing these two slopes confirmed that the rate of TC increase over time was significantly greater in the CC treatment compared to the NC treatment (p = 0.002), although both demonstrated positive trajectories over time.

Furthermore, a significant two-way interaction of depth and P fertilization was detected for soil TC (Table 5-2; Figure 5-3c). Contrast analysis showed that the effect of depth on TC was greater under the BD treatment than the CN treatment, as indicated by a larger difference between the 0 to 2.5-cm and 5 to 15-cm depths (9.16 g kg^{-1} vs. 8.02 g kg^{-1} for the BD and CN, respectively).

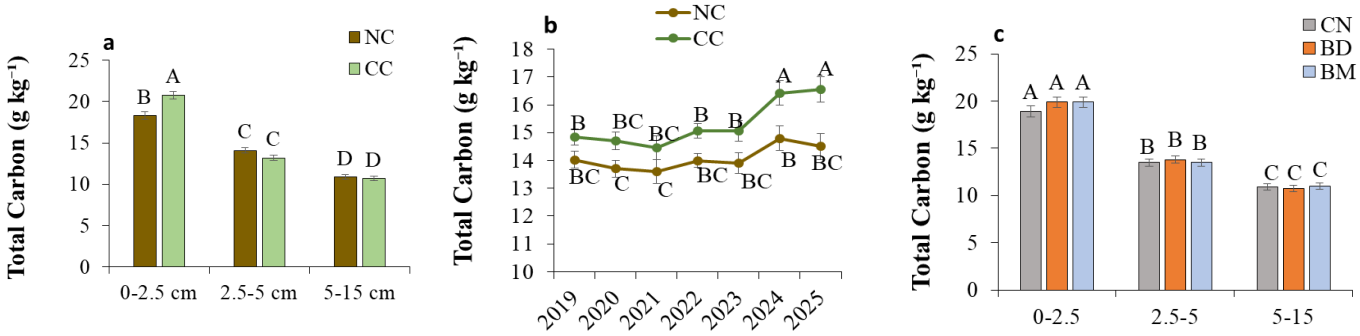


Figure 5-3. The interaction of cover crop and depth on soil total carbon (a), and the interaction of year and cover crop on soil total carbon (b) and the interaction of depth and P fertilization on soil total carbon (c). Means within a treatment containing the same letter are not significantly different at α=0.05. Abbreviations: control (CN), build and drawdown (BD), build and maintain (BM), no cover crop (NC), and with cover crop (CC).

Total Nitrogen

Soil total N (TN) was strongly influenced by a significant depth × cover crop interaction ($p < 0.0001$), while a significant three-way interaction of year × cover crop × P fertilization ($p = 0.0459$) was uniquely observed for this parameter (Table 5-2). Furthermore, a significant two-way interaction of depth and P fertilization was detected for soil TN ($p = 0.0087$; Figure 5-4a). Contrast analysis showed that the effect of depth on soil TN was more pronounced under the BD treatment than the CN treatment, as indicated by a larger concentration difference between the 0–2.5 and 5–15 cm depths (0.651 g kg^{-1} vs. 0.565 g kg^{-1} for the BD and CN treatments, respectively). For the depth × cover crop interaction (Figure 5-4b), soil TN declined with soil depth in both CC and NC treatments, with the highest values at 0–2.5 cm and the lowest at 5–15 cm. The CC treatment had significantly greater TN than NC at the 0–2.5 and 2.5–5 cm depths, whereas no significant difference was observed between treatments at the 5–15 cm depth.

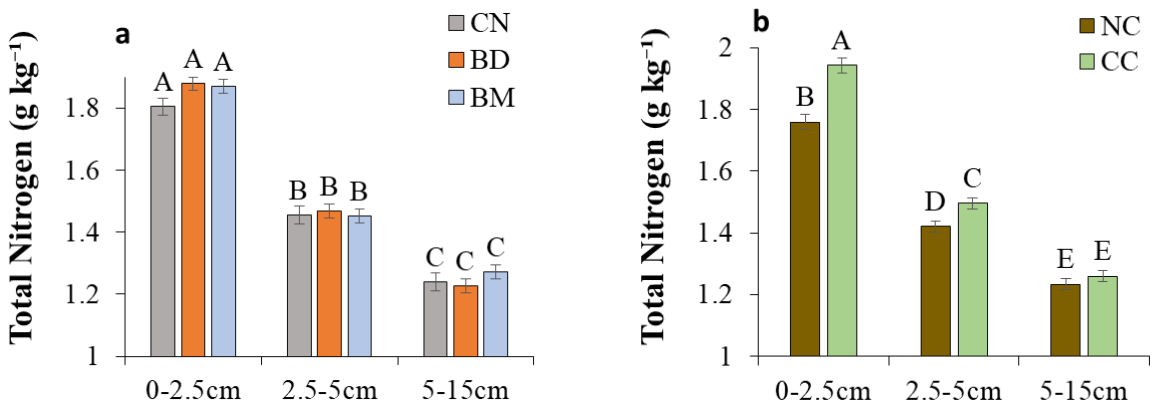


Figure 5-4. The interaction of P fertilization and depth on soil total nitrogen (a), and the interaction of depth and cover crop on soil total nitrogen (b). Means within a panel containing the same letter are not significantly different at $\alpha = 0.05$. Abbreviations: control (CN), build and drawdown (BD), build and maintain (BM), no cover crop (NC), and with cover crop (CC).

A significant three-way interaction among year, P fertilization, and cover cropping was detected for soil TN concentration (Table 5-2; Figure 5-5). In the cover crop treatment (Figure 5-5a), TN concentration exhibited dynamic temporal variations rather than a strict linear trend, with prominent peaks occurring in 2022 and 2024. Across most sampling years, the BM treatment generally maintained the greatest TN concentrations, followed by the BD treatment, whereas the CN control remained the lowest. Conversely, in the no cover crop treatment (Figure 5-5b), TN concentrations were generally lower than those observed with cover crops, and differences among the P fertilization treatments were not statistically significant across the study period.

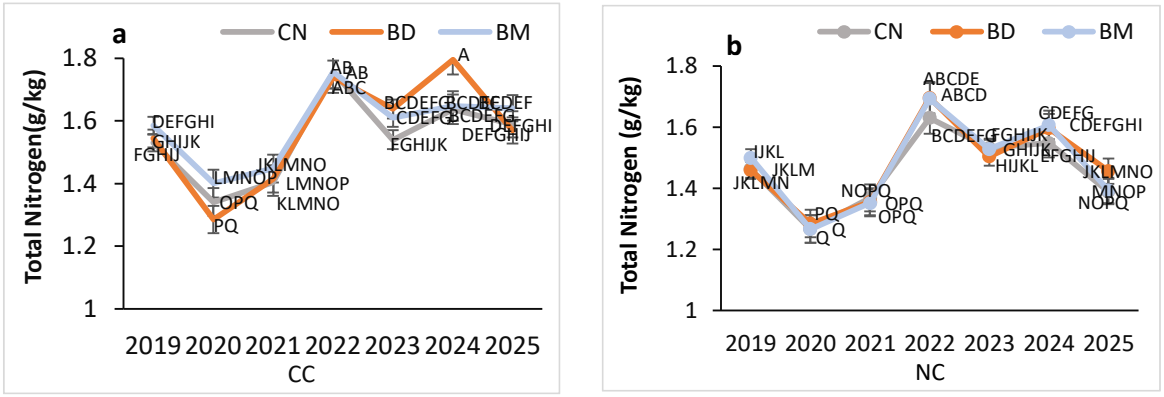


Figure 5-5. The three-way interaction of year, P fertilization, and cover cropping on soil total nitrogen concentration (g kg^{-1}) in the surface soil layer. Panel (a) represents the cover crop (CC) treatment, and panel (b) represents the no cover crop (NC) treatment. Means within a year followed by the same letter are not significantly different at alpha = 0.05. Error bars represent the standard error of the mean. Abbreviations: control (CN), build-and-drawdown (BD), build-and-maintain (BM), no cover crop (NC), and with cover crop (CC).

Soil pH Dynamics

Soil pH was significantly influenced by the main effects of sampling year ($p < 0.001$) and soil depth ($p < 0.001$), as well as the two-way interactions of depth × cover crop ($p < 0.001$) and depth × year ($p < 0.001$; Table 5-2). In contrast, the main effect of P fertilization on soil pH was not statistically significant at the $\alpha = 0.05$ level ($p = 0.0505$), although a slight numerical trend toward lower mean soil pH was observed in the BM treatment (6.64) compared to BD (6.80) and CN (6.85).

Across all treatments and years, soil pH exhibited strong vertical stratification, generally increasing with soil depth from the surface 0–2.5 cm layer to the deeper 5–15 cm layer (Figure 5-6; Table 5-3). For the depth × cover crop interaction (Figure 5-6a), cover cropping (CC) significantly reduced soil pH in the surface 0–2.5 cm layer compared to no cover crop (NC) (6.72 vs. 6.92), whereas no significant differences between CC and NC were observed in the 2.5–5 cm (6.65 vs. 6.66) or 5–15 cm (6.72 vs. 6.69) depths.

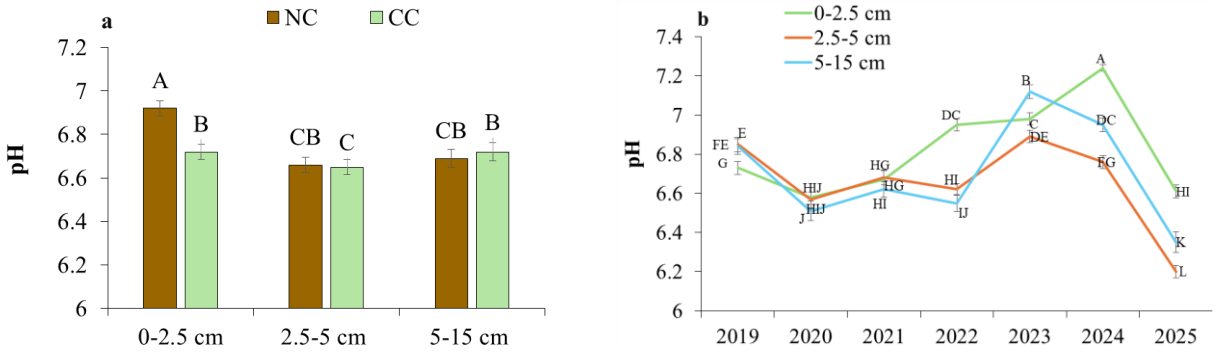


Figure 5-6. The interaction of soil depth and cover cropping (a), and the interaction of soil depth and sampling year (b) on soil pH averaged across other treatments (2019–2025). Means within a panel containing the same letter are not significantly different at α = 0.05. Error bars represent the standard error of the mean. Abbreviations: no cover crop (NC) and with cover crop (CC).

Furthermore, the significant depth × year interaction demonstrated pronounced temporal fluctuations in soil pH across the three depth intervals over the 7-year period (Table 5-3). In 2019, soil pH in the 0–2.5 cm surface layer (6.73) was significantly lower than in the 2.5–5 cm (6.85) and 5–15 cm (6.84) layers. Soil pH declined across all depths in 2020 (ranging from 6.51

to 6.58) and remained relatively low in 2021 (6.62 to 6.68). Between 2022 and 2024, surface soil pH (0–2.5 cm) increased substantially, peaking at 7.24 in 2024 and remaining significantly higher than in the subsurface layers during 2022 and 2024. However, in 2025, soil pH decreased sharply across all three depth increments, reaching 6.61 in the 0–2.5 cm layer, 6.20 in the 2.5–5 cm layer, and 6.35 in the 5–15 cm layer (Figure 5-6b; Table 5-3).

Table 5-3. The interaction of soil depth and sampling year on soil pH across cover crop and P fertilization treatments (2019–2025).

Soil Depth (cm)	2019	2020	2021	2022	2023	2024	2025
0–2.5	6.73 G	6.58 HIJ	6.67 HG	6.95 DC	6.98 C	7.24 A	6.61 HI
2.5–5	6.85 E	6.57 HIJ	6.68 HG	6.62 HI	6.89 DE	6.76 FG	6.20 L
5–15	6.84 FE	6.51 J	6.62 HI	6.55 IJ	7.12 B	6.95 DC	6.35 K

Note: Means followed by the same uppercase letter across all depth × year combinations are not significantly different at $\alpha = 0.05$.

Annual P budget dynamics

Annual P budget dynamics, calculated as the difference between P fertilizer inputs (P_{in}) and crop P removal through grain harvest (P_{out}), varied substantially across the distinct fertilization strategies (Figure 5-7). In the unfertilized control (CN) and during the drawdown phase of the BD treatment (2020–2022), no P fertilizer was applied (P_{in} = 0 kg P ha^{-1} yr^{-1}). The lack of fertilizer input, combined with continuous P removal via crop uptake (P_{out}), drove the consistently negative annual P budgets observed during this period. Importantly, the annual P budget for the BD treatment during this drawdown phase (2020–2022) was significantly more

negative than that of the CN treatment because the historically higher soil P fertility in the BD plots (from the 2015–2019 build phase) supported greater crop yields, resulting in substantially higher crop P removal (P_{out}) relative to the unfertilized control.

In contrast, the BM treatment received continuous annual P inputs; however, its net P budget fluctuated depending on crop removal rates and interannual variability in fertilizer application rates in 2020 and 2021. Notably in 2020, the BM strategy exhibited a negative budget because exceptionally high crop P removal ($P_{out} \approx 30$ kg P ha^{-1} yr^{-1}) outpaced fertilizer inputs ($P_{in} \approx 17$ kg P ha^{-1} yr^{-1}). Overall, across the monitoring period, the BM strategy generally maintained relatively consistent P inputs, whereas the BD strategy exhibited pronounced fluctuations due to the intentional cessation and subsequent reintroduction of P fertilizer.

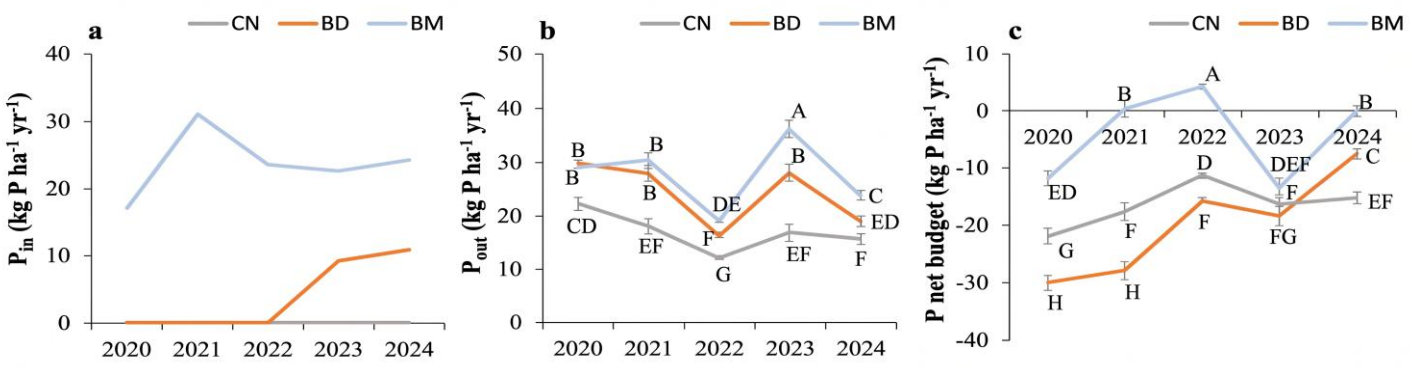


Figure 5-7. Annual phosphorus (P) balance components (kg P ha^{-1} yr^{-1}) from 2020 to 2024 under different fertilization strategies: (a) annual P fertilizer inputs (P_{in}), (b) annual crop P removal through grain harvest (P_{out}), and (c) the resulting annual net P budget ($P_{in} - P_{out}$). Means within a year followed by the same letter are not significantly different at $\alpha = 0.05$. Error bars represent the standard error of the mean. Abbreviations: control (CN), build and drawdown (BD), and build and maintain (BM).

Discussion

Cover crops

The effect of cover crops on Mehlich-3 P was a notable finding and aligns with the sequential extraction results (Chapter 3), where cover crops significantly reduced the concentration of operationally defined highly labile inorganic P fractions (Resin-P_i and $NaHCO_3$-P_i). This reduction is most likely driven by greater plant P uptake and microbial immobilization, as evidenced by higher plant P uptake in cover crop treatments compared to those without cover crops (Chapter 3; Bourns et al., 2024). Similar results have been reported by Kaur et al. (2024), where they have found that incorporation of hairy vetch in a corn–rye–soybean rotation reduced Mehlich-3 P by 26–29% compared to both no-cover and oat–radish systems, indicating that not all cover crops exert the same influence on soil P availability. In addition, they have reported that this reduction in Mehlich-3 P was concomitant with increased plant P uptake. Similarly, Welch et al. (2016) observed lower soil P levels in treatments with a forage radish and buckwheat cover crop mixture compared to the no cover crop control. Additionally, the greater DRP runoff losses previously documented under cover cropping at this experimental site (Carver et al., 2022; Sakib et al., 2026) may also contribute to the lower Mehlich-3 extractable P concentrations observed in the surface soil of cover-cropped plots.

Another study conducted by Dada et al. (2023) showed that including annual ryegrass decreased Mehlich-3 P at the 0 to 2 and 2 to 4-cm depths compared to no cover crop treatments. They further stated that this reduction in Mehlich-3 P could be due to P uptake by roots of annual ryegrass and soil sorption of P released from roots after freeze-thaw cycling. In another study

conducted by Gonzalez et al. (2024), including cereal rye in the management practices decreased Mehlich-3 P. They attributed this to the slower decomposition rate of cereal rye, which further lowers Mehlich-3 P by reducing phosphate release from residues and delaying mineralization of organic P compounds, thereby temporarily retaining phosphate and organic P compounds in the biomass and reducing its presence in Mehlich-3 extractable soil pools. Our findings from sequential extraction (Chapter 3) further support this explanation, where we have found significantly greater NaOH-P_o concentration for cover crop treatments, suggesting that P may have been tied up in cover crop residues, resulting in greater NaOH-P_o and lower Mehlich-3 P for this treatment.

In contrast, there are some studies that have shown that including a cover crop could increase Mehlich-3 P. For example, White and Weil (2011) found that forage radish increases Mehlich-3 P in localized zones because it rapidly takes up phosphate and releases it during taproot decomposition, creating concentrated areas of elevated soil test P near root channels. Similarly, in a tropical dryland maize system, Barbosa et al. (2026) reported that a cover crop mixture primarily dominated by *Canavalia ensiformis* (Jack bean, a fast-decomposing legume) and *Pennisetum glaucum* (Pearl millet) increased Mehlich-3 P by up to 38% under no-fertilizer conditions, likely due to enhanced P cycling and biological mobilization. Importantly, Barbosa et al. (2026) noted that this Mehlich-3 P increase was restricted to the unfertilized plots; under high P fertilization regimes, the cover crops had no significant additive effect on Mehlich-3 P, suggesting that the net direction of the cover crop response is governed by multiple interacting factors, including initial soil P saturation, the magnitude of cover crop P uptake, residue decomposition kinetics, and concurrent hydrological P losses (such as DRP runoff).

The rise in TC observed with cover crop addition is likely driven by greater aboveground biomass production and the resulting increased C inputs (Blanco-Canqui et al., 2013). Similarly, a meta-analysis has revealed that including cover crops into rotations significantly increased soil organic C, with an overall mean change of 15.5% (Jian et al., 2020). An increase in soil C might also be due to the enhanced retention of soil C by reduced runoff and erosion, as has been reported by Blanco-Canqui et al. (2015) and Jian et al. (2020). At this site, previous monitoring demonstrated a 60% to 90% decrease in annual erosion with cover crop use compared to the no-cover treatment (Carver et al., 2022), which is further supported by recent assessments reporting a 68% reduction in erosion (Sakib et al., 2026).

The significant increase in soil TC observed during this study differs from some shorter-term studies, such as the findings of Blanco-Canqui et al. (2014), who reported no increase over a three-year period. The discrepancy between our findings and these studies can be attributed to both the long-term duration of our experiment and edaphic differences across study sites, particularly soil texture. As suggested by Acuña and Villamil (2014), significant accumulation of TC from cover crops often requires several consecutive years of sustained residue inputs to become detectable. Furthermore, soil textural differences strongly modulate the rate of C stabilization; coarse-textured, sandier soils have limited mineral surface area and aggregate protection and therefore often take longer to exhibit detectable C accrual compared to fine-textured soils such as the Smolan silty clay loam in our study, where clay and silt fractions facilitate rapid organo-mineral stabilization (Blanco-Canqui & Ruis, 2020; Jian et al., 2020). Because our study encompasses a longer continuous management period on a fine-textured soil, the cumulative effect of cover cropping on surface TC became clearly observable.

As with TC, the increase in total N associated with cover crop use is likely attributable to greater plant biomass inputs to the soil surface. Studies by Hargrove (1986) and Kuo et al. (1997a; 1997b) showed that cover crops can raise soil N concentrations through the production and accumulation of additional biomass. Similarly, a global systematic review concluded that cover cropping generally increases soil TN, with an average increase of approximately 20%, and also enhances biologically-active N pools such as microbial biomass N and particulate organic matter N. These effects were most pronounced in surface soils and in long-term cover cropping systems, indicating that soil nitrogen accumulation is a gradual process driven by sustained OM inputs (Hao et al., 2023). In our study, linear contrast analysis (Figure 5-5) confirmed that TN exhibited significant variations across the multiple sampling years under both cover crop and no-cover treatments, with the highest overall TN concentrations consistently recorded in the cover cropped plots.

The significant three-way interaction of year, P fertilization, and cover cropping on soil TN underscores the synergetic effect of combining conservation practices with nutrient management (Figure 5-5). Although the TN concentrations did not exhibit a strictly linear dramatic acceleration, visual inspection of the means over the study period (Figure 5-5a) reveals that in the presence of cover crops, higher P fertilization rates (BM and BD) consistently maintained higher TN concentrations over the years compared to the unfertilized control. This synergistic response is primarily driven by the fact that adequate P availability stimulates cover crop root development and aboveground biomass production, thereby increasing the total amount of N captured and returned to the soil surface via residue decomposition. Similar synergistic effects have been documented by Kuo et al. (1997b), who reported that optimal fertilization

enhances winter cover crop biomass, leading to proportionally greater soil nitrogen accumulation.

In contrast, when cover crops were absent, P fertilization strategies failed to induce any changes in soil TN, with all treatments overlapping at a low baseline across the entire study period (Figure 5-5b). We hypothesized that P fertilizer additions would not substantially alter soil TN storage unless they were coupled with the biological mechanism of cover crop biomass accumulation. This finding highlights the critical importance of integrating cover cropping into long-term P management plans to enhance overall soil fertility.

Cover Cropping, P Fertilization, and Soil pH Interactions

Cover crop integration significantly influenced vertical soil pH stratification, resulting in slightly lower pH values in the uppermost 0–2.5 cm layer under CC compared to NC (Figure 5-6a). However, the direction and magnitude of cover crop-induced pH shifts across agricultural systems are not uniform and depend strongly on soil type, initial soil pH, soil pH buffering capacity, and cover crop species. Specifically, measurable surface acidification is more likely to occur in soils with a higher initial pH (Yan and Arthur 2025), whereas strongly buffered, fine-textured soils such as the Smolan silty clay loam in this study resist rapid bulk pH shifts.

Even modest, localized decreases in surface soil pH within the 0–2.5 cm layer carry important implications for soil P solubility and speciation. Because calcium-associated P (Ca–P) minerals become increasingly soluble as pH declines below neutrality, minor proton-driven acidification induced by cover crop residues and root exudates can promote the dissolution of

sparingly soluble Ca–P phases, releasing orthophosphate into more labile soil pools (Weeks & Hettiarachchi, 2020).

In addition to cover crop effects, long-term P fertilization strategies contributed to subtle pH divergence near the soil surface, with fertilized plots (particularly under the BM strategy) exhibiting numerically lower surface pH than the unfertilized CN control. In continuous no-till systems where fertilizers are surface-applied without mechanical incorporation, repeated inputs of ammonium-based P fertilizers—such as monoammonium phosphate (MAP) and ammonium polyphosphate (APP)—drive localized acidification primarily through the microbial nitrification of ammonium (NH_4^+) to nitrate (NO_3^-), which generates two moles of H^+ per mole of NH_4^+ oxidized (Cade-Menun et al., 2026). Over multi-year management cycles, this nitrification-derived acidity, combined with surface organic matter accumulation, reinforces vertical pH stratification at the soil–residue interface.

Phosphorus fertilizer management and P budget dynamics

Higher nutrient accumulation at the soil surface, caused by limited soil mixing, is a well-recognized phenomenon in no-till agricultural systems (Buah et al., 2000; Fernandez et al., 2012; Smith et al., 2017). Consequently, placing soil amendments below the surface is often recommended to minimize nutrient stratification (Schwab et al., 2006). In the present study, long-term P fertilization in both the BM and BD treatments expectedly led to increased total P (TP) concentrations in the upper soil layers (0–2.5 and 2.5–5 cm) compared to the unfertilized control (CN). However, the temporal dynamics of Mehlich-3 P exhibited a more complex response that can be explicitly elucidated by examining the P budget (P_{in} - P_{out}).

In this no-till system, the fluctuations in Mehlich-3 P concentrations across the soil profile were strongly dependent on the fertilization strategy. Linear contrast analysis indicated that Mehlich-3 P under the BM treatment significantly increased at both the 2.5–5 cm ($p < 0.001$) and 5–15 cm ($p = 0.0005$) depths over time, while remaining stable at the 0–2.5 cm surface layer ($p = 0.252$). This subsurface accumulation is an expected outcome after more than a decade of annual subsurface band injection of P fertilizer (~5 cm depth), and vertical P redistribution into these zones can also be facilitated by plant root turnover and preferential transport along decaying root channels. Conversely, under the BD strategy where fertilization ceased during the drawdown phase, Mehlich-3 P significantly decreased in the 0–2.5 cm surface layer ($p < 0.001$) but remained relatively stable in the deeper layers. Because crops actively acquire phosphate from deeper within the soil profile to sustain growth alongside surface pools, surface-level dynamics alone should not be over-interpreted as a complete proxy for whole-profile legacy P depletion or accumulation (Buah et al., 2000; Fernández et al., 2012; Schwab et al., 2006).

In the unfertilized control (CN), where no P fertilizer was applied, the P budget remained consistently negative, driven entirely by P removal via crop harvest. This ongoing deficit resulted in a progressive decline in P_{out} over time, directly reflecting a reduction in crop biomass and tissue P concentrations under prolonged P deficiency. Despite this continuous depletion, higher TP and Mehlich-3 P concentrations were still observed at the immediate soil surface (0–2.5 cm) relative to deeper layers, a pattern attributable to the continuous biological cycling and deposition of P via crop residues (Scheiner & Lavado, 1998).

For the build-and-drawdown (BD) treatment, the cessation of P fertilizer applications created a highly negative P budget, as enhanced crop productivity from historical reserves maintained P_{out} above the CN even though P_{in} was zero. Despite this net P depletion, the BD treatment maintained higher Mehlich-3 P concentrations in the surface soil than the unfertilized control. This expected baseline difference occurs because the control had not received any P fertilizer during the preceding 5-year build phase either. Ultimately, this indicates that residual P accumulated from previous fertilizer applications in the BD treatment supplied bioavailable P even in the absence of external inputs. However, data from parallel agronomic evaluations at this site reveal that this drawdown approach did not perfectly sustain maximum crop yields across all years. Bourns et al. (2026) reported a significant decline in grain yield for the drawdown treatment in 2021 (though not in 2020 or 2022), and Sakib et al. (2026) documented that the subsequent sufficiency (SF) phase yielded less than the BM treatment in 2023, before recovering to similar levels in 2024 and 2025. This historical record clearly demonstrated that while legacy P supports crop production significantly better than the unfertilized control, it may not be adequate to maintain absolute maximum yield potentials during specific climatically challenging years without supplemental P.

In contrast, the build-and-maintain (BM) and build-and-drawdown (BD) strategies represent fundamentally divergent management paradigms. The BM strategy was designed to supply continuous annual fertilizer inputs to offset crop removal, thereby keeping soil P levels consistently elevated. While this continuous application effectively maintained agronomic maximum yields, it progressively accumulated TP, primarily in the upper soil layers. On the other hand, the BD strategy explicitly leveraged historical P accumulation. By intentionally

halting fertilizer inputs during the drawdown phase, the BD approach forced a severely negative P budget, relying on legacy P reserves to sustain crop demands. Our data explicitly demonstrated that this strategic drawdown successfully reduced surface Mehlich-3 P concentrations over time without the need for continuous external inputs.

Although the BM treatment received continuous P inputs, its temporal shifts in surface Mehlich-3 P were directly linked to annual fluctuations in the P budget. For instance, in 2020, exceptionally high crop yields caused crop P removal (P_{out}, ~30 kg P ha^{-1} yr^{-1}) to substantially exceed the applied fertilizer (P_{in}, ~17 kg P ha^{-1} yr^{-1}). This specific imbalance resulted in a transient negative P budget and a temporary depletion of the labile surface P pool. However, in subsequent years (2021 and 2022), positive P budgets where fertilizer inputs once again exceeded crop removal successfully replenished the extractable P pool. While this continuous application strategy effectively prevented P-related yield limitations and maintained stable P levels, it inherently perpetuated excessive soil P accumulation over the long term. Consequently, this could significantly increase the risk of dissolved reactive P (DRP) transfer to surface waters via runoff (Hooda et al., 2001; McDowell et al., 2001; Wortmann et al., 2018).

The absence of a significant interaction between cover cropping and P fertilization for Mehlich-3 P (Table 5-2) further strengthens this management framework. Consistent with our sequential extraction findings (Chapter 3), this indicates that cover crops reduce labile soil P primarily through biological immobilization and redistribution into organic pools (e.g., NaOH-P_o). While the interaction between cover crop and soil depth for Mehlich-3 P approached significance ($p = 0.0668$), the overall trend suggests that this effect was generally consistent across all P fertilization rates. As a result, cover cropping can be integrated into both drawdown

and maintenance systems as an independent biological driver that modulates the chemical speciation of legacy P without interfering with broader fertilizer-driven agronomic objectives.

Conclusion

Managing P in stratified, no-till agroecosystems necessitates strategies that optimize nutrient use efficiency and protect water quality. Our findings indicate that continuous P applications under a build-and-maintain (BM) strategy result in the continuous accumulation of TP and Mehlich-3 P in the upper soil profile, increasing the potential risk of dissolved reactive P losses. In contrast, the build-and-drawdown (BD) strategy demonstrated that accumulated legacy P reserves can effectively supply crop requirements during periods of restricted fertilizer application. By incorporating the P budget into our analysis, we confirmed that legacy P in the BD treatment maintained higher Mehlich-3 P concentrations than the unfertilized control despite significant net P depletion through crop removal, highlighting the feasibility of reducing external P inputs from a crop production standpoint.

The integration of cover crops enhanced overall soil health by increasing surface TC and TN concentrations. The reduction in Mehlich-3 P observed under cover cropping occurred independent of P fertilization strategies, suggesting that cover crops act as an independent biological driver that redistributes readily available P into organic pools or crop biomass. Ultimately, this study suggests that shifting from a continuous build-and-maintain paradigm to a strategic build-and-drawdown approach is an effective strategy for reducing legacy P buildup. When combined with cover cropping, this integrated framework supports long-term soil fertility in no-till agricultural systems as well.

References

Acuña, J. C., & Villamil, M. B. (2014). Short-term effects of cover crops and compaction on soil properties and soybean production in Illinois. Agronomy Journal, 106(3), 860–870. https://doi.org/10.2134/agronj2013.0366

Barbosa, L. D., da Luz, J. H., dos Santos, R. A., de Souza, J. W., de Oliveira, H. P., Silva, D. M., Soltangheisi, A., Pavinato, P. S., & dos Santos, V. R. (2026). Cover crops modulate soil phosphorus dynamics under P fertilizer sources in dryland maize production on tropical soil. Geoderma Regional, 36, e01065. https://doi.org/10.1016/j.geodrs.2026.e01065

Bindraban, P. S., Dimkpa, C. O., & Pandey, R. (2020). Exploring phosphorus fertilizers and fertilization strategies for improved human and environmental health. Biology and Fertility of Soils, 56(3), 299–317. https://doi.org/10.1007/s00374-019-01430-2

Blanco-Canqui, H., & Ruis, S. J. (2020). Cover crop impacts on soil physical properties: A review. Soil Science Society of America Journal, 84(5), 1527–1576. https://doi.org/10.1002/saj2.20129

Blanco-Canqui, H., Ferguson, R. B., Jin, V. L., Schmer, M. R., Wienhold, B. J., & Tatarko, J. (2014). Can cover crop and manure maintain soil properties after stover removal from irrigated no-till corn? Soil Science Society of America Journal, 78(4), 1368–1377. https://doi.org/10.2136/sssaj2014.01.0022

Blanco-Canqui, H., Holman, J. D., Schlegel, A. J., Tatarko, J., & Shaver, T. M. (2013). Replacing fallow with cover crops in a semiarid soil: Effects on soil properties. Soil Science Society of America Journal, 77(3), 1026–1034. https://doi.org/10.2136/sssaj2013.01.0006

Blanco-Canqui, H., Shaver, T. M., Lindquist, J. L., Shapiro, C. A., Elmore, R. W., Francis, C. A., & Hergert, G. W. (2015). Cover crops and ecosystem services: Insights from studies in temperate soils. Agronomy Journal, 107(6), 2449–2474. https://doi.org/10.2134/agronj15.0086

Bourns, M. A., Nelson, N. O., Carver, R. E., Roozeboom, K. L., Kluitenberg, G. J., Tomlinson, P. J., Kang, Q., & Hettiarachchi, G. M. (2024). Cover crops impact phosphorus cycling and environmental efficiency in a corn–soybean system. Agronomy Journal, 116(1), 109–120. https://doi.org/10.1002/agj2.21498

Bourns, M., Yeager, E., Nelson, N., Kluitenberg, G., Roozeboom, K., Hettiarachchi, G., Tomlinson, P., & Presley, D. (2026). Phosphorus drawdown improves net return and water quality in a no-till corn–soybean system. Journal of Soil and Water Conservation, 81(3), 222–235. https://doi.org/10.1080/00224561.2026.2651052

Buah, S. S. J., Polito, T. A., & Killorn, R. (2000). No-tillage corn response to placement of fertilizer nitrogen, phosphorus, and potassium. Agronomy Journal, 92(5), 937–942. https://doi.org/10.2134/agronj2000.925937x

Cade-Menun, B. J., Bainard, L. D., Crittenden, S., Fernandez, M. R., Lafond, J., Nyiraneza, J., St. Luce, M., & Ziadi, N. (2026). Ammonium-based fertilizers alter pH and cation concentrations in agricultural soils of Saskatchewan, Manitoba, and Quebec. Canadian Journal of Soil Science, 106(4), 1–22. https://doi.org/10.1139/cjss-2025-0099

Carver, R. E., Nelson, N. O., Roozeboom, K. L., Kluitenberg, G. J., Tomlinson, P. J., Kang, Q., & Abel, D. S. (2022). Cover crop and phosphorus fertilizer management impacts on surface water quality from a no-till corn–soybean rotation. Journal of Environmental Management, 301, 113818. https://doi.org/10.1016/j.jenvman.2021.113818

Dada, A. O., Armstrong, S. D., & Smith, D. R. (2023). Phosphorus sorption and desorption as affected by long-term cover cropping at two soil surface depths. Agrosystems, Geosciences & Environment, 6(1), e20338. https://doi.org/10.1002/agg2.20338

Fernández, F. G., Farmaha, B. S., & Nafziger, E. D. (2012). Soil fertility status of soils in Illinois. Agronomy Journal, 104(5), 1460–1464. https://doi.org/10.2134/agronj2012.0016

Gonzalez, J. M., Dick, W. A., Islam, K. R., Watts, D. B., Fausey, N. R., Flanagan, D. C., Batte, M. T., VanToai, T. T., Reeder, R. C., & Shedekar, V. S. (2024). Cover crops, crop rotation, and gypsum, as conservation practices, impact Mehlich-3 extractable plant nutrients and trace metals. International Soil and Water Conservation Research, 12(3), 650–662. https://doi.org/10.1016/j.iswcr.2023.08.004

Hallama, M., Pekrun, C., Lambers, H., & Kandeler, E. (2019). Hidden miners–the roles of cover crops and soil microorganisms in phosphorus cycling through agroecosystems. Plant and Soil, 434(1–2), 7–45. https://doi.org/10.1007/s11104-018-3810-7

Hao, X., Abou Najm, M., Steenwerth, K. L., Nocco, M. A., Basset, C., & Daccache, A. (2023). Are there universal soil responses to cover cropping? A systematic review. Science of the Total Environment, 861, 160600. https://doi.org/10.1016/j.scitotenv.2022.160600

Hargrove, W. L. (1986). Winter legumes as a nitrogen source for no-till grain sorghum. Agronomy Journal, 78(1), 70–74. https://doi.org/10.2134/agronj1986.00021962007800010017x

Haruna, S. I., Anderson, S. H., Udawatta, R. P., Gantzer, C. J., Phillips, N. C., Cui, S., & Gao, Y. (2020). Improving soil physical properties through the use of cover crops: A review. Agrosystems, Geosciences & Environment, 3(1), e20105. https://doi.org/10.1002/agg2.20105

Hooda, P. S., Truesdale, V. W., Edwards, A. C., Withers, P. J. A., Aitken, M. N., Miller, A., & Rendell, A. R. (2001). Manuring and fertilization effects on phosphorus accumulation in soils and potential environmental implications. Advances in Environmental Research, 5(1), 13–21. https://doi.org/10.1016/S1093-0191(00)00064-0

Jian, J., Du, X., Reiter, M. S., & Stewart, R. D. (2020). A meta-analysis of global cropland soil carbon changes due to cover cropping. Soil Biology and Biochemistry, 143, 107735. https://doi.org/10.1016/j.soilbio.2020.107735

Kaur, H., Singh, G., Williard, K., Schoonover, J., Nelson, K. A., & Kaur, G. (2024). Tillage and cover cropping influence phosphorus dynamics in soil and water pools. Agrosystems, Geosciences & Environment, 7(4), e20570. https://doi.org/10.1002/agg2.20570

Kuo, S., Sainju, U. M., & Jellum, E. J. (1997a). Winter cover crop effects on soil organic carbon and carbohydrate in soil. Soil Science Society of America Journal, 61(1), 145–152. https://doi.org/10.2136/sssaj1997.03615995006100010022x

Kuo, S., Sainju, U. M., & Jellum, E. J. (1997b). Winter cover cropping influence on nitrogen in soil. Soil Science Society of America Journal, 61(5), 1392–1399. https://doi.org/10.2136/sssaj1997.03615995006100050015x

Leikam, D. F., Lamond, R. E., & Mengel, D. B. (2003). Providing flexibility in phosphorus and potassium fertilizer recommendations. Better Crops with Plant Food, 87(3), 6–10.

Macnack, N. E., Chim, B. K., Amedy, B., & Arnall, D. B. (2017). Fertilization based on sufficiency, build-up and maintenance concept (Fact Sheet PSS-2266). Oklahoma State University Extension. https://extension.okstate.edu/fact-sheets/fertilization-based-on-sufficiency-build-up-and-maintenance-concept.html

Maltais-Landry, G., & Frossard, E. (2015). Similar phosphorus transfer from cover crop residues and water-soluble mineral fertilizer to soils and a subsequent crop. Plant and Soil, 393(1–2), 193–205. https://doi.org/10.1007/s11104-015-2477-6

McClelland, S. C., Paustian, K., & Schipanski, M. E. (2021). Management of cover crops in temperate climates influences soil organic carbon stocks: A meta-analysis. Ecological Applications, 31(3), e02278. https://doi.org/10.1002/eap.2278

McDowell, R. W., Sharpley, A. N., Condron, L. M., Haygarth, P. M., & Brookes, P. C. (2001). Processes controlling soil phosphorus release to runoff and implications for agricultural management. Nutrient Cycling in Agroecosystems, 59(3), 269–284. https://doi.org/10.1023/A:1014419206761

Mehlich, A. (1984). Mehlich 3 soil test extractant: A modification of Mehlich 2 extractant. Communications in Soil Science and Plant Analysis, 15(12), 1409–1416. https://doi.org/10.1080/00103628409367568

Nelson, N. O., Roozeboom, K. L., Yeager, E. A., Williams, J. R., Zerger, S. E., Kluitenberg, G. J., Tomlinson, P. J., Abel, D. S., & Carver, R. E. (2023). Agronomic and economic implications of cover crop and phosphorus fertilizer management practices for water quality improvement. Journal of Environmental Quality, 52(1), 113–125. https://doi.org/10.1002/jeq2.20427

Olsen, S. R., & Sommers, L. E. (1982). Phosphorus. In A. L. Page, R. H. Miller, & D. R. Keeney (Eds.), Methods of soil analysis: Part 2—Chemical and microbiological properties (2nd ed., pp. 403–430). American Society of Agronomy & Soil Science Society of America. https://doi.org/10.2134/agronmonogr9.2.2ed.c24

Patel, S., Shapiro, C. A., & Iqbal, J. (2024). Long-term comparison of targeted soil test values and crop removal as a phosphorus fertilization strategy in corn. Agronomy Journal, 116(6), 3240–3255. https://doi.org/10.1002/agj2.21677

Poeplau, C., & Don, A. (2015). Carbon sequestration in agricultural soils via cultivation of cover crops—A meta-analysis. Agriculture, Ecosystems & Environment, 200, 33–41. https://doi.org/10.1016/j.agee.2014.10.024

Robbins, S. G., & Voss, R. D. (1991). Phosphorus and potassium stratification in conservation tillage systems. Journal of Soil and Water Conservation, 46(4), 298–300.

Sakib, T. U., Hettiarachchi, G. M., Kluitenberg, G. J., Roozeboom, K. L., Tomlinson, P. J., Presley, D. R., & Nelson, N. O. (2026). Drawdown phosphorus management in cover cropping systems: A strategy for mitigating phosphorus loss in agroecosystems. Journal of Environmental Quality. (In review).

SAS Institute. (2020). SAS/STAT 15.2 user's guide (Version 9.4). SAS Institute Inc.

Scheiner, J. D., & Lavado, R. S. (1998). The role of crop residues in the soil phosphorus cycling. Agronomie, 18(10), 655–661. https://doi.org/10.1051/agro:19981004

Schipanski, M. E., Barbercheck, M., Douglas, M. R., Finney, D. M., Haider, K., Kaye, J. P., Kemanian, A. R., Mortensen, D. A., Ryan, M. R., Tooker, J., & White, C. (2014). A framework for evaluating ecosystem services provided by cover crops in agroecosystems. Agricultural Systems, 125, 12–22. https://doi.org/10.1016/j.agsy.2013.11.004

Schwab, G. J., Whitney, D. A., Kilgore, G. L., & Sweeney, D. W. (2006). Tillage and phosphorus management effects on crop production in soils with phosphorus stratification. Agronomy Journal, 98(3), 430–435. https://doi.org/10.2134/agronj2005.0050

Sharpley, A. N. (2003). Soil mixing to decrease surface stratification of phosphorus in manured soils. Journal of Environmental Quality, 32(4), 1375–1384. https://doi.org/10.2134/jeq2003.1375

Sharpley, A. N., & Smith, S. J. (1994). Wheat tillage and water quality in the Southern Plains. Soil and Tillage Research, 30(1), 33–48. https://doi.org/10.1016/0167-1987(94)90069-8

Sharpley, A. N., Bergström, L., Aronsson, H., Bechmann, M., Bolster, C. H., Börling, K., Djodjic, F., Jarvie, H. P., Schoumans, O. F., Stamm, C., Tonderski, K. S., Ulén, B., Uusitalo, R., & Withers, P. J. A. (2015). Future agriculture with minimized phosphorus losses to waters: Research needs and direction. Ambio, 44(Suppl. 2), S163–S179. https://doi.org/10.1007/s13280-014-0612-x

Smith, D. R., Huang, C., & Haney, R. L. (2017). Phosphorus fertilization, soil stratification, and potential water quality impacts. Journal of Soil and Water Conservation, 72(5), 417–424. https://doi.org/10.2489/jswc.72.5.417

Soltangheisi, A., Rodrigues, M., Coelho, M. J. A., Gasperini, A. M., Sartor, L. R., & Pavinato, P. S. (2018). Changes in soil phosphorus lability promoted by phosphate sources and cover crops. Soil and Tillage Research, 179, 20–28. https://doi.org/10.1016/j.still.2018.01.006

Soltangheisi, A., Teles, A. P. B., Sartor, L. R., & Pavinato, P. S. (2020). Cover cropping may alter legacy phosphorus dynamics under long-term fertilizer addition. Frontiers in Environmental Science, 8, 13. https://doi.org/10.3389/fenvs.2020.00013

Sommers, L. E., & Nelson, D. W. (1972). Determination of total phosphorus in soils: A rapid perchloric acid digestion procedure. Soil Science Society of America Journal, 36(6), 902–904. https://doi.org/10.2136/sssaj1972.03615995003600060020x

Syers, J. K., Johnston, A. E., & Curtin, D. (2008). Efficiency of soil and fertilizer phosphorus use: Reconciling changing concepts of soil phosphorus behaviour with agronomic information (FAO Fertilizer and Plant Nutrition Bulletin No. 18). Food and Agriculture Organization of the United Nations.

Thomas, R. L., Sheard, R. W., & Moyer, J. R. (1967). Comparison of conventional and automated procedures for nitrogen, phosphorus, and potassium analysis of plant material using a single digestion. Agronomy Journal, 59(3), 240–243. https://doi.org/10.2134/agronj1967.00021962005900030010x

Weeks, J. J., Jr., & Hettiarachchi, G. M. (2020). Source and formulation matter: New insights into phosphorus fertilizer fate and transport in mildly calcareous soils. Soil Science Society of America Journal, 84(3), 731–746. https://doi.org/10.1002/saj2.20054

Welch, R. Y., Behnke, G. D., Davis, A. S., Masiunas, J., & Villamil, M. B. (2016). Using cover crops in headlands of organic grain farms: Effects on soil properties, weeds and crop yields. Agriculture, Ecosystems & Environment, 216, 322–332. https://doi.org/10.1016/j.agee.2015.10.014

White, C. M., & Weil, R. R. (2011). Forage radish cover crops increase soil test phosphorus surrounding radish taproot holes. Soil Science Society of America Journal, 75(1), 121–130. https://doi.org/10.2136/sssaj2010.0095

Wortmann, C. S., Dobermann, A. R., Ferguson, R. B., Hergert, G. W., Shapiro, C. A., Tarkalson, D. D., & Walters, D. T. (2009). High-yielding corn response to applied phosphorus, potassium, and sulfur in Nebraska. Agronomy Journal, 101(3), 546–555. https://doi.org/10.2134/agronj2008.0103x

Wortmann, C. S., Shapiro, C. A., Shaver, T. M., & Mainz, M. (2018). High soil test phosphorus effect on corn yield. Soil Science Society of America Journal, 82(5), 1160–1167. https://doi.org/10.2136/sssaj2018.02.0068

Xu, S., Zhang, W., Goodwin, P. H., Wang, Y., Zheng, S. J., & Li, X. (2024). Effect of cover crop on soil fertility and bacterial diversity in a banana plantation in southwestern China. Soil and Tillage Research, 240, 106092. https://doi.org/10.1016/j.still.2024.106092

Yan, F., & Arthur, E. (2025). Cover crops alter soil physicochemical properties: A global meta-analysis. *Geoderma, 460*, 117436. https://doi.org/10.1016/j.geoderma.2025.117436

Chapter 6 - Effects of Cover Cropping and Phosphorus Fertilization on Soil Iron Chemistry: Evidence from Selective Extractions and Fe-XANES

Abstract

Cover crops are widely promoted for soil conservation, but their integration into no-till systems has been associated with unintended increases in dissolved reactive phosphorus (DRP) losses. Because iron (Fe) plays a critical role in regulating phosphorus (P) mobility through sorption and precipitation, we hypothesized that increased DRP losses under cover cropping are linked to cover crop-induced changes in soil Fe speciation and reactivity. This study evaluated the interactive effects of cover cropping and P fertilization strategies (control [CN], build-and-drawdown [BD], and build-and-maintain [BM]) on soil Fe fractionation in a no-till corn–soybean rotation using selective chemical extractions and bulk Fe K-edge X-ray absorption near-edge structure (XANES) spectroscopy.

Chemical extractions revealed that cover cropping significantly increased sodium pyrophosphate-extractable Fe (organically-associated Fe) under both the BM and BD strategies, while proportionally decreasing ammonium oxalate-extractable Fe (amorphous Fe oxides). This redistribution suggests that cover cropping enhances Fe complexation with OM, effectively reducing the abundance of highly reactive inorganic mineral surfaces available for P sorption. Rather than widespread reductive dissolution, these trends point to ligand-promoted dissolution driven by root exudates, which destabilizes Fe oxides without necessarily altering the bulk Fe oxidation state. Correspondingly, bulk Fe-XANES analysis did not reveal a pronounced shift

toward reduced Fe(II) species across treatments. The apparent stability of the XANES absorption edge supports the conclusion that Fe mobilization occurred primarily via organic complexation.

Furthermore, the lack of discernible organo-Fe spectral features in bulk XANES is largely attributed to the masking effect of dominant, structurally stable phyllosilicate minerals in these soils, compounded by the dilution of localized rhizosphere processes within the bulk soil matrix. Ultimately, the ligand-driven transition of Fe toward organic complexes diminishes the sorption capacity of soils for P compounds, providing a mechanistic explanation for increased DRP losses. Future investigations should employ spatially resolved techniques, such as μ-XANES, on cryogenically preserved rhizosphere samples to overcome the masking and dilution limitations of bulk soil analysis.

Introduction

An improved understanding of how agricultural management affects phosphorus (P) availability is critical because P is essential for food production, yet excess P can be lost from agricultural fields, contributing to water quality degradation and eutrophication (Soltangheisi et al., 2020; Syers et al., 2008). Cover crops are widely promoted as a soil conservation practice because they reduce erosion, improve soil health, and provide numerous ecosystem benefits (Welch et al., 2016; White & Weil, 2011). However, less is known about how cover crops influence soil P cycling and speciation. Recent research in this study site has shown that cover crops can consistently increase dissolved reactive phosphorus (DRP) concentrations in runoff water (Carver et al., 2022). This increase in DRP loss is concerning because DRP is highly bioavailable and can readily contribute to harmful algal blooms in downstream aquatic ecosystems (Soltangheisi et al., 2020). Although the mechanisms responsible for increased DRP

losses under cover crops remain uncertain, they may be linked to cover crop-induced changes in soil P chemistry and speciation.

Iron (Fe) is one of the most important controls on P retention and mobility in soils because Fe minerals strongly sorb and precipitate phosphate, polyphosphates and some organic P compounds, thereby regulating P availability and transport (Gerke, 2010; Soltangheisi et al., 2018). Consequently, changes in Fe speciation could have a strong effect on the bioavailability of Fe itself and other nutrients, including P, because of the close linkage between these two important nutrients (Condron et al., 2005; Karlsson et al., 2008; Sundman et al., 2016).

Cover crops may alter soil OM inputs and microbial activity and trigger redox transformations, all of which can modify Fe speciation and, in turn, affect P dynamics (Chacon et al., 2006; Schreeg et al., 2013). On the other hand, the increase in Fe mobilization under cover crops can be interpreted as ligand-promoted dissolution, whereby low-molecular-weight organic acids (LMWOAs) and siderophore-like ligands form surface and aqueous Fe–ligand complexes that destabilize Fe oxides and enhance Fe release without requiring a concomitant shift in Fe oxidation state (Reichard et al., 2007). Therefore, enhanced Fe solubilization in the rhizosphere should not be equated *a priori* with reductive dissolution unless supported by Fe-XANES edge or pre-edge evidence.

Soil OM can influence phosphate availability through both direct and indirect mechanisms. Directly, organic compounds may compete with phosphate for adsorption sites on mineral surfaces, reducing phosphate sorption and increasing soluble P concentrations (Lindegren & Persson, 2009). Soil OM can also form phosphate–metal–OM complexes, in which phosphate may be more bioavailable than when associated with inorganic mineral surfaces or precipitates (Gerke, 2010).

Indirectly, OM can alter P speciation by changing Fe speciation (Chacon et al., 2006; Lindsay, 1981; Schreeg et al., 2013). Increased OM inputs can stimulate microbial reduction of Fe(III)-bearing minerals, including Fe(III) oxides, oxyhydroxides, and hydroxides, as microorganisms use organic carbon (C) as an electron donor during Fe reduction. The reductive dissolution of reactive Fe(III) minerals converts Fe(III) to Fe(II), dissolves Fe oxides, and can release previously sorbed or precipitated phosphate into solution (Chacon et al., 2006; Lindsay, 1981). In addition, strong complexation between Fe(III) and OM may inhibit the formation of Fe(III) (hydr)oxides, Fe(III) phosphates precipitates, and ternary P–Fe–OM complexes, thereby increasing P solubility (Sundman et al., 2016). Similarly, Karlsson et al. (2008) reported that Fe-OM complexes are sufficiently strong to hinder Fe hydrolysis, thereby affecting Fe reactivity and ultimately its speciation, which could also affect the speciation and availability of other nutrients, including phosphorus.

Furthermore, although aluminum (Al) is not a redox-sensitive element like Fe, Al (hydr)oxides can similarly undergo ligand-promoted dissolution and transformation in the presence of root exudates and organic acids. This process modifies the reactivity of Al minerals and significantly impacts P availability and sorption dynamics in soils (Violante et al., 2010). Therefore, investigating Fe speciation provides an opportunity to better understand the mechanisms governing P transformations in cover-cropped soils and may help explain the increases in DRP observed in runoff from these systems. Accordingly, the objective of this study was to evaluate the effect of cover cropping and P fertilization on soil Fe fractionation and speciation. We hypothesized that cover crop treatments would result in greater amounts of organically associated Fe and Al, effectively reducing the availability of these metals to react with P and form insoluble Al-P and Fe-P precipitates. To evaluate these operationally defined

organically-bound pools, we conducted sodium pyrophosphate extractions. Additionally, we hypothesized that the reactivity of the broader inorganic Fe and Al oxide pools would differ across treatments; thus, ammonium oxalate extractions were performed. Finally, we hypothesized that changes in the oxidation state of Fe could be indicative of shifts in Fe speciation under cover cropping, driven by either reductive dissolution or ligand-promoted dissolution. To investigate this, we conducted bulk Fe K-edge XANES spectroscopy.

Material and Methods

Experimental site and design

This research was conducted at the Kansas Agricultural Watershed (KAW) field laboratory near Manhattan, Kansas, from 2014 through 2026. The site is managed under a continuous no-till system with a corn–soybean rotation. Soils at the location are mapped as eroded Smolan silty clay loam (fine, smectitic, mesic Pachic Argiustoll) on slopes ranging from 3 to 7%. Prior to the establishment of the experimental plots, the field was operated under a conventionally tilled winter wheat (*Triticum aestivum*)–soybean rotation, with the most recent tillage occurring in the fall of 2014. The region receives an average of 889 mm of precipitation annually based on 30-year records and experiences a continental climate characterized as hot and humid, with a mean annual temperature of 12.9 °C.

The experiment employed a randomized complete block design with a 2 × 3 factorial treatment structure. The two cover crop management treatments included plots with a winter cover crop (CC) and plots without a cover crop (NC). The three P fertilization strategies included a control with no added P (CN), a build-and-drawdown (BD) approach, and a continuous build-

and-maintain (BM) approach. Each treatment combination was replicated three times (n = 18), with replications blocked by landscape position.

Soil Sample Collection and Processing

Selective extractions (sodium pyrophosphate and ammonium oxalate) were performed on soil samples collected annually from 2020 to 2023. Composite soil samples, each consisting of 21 cores, were collected after the fall harvest from three depth intervals (0 to 2.5, 2.5 to 5, and 5 to 15 cm) at three geo-referenced subplot locations within each plot. Samples were air-dried, ground, and sieved to pass a <2 mm mesh.

To align with concurrent analyses, composite soil samples representing the 0 to 5-cm depth were prepared by combining 10 g of soil from the 0 to 2.5-cm depth and 10 g from the 2.5 to 5-cm depth for each sampling point, operating under the assumption that soil bulk densities were uniform across the upper 5 cm. The resulting subsamples from the three geo-referenced points were then thoroughly mixed to form a single 0 to 5-cm composite sample for each plot. The baseline physicochemical properties of the soil across all treatments in 2023, including pH, total C, and Mehlich-3 extractable P, are summarized in Table 6-1.

Table 6-1. Baseline soil physicochemical properties (pH, total carbon, and Mehlich-3 extractable P) across experimental treatments in 2023.

Treatment Name	Treatment Number	pH	Total Carbon (g kg^{-1})	Mehlich-3 P (mg kg^{-1})
CN-NC	102-205-304	7.16	15.7	6.67
CN-CC	101-202-306	7.06	16.3	6.28
BD-NC	106-204-302	7.01	15.8	42.67
BD-CC	103-206-301	6.86	18.0	38.00
BM-NC	104-203-303	6.78	15.8	83.33
BM-CC	105-201-305	6.77	17.8	82.17

Note: Values represent composite samples from the 0–5 cm depth collected in fall 2023. Total carbon and Mehlich-3 P data are extensively analyzed and discussed in Chapter 5.

Soil pH Dynamics in the Surface Layer

Analysis of variance for soil pH in the 0–5 cm layer across the 2020–2023 study period revealed significant main effects of P fertilization ($p = 0.0141$) and sampling year ($p < 0.0001$). Across sampling years, the unfertilized control (CN) maintained the highest mean pH (6.89 a), which was significantly greater than both the build-and-drawdown (BD, pH 6.71 b) and build-and-maintain (BM, pH 6.64 b) treatments. Although the main effect of cover cropping on soil pH was not statistically significant at the $\alpha = 0.05$ level ($p = 0.1917$), there was a consistent biological trend toward surface acidification in the presence of cover crops (CC mean pH = 6.71) compared to no cover crops (NC mean pH = 6.79).

Pyrophosphate Extraction

To extract organically associated Fe and Al, 0.3 g of soil was weighed into 50-mL centrifuge tubes and combined with 25 mL of sodium pyrophosphate (0.1 M). The samples were shaken overnight using an end-to-end shaker for 16 hours and subsequently centrifuged at 20,000 × g for 10 minutes. The supernatants were filtered through 0.45 µm syringe filters, and the

filtrate was analyzed for Al and Fe concentrations using inductively coupled plasma (ICP) spectrometry.

Ammonium Oxalate Extraction

To extract amorphous and poorly crystalline Fe and Al oxides, 0.75 g of soil was weighed into 50-mL centrifuge tubes and combined with 30 mL of ammonium oxalate solution (0.2 M ammonium oxalate/oxalic acid). The tubes were wrapped in aluminum foil to maintain complete darkness and prevent the photo-induced dissolution of crystalline oxides. The samples were placed horizontally on a reciprocating shaker for 2 hours at room temperature. To ensure constant temperature and light exclusion, the foiled tubes were placed into foam racks for thermal insulation. Following the 2-hour extraction, the tubes were centrifuged at 10,000 rpm for 10 minutes. The supernatant from each tube was passed through a 0.45 μm nylon syringe filter into 15-mL vials, and the concentrations of Fe, Al, and P were determined using ICP spectrometry.

Iron K-edge XANES Study

Data Collection

For the X-ray absorption near-edge structure (XANES) analysis, soil samples from 2015 (baseline prior to treatment differentiation), 2022 (the conclusion of the build-and-drawdown P fertilization phase), and 2023 (the initiation of the sufficiency P fertilization approach) were selected. Specifically, six composite soil samples were analyzed for both 2015 and 2023, and 18 composite soil samples were analyzed for 2022. Bulk Fe K-edge XANES data were collected at beamline 7-ID-2 of the National Synchrotron Light Source II (NSLS-II) at Brookhaven National Laboratory (Upton, NY, USA).

Samples were finely ground and spread thinly onto double-sided C tape (SPI Supplies) secured to a sample holder. The sample holder was subsequently transferred to a vacuum chamber for analysis to minimize air scattering. All Fe XANES spectra, alongside a vivianite standard utilized for energy calibration, were collected in fluorescence mode using a solid-state drift detector. To effectively account for soil mineralogical heterogeneity, eight replicate scans were collected per soil sample across an energy range of 6950 to 7350 eV. Background correction, normalization, and linear combination fitting of the experimental spectra were performed in Athena v.0.9.25 (Ravel & Newville, 2005) following the standardized procedures described by Werner and Prietzel (2015). Previously collected Fe reference standards were included in the database, and vivianite standard spectra were acquired simultaneously during each analytical run to ensure precise spectral energy alignment (Khatiwada et al., 2012; Weeks & Hettiarachchi, 2020).

Data Analysis

During data processing, each of the eight XANES scans collected per sample was examined individually to ensure no excessive noise or anomalies were present. Acceptable scans were merged to improve the signal-to-noise ratio, producing a single averaged spectrum for each sample. Truncated data files were then generated to strictly isolate the XANES region, as the extended X-ray absorption fine structure (EXAFS) region contained excessive noise that would otherwise compromise robust data fitting.

A normalization range of 15 to 83 eV relative to the edge energy (E_0) was applied consistently across all samples. Based on a representative E_0 of 7124.57 eV, this corresponds to an absolute energy range of 7109.57 to 7207.57 eV. To interpret the XANES spectra and perform linear combination fitting (LCF) to delineate differences in Fe oxidation state and

coordination, a comprehensive set of model standards representing various Fe oxidation states and mineral phases was selected. Iron(II) oxalate and FeS were utilized as representative reduced Fe(II) compounds. Oxidized Fe(III) species were represented by Fe(III) oxalate, ferrihydrite, and goethite, with the latter two serving as poorly crystalline and highly crystalline Fe oxyhydroxides, respectively. Additionally, biotite was included as a representative Fe-bearing silicate mineral containing structurally bound iron.

For the final LCF analysis, all component weights were mathematically constrained between 0 and 1, and the option to force the component weights to sum to exactly 1.0 was applied. Linear combination fitting was iteratively performed using the selected model compounds to determine the combination that best represented the experimental sample spectra. Fit quality was systematically evaluated based on the lowest R-factor values and visual agreement between the fitted and experimental spectral curves. The optimal combination of model compounds for each sample was selected based strictly on the lowest overall R-factor and the most accurate replication of the specific spectral shape.

Results

Pyrophosphate-Extractable Fe and Al

Pyrophosphate extraction was used to quantify Fe and Al associated with OM and reactive mineral phases in the soil. This method primarily extracts organically-complexed Fe and Al by forming soluble metal–pyrophosphate complexes and disrupting OM–metal associations under alkaline conditions. However, pyrophosphate extraction may also release a portion of noncrystalline and poorly crystalline Fe and Al oxide/hydroxide phases, particularly those associated with organic coatings, and therefore represents a pool of organically associated and

reactive Fe and Al rather than exclusively organic-bound forms (Ulery & Drees, 2008). Additionally, in the fertilized treatments, fertilizer-derived condensed phosphates (such as pyrophosphate) may also contribute to the complexation of these metals in the field.

The interaction of P fertilization and cover cropping on pyrophosphate-extractable Al (Pyrophosphate-Al) was significant (Figure 6-1a). Under the BM treatment, the presence of a cover crop resulted in significantly greater Pyrophosphate-Al compared with the no-cover-crop treatment. A similar pattern was observed under the BD treatment, where Pyrophosphate-Al was slightly higher with a cover crop than without; however, this difference was not statistically significant. The CN treatment also showed no difference between cover crop and no-cover-crop treatments. These results suggest that the effect of cover crops on Pyrophosphate-Al was strictly evident under the high-input BM fertilization strategy, but not under the BD and CN treatments.

The interaction of P fertilization and cover cropping on pyrophosphate-extractable Fe (Pyrophosphate-Fe) was also significant (Figure 6-1b). In the absence of a cover crop, Pyrophosphate-Fe concentrations did not differ significantly among the BM, BD, and CN treatments. However, under cover crop (CC) treatments, Pyrophosphate-Fe concentrations increased substantially in the BM and BD treatments, making them significantly greater than the CN treatment. These results indicate that cover crops actively promoted the accumulation of organically-associated Fe under the BM and BD strategies, but failed to do so under the unfertilized CN treatment.

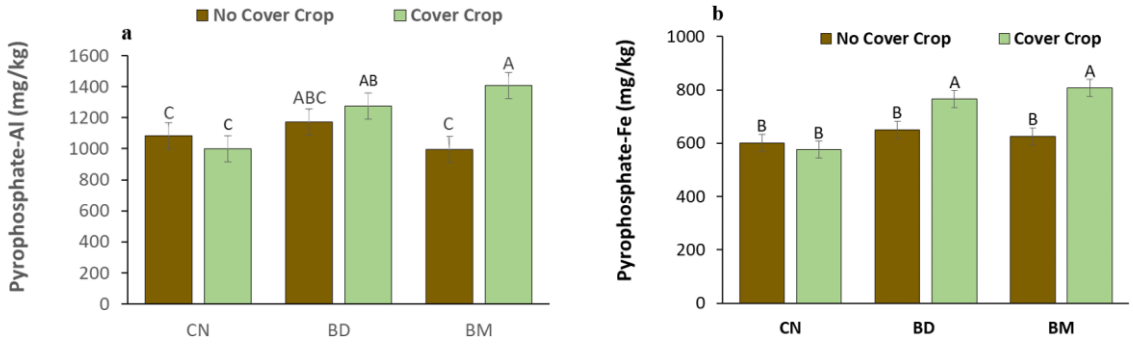


Figure 6-1. The interaction of P fertilization and cover cropping on pyrophosphate-extractable Al (a) and pyrophosphate-extractable Fe (b). Means within a treatment containing the same letter are not significantly different at *α*=0.05. Abbreviations used include control (CN), build-and-drawdown (BD), and build-and-maintain (BM) of phosphorus fertilizer application. (Data are averaged from 2020 to 2023).

Oxalate-Extractable Fe, Al, and P

Ammonium oxalate extraction was used to quantify poorly crystalline and short-range-order Fe and Al mineral phases in the soil. Under acidic conditions, oxalate selectively dissolves reactive Fe and Al oxides, hydroxides, and aluminosilicate phases, including poorly crystalline minerals such as ferrihydrite, allophane, and imogolite. However, due to the strong complexing ability of oxalate, this extraction may also release organically-bound Fe and Al, and therefore represents a broader pool of reactive poorly crystalline and organically associated Fe and Al rather than exclusively mineral-derived forms (Ulery & Drees, 2008).

The interaction of P fertilization and cover cropping was significant on oxalate-extractable Fe (Oxalate-Fe). Oxalate-Fe varied considerably among P fertilization and cover crop

treatments (Figure 6-2a). Under no P fertilization (CN), the presence of a cover crop increased Oxalate-Fe compared with the no-cover-crop treatment. Under the build-and-drawdown (BD) treatment, Oxalate-Fe concentrations were similar between cover crop and no-cover-crop treatments. In sharp contrast, under the build-and-maintain (BM) treatment, Oxalate-Fe was highest in the no-cover-crop treatment, while the cover crop treatment significantly reduced these values. Overall, the BM treatment without cover crop exhibited the greatest Oxalate-Fe concentration, whereas the lowest value was observed in the CN treatment without cover crop.

The interaction of year and P fertilization was significant for oxalate-extractable P (Oxalate-P). From 2020 to 2022, there was a slight increase in Oxalate-P in the BM treatment, followed by a slight, non-significant decrease from 2022 to 2023. For the BD and CN treatments, Oxalate-P remained relatively stable from 2020 to 2023 (Figure 6-2b).

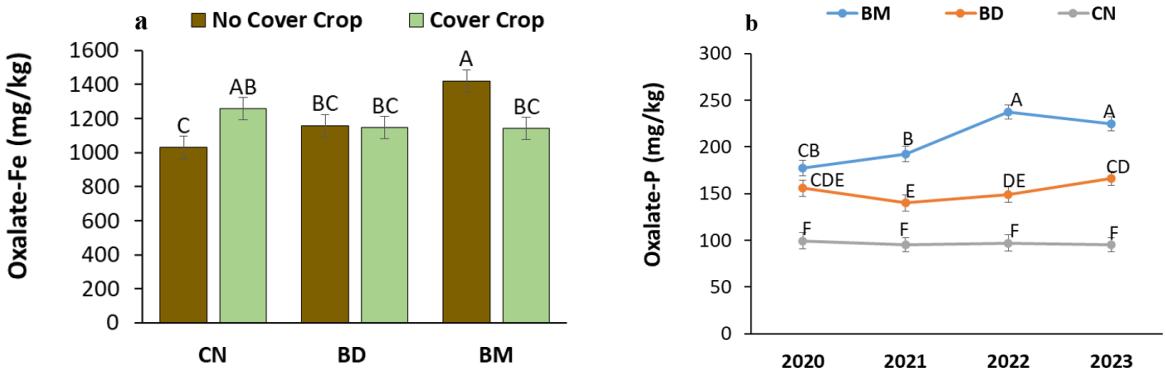


Figure 6-2. The interaction of P fertilization and cover cropping on oxalate-extractable Fe (a) and the interaction of P fertilization and year on oxalate-extractable P (b). Means within a treatment containing the same letter are not significantly different at α=0.05. Abbreviations used include control (CN), build-and-drawdown (BD), and build-and-maintain (BM) of phosphorus fertilizer application. (Data are from 2020 to 2023).

To better visualize the relationship between operationally-defined organic and inorganic reactive Fe pools, an overlay of Pyrophosphate-Fe and Oxalate-Fe is presented in Figure 6-3. This comparative visualization highlights that organically-associated Fe (pyrophosphate-extractable) constitutes a substantial proportion of the total reactive Fe pool (oxalate-extractable) across multiple treatments. Notably, under cover crop treatments in the BD and BM fertilization regimes, the contribution of the organically associated Fe fraction to the overall reactive Fe pool appears distinctly enhanced. This proportional shift further supports the potential role of cover crops in actively promoting the formation of Fe-OM complexes at the expense of inorganic amorphous Fe oxides.

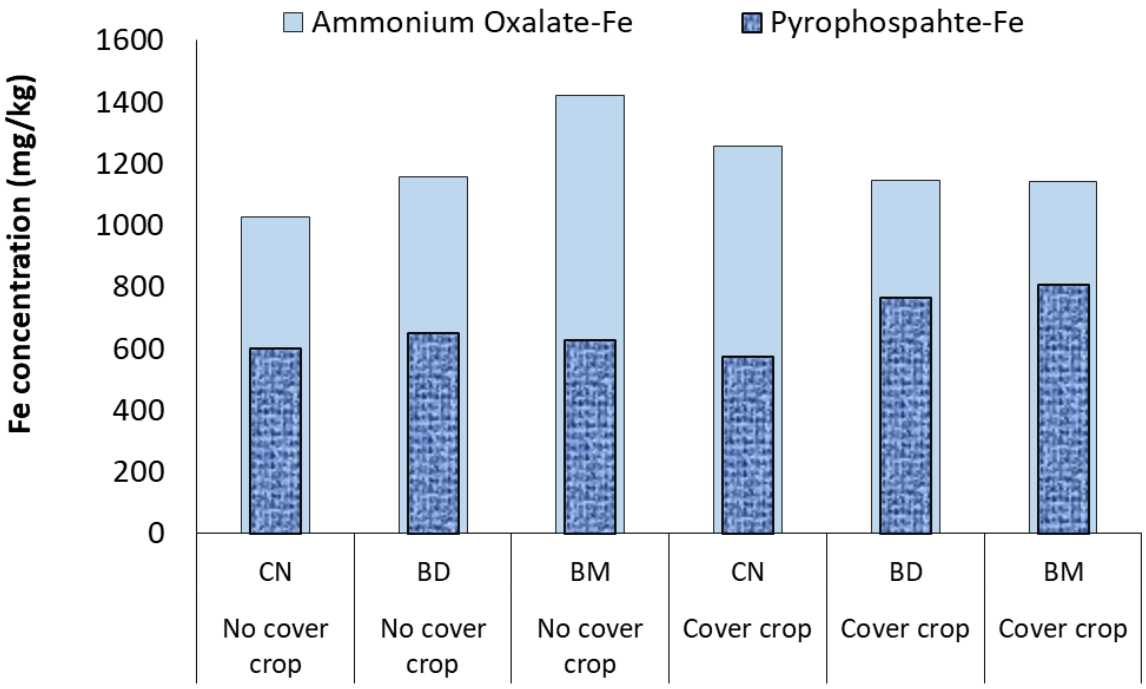


Figure 6-3. Overlay of ammonium oxalate-extractable Fe (representing total reactive and poorly crystalline Fe) and sodium pyrophosphate-extractable Fe (representing organically associated Fe) across different phosphorus fertilization and cover crop treatments. The overlaid bars illustrate the proportion of organically bound Fe (foreground) relative to the broader reactive Fe pool (background).

Iron K-edge XANES Spectroscopy

Iron K-edge XANES spectroscopy was used to evaluate Fe oxidation state and local coordination environment by examining changes in absorption edge position, white-line intensity, and overall spectral features. Iron K-edge XANES provides a robust oxidation-state-sensitive indicator because Fe(II)-rich phases generally display lower edge or pre-edge energies, whereas Fe(III)-rich phases are shifted to higher energies. Thus, approximate Fe(II)-dominated

and Fe(III)-dominated edge windows near 7112–7118 eV and 7120–7128 eV, respectively, should be interpreted as calibration-dependent but chemically meaningful reference ranges (Wilke et al., 2001), especially when correcting for any calibration differences.

The normalized Fe K-edge XANES spectra of soils collected in 2015 and 2022 showed similar overall spectral characteristics across treatments, with the absorption edge occurring near 7118–7120 eV and the white-line peak centered around 7128–7130 eV, suggesting that Fe phases were predominantly similar among treatments and sampling years (Figure 6-4). However, some discernible differences in edge position and spectral shape were observed in specific treatments, particularly BD-NC, BM-NC, and BM-CC, indicating potential changes in the Fe local coordination environment over the seven-year period. In contrast, spectra from CN-NC, CN-CC, and BD-CC showed greater similarity between years, suggesting relatively stable bulk Fe speciation in these treatments. Overall, a lack of systematic edge shift among treatments supports minimal change in bulk Fe valence, even if ligand-driven Fe redistribution occurred at the micro-scale.

The relative contributions of the Fe reference spectra obtained from Fe-XANES linear combination fitting (LCF) for all treatments in 2015 are summarized in Table 6-2. The fitted percentages represent the spectral similarity of the sample to the selected reference compounds and are used to infer broad patterns in Fe bonding environments rather than direct quantitative mineralogy. For example, in the CN-CC treatment, LCF indicated that approximately 45.1% of the Fe occurred in an environment spectrally similar to Fe(III)-oxalate, suggesting Fe associations with OM, while 54.9% was best represented by biotite.

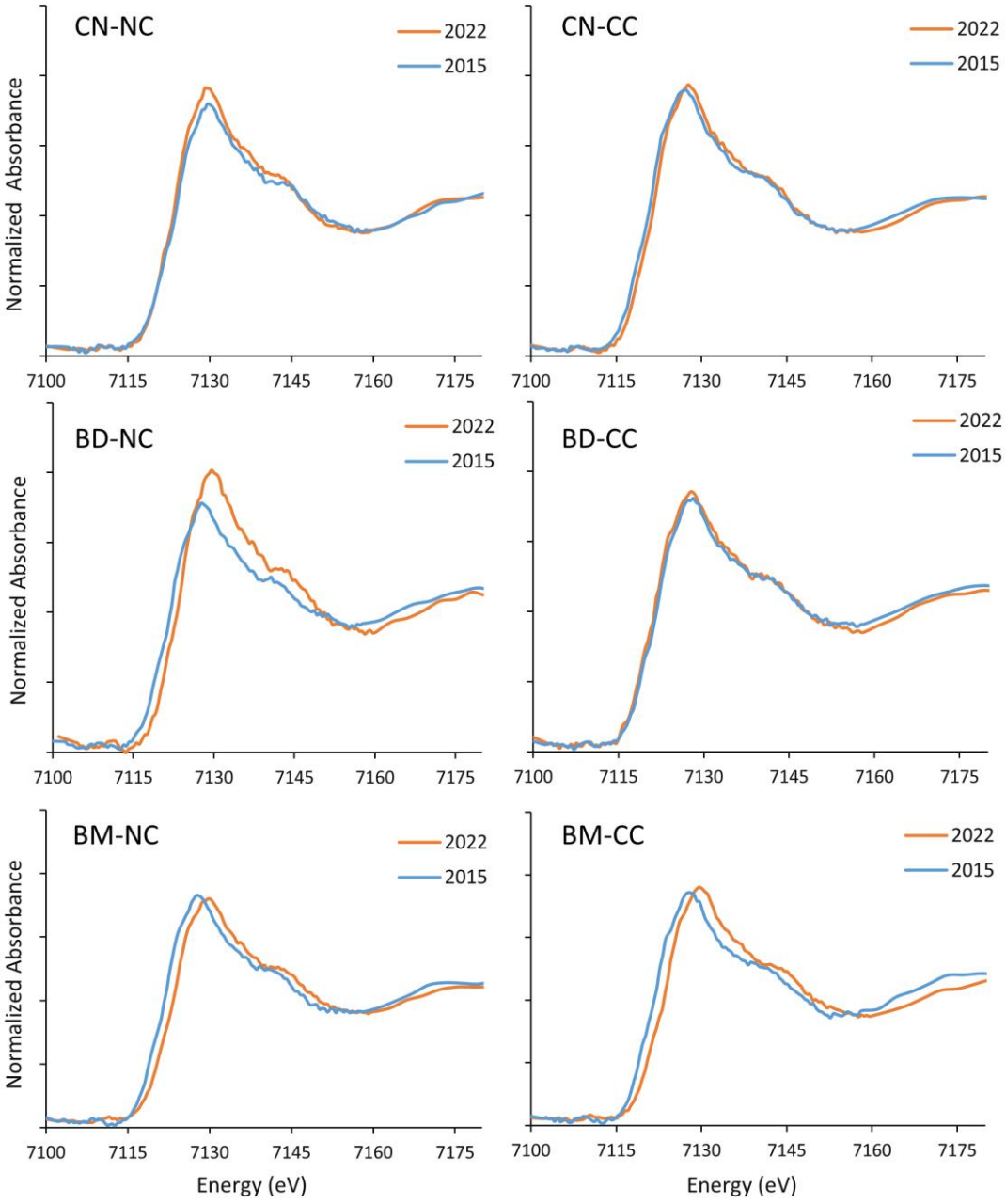


Figure 6-4. Normalized Fe K-edge X-ray absorption near-edge structure spectra of soil collected in 2015 and 2022. CN-CC, control-with cover crops; CN-NC, control-no cover crops; BD-CC, build-and-drawdown with cover crops; BD-NC, build-and-drawdown-no cover crops; BM-CC, build-and-maintain with cover crops; BM-NC, build-and-maintain no cover crops.

Table 6-2. The relative contributions of the Fe reference spectra obtained from Fe-XANES linear combination fitting for all treatments in 2015.

Treatment Name	Treatment Number	Fe(II) oxalate (%)	Fe(III) oxalate (%)	Biotite (%)	Goethite (%)	FeS (%)	Ferrihydrite (%)
CN-CC	101-202-306	-	45.1	54.9	-	-	-
CN-NC	102-205-304	-	-	45.3	54.7	-	-
BD-CC	103-206-301	-	23.4	57.9	18.7	-	-
BM-NC	104-203-303	-	18.4	63.5	18.1	-	-
BM-CC	105-201-305	-	17.1	67.3	15.6	-	-
BD-NC	106-204-302	-	23.3	54.0	22.8	-	-

Note: CN-CC, control with cover crop; CN-NC, control with no cover crop; BD-CC, build-and-drawdown with cover crop; BD-NC, build-and-drawdown with no cover crop; BM-CC, build-and-maintain with cover crop; BM-NC, build-and-maintain with no cover crop. Dash (–) indicates that the reference standard was not included in the best-fit linear combination model.

Figure 6-5 shows the normalized Fe K-edge XANES spectra for samples from 2022 and 2023. All spectra displayed a distinct absorption edge at approximately 7118–7120 eV, followed by a discernible white-line peak centered around 7128–7130 eV. Differences between years were generally subtle and treatment-dependent. In the control treatment, the CN-NC spectra from 2022 and 2023 overlapped closely. The CN-CC treatment yielded the noisiest Fe-XANES spectrum among all samples. Additionally, the CN-CC treatment exhibited greater year-to-year variation, with the 2023 spectrum revealing a slightly altered oscillatory structure in the post-edge region. Within the BD treatments, the BD-NC spectra displayed a minimal shift in 2023 relative to 2022, whereas the BD-CC spectra were highly similar across both years. The build-

and-maintain treatments (BM-NC and BM-CC) exhibited the least interannual variability, largely overlapping between 2022 and 2023. The relative contributions of the Fe reference spectra derived from the linear combination fitting for all treatments in 2022 and 2023 are detailed in Table 6-3 and Table 6-4, respectively.

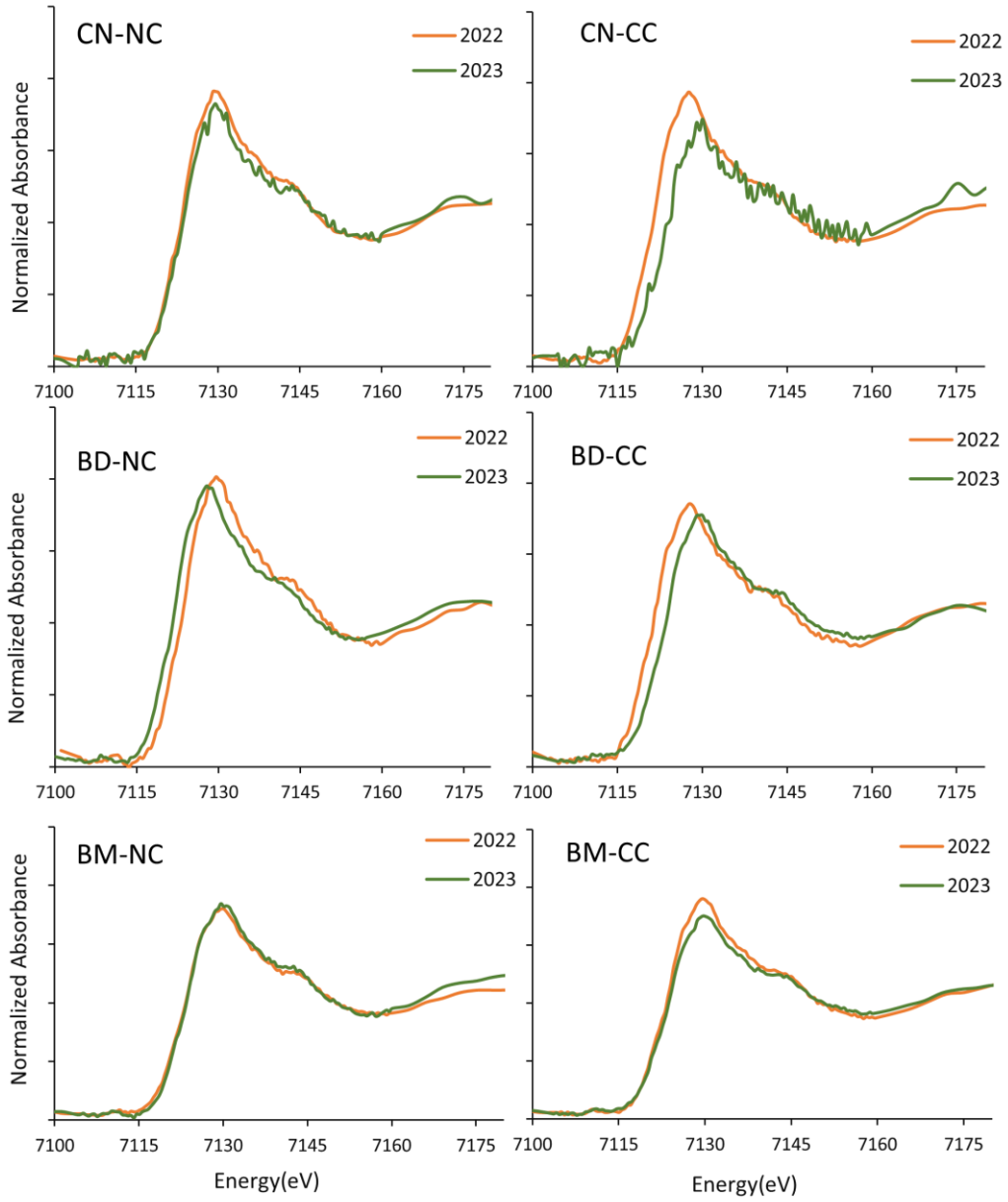


Figure 6-5. Normalized Fe K-edge X-ray absorption near-edge structure spectra of soil collected in 2022 and 2023. CN-CC, control-with cover crops; CN-NC, control-no cover crops; BD-CC, build-and-drawdown with cover crops; BD-NC, build-and-drawdown-no cover crops; BM-CC, build-and-maintain with cover crops; BM-NC, build-and-maintain no cover crops.

Table 6-3. The relative contributions of the Fe reference spectra obtained from Fe-XANES linear combination fitting for all treatments in 2022.

Treatment Name	Treatment Number	Fe(II) oxalate (%)	Fe(III) oxalate (%)	Biotite (%)	Goethite (%)	FeS (%)	Ferrihydrite (%)
CN-CC	101-202-306	-	23.9	69.0	7.2	-	-
CN-NC	102-205-304	-	-	52.4	47.6	-	-
BD-CC	103-206-301	-	28.1	60.4	11.6	-	-
BM-NC	104-203-303	-	-	51.3	48.7	-	-
BM-CC	105-201-305	-	-	51.3	48.7	-	-
BD-NC	106-204-302	-	-	55.0	45.0	-	-

Note: CN-CC, control with cover crop; CN-NC, control with no cover crop; BD-CC, build-and-drawdown with cover crop; BD-NC, build-and-drawdown with no cover crop; BM-CC, build-and-maintain with cover crop; BM-NC, build-and-maintain with no cover crop. Dash (–) indicates that the reference standard was not included in the best-fit linear combination model.

Table 6-4. The relative contributions of the Fe reference spectra obtained from Fe-XANES linear combination fitting for all treatments in 2023.

Treatment Name	Treatment Number	Fe(II) oxalate (%)	Fe(III) oxalate (%)	Biotite (%)	Goethite (%)	FeS (%)	Ferrihydrite (%)
CN-CC	101-202-306	-	-	42.5	57.5	-	-
CN-NC	102-205-304	-	-	45.4	54.6	-	-
BD-CC	103-206-301	-	-	48.4	51.6	-	-
BM-NC	104-203-303	-	-	47.2	52.8	-	-
BM-CC	105-201-305	-	-	42.7	57.3	-	-
BD-NC	106-204-302	-	16.1	73.0	10.9	-	-

Note: CN-CC, control with cover crop; CN-NC, control with no cover crop; BD-CC, build-and-drawdown with cover crop; BD-NC, build-and-drawdown with no cover crop; BM-CC, build-and-maintain with cover crop; BM-NC, build-and-maintain with no cover crop. Dash (–) indicates that the reference standard was not included in the best-fit linear combination model.

Discussion

Pyrophosphate- and ammonium oxalate-extractable Fe and Al

The greater pyrophosphate-extractable Fe and Al observed under cover cropping suggest that a larger proportion of these metals occurred in forms extractable by sodium pyrophosphate, consistent with increased associations between Fe and Al and soil OM. Conversely, the larger

non-pyrophosphate fraction in the no-cover-crop treatment indicates that a greater proportion of Fe and Al remained in forms not extracted by pyrophosphate, including amorphous inorganic oxides. Because pyrophosphate extraction provides an operational estimate rather than a direct measure of organically-complexed metals (Parfitt & Childs, 1988), these results should be interpreted as evidence of shifts in operationally-defined Fe and Al fractions rather than unequivocal changes in organo-metallic complexes.

The Role of Soil pH in Iron Solubilization and Complexation

The observed shifts in extractable Fe pools — specifically the proportional transition from amorphous inorganic Fe oxides to organically-associated Fe — are intrinsically linked to the localized soil pH dynamics in the 0–5 cm surface layer. The continuous application of ammonium polyphosphate fertilizers in the BM and BD treatments caused significant surface soil acidification (reducing pH from 6.89 in the control to 6.64 and 6.71, respectively). In addition to fertilizer-induced acidity, the presence of cover crops contributed to a consistent trend of further surface acidification (lowering the bulk pH to 6.71 compared to 6.79 in NC plots).

This localized acidification is a critical driver for ligand-promoted dissolution. As pH decreases, the solubility of amorphous and poorly crystalline Fe(III) oxides naturally increases, and protonation of the mineral surfaces weakens Fe–O bonds. Simultaneously, actively growing cover crop roots exude LMWOAs (e.g., citrate and malate) and release protons to balance cation uptake. This combination of lower surface pH and an influx of organic ligands creates optimal thermodynamic and kinetic conditions for OM to complex with the newly solubilized Fe.

Therefore, the significantly greater pyrophosphate-extractable Fe concentration (organo-Fe complexes) observed under the cover-cropped BM and BD treatments is directly facilitated by this slightly more acidic environment. The lower pH destabilizes the inorganic Fe oxides,

allowing the cover crop-derived organic C to outcompete phosphate for the available Fe, ultimately forming stable Fe–OM complexes. By sequestering Fe into these organic complexes, the abundance of reactive inorganic mineral surfaces available to retain phosphate is reduced, thereby increasing the vulnerability of DRP to runoff losses. Additionally, because the fertilized treatments received ammonium polyphosphate—which contains pyrophosphate and polyphosphate chains (as confirmed by ^{31}P-NMR in Chapter 4)—and given that pyrophosphate acts as a strong chelating agent capable of complexing Fe and Al in laboratory extractions, it is also plausible that fertilizer-derived condensed phosphates directly complexed a portion of soil Fe and Al in the field. Future mechanistic studies should investigate the extent to which polyphosphate fertilizers directly participate in metal complexation and organo-mineral disruption in agricultural soils.

Nevertheless, the observed trends are consistent with greater inputs of root exudates, dissolved OM, and LMWOAs under cover cropping (Sakib et al., 2026), which are expected to promote Fe and Al interactions with OM and alter their distribution among soil fractions. Consequently, a reduction in the abundance or reactivity of inorganic Fe and Al oxide surfaces, together with competition between organic ligands and phosphate for sorption sites, may have reduced phosphate sorption and contributed to the greater dissolved reactive P previously reported under cover cropping at this experimental site (Carver et al., 2022).

To explicitly visualize the redistribution of reactive Fe pools, ammonium oxalate-extractable Fe and sodium pyrophosphate-extractable Fe were overlaid (Figure 6-3). This comparative overlay demonstrated that while cover cropping reduced the total pool of poorly crystalline Fe (Oxalate-Fe) under the BM treatment, it simultaneously increased the organically-associated Fe fraction (Pyrophosphate-Fe). Consequently, the proportion of organically-

associated Fe relative to the overall reactive Fe pool was substantially higher in cover-cropped soils. This proportional shift suggests that cover cropping promotes Fe complexation with soil OM at the expense of amorphous inorganic Fe oxides, thereby reducing the availability of highly reactive mineral surfaces for phosphate sorption.

The greater ammonium oxalate-extractable P observed under the build-and-maintain (BM) treatment suggests that a larger proportion of applied P was retained by the overall reactive Fe and Al pool. Because ammonium oxalate extracts both amorphous inorganic minerals and organically-complexed metals, this retained P cannot be exclusively attributed to amorphous phases; rather, organically-associated Fe and Al may also participate in P stabilization through ternary complex formation.

Furthermore, the greater ammonium oxalate-extractable P under higher P fertilization likely reflects increased P loading to the soil system, resulting in progressive occupation of available sorption sites and greater accumulation of P associated with extractable Fe and Al pools. Because ammonium oxalate extracts P associated with poorly crystalline minerals, organically associated Fe and Al, as well as some readily exchangeable P pools, the greater Oxalate-P recovery in the BM treatment likely reflects the overall increase in total soil P from continued fertilization rather than specific accumulation within a single phase.

Iron K-edge XANES Spectroscopy

The chemical extractions indicated greater pyrophosphate-extractable Fe under cover cropping, demonstrating a shift toward organically associated Fe fractions; however, the bulk Fe-XANES and linear combination fitting (LCF) results did not exhibit a proportional increase in the distinct Fe(III)-oxalate fraction or a shift toward reduced Fe(II) species. This apparent discrepancy can be resolved by considering the fundamental mechanisms of Fe mobilization in

the rhizosphere, the inherent differences between operational chemical extractions and bulk spectroscopic techniques, and the lack of sensitivity of the bulk XANES technique for organically-associated Fe (Karlsson et al., 2008; Prietzel et al., 2007; Rennert, 2019).

While we originally hypothesized that cover crops might promote the reductive dissolution of Fe(III) oxides, yielding a distinct Fe(II) signature, the lack of a systematic edge shift toward lower energies across treatments strongly suggests an alternative pathway. The increase in Fe mobilization and subsequent P release under cover crops is more accurately interpreted as ligand-promoted dissolution. In this mechanism, LMWOAs exuded by cover crop roots form stable Fe–ligand complexes that destabilize Fe oxides and enhance Fe release into the soil solution without requiring a concomitant shift in the Fe oxidation state (Reichard et al., 2007). Therefore, enhanced Fe solubilization in these systems is primarily driven by organic complexation (as captured by the pyrophosphate extractions) rather than reductive dissolution, explaining the stability of the bulk XANES absorption edge.

Furthermore, the lack of a pronounced spectroscopic response to these organic complexes is largely governed by a masking effect within the soil matrix. Bulk Fe-XANES is sensitive to the average coordination environment of all Fe in the sample. In the soils of this study region, the Fe inventory is heavily dominated by structurally-bound Fe within phyllosilicates (e.g., biotite) and highly crystalline Fe oxides. Because bulk Fe-XANES represents a spatially averaged signal, minor pools of organically-complexed Fe can be severely underrepresented when the overall signal is dominated by these dominant, unreactive mineral phases (Prietzel et al., 2007). Consequently, the absence of a strong bulk-XANES organo-Fe signature should be interpreted as “not resolved at the bulk scale” rather than a definitive absence of these complexes.

Additionally, the biogeochemical processes driving these ligand-promoted transformations are highly transient and spatially confined to millimeter-scale gradients around the roots. The absence of a strong treatment effect in the XANES spectra is consistent with a rhizosphere dilution effect: localized organic exudation, Fe solubilization, and complexation occur strictly within the rhizosphere microzones and are therefore readily diluted when homogenized with the much larger, unaffected bulk-soil matrix during sampling (van Veelen et al., 2020). Accordingly, bulk Fe-XANES is a highly conservative tool for detecting the delicate, micro-scale redistributions of Fe generated by cover crop roots, which are more sensitively captured by targeted wet-chemical extractions.

Taken together, the findings demonstrate that cover crops enhance the formation of Fe–OM associations most likely through ligand-promoted dissolution, effectively decreasing the abundance of reactive inorganic Fe(III) oxides that normally retain phosphate. Consequently, phosphate is maintained in more soluble and bioavailable forms, providing a robust mechanistic explanation for the previously observed increases in DRP losses from this site.

Conclusion

This study evaluated the effects of cover cropping and P fertilization strategies on soil Fe fractionation and speciation to elucidate the mechanisms governing P dynamics in a no-till agricultural system. Targeted chemical extractions demonstrated that cover cropping significantly increased the organically-associated Fe pool (pyrophosphate-extractable Fe), particularly under the build-and-maintain and build-and-drawdown P fertilization strategies. A comparative overlay of reactive Fe pools further confirmed that cover crops promoted a proportional shift from amorphous inorganic Fe oxides toward Fe–OM complexes.

Rather than undergoing reductive dissolution, the results strongly indicate that Fe mobilization in these cover-cropped soils is driven by ligand-promoted dissolution. The exudation of LMWOAs by cover crop roots facilitates the formation of stable Fe-OM complexes without altering the bulk Fe oxidation state, as corroborated by the stable absorption edges observed in the bulk Fe-XANES spectra. While bulk XANES analysis was inherently limited by the masking effect of dominant phyllosilicate minerals and the dilution of localized rhizosphere processes within the bulk soil matrix, it effectively ruled out widespread reductive shifts as the primary driver of phosphate release.

Ultimately, the ligand-driven transition of Fe from highly reactive mineral surfaces to organic complexes diminishes the capacity of the soil for strong phosphate sorption. This mechanistic shift provides a critical explanation for the increased susceptibility of DRP to transport and loss in cover-cropped systems. Future studies aiming to capture these micro-scale biogeochemical transformations should employ targeted in situ microspectroscopic techniques (e.g., μ-XANES) focused directly on the rhizosphere to overcome the dilution and masking limitations inherent to bulk soil analysis. This limitation may also be overcome by carefully sampling rhizosphere soils.

References

Carver, R. E., Nelson, N. O., Roozeboom, K. L., Kluitenberg, G. J., Tomlinson, P. J., Kang, Q., & Abel, D. S. (2022). Cover crop and phosphorus fertilizer management impacts on surface water quality from a no-till corn-soybean rotation. Journal of Environmental Management, 301, 113818. https://doi.org/10.1016/j.jenvman.2021.113818

Chacon, N., Silver, W. L., Dubinsky, E. A., & Cusack, D. F. (2006). Iron reduction and soil phosphorus solubilization in humid tropical forests soils: The roles of labile carbon pools and an electron shuttle compound. Biogeochemistry, 78(1), 67–84. https://doi.org/10.1007/s10533-005-2343-3

Condron, L. M., Turner, B. L., & Cade-Menun, B. J. (2005). Chemistry and dynamics of soil organic phosphorus. In J. T. Sims & A. N. Sharpley (Eds.), Phosphorus: Agriculture and the environment (pp. 87–121). American Society of Agronomy, Crop Science Society of America, & Soil Science Society of America. https://doi.org/10.2134/agronmonogr46.c4

Gerke, J. (2010). Humic (organic matter)–Al(Fe)–phosphate complexes: An underestimated phosphate form in soils and source of plant-available phosphate. Soil Science, 175(9), 417–425. https://doi.org/10.1097/SS.0b013e3181f1b4dd

Karlsson, T., Persson, P., Skyllberg, U., Mörth, C.-M., & Giesler, R. (2008). Characterization of iron(III) in organic soils using extended X-ray absorption fine structure spectroscopy. Environmental Science & Technology, 42(15), 5449–5454. https://doi.org/10.1021/es800059e

Khatiwada, R., Hettiarachchi, G. M., Mengel, D. B., & Fei, M. (2012). Speciation of phosphorus in a fertilized, reduced-till soil system: In-field treatment incubation study. Soil Science Society of America Journal, 76(6), 2006–2018. https://doi.org/10.2136/sssaj2011.0299

Lindegren, M., & Persson, P. (2009). Competitive adsorption between phosphate and carboxylic acids: Quantitative effects and molecular mechanisms. European Journal of Soil Science, 60(6), 982–993. https://doi.org/10.1111/j.1365-2389.2009.01171.x

Lindsay, W. L. (1981). Solid phase-solution equilibria in soils. In R. H. Dowdy, J. A. Ryan, V. V. Volk, & D. E. Baker (Eds.), Chemistry in the soil environment (ASA Special

Publication No. 40, pp. 183–202). American Society of Agronomy & Soil Science Society of America. https://doi.org/10.2134/asaspecpub40.c10

Parfitt, R. L., & Childs, C. W. (1988). Estimation of forms of Fe and Al—A review, and analysis of contrasting soils by dissolution and Mössbauer methods. Australian Journal of Soil Research, 26(1), 121–144. https://doi.org/10.1071/SR9880121

Prietzel, J., Thieme, J., Eusterhues, K., & Eichert, D. (2007). Iron speciation in soils and soil aggregates by synchrotron-based X-ray microspectroscopy (XANES, μ-XANES). European Journal of Soil Science, 58(5), 1027–1041. https://doi.org/10.1111/j.1365-2389.2006.00882.x

Ravel, B., & Newville, M. (2005). ATHENA, ARTEMIS, HEPHAESTUS: Data analysis for X-ray absorption spectroscopy using IFEFFIT. Journal of Synchrotron Radiation, 12(4), 537–541. https://doi.org/10.1107/S0909049505012719

Reichard, P. U., Kretzschmar, R., & Kraemer, S. M. (2007). Dissolution mechanisms of goethite in the presence of siderophores and organic acids. Geochimica et Cosmochimica Acta, 71(23), 5635–5650. https://doi.org/10.1016/j.gca.2006.12.022

Rennert, T. (2019). Wet-chemical extractions to characterise pedogenic Al and Fe species—A critical review. Soil Research, 57(1), 1–16. https://doi.org/10.1071/SR18299

Sakib, T. U., Hettiarachchi, G. M., Kluitenberg, G. J., Roozeboom, K. L., Tomlinson, P. J., Presley, D. R., & Nelson, N. O. (2026). Drawdown phosphorus management in cover cropping systems: A strategy for mitigating phosphorus loss in agroecosystems. Journal of Environmental Quality. (In review).

Schreeg, L. A., Mack, M. C., & Turner, B. L. (2013). Leaf litter inputs decrease phosphate sorption in a strongly weathered tropical soil over two time scales. Biogeochemistry, 113(1–3), 507–524. https://doi.org/10.1007/s10533-012-9781-5

Soltangheisi, A., Rodrigues, M., Coelho, M. J. A., Gasperini, A. M., Sartor, L. R., & Pavinato, P. S. (2018). Changes in soil phosphorus lability promoted by phosphate sources and cover crops. Soil and Tillage Research, 179, 20–28. https://doi.org/10.1016/j.still.2018.01.006

Soltangheisi, A., Teles, A. P. B., Sartor, L. R., & Pavinato, P. S. (2020). Cover cropping may alter legacy phosphorus dynamics under long-term fertilizer addition. Frontiers in Environmental Science, 8, 13. https://doi.org/10.3389/fenvs.2020.00013

Sundman, A., Karlsson, T., Sjöberg, S., & Persson, P. (2016). Impact of iron–organic matter complexes on aqueous phosphate concentrations. Chemical Geology, 426, 109–117. https://doi.org/10.1016/j.chemgeo.2016.02.008

Syers, J. K., Johnston, A. E., & Curtin, D. (2008). Efficiency of soil and fertilizer phosphorus use: Reconciling changing concepts of soil phosphorus behaviour with agronomic information (FAO Fertilizer and Plant Nutrition Bulletin No. 18). Food and Agriculture Organization of the United Nations.

Ulery, A. L., & Drees, L. R. (Eds.). (2008). Methods of soil analysis: Part 5—Mineralogical methods (SSSA Book Series No. 5). Soil Science Society of America. https://doi.org/10.2136/sssabookser5.5

van Veelen, A., Koebernick, N., Scotson, C. S., McKay-Fletcher, D., Huthwelker, T., Borca, C. N., Mosselmans, J. F. W., & Roose, T. (2020). Root-induced soil deformation influences Fe, S and P: Rhizosphere chemistry investigated using synchrotron XRF and XANES. New Phytologist, 225(4), 1476–1490. https://doi.org/10.1111/nph.16242

Violante, A., Cozzolino, V., Perelomov, L., Caporale, A. G., & Pigna, M. (2010). Mobility and bioavailability of heavy metals and metalloids in soil environments. Journal of Soil Science and Plant Nutrition, 10(3), 268–292. https://doi.org/10.4067/S0718-95162010000100005

Weeks, J. J., Jr., & Hettiarachchi, G. M. (2020). Source and formulation matter: New insights into phosphorus fertilizer fate and transport in mildly calcareous soils. Soil Science Society of America Journal, 84(3), 731–746. https://doi.org/10.1002/saj2.20054

Welch, R. Y., Behnke, G. D., Davis, A. S., Masiunas, J., & Villamil, M. B. (2016). Using cover crops in headlands of organic grain farms: Effects on soil properties, weeds and crop yields. Agriculture, Ecosystems & Environment, 216, 322–332. https://doi.org/10.1016/j.agee.2015.10.014

Werner, F., & Prietzel, J. (2015). Standard protocol and quality assessment of soil phosphorus speciation by P K-edge XANES spectroscopy. Environmental Science & Technology, 49(17), 10521–10528. https://doi.org/10.1021/acs.est.5b03096

White, C. M., & Weil, R. R. (2011). Forage radish cover crops increase soil test phosphorus surrounding radish taproot holes. Soil Science Society of America Journal, 75(1), 121–130. https://doi.org/10.2136/sssaj2010.0095

Wilke, M., Farges, F., Petit, P.-E., Brown, G. E., Jr., & Martin, F. (2001). Oxidation state and coordination of Fe in minerals: An Fe K-XANES spectroscopic study. American Mineralogist, 86(5–6), 714–730. https://doi.org/10.2138/am-2001-5-612

Chapter 7 - General Summary, Synthesis, and Conclusions

Research Overview and Rationale

Achieving sustainable phosphorus (P) management in modern agroecosystems requires reconciling two often competing imperatives: maintaining sufficient soil fertility to support high crop yields and minimizing dissolved reactive P (DRP) losses to surface waters. In the central United States, the widespread adoption of continuous no-till management in corn (*Zea mays* L.)–soybean (*Glycine max* [L.] Merr.) rotations, combined with historical build-and-maintain (BM) fertilization regimes, has led to pronounced vertical stratification of P and the accumulation of substantial legacy P reserves in the near-surface soil (0–5 cm). While winter cover cropping (CC) is widely promoted to control soil erosion and particulate P transport, edge-of-field monitoring has revealed that cover crops can paradoxically elevate surface runoff DRP concentrations. Resolving this environmental trade-off requires a mechanistic understanding of how cover crops and contrasting P fertilization strategies—specifically control (CN, no P addition), build-and-drawdown (BD) or sufficiency (SF), and build-and-maintain (BM)—interact to govern the chemical speciation, biological cycling, and mineralogical retention of soil P.

To address these knowledge gaps, this dissertation employed a multi-scale, multi-technique analytical framework at the Kansas Agricultural Watershed (KAW) field laboratory near Manhattan, Kansas, on a fine, smectitic, mesic Pachic Argiustoll (Smolan silty clay loam). By integrating long-term agronomic P budgets and stratified soil fertility indicators (Chapter 5) with operational sequential P fractionation (Chapter 3), molecular-level organic and inorganic P speciation via liquid-state ^{31}P nuclear magnetic resonance (^{31}P-NMR) spectroscopy (Chapter 4), and solid-phase iron (Fe) and aluminum (Al) biogeochemistry via selective chemical extractions and synchrotron-based Fe K-edge X-ray absorption near-edge structure (XANES) spectroscopy

(Chapter 6), this research provides a comprehensive mechanistic synthesis of soil P dynamics under conservation management.

Synthesis of Key Findings across Chapters

1. **Agronomic Fluxes, Vertical Stratification, and Soil Fertility Dynamics (Chapters 3 and 5):** Long-term evaluation of soil fertility indicators across three depth intervals (0–2.5, 2.5–5, and 5–15 cm) confirmed severe vertical stratification of Mehlich-3 P, total P, total carbon (TC), and total nitrogen (TN) within the continuous no-till profile, with the highest nutrient concentrations restricted to the top 0–2.5 and 2.5–5 cm layers. Phosphorus fertilization was the primary driver of net P balance and surface soil test P (STP) accumulation. Continuous annual applications under the BM strategy generally maintained positive cumulative net P budgets and kept Mehlich-3 P concentrations above the agronomic critical threshold (20 mg kg^{-1}), with severe stratification resulting in Mehlich-3 P concentrations exceeding 80 mg kg^{-1} in the uppermost 0–2.5 cm surface layer. Conversely, ceasing P applications under the BD strategy resulted in a negative net P budget, allowing crops to progressively draw down legacy Mehlich-3 P in the surface soil toward the critical threshold without reducing grain yields relative to the BM strategy during most study years. Across the 8-year study period (2015–2022), integrating winter cover crops significantly increased total annual plant P assimilation (average annual uptake across cash crops and cover crops, kg P ha^{-1} yr^{-1}) and annual P redeposition (return of unharvested residue P to the soil surface). Furthermore, cover cropping

significantly enhanced surface TC and TN stocks, demonstrating its vital role in building near-surface soil organic matter (OM) in stratified no-till systems.

2. **Operational Phosphorus Fractionation and Biological Redistribution (Chapter 3):** Modified Hedley sequential fractionation of the 0–5 cm topsoil from 2019 to 2022 demonstrated that P fertilization predominantly governed the accumulation of P in the fractions associated with readily soluble and labile (Resin-P_i and $NaHCO_3$-P_i) and moderately labile (NaOH-P_i) inorganic pools, consistently following the gradient of BM > BD > CN. A significant interaction between cover cropping and P fertilization revealed that cover crops actively depleted readily soluble and labile pools (Resin-P_i and $NaHCO_3$-P_i) in the fertilized treatments (BD and BM), but had no significant depleting effect in the P-deficient CN plots. Also, cover cropping significantly enriched the moderately stable, organic P fraction (NaOH-P_o) across treatments. The highly recalcitrant fractions (HCl-P_i and Residual-P), remained statistically unaffected by either cover cropping or P fertilization strategies, although Residual-P exhibited temporal fluctuations across sampling years. These operational fractionation results demonstrate that cover crops do not merely mine recalcitrant P; rather, they scavenge labile pools from fertilized topsoil, assimilate it into winter biomass, and biologically redistribute it into moderately stable organic P reservoirs.

3. **Molecular Speciation of Inorganic and Organic Phosphorus via Solution ^{31}P-NMR (Chapter 4):** Because operational sequential extractions lack strict

chemical specificity, liquid-state ^{31}P-NMR spectroscopy on NaOH-EDTA extracts was utilized to resolve the molecular composition of the topsoil P pools. The proportion of total soil P extracted by NaOH-EDTA and the concentration of orthophosphate increased significantly with P fertilization intensity, mirroring the Resin-P_i, $NaHCO_3$-P_i, and Mehlich-3 P trends. Furthermore, fertilization elevated condensed inorganic phosphates, specifically pyrophosphate and polyphosphates, reflecting both ammonium polyphosphate fertilizer inputs and enhanced microbial P storage. ^{31}P-NMR spectroscopy revealed that cover cropping significantly increased the concentration of *myo*-inositol hexakisphosphate (*myo*-IHP, phytate), while interacting with P fertilization to alter specific uncharacterized orthophosphate monoester peaks. This molecular evidence confirms that cover crops actively assimilate labile soil P and convert it into plant-derived organic P forms that accumulate in the topsoil upon residue decomposition.

4. **Organo-Mineral Interactions and Soil Iron Chemistry via Selective Extractions and Fe K-edge XANES (Chapter 6):** Selective extraction procedures (sodium pyrophosphate and acid ammonium oxalate) combined with synchrotron-based Fe K-edge XANES spectroscopy elucidated the mineralogical mechanisms affecting P retention in the 0–5 cm layer. Cover cropping and associated OM inputs significantly increased pyrophosphate-extractable Fe and Al under the fertilized strategies (BM and BD) while proportionally reducing ammonium oxalate-extractable amorphous Fe oxides, indicating enhanced formation of organo-metallic complexes. Complexation of Fe by OM reduces the availability of reactive inorganic Fe oxide surfaces for phosphate sorption,

directly contributing to the increased DRP losses observed in cover-cropped treatments.

Mechanistic Synthesis: Resolving the Cover Crop–Phosphorus Paradox

Synthesizing the chemical, spectroscopic, and agronomic lines of evidence across Chapters 3 through 6 provides a unified mechanistic explanation for the dual behavior of cover crops in no-till agroecosystems. During the fall and spring growing seasons, cereal rye cover crops act as an active biological sink, scavenging highly labile P pools (Resin-P_i, $NaHCO_3$-P_i, and Mehlich-3 P) from the stratified 0–5 cm soil layer and immobilizing it within living plant tissue and rhizosphere microbial biomass. Upon herbicide termination and residue decomposition, a substantial fraction of this assimilated P—along with root-derived C—is humified and stabilized within the soil matrix as NaOH-extractable organic P (NaOH-P_o).

When cover crops are grown under a continuous BM fertilization regime, the near-surface soil remains oversaturated with phosphate due to annual fertilizer additions, and the cover crop engages in luxury P consumption. Under these high-fertility conditions, freeze–thaw cycles and rainfall following termination cause the rapid leaching of water-soluble intracellular phosphate from decaying surface residues, while organic ligands released during decomposition compete with phosphate for Fe and Al sorption sites. Consequently, in BM systems, biological P release from surface residues may exceed the soil's capacity to retain P, potentially contributing to the elevated DRP runoff losses previously documented at this watershed. Conversely, when cover cropping is paired with a BD (drawdown) strategy, withholding P fertilizer forces both the cash crop and the cover crop to rely on legacy P reserves. This progressively draws down labile P pools toward the agronomic critical threshold while preserving crop yields.

Practical Implications for Sustainable Phosphorus Management

- **Transitioning from Build-and-Maintain to Drawdown Management:** In no-till soils with historical P accumulation (STP exceeding agronomic critical levels), continuing annual P applications under a BM philosophy is agronomically unnecessary and environmentally hazardous. Adopting a drawdown (BD) phase allows producers to rely on legacy P reserves, reduce fertilizer input costs, and lower surface labile phosphate concentrations without sacrificing corn or soybean yields.

- **Coupling Cover Crops with Phosphorus Drawdown:** Cover crops should not be viewed as a standalone solution for dissolved P mitigation in P-saturated soils. Instead, their environmental benefit is maximized when integrated with P drawdown management, where their biological scavenging capacity accelerates the conversion of highly labile inorganic P pools into less labile organic P pools.

Future Research Directions

1. **Rhizosphere versus Bulk Soil Sampling and Spatially Resolved Microspectroscopy:** As highlighted in Chapter 6, biogeochemical transformations driven by cover crop roots—such as proton release, ligand-promoted Fe dissolution, and organo-metallic complexation—are spatially concentrated within millimeter-scale rhizosphere gradients and can be masked or diluted when analyzing homogenized bulk soil samples. Future field investigations should be conducted directly within the established KAW plots during active spring cereal rye growth by excavating intact root–soil monoliths and

physically separating rhizosphere soil (soil tightly adhering to root surfaces) from bulk inter-row soil. Combining wet-chemical extractions (Hedley, pyrophosphate, and oxalate extractions) on separated rhizosphere soil with synchrotron-based microspectroscopy (μ-XRF elemental mapping and Fe/P K-edge μ-XANES on intact, cryogenically preserved root–soil cores) will directly resolve micro-scale P and Fe speciation gradients.

2. **Quantifying Root Exudates, Organic Acid Production, and Microbial and Enzymatic Activities:** While this dissertation inferred biological P mobilization and immobilization from shifts in operational and molecular P pools, future studies should directly quantify the biological drivers through coupled field and controlled-environment greenhouse experiments. At the KAW field site, seasonal soil sampling (at fall cover crop establishment, spring vegetative peak, and post-termination) should be paired with extracellular enzyme assays—specifically acid and alkaline phosphatases and phytases (for organic P mineralization), pyrophosphatases (for polyphosphate hydrolysis), and C- and N-degrading enzymes governing organic matter decomposition—alongside microbial community profiling and functional gene quantification (e.g., *phoD* and *gcd*). Complementing the field measurements, controlled greenhouse rhizobox experiments using Smolan silty clay loam collected from the KAW plots should be conducted to non-destructively sample root exudates *in situ* (e.g., via micro-suction cups or anion-exchange membranes) and quantify the production rates and composition of low-molecular-weight organic acids (citrate, malate, and oxalate) across contrasting P fertility regimes.
3. **Subsoil Phosphorus Dynamics and Deep Root Foraging:** While Chapters 3, 4, and 6 focused intensively on the biogeochemically active 0–5 cm interface, and Chapter 5 extended to 15 cm, cash crops and deep-rooted cover crops under prolonged P drawdown

likely acquire P from deeper soil horizons. Future field investigations at the KAW site and broader regional long-term P trials should collect deep soil cores (e.g., 15–30, 30–60, and 60–100 cm) to evaluate subsoil P fractionation, root distribution, and deep legacy P depletion during extended drawdown and sufficiency phases.

4. **Coupled Solid-Phase P K-edge XANES and Laboratory Incubation of Condensed Phosphate Interactions:** Future spectroscopic analyses on archived and newly collected KAW surface soils (0–2.5 and 2.5–5 cm) should integrate solid-phase P K-edge XANES spectroscopy to directly resolve Ca- versus Fe- and Al-bound inorganic phosphates. Furthermore, given that ammonium polyphosphate (APP) fertilizers supply pyrophosphate and polyphosphates to the soil while sodium pyrophosphate serves as a laboratory extractant for organically complexed metals, controlled laboratory batch incubation studies are warranted. Specifically, incubating surface soil from the KAW control plots with graded rates of APP versus orthophosphate (monopotassium phosphate) under sterile and non-sterile conditions—and tracking temporal shifts in pyrophosphate- and oxalate-extractable Fe and Al alongside solution ^{31}P-NMR—will partition direct fertilizer-derived polyphosphate chelation from root- and microbe-driven organic complexation.
5. **Crop Residue ^{31}P-NMR and Evaluating Tillage Inclusions:** Despite the mechanistic insights gained into soil P and Fe dynamics, a critical knowledge gap remains regarding the exact source of DRP losses in runoff under cover-cropped systems. It is currently unresolved whether the mobilized DRP originates primarily from the underlying mineral soil (e.g., via ligand-promoted dissolution and desorption) or directly from the leaching of decomposing cover crop residues resting on the soil surface. To definitively partition these

sources, future research must incorporate specific crop residue ^{31}P-NMR spectroscopy to characterize P speciation and release dynamics directly within the plant tissues during decomposition. Furthermore, the intense vertical stratification of P, C, and acidity at the immediate soil surface (0–2.5 cm) is fundamentally driven by the strict, continuous no-till management applied in this study. This severe surface stratification substantially increases the vulnerability of DRP to runoff. To mitigate this, integrating occasional tillage (strategic or rotational tillage) into these conservation systems could prove highly beneficial. Occasional tillage may redistribute surface-stratified legacy P and accumulated plant residues into deeper soil layers, potentially reducing the direct interaction between high surface-soil P concentrations and surface runoff.

Appendix A - Supplementary ^{31}P-NMR Data

The least squares means and standard errors of the transformed data for soil phosphorus compounds and compound classes determined by solution ^{31}P-NMR spectroscopy are presented in Table A1. Because the raw concentration data violated the assumptions of normality and compositional independence, statistical analyses and ANOVA significance testing in Chapter 4 were conducted on transformed data using log (n + 0.5) for broad compound classes (P_i, P_o, Total Polyphosphates, Total IHP, Total Monoesters, Total Diesters, C_{mono}, C_diest, and M:D ratios) and centered log-ratio (CLR) transformations for individual phosphorus species (Abdi et al., 2015). Negative values in Table A1 reflect log- or CLR-transformed coordinates of low-abundance compounds rather than negative physical concentrations; the corresponding back-transformed concentrations (mg P kg^{-1}) for main effects are presented in Chapter 4 (Tables 4-5 and 4-6, and Figures 4-4 and 4-5).

Table A 1. Least squares means and standard errors (Mean ± SE) of transformed soil phosphorus compound concentrations (log (*n* + 0.5) or centered log-ratio transformed) across main effects and treatment interactions, determined by ^{31}P-NMR spectroscopy.

Variable (Compound)	Cover: NC	Cover: CC	Fert: CN	Fert: SF	Fert: BM	NC-CN	NC-SF	NC-BM	CC-CN	CC-SF	CC-BM
Cdiest	1.171 ± 0.026	1.191 ± 0.026	1.126 ± 0.032	1.185 ± 0.032	1.232 ± 0.032	1.131 ± 0.045	1.164 ± 0.045	1.217 ± 0.045	1.120 ± 0.045	1.206 ± 0.045	1.247 ± 0.045
D-*chiro*-IHP	-0.199 ± 0.117	-0.025 ± 0.117	-0.079 ± 0.143	0.020 ± 0.143	-0.276 ± 0.143	-0.007 ± 0.202	-0.188 ± 0.202	-0.403 ± 0.202	-0.151 ± 0.202	0.227 ± 0.202	-0.150 ± 0.202
Cmono	1.550 ± 0.020	1.574 ± 0.020	1.570 ± 0.024	1.597 ± 0.024	1.519 ± 0.024	1.576 ± 0.034	1.577 ± 0.034	1.496 ± 0.034	1.564 ± 0.034	1.617 ± 0.034	1.541 ± 0.034
DNA	-0.506 ± 0.169	-0.821 ± 0.169	-0.481 ± 0.207	-1.080 ± 0.207	-0.431 ± 0.207	-0.174 ± 0.292	-0.954 ± 0.292	-0.391 ± 0.292	-0.788 ± 0.292	-1.206 ± 0.292	-0.471 ± 0.292
Degradation	0.994 ± 0.029	1.033 ± 0.029	0.960 ± 0.036	1.044 ± 0.036	1.037 ± 0.036	0.954 ± 0.050	1.011 ± 0.050	1.018 ± 0.050	0.965 ± 0.050	1.078 ± 0.050	1.057 ± 0.050

Variable (Compound)	Cover: NC	Cover: CC	Fert: CN	Fert: SF	Fert: BM	NC-CN	NC-SF	NC-BM	CC-CN	CC-SF	CC-BM
Total Diesters	0.723 ± 0.041	0.706 ± 0.041	0.663 ± 0.050	0.660 ± 0.050	0.820 ± 0.050	0.695 ± 0.071	0.661 ± 0.071	0.812 ± 0.071	0.632 ± 0.071	0.659 ± 0.071	0.828 ± 0.071
M:D ratio	0.997 ± 0.047	1.038 ± 0.047	1.064 ± 0.057	1.111 ± 0.057	0.878 ± 0.057	1.032 ± 0.081	1.095 ± 0.081	0.865 ± 0.081	1.095 ± 0.081	1.128 ± 0.081	0.890 ± 0.081
Total Monoesters	1.653 ± 0.021	1.681 ± 0.021	1.661 ± 0.025	1.701 ± 0.025	1.638 ± 0.025	1.664 ± 0.036	1.678 ± 0.036	1.616 ± 0.036	1.659 ± 0.036	1.724 ± 0.036	1.660 ± 0.036
Monoester 1	-0.306 ± 0.059	-0.300 ± 0.059	-0.387 ± 0.072	-0.095 ± 0.072	-0.426 ± 0.072	-0.220 ± 0.102	-0.111 ± 0.102	-0.586 ± 0.102	-0.554 ± 0.102	-0.079 ± 0.102	-0.267 ± 0.102
Monoester 2	2.066 ± 0.036	1.949 ± 0.036	2.337 ± 0.044	2.015 ± 0.044	1.669 ± 0.044	2.447 ± 0.062	2.037 ± 0.062	1.714 ± 0.062	2.227 ± 0.062	1.994 ± 0.062	1.625 ± 0.062
Monoester 3	-0.231 ± 0.061	0.137 ± 0.061	0.134 ± 0.075	0.080 ± 0.075	-0.354 ± 0.075	-0.220 ± 0.106	0.112 ± 0.106	-0.586 ± 0.106	0.487 ± 0.106	0.048 ± 0.106	-0.123 ± 0.106
Nucl	0.900 ± 0.057	0.846 ± 0.057	0.997 ± 0.070	0.842 ± 0.070	0.781 ± 0.070	1.039 ± 0.098	0.810 ± 0.098	0.851 ± 0.098	0.954 ± 0.098	0.873 ± 0.098	0.710 ± 0.098
OrthoP	3.162 ± 0.036	3.082 ± 0.036	2.402 ± 0.044	3.258 ± 0.044	3.706 ± 0.044	2.426 ± 0.062	3.226 ± 0.062	3.834 ± 0.062	2.379 ± 0.062	3.289 ± 0.062	3.579 ± 0.062
OthDi 1	-0.042 ± 0.107	0.002 ± 0.107	-0.081 ± 0.131	-0.078 ± 0.131	0.098 ± 0.131	-0.120 ± 0.185	-0.183 ± 0.185	0.176 ± 0.185	-0.041 ± 0.185	0.027 ± 0.185	0.021 ± 0.185
OthDi 2	-1.256 ± 0.172	-1.401 ± 0.172	-1.080 ± 0.210	-1.815 ± 0.210	-1.090 ± 0.210	-0.970 ± 0.298	-1.640 ± 0.298	-1.158 ± 0.298	-1.190 ± 0.298	-1.990 ± 0.298	-1.023 ± 0.298
Pchol	-1.235 ± 0.081	-1.084 ± 0.081	-1.118 ± 0.099	-1.086 ± 0.099	-1.275 ± 0.099	-1.066 ± 0.140	-1.101 ± 0.140	-1.537 ± 0.140	-1.169 ± 0.140	-1.071 ± 0.140	-1.013 ± 0.140
Phn	-0.275 ± 0.038	-0.295 ± 0.038	-0.484 ± 0.047	-0.290 ± 0.047	-0.081 ± 0.047	-0.524 ± 0.067	-0.305 ± 0.067	0.004 ± 0.067	-0.444 ± 0.067	-0.275 ± 0.067	-0.166 ± 0.067
P_i	1.840 ± 0.025	1.844 ± 0.025	1.513 ± 0.030	1.899 ± 0.030	2.114 ± 0.030	1.511 ± 0.043	1.876 ± 0.043	2.132 ± 0.043	1.516 ± 0.043	1.921 ± 0.043	2.096 ± 0.043
P_o	1.747 ± 0.019	1.779 ± 0.019	1.735 ± 0.023	1.793 ± 0.023	1.760 ± 0.023	1.737 ± 0.033	1.773 ± 0.033	1.731 ± 0.033	1.733 ± 0.033	1.813 ± 0.033	1.790 ± 0.033
Total Poly	0.549 ± 0.134	0.349 ± 0.134	0.547 ± 0.164	0.234 ± 0.164	0.566 ± 0.164	0.676 ± 0.233	0.389 ± 0.233	0.582 ± 0.233	0.419 ± 0.233	0.079 ± 0.233	0.549 ± 0.233
Pyro	0.965 ± 0.053	0.962 ± 0.053	0.874 ± 0.065	0.896 ± 0.065	1.119 ± 0.065	0.779 ± 0.091	0.955 ± 0.091	1.160 ± 0.091	0.970 ± 0.091	0.837 ± 0.091	1.078 ± 0.091
scyllo-IHP	-0.687 ± 0.086	-0.799 ± 0.086	-0.581 ± 0.105	-0.787 ± 0.105	-0.861 ± 0.105	-0.482 ± 0.148	-0.735 ± 0.148	-0.843 ± 0.148	-0.680 ± 0.148	-0.840 ± 0.148	-0.878 ± 0.148
Total IHP	0.913 ± 0.030	0.967 ± 0.030	0.864 ± 0.037	0.988 ± 0.037	0.967 ± 0.037	0.853 ± 0.052	0.939 ± 0.052	0.945 ± 0.052	0.875 ± 0.052	1.036 ± 0.052	0.989 ± 0.052
Total Phn	0.369 ± 0.019	0.393 ± 0.019	0.255 ± 0.023	0.394 ± 0.023	0.495 ± 0.023	0.234 ± 0.033	0.376 ± 0.033	0.498 ± 0.033	0.275 ± 0.033	0.412 ± 0.033	0.492 ± 0.033
TotPoly	1.046 ± 0.037	1.050 ± 0.037	0.970 ± 0.045	1.020 ± 0.045	1.153 ± 0.045	0.959 ± 0.064	1.043 ± 0.064	1.134 ± 0.064	0.980 ± 0.064	0.998 ± 0.064	1.172 ± 0.064

Variable (Compound)	Cover: NC	Cover: CC	Fert: CN	Fert: SF	Fert: BM	NC-CN	NC-SF	NC-BM	CC-CN	CC-SF	CC-BM
α-glyc	-0.593 ± 0.059	-0.481 ± 0.059	-0.651 ± 0.072	-0.422 ± 0.072	-0.538 ± 0.072	-0.748 ± 0.101	-0.493 ± 0.101	-0.538 ± 0.101	-0.554 ± 0.101	-0.351 ± 0.101	-0.538 ± 0.101
β-glyc	0.118 ± 0.052	0.203 ± 0.052	0.045 ± 0.064	0.280 ± 0.064	0.156 ± 0.064	-0.037 ± 0.091	0.217 ± 0.091	0.173 ± 0.091	0.126 ± 0.091	0.344 ± 0.091	0.139 ± 0.091
cM:D ratio	0.471 ± 0.019	0.473 ± 0.019	0.526 ± 0.024	0.498 ± 0.024	0.392 ± 0.024	0.525 ± 0.033	0.500 ± 0.033	0.387 ± 0.033	0.526 ± 0.033	0.496 ± 0.033	0.397 ± 0.033
g6P	-1.072 ± 0.106	-1.114 ± 0.106	-0.917 ± 0.129	-0.970 ± 0.129	-1.390 ± 0.129	-0.809 ± 0.183	-0.870 ± 0.183	-1.537 ± 0.183	-1.026 ± 0.183	-1.071 ± 0.183	-1.244 ± 0.183
myo-IHP	0.423 ± 0.057	0.661 ± 0.057	0.317 ± 0.070	0.729 ± 0.070	0.579 ± 0.070	0.234 ± 0.099	0.710 ± 0.099	0.327 ± 0.099	0.401 ± 0.099	0.749 ± 0.099	0.832 ± 0.099
neo-IHP	-0.242 ± 0.041	-0.242 ± 0.041	-0.280 ± 0.051	-0.237 ± 0.051	-0.208 ± 0.051	-0.360 ± 0.072	-0.242 ± 0.072	-0.124 ± 0.072	-0.201 ± 0.072	-0.232 ± 0.072	-0.293 ± 0.072
4.2 ppm	-0.381 ± 0.066	-0.507 ± 0.066	-0.387 ± 0.081	-0.458 ± 0.081	-0.487 ± 0.081	-0.482 ± 0.114	-0.565 ± 0.114	-0.097 ± 0.114	-0.292 ± 0.114	-0.351 ± 0.114	-0.878 ± 0.114
5.0 ppm	-0.428 ± 0.096	-0.311 ± 0.096	-0.302 ± 0.117	-0.342 ± 0.117	-0.464 ± 0.117	-0.499 ± 0.166	-0.333 ± 0.166	-0.450 ± 0.166	-0.105 ± 0.166	-0.351 ± 0.166	-0.477 ± 0.166
sIP5	-0.730 ± 0.105	-0.811 ± 0.105	-0.825 ± 0.129	-0.694 ± 0.129	-0.793 ± 0.129	-0.883 ± 0.182	-0.735 ± 0.182	-0.573 ± 0.182	-0.768 ± 0.182	-0.653 ± 0.182	-1.013 ± 0.182

Note: Broad compound classes (P_i, P_o, TotPoly, Total IHP, Total Monoesters, Total Diesters, Total Phn, Degradation, C_{mono}, C_diest, and M:D and cM:D ratios) were transformed using log(n + 0.5), whereas individual phosphorus species were transformed using centered log-ratio (CLR) transformation (Abdi et al., 2015). Abbreviations: C_diest, corrected orthophosphate diesters; C_{mono}, corrected orthophosphate monoesters; M:D ratio, uncorrected monoester-to-diester ratio; cM:D ratio, corrected monoester-to-diester ratio; Nucl, mononucleotides; OrthoP, orthophosphate; OthDi 1 and OthDi 2, other diesters 1 and 2; Pchol, choline phosphate; Phn, phosphonates; P_i, total inorganic P; P_o, total organic P; Poly, polyphosphate; Pyro, pyrophosphate; TotPoly, total polyphosphates; α-glyc, α-glycerophosphate; β-glyc, β-glycerophosphate; g6P, glucose 6-phosphate; IHP, inositol hexakisphosphate; sIP5, scyllo-inositol pentakisphosphate; 4.2 ppm and 5.0 ppm, uncharacterized monoester peaks at 4.2 and 5.0 ppm. Treatments: NC, no cover crop; CC, cover crop; CN, control (no P fertilizer); SF, sufficiency P fertilizer; BM, build-and-maintain P fertilizer.

The untransformed interaction means and standard errors (expressed in mg P kg^{-1}) for the uncharacterized orthophosphate monoester peaks that exhibited significant Cover Crop × Fertilizer interactions (Monoester 1, Monoester 3, and the unknown peak at 4.2 ppm; Table 4-4) are presented in Table A2.

Table A 2. Interactive effects of cover crop and phosphorus (P) fertilization treatments on the concentrations of specific uncharacterized orthophosphate monoesters (mg P kg^{-1}) determined by ^{31}P-NMR spectroscopy. Values represent least-squares means ± standard errors.

P Fertilization Strategy	Cover Crop Management	Monoester 1 (mg P kg^{-1})	Monoester 3 (mg P kg^{-1})	Unknown peak at 4.2 ppm (mg P kg^{-1})
CN (Control)	NC (No Cover Crop)	1.65 ± 0.10 b	1.65 ± 0.11 b	1.27 ± 0.11 b
	CC (Cover Crop)	1.24 ± 0.10 c	3.51 ± 0.11 a	1.61 ± 0.11 ab
SF (Sufficiency)	NC (No Cover Crop)	2.30 ± 0.10 ab	2.87 ± 0.11 a	1.46 ± 0.11 ab
	CC (Cover Crop)	2.53 ± 0.10 a	2.88 ± 0.11 a	1.93 ± 0.11 a
BM (Build and Maintain)	NC (No Cover Crop)	1.47 ± 0.10 c	1.47 ± 0.11 b	2.40 ± 0.11 a
	CC (Cover Crop)	2.37 ± 0.10 ab	2.74 ± 0.11 a	1.29 ± 0.11 b

Note: Means within a column followed by the same letter are not significantly different at α = 0.05.

Reference

Abdi, D., Cade-Menun, B. J., Ziadi, N., & Parent, L.-É. (2015). Compositional statistical analysis of soil ^{31}P-NMR forms. *Geoderma*, 257–258, 40–47. https://doi.org/10.1016/j.geoderma.20